Regulation of Quorum-sensing in *Vibrio cholerae*

By

Lucas Maximilian Walker

A thesis submitted to the University of Birmingham

For the degree of
Doctor of Philosophy

School of Biosciences

University of Birmingham

December, 2021

Abstract

Vibrio cholerae has spread across the world in seven recorded pandemics. Millions of recorded cases, and thousands of deaths, still occur world-wide each year. Survival of *V. cholerae* in the host and aquatic environments requires the careful regulation of gene expression. In part, this relies on quorum-sensing; a tool used by bacteria to respond to changes in population density. Two key transcription factors involved in the quorum-sensing cascade of *V. cholerae* are LuxO and HapR. Interestingly, the genes encoding these factors are highly variable amongst clinical isolates of pandemic cholera. Despite the importance of HapR and LuxO in escape from the host mucosa, natural competence, and expression of virulence factors, genome-wide DNA-binding targets have not yet been identified. Furthermore, it is not known how these proteins interact with other global regulators.

In this study, we assess the role of HapR and LuxO in pandemic *V. cholerae*. We show that mutations common in clinical isolates of *V. cholerae* abolish HapR expression. We determine DNA-binding targets of HapR and LuxO across the *V. cholerae* E7946 genome and identify genes with a diverse range of functions that are regulated by HapR. Additionally, we demonstrate how HapR and the cyclic AMP receptor protein (CRP) co-regulate transcription from the *murQP* promoter. Specifically, we show that these transcription factors bind DNA co-operatively.

Acknowledgements

There are many people I would like to thank for their support and encouragement throughout the past four years. First and foremost, my sincerest thanks go to Professor David Grainger for supervising the project, for keeping me motivated and ensuring I was always on the right track. Also, special thanks go to Dr. James Haycocks for all the times he has helped me in the lab, given me advice, put up with my constant questions and purchased materials for me (meaning I never once had to use New Core). I would also like to thank the whole of the Grainger group, past and present, for making it a such a great place to work and for enduring all of my puns.

Thanks also go to Professor Steve Busby for all of his advice during this project and for all the equipment and reagents we invariably had to 'borrow'. I would also like to thank Dr. Ankur Dalia of Indiana University for his help with HapR purification. Thanks to Fay and Norman in Genomics for all the sequencing data.

A big thank you goes to the staff at Costa for the many, many flat whites and breakfast rolls that have gotten me through the years. Thanks to Davey, Dorian and Paul in Biosciences stores for all of their work.

I would like to thank my parents for supporting me while I have been a full-time student for a total of eight years now. Finally, a huge thank you to my incredible partner Natasha for her patience and understanding and without whom I would not have managed any of this.

Table of Contents

List of Figures

List of Tables

Abbreviations

7PET	Seventh pandemic El Tor
A	Adenine
A	(Ala) Alanine
AAA ATPase	ATPases Associate with diverse cellular Activities
APS	Ammonium persulphate
AR	Activating Region
ATP	Adenosine triphosphate
ATPase	Adenosine triphosphatase
bEBP	Bacterial Enhancer Binding Protein
bp	Base pair
BSA	Bovine serum albumin
C	Cytosine
CBP	Chitin binding protein
Ci	Sievert
^{o}C	Celsius (degree)
ChIP	Chromatin Immunoprecipitation
ChIP-seq	ChIP and DNA sequencing
CIP	Calf intestinal phosphatase
CRP	Cyclic-AMP Receptor Protein
cAMP	3'-5'-cyclic adenosine monophosphate
CTD	Carboxy-terminal domain
CTP	Cytosine triphosphate
CTX	Cholera toxin

D (Asp)	Aspartic acid
dH2O	Distilled water
DNA	Deoxyribonucleic acid
DnaseI	Deoxyribonuclease I
dNTP	2'-deoxyribonucleoside 5'-triphosphate (N = A, C, G, T)
E (Glu)	Glutamic acid
E. coli	*Escherichia coli*
EDTA	Diaminoethanetetra-acetic acid
EIIA^{Glc}	Glucose-specific enzyme II A
EMSA	Electrophoretic mobility shift assays
G	Guanosine
G (Glu)	Glutamine
GlcNAc	N-Acetylglucosamine
GTP	Guanosine triphosphate
H (His)	Histidine
H-NS	Histone-like Nucleoid Structuring protein
IHF	Integration host factor
IPTG	Isopropyl β-D-1-thiogalactopyranoside
K (Lys)	Lysine
kb	Kilobase
kDa	Kilodalton
LB	Luria Broth
mRNA	Messenger ribonucleic acid
nt	Nucleotide

NTD	Amino-terminal domain
MCP	Methyl-accepting chemotaxis protein
MEME	Multiple EM for Motif Elicitation
MurNAc	N-Acetylmuramic acid
N (Asn)	Asparagine
OD	Optical Density
ONPG	o-nitrophenyl-β-D-galactopyranoside
ORF	Open reading frame
PAGE	Polyacrylamide gel electrophoresis
PCR	Polymerase chain reaction
PNK	Polynucleotide kinase
Ppi	Pyrophosphate
Qrr	Quorum-regulatory RNA
R (Arg)	Arginine
RNA	Ribonucleic acid
RNA-seq	RNA sequencing
RNAP	RNA polymerase
Rnase	Ribonuclease
rRNA	Ribosomal RNA
S (Ser)	Serine
S. aureus	*Staphylococcus aureus*
SDS	Sodium dodecyl sulphate
SNP	Single nucleotide polymorphism
sRNA	Small RNA

T	Thymine
T (Thr)	Threonine
TBS	Tris-buffered saline
TBE	Tris-borate EDTA
TCP	Toxin co-regulated pilus
TE	Tris-EDTA
TEMED	N,N,N',N'-tetramethylethylene diamine
TNSC	Transcription buffer
Tris	Tris (hydroxymethyl) aminoethane
tRNA	Transfer RNA
TSS	Transcription start site
U	Uracil
UTP	Uracil triphosphate
UP element	Upstream promoter element
V	Volts
V. cholerae	*Vibrio cholerae*
V. harveyi	*Vibrio harveyi*
V. vulnificus	*Vibrio vulnificus*
w/v	Weight per volume
W	Watts
WT	Wild-type
v/v	Volume per volume

Chapter 1
Introduction

2.6 Gene regulation in bacteria

Prokaryotic organisms survive in the environment through the careful regulation of gene expression. A diverse range of mechanisms are utilised to achieve this. Many of these mechanisms centre around regulating the activity of the DNA-dependent RNA polymerase (RNAP), particularly during transcription initiation (for detailed reviews see Browning and Busby, 2004, Browning and Busby, 2016, and Borukhov and Nudler, 2008). Other mechanisms, such as the post-transcriptional regulation of gene expression by small RNAs (sRNAs), are also used (Dutta and Srivastava, 2018). Together, these mechanisms allow co-ordination of responses to environmental cues, including nutrient availability, population density, and stress factors.

1.2 Bacterial RNA polymerase

RNAP is an enzyme, the sequence of which is highly conserved across all bacterial species. The core enzyme consists of five subunits (αI, αII, β, β′ and ω), which form a complex of around 400 kDa in mass (Borukhov and Nudler, 2008; Cramer et al., 2001; Nudler et al., 1998; Minakhin et al., 2001; Zhang et al., 1999). The function of RNAP is to bind DNA and initiate transcription, to generate a complementary strand of RNA. This RNA can code for a protein (messenger RNA), be non-coding transfer RNA (tRNA), or ribosomal RNA (rRNA) (Borukhov and Nudler, 2008).

1.3 Sigma factors and Promoters

1.3.1 Structure and function of sigma factors

A promoter is a sequence of DNA to which RNAP binds to initiate transcription. The recognition of promoter DNA sequences by RNAP requires proteins called sigma factors (see figure 1.1) (Burgess and Anthony, 2001). Different sigma factors are categorised by the function of genes they regulate (their regulon). For example, σ^{70} (RpoD) is the 'housekeeping' sigma factor in *E. coli* and has the largest regulon (Cho et al., 2014). Conversley, σ^{54} (RpoN) controls *E. coli* genes involved in nitrogen metabolism and has a smaller regulon (Tsang and Hoover, 2014). The 'stationary phase' σ^{38} factor (RpoS) governs theepharosen of genes for survival of bacteria in nutrient-poor environments (Hengge-Aronis, 1993). Other *E. coli* sigma factors control the heat shock response (σ^{32}, RpoH), flagellar biosynthesis (σ^{28}, RpoF), cell envelope stress response (σ^{24}, RpoE) and iron stress response (σ^{19}, FecI) (Yura et al., 1993; Slamti et al., 2007; Starnbach and Lory, 1992; Hayden and Ades, 2008; Angerer et al., 1995). Sigma factors can have slightly different roles in different species of bacteria. For example, in *Vibrio cholerae*, σ^{54} is required for the transcription of flagellar genes and σ^{38} is critical for virulence and escape from the host epithelium during infection (Yildiz and Schoolnik, 1998; Nielsen et al., 2006; Dong and Mekalanos, 2012). Most sigma factors are in the σ^{70} family, the exception being those related to σ^{54}. Σ^{70} family sigma factors are generally comprised of three domains (σ2, σ3 and σ4) with linker regions between them (Borukhov and Severinov, 2002). A σ1 domain is often, but not always, present.

1.3.2 Promoter recognition by sigma factors

The σ^{70} factor recognises 6 bp sequences 35 and 10 bp upstream of the transcription start site (TSS) (Murakami et al., 2002; Campbell et al., 2002). These are referred to as the '-35' and '-10' elements and have the consensus 5'-TTGACA-3' and 5'-TATAAT-3' respectively (figure 1.1a). At some promoters, the sequence 5'-TGn-3' is located immediately upstream of the -10 element to make an 'extended -10' (Sanderson et al., 2003; Kumar et al., 1993). At promoters with an extended -10 sequence, the -35 element is less important for promoter recognition by σ^{70} (Kumar et al., 1993). An AT-rich sequence of around 20 bp, often found upstream of the -35 element is referred to as the 'UP element'. This facilitates binding of the RNAP α subunit C-terminal domain (α-CTD) to DNA (Ross et al., 2001). The kinetics of association between RNAP and DNA is partly dictated by the sequence these four elements, which are not always of perfect consensus (Browning and Busby, 2004). Other σ^{70} family sigma factors also recognise promoter elements, but the sequence and positions of these elements vary. All σ^{70} family factors stabilise spontaneous DNA opening to drive transcription initiation.

At promoters recognised by σ^{54}, the RNAP σ^{54} holoenzyme is not sufficient to drive transcription initiation. Unable to stabilise spontaneous DNA opening, σ^{54} requires energy from ATP-hydrolysis provided by an activator protein (Wang and Gralla, 1998; Rombel et al., 1998). Consensus DNA-binding sites for σ^{54} are distinct from those for σ^{70} and more conserved across bacterial species (Merrick, 1993). Interactions between σ^{54} and DNA occur at -12 and -24 sequences with the consensus 5'-TGC-3' and 5'-'GG'-3' respectively (Merrick, 1993). Σ^{54} has three regions (I to III), each of which have a different function. Region I is the site of interaction between the -12 element and the RNAP complex, as well as the site of

activator ATPase binding (Yang et al., 2015). Region II is less well understood, and is highly variable in length, although it is believed to modulate DNA binding and unwinding in many bacterial species (Yang et al., 2015). Highly conserved Region III makes the strongest contacts with core RNAP and the promoter (Yang et al., 2015).

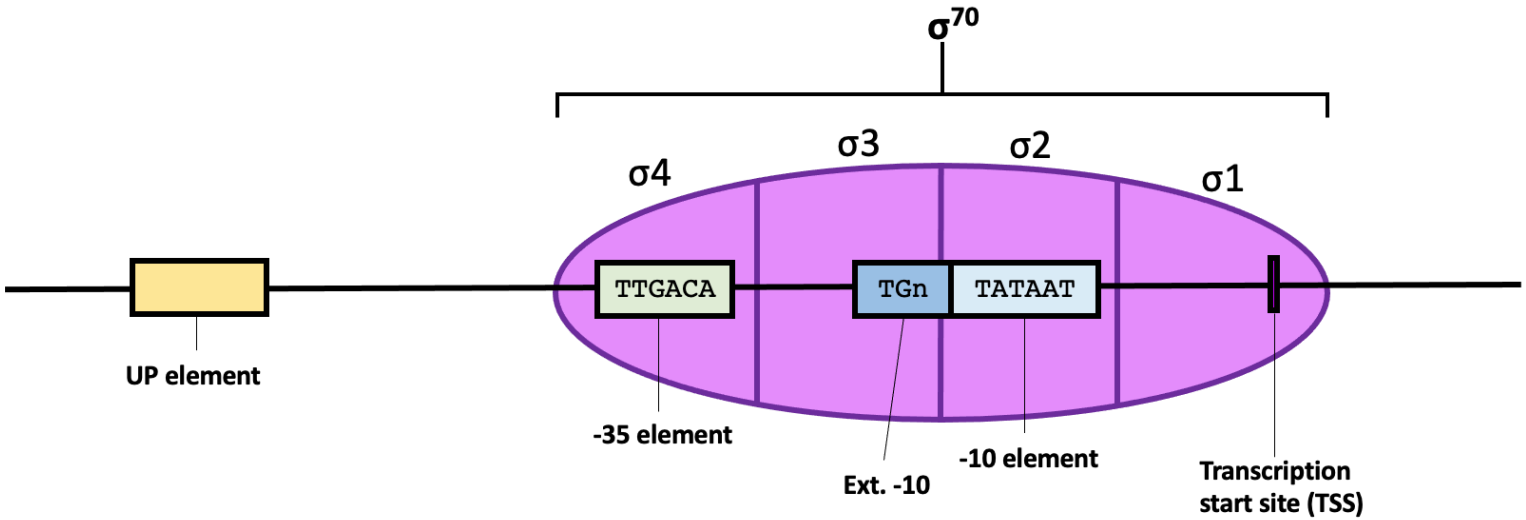

Figure 1.1 – A canonical σ^{70} promoter in *E. coli*. Consensus sequences of the -35 and (extended) -10 elements given. Positioning of σ^{70} domains relative to the promoter shown. *Adapted from Browning and Busby (2008).*

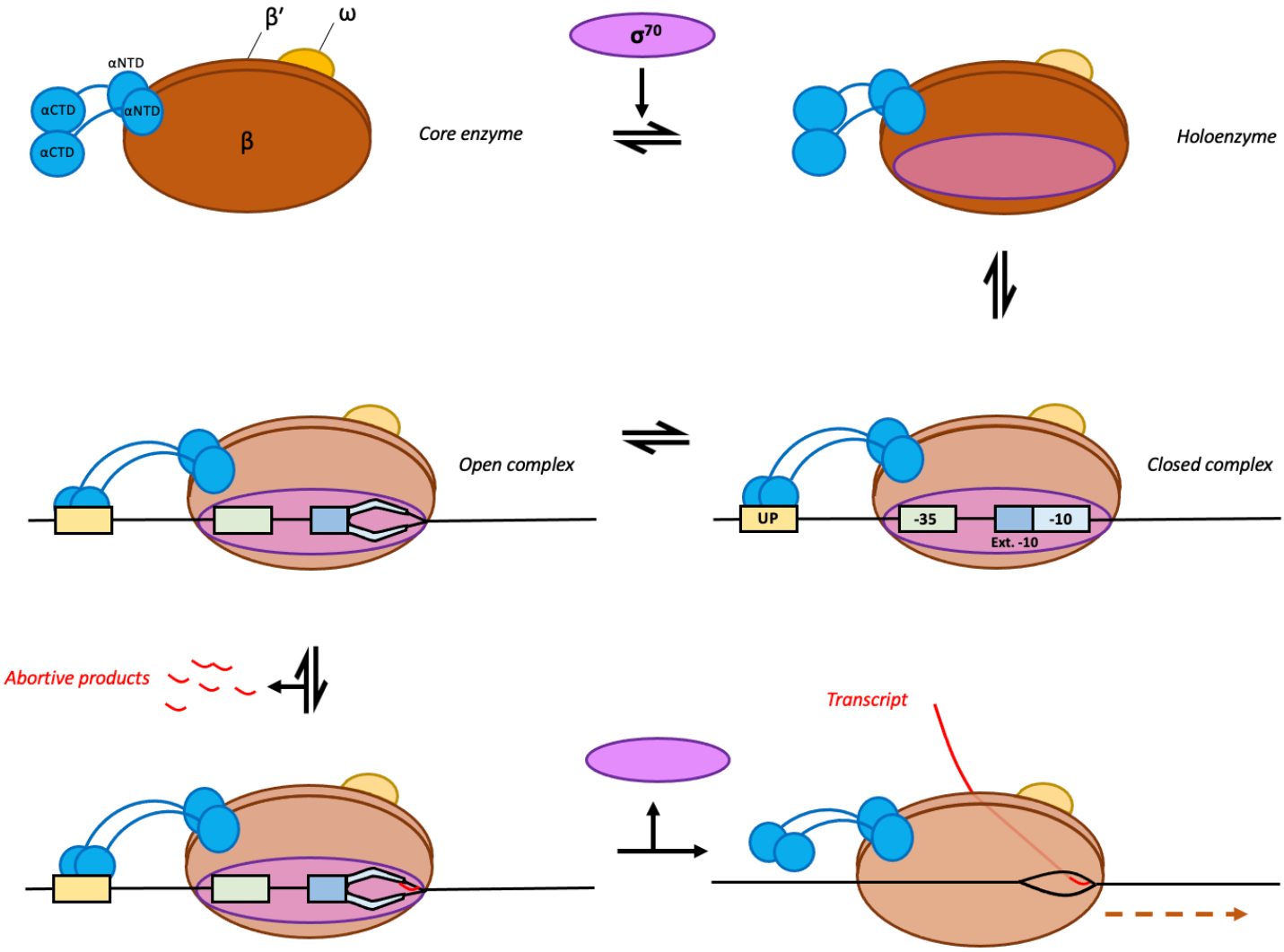

Figure 1.2 – Initiation of transcription by RNA polymerase from a canonical σ^{70} promoter. Core polymerase binds to σ^{70} to form the polymerase holoenzyme. This binds to the promoter to form the 'closed complex'. Unwinding of the DNA helix by polymerase leads to the formation of the 'open complex'. Cycles of abortive initiation occur, resulting in the production of 2-15 bp abortive products until sufficient free energy allows for the elongation complex to form. Σ^{70} dissociates from polymerase and the full-length transcript can be produced. *Adapted from Browning and Busby (2016) and Borukhov and Nudler (2008).*

1.4 Transcription initiation

Prior to DNA binding, core polymerase binds to a sigma factor to form the RNAP holoenzyme (see figure 1.2). At housekeeping promoters, the σ2 domain of σ^{70} contacts the -10 promoter element forming the 'closed complex' (Li and McClure, 1998). Where present, -35 elements stabilise binding by the domain σ4. UP elements are contacted by the α-CTD. The 'open complex' is formed as the two strands of the DNA are separated. This begins at the -11 position and bends the DNA. The two DNA strands are positioned within the RNAP 'clamp' (deHaseth and Helmann, 1995). Three catalytic aspartate residues within the β' subunit of RNAP contact the transcription start site (TSS, +1) of the DNA template strand (Vassylyev et al., 2007). Nucleotides are fed into the catalytic core of RNAP via a funnel in the β' subunit, where (if complementary to the nucleotide of the DNA template strand) they are added to the RNA chain. Upon addition, the DNA/RNA complex moves one base-pair, allowing the next nucleotide to be added (Cheetham and Steitz, 1999). Initially, RNA chains are released prematurely at between 2 and 15 nucleotides in length; this is referred to as 'abortive transcription' and can occur cyclically until RNAP 'escapes' its contacts with the promoter (when there is sufficient free energy) and move along the DNA to produce the full-length transcript (Revyakin et al., 2006). Σ^{54} factors have also been shown produce abortive RNA products, though 'promoter escape' occurs more rapidly (Tintut et al., 1995).

1.5 Transcription factors

Controlling transcription is one way that bacteria respond to environmental change. Transcription factors are proteins that up- or downregulate transcription (see Seshasayee et al., 2011, for a review). Transcription factors can be activators (upregulating transcription) or repressors (downregulating transcription). Importantly, a single transcription factor may act in both capacities depending on the position of its DNA target site relative to the promoter and other sites of transcription factor interaction (Browning and Busby, 2004). A single gene or operon may be controlled by a combination of activators and repressors, allowing a variety of signals to feed into a single pathway. The cAMP receptor protein (CRP, discussed later) is a well-described transcription factor that can regulate transcription in multiple ways (Busby and Ebright, 1997).

1.5.1 Transcription activation

Activators are divided into three classes (see figure 1.3); class I, class II and conformational activators (Lee et al., 2012). Class I activators bind upstream of promoters and increase promoter recognition by RNAP through contacts with the C-terminal domains of the α subunits (Zhou et al., 2014). Class II activators bind near to the -35 element and contact the sigma factor via the σ4 subdomain (Niu et al., 1996). Conformational activators change DNA organisation to allow RNAP binding. Often, this is by twisting DNA to correctly align promoter elements. Not all activators conform to these descriptions; some counteract the activity of repressors or help drive DNA unwinding via ATP-hydrolysis. The latter is required at σ^{54}-dependent promoters (Browning and Busby, 2016).

1.5.2 Repression of transcription

Repressors can also be categorised into three classes (see figure 1.4). Some act by preventing RNAP from binding the promoter (steric hindrance) (Rojo, 1999). Others counteract activators (anti-activation) (Valentin-Hansen et al., 1996). Much like conformational activators, some repressors bend DNA to exclude RNAP from interacting with a promoter (looping) (Rojo, 1999).

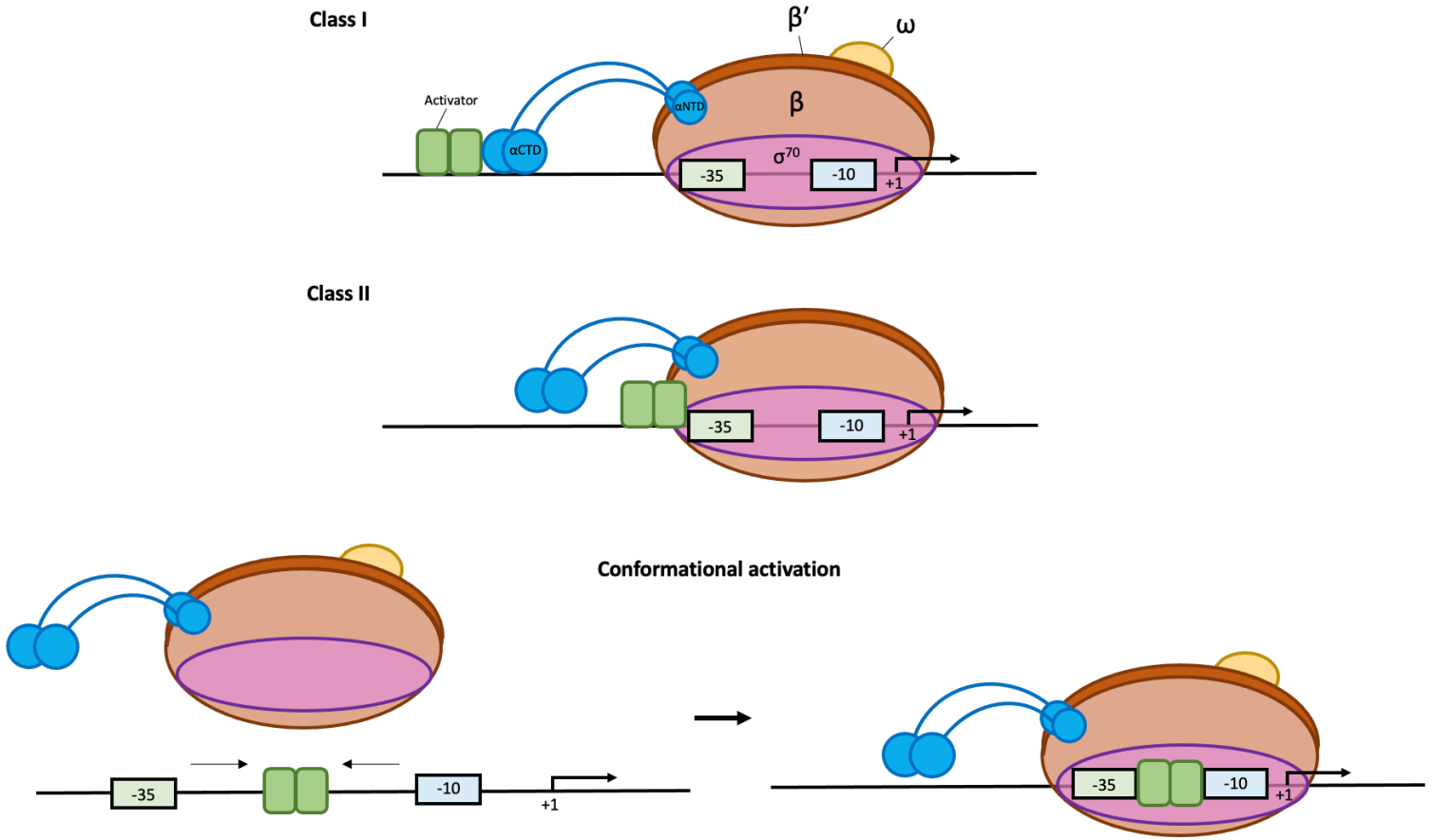

Figure 1.3 – Mechanisms of transcription activation. Class I activators bind upstream of a promoter and recruit polymerase via contacts with the α-subunits, whereas class II activators bind near the -35 element and associate with σ^{70} and αNTD. Conformational activators bind DNA, for example, to re-orientate the -10 and -35 elements and enable σ^{70} binding. *Adapted from Browning and Busby (2004) and Browning and Busby (2016).*

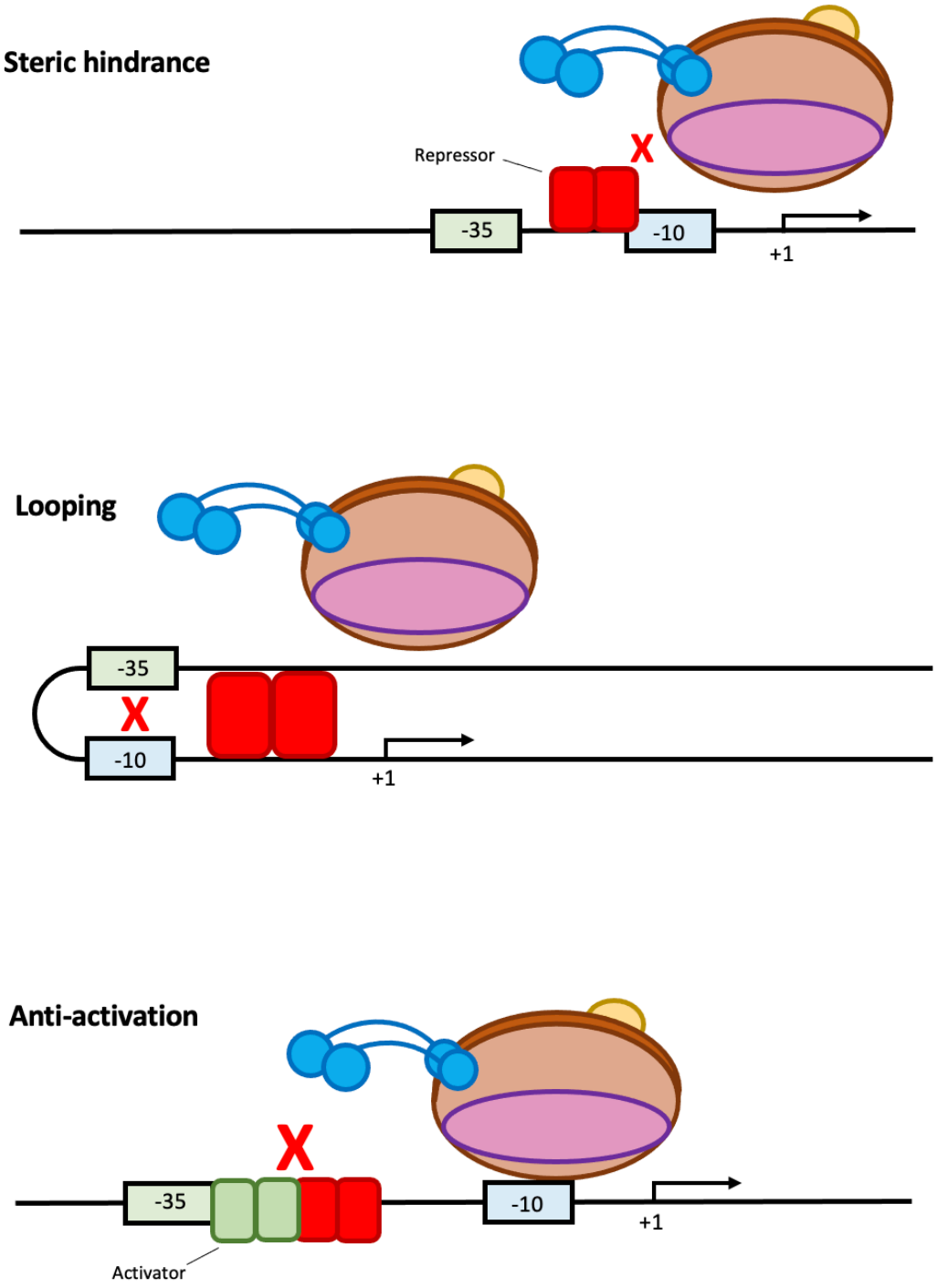

Figure 1.4 – Mechanisms of transcription repression. Repressors can bind to promoter elements and directly inhibit polymerase binding (steric hindrance). Repressors may also act indirectly by re-orientating DNA to 'mask' promoter elements (looping), or by binding to transcription activators and inhibiting their function (anti-activation). *Adapted from Browning and Busby (2004) and Browning and Busby (2016)*.

1.6 CRP and transcription regulation

1.6.1 CRP structure and binding to DNA

CRP is a transcription factor dependent on the second messenger cyclic AMP (cAMP) (Kolb et al., 1993). The structure of CRP is shown in figure 1.5. Two CRP monomers dimerise by interaction of the N-terminal domain. The dimer interacts with DNA via a C-terminal helix-turn-helix motif (Kolb et al., 1993; Busby and Ebright, 1999). Each monomer has three distinct activating regions; protein surfaces that can interact with RNAP. Activating regions (Ars) 1 and 3 comprise residues 156-164 and 52-58 respectively. AR2 consists of residues 19, 21, 96 and 101 (de Crombrugghe et al., 1984; Niu et al., 1996, 1994). CRP dimers bind to a palindromic DNA sequence consensus 5'-TGTGAN_6TCACA-3' (Shimada et al., 2011; Manneh-Roussel et al., 2018). Dimerisation and recognition of this sequence is dependent on cAMP; insertion of cAMP into the ligand binding pocket causes a conformational change in the DNA-binding domain of CRP (de Crombrugghe et al., 1984). Activation of transcription by CRP can occur through multiple mechanisms involving different Ars.

1.6.2 Class I CRP promoters

At class I promoters, CRP binds upstream of the core promoter elements and recruits RNAP through contacts between AR1 on the downstream CRP monomer and residue 287 of α-CTD (Zhou et al., 1993; Savery et al., 1998). The site of CRP binding at class I activated promoters can vary but is always on the same face of the DNA helix as RNAP (Ebright, 1993).

1.6.3 Class II CRP promoters

The CRP binding site at class II promoters is usually located at position -41.5 (Busby and Ebright, 1997). Here, CRP can contact α-CTD via AR1 and four negatively charged residues

(162-165) in the α subunit N-terminal domain (α-NTD) via AR2 (Niu et al., 1996; Savery et al., 1998). Domain 4 of σ^{70} interacts with AR3 (Rhodius and Busby, 2000).

1.6.4 Class III CRP promoters

Class III promoters have multiple CRP sites or a combination of CRP and sites for other transcription factors (Browning and Busby, 2004). For example, CRP and FNR co-activate transcription from the *ansB* promoter in *E. coli*, with binding sites centred around -91.5 and -41.5 respectively (Scott et al., 1995). Regulators at Class III promoters can employ a combination of class I and class II-like interactions with RNAP, as illustrated in figure 1.6 (Busby and Ebright, 1999).

1.6.5 CRP-regulated genes

In *E. coli*, CRP regulates over 180 genes, many of which are involved in the metabolism of alternative carbon sources in the absence of glucose (Kolb et al., 1993; Zheng et al., 2004). A ChIP-seq study in *Vibrio cholerae* identified 119 DNA binding targets for CRP and *E. coli* and *V. cholerae* CRP are 95 % identical (Skorupski and Taylor, 1997b; Manneh-Roussel et al., 2018). In *V. cholerae*, CRP downregulates biofilm formation and virulence gene expression via induction of the high-cell density regulator, HapR (discussed later). Furthermore, CRP is vital for the colonisation of the intestinal tracts of fish and down-regulation of toxin production (Manneh-Roussel et al., 2018; Skorupski and Taylor, 1997b, 1997a).

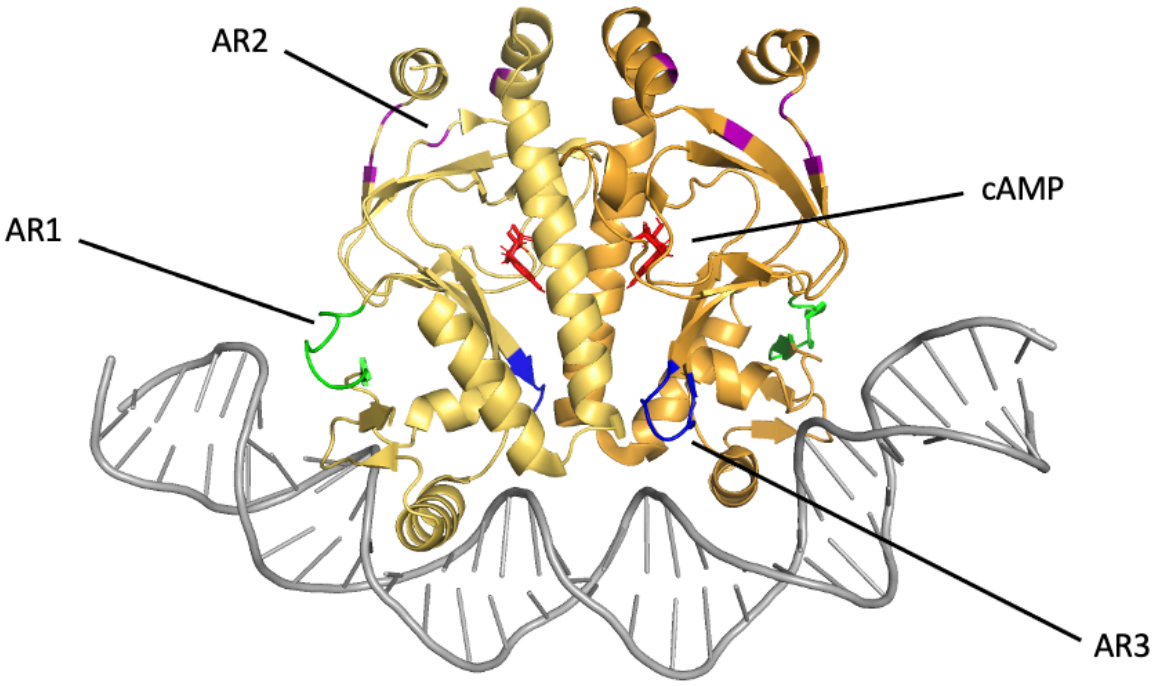

Figure 1.5 – Structure of a CRP/DNA complex. Monomers of the CRP dimer coloured separately in yellow and orange. Molecules of cyclic AMP (cAMP) shown in red. Associated DNA shown in grey. DNA is bound at the major groove via C-terminal α-helices. Activating regions 1, 2 and 3 coloured in purple, blue and green respectively. Image generated using PyMOL. Structure resolved by Parkinson et al., 1996.

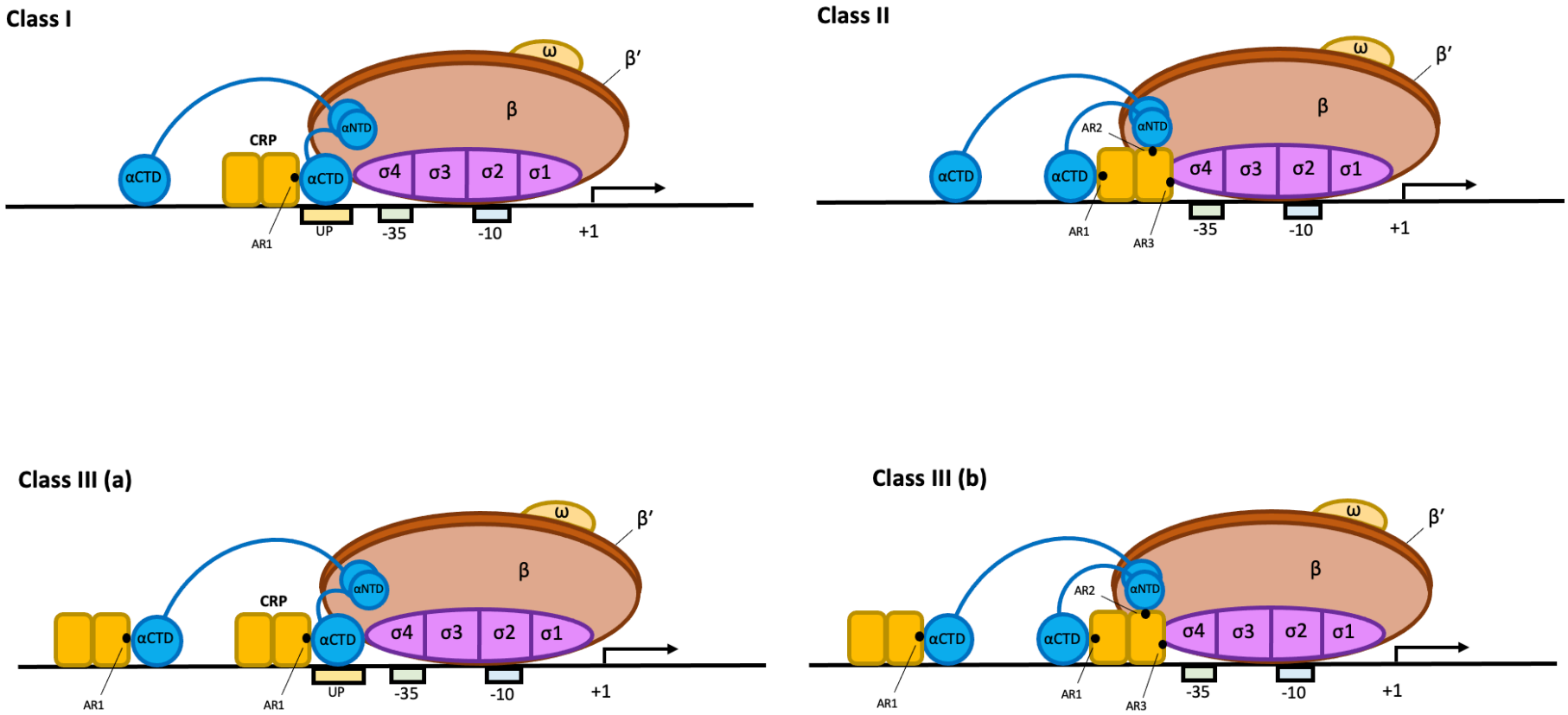

Figure 1.6 – CRP-dependent activation of transcription. Interactions between CRP (yellow), RNA polymerase subunits and promoter DNA. Model of class I and class II activation shown with activating regions of CRP (AR1, AR2 and AR3) indicated where interactions occur. **Class I** activation; AR1 of the downstream CRP interacting with residue 287 of αCTD. **Class II** activation; contacts are made between AR1 of the upstream CRP interacting with residue 287 of αCTD, AR2 and AR3 of the downstream CRP contacts the αNTD and σ4 respectively. Two different examples of class III activation presented. Adapted from Busby and Ebright (1999).

1.7 *Vibrio cholerae* and the Seventh Pandemic

1.7.1 Epidemiology of *V. cholerae*

V. cholerae has spread across human populations in a series of pandemics; the current being the seventh (Ali et al., 2012). The bacterium can be classified by serogroup and biotype. The serogroup is defined by the structure of the O-antigen on the surface lipopolysaccharide (Chatterjee and Chaudhuri, 2003). Infectious cases of *V. cholerae* are of either the O1 or O139 serogroup. The former is responsible for the vast majority of *V. cholerae* infections (Ali et al., 2012; Chin et al., 2011). O1 serotyped *V. cholerae* can be further classified into 'Inaba', 'Ogawa' or 'Hikojima' subtypes based on the constituent elements of the O1 antigen (Stroeher et al., 1992). O1 is yet further identified by biotype, either Classical or El Tor, based on a few differentiating properties such as haemolysin production (Stroeher et al., 1992). The vast majority of the **s**eventh **p**andemic of cholera is caused by the O1 serogroup and **E**l **T**or biotype of *V. cholerae* – and henceforth will be referred to as **7PET** (Chin et al., 2011). By contrast, the previous six pandemics are believed to be predominantly of the Classical biotype. 7PET cholera was first identified in the Bay of Bengal around 1910 and remains endemic there (Kaper et al., 1995). *V. cholerae* spreads prolifically in areas of poor sanitation or where local infrastructure (such as water and sewage lines) is severely damaged; often due to conflict or natural disasters (Ali et al., 2012). One of the most recent large-scale outbreaks of *V. cholerae* in Yemen has recorded over 1.2 million cases in two years (WHO, 2020).

Previously, *V. cholerae* was thought to be spread around the globe by environmental events such as El Niño (Colwell, 1996). However, recent work has suggested that humans are more likely responsible for the spread of epidemic *V. cholerae* (Weill et al., 2017). Large-scale

genomic studies have shown that global dissemination of 7PET *V. cholerae* occurred in 'waves of transmission' (Mutreja et al., 2011). These waves originate from the endemic regions around the Bay of Bengal, and predominantly target Africa and South Asia initially, with some waves subsequently spreading onwards to South America (Mutreja et al., 2011).

1.7.2 The life cycle of *V. cholerae*

1.7.2.1 The aquatic environment and chitin utilisation

Key to the survival and transmission of *V. cholerae* is adaptation to two ecological niches: brackish waters (the aqueous environment) and the intestinal tracts of humans (the host environment) (Alam et al., 2007). *V. cholerae* can also colonise the intestines of several fish species (Halpern and Izhaki, 2017). The infection cycle of *V. cholerae* is illustrated in figure 1.7. In the aqueous environment, *V. cholerae* forms biofilms on chitin, a polymer of N-acetylglucosamine (GlcNAc), found in the exoskeletons of arthropods (Alam et al., 2006). Chitin can be utilised by *V. cholerae* as a carbon and nitrogen source (Meibom et al., 2004; Alam et al., 2006). This metabolism is governed by the regulator ChiS, which controls the expression of the *chb* operon (Klancher et al., 2020b; Yamamoto et al., 2014; Li and Roseman, 2004). Two enzymes, ChiA-1 and ChiA-2 are exported into the extracellular environment and break down chitin (Li and Roseman, 2004). Growth on chitin also induces the natural competence cascade, allowing the uptake of exogenous DNA from the environment (Meibom et al., 2005). ChiS also induces expression of TfoS, a regulator which promotes expression of another protein, TfoX (Dalia et al., 2014). In tandem with the quorum-sensing master regulator HapR, TfoX activates expression of QstR, which in turn, switches on competence-related genes (Scrudato and Blokesch, 2013). CRP also regulates genes which control nutrient acquisition and competence on chitin (Blokesch, 2012).

1.7.2.2 Survival in the host

V. cholerae is ingested by consumption of contaminated food or water (Alam et al., 2007). In the host stomach, pH is low and so *V. cholerae* induces an acid tolerance response. This involves increased expression of the *cadAB* operon mediated by the transcription factor, CadC (Dell et al., 1994). CadA converts lysine to cadaverine, utilising protons and thus raising the intracellular pH. Cadaverine is then exported by CadB (Merrell and Camilli, 1999; Sabo et al., 1974). In the intestinal lumen of host organisms, bile and associated antimicrobial peptides (AMPs) act to protect the intestinal epithelium by disrupting cell walls of invading bacteria (Conner et al., 2016). *V. cholerae* responds by modifying lipopolysaccharides (LPS) on its cell surface, for example, via acylation by MsbB (Matson et al., 2010). Altered expression of porins, OmpT and OmpU, and induction of the efflux pump VexAB, is also important (Wibbenmeyer et al., 2002; Bina et al., 2006). To reach intestinal epithelial cells, *V. cholerae* first adheres to the mucosal surface using the GlcNAc binding protein, GbpA (Zampini et al., 2005). The haemagglutinin protease, HapA, is then upregulated by HapR to degrade the mucous layer. This allows *V. cholerae* to migrate through the mucosa (Jobling and Holmes, 1997; Silva et al., 2003).

1.7.2.3 Virulence gene expression

Virulence genes are ultimately required for *V. cholerae* to colonise the host. Components of bile, a fluid produced in the host liver, inhibit the expression of virulence genes such as *toxT* (Lowden et al., 2010). As *V. cholerae* moves towards the epithelium, increasing concentrations of bicarbonate counter *toxT* inhibition (Abuaita and Withey, 2009). ToxT controls the expression of multiple virulence factors, including cholera toxin (CTX) and the toxin co-regulated pilus (TCP). ToxT, regulates TCP expression indirectly and via another

regulator, TcpPH (Hulbert and Taylor, 2002; Häse and Mekalanos, 1998). TCP is a type IV pilus, which promotes the formation of microcolonies and so attachment to the epithelium (Helene Thelin and Taylor, 1996; Herrington et al., 1988). Upon attachment, *V. cholerae* induces biofilm formation and upregulates virulence gene expression via ToxT (Sengupta et al., 2016).

CTX is comprised of a single subunit A (made up of the two domains, A_1 and A_2) surrounded by five B subunits (Dallas and Falkow, 1980). CTX binds to the host monosialoganglioside GM1 receptor on the surface of epithelial cells via a B subunit (Kaper et al., 1995). Cleavage of the A_1 and A_2 subunits, by proteases including HapA, releases the A_1 subunit (Lencer et al., 1997; Booth et al., 1984). A_1 activity causes a G-protein to perpetually activate adenylate cyclase, an enzyme which converts ATP to cAMP (Spangler, 1992). Elevated cAMP levels cause chloride ions to leak from host cells. This creates an osmotic gradient through which water flows into the intestinal lumen. This is responsible for the 'rice water' stools in cholera patients (Chaudhuri and Chatterjee, 2009; Kaper et al., 1995).

1.7.2.4 Host dissemination

Dissemination from the host is mediated by the sigma factor, RpoS, which upregulates HapR. Together, HapR and RpoS control the expression of motility and chemotaxis genes which drive the detachment of *V. cholerae* from the intestinal epithelium (Nielsen et al., 2006). Transition between the toxin-producing and mucosal escape states was shown by one study to occur in only a subset of the *V. cholerae* population. The study proposed that a bistable switch gives rise to two populations: one which continues to produce TCP and CTX, and one which disseminates from the host (Nielsen et al., 2010). Bistable switches have

been described in several species (see Dubnau and Losick, 2006 for a review) and allow individuals of a genetically identical bacterial population to behave differently in the same environment (Ferrell, 2002). Small changes in the concentration of a signal are amplified by expression feedback loops (either positive or double-negative). Therefore, a cellular response controlled by a bistable switch can exist only in an 'OFF' or 'ON' state. In *V. cholerae*, TCP expression is coupled with expression of ToxT, which further upregulates the *tcp* genes, resulting in a positive feedback loop that switches the cells to a virulent state (Nielsen et al., 2010).

1.7.2.5 Biofilm formation

The formation of biofilms is crucial for many stages of the *V. cholerae* infection cycle (figure 1.7). Biofilms provide protection from stressors, including nutrient depravation, temperature, acidity and antimicrobial compounds (Flemming and Wingender, 2010). Biofilm-associated *V. cholerae* cells also display increased infectivity in host organisms compared to planktonic cells (Faruque et al., 2006). *V. cholerae* biofilms are comprised primarily of an exopolysaccharide, VPS, and the matrix proteins Bap1, RbmA and RbmC (Silva and Benitez, 2016). Exopolysaccharides provide a three-dimensional structure in which cells aggregate (summarised by Flemming and Wingender, 2010). The three matrix proteins promote adhesion between cells and to surfaces (Absalon et al., 2011; Fong and Yildiz, 2007; Fong et al., 2006). The major regulators of biofilms in *V. cholerae* are VpsR and VpsT; transcriptional activators of biofilm-related genes (Zamorano-Sánchez et al., 2015). Biofilm formation is also regulated positively by factors such as c-di-GMP and AphA, and negatively regulated by CRP and HapR (Fong and Yildiz, 2008; Yang et al., 2010; Lin et al., 2007).

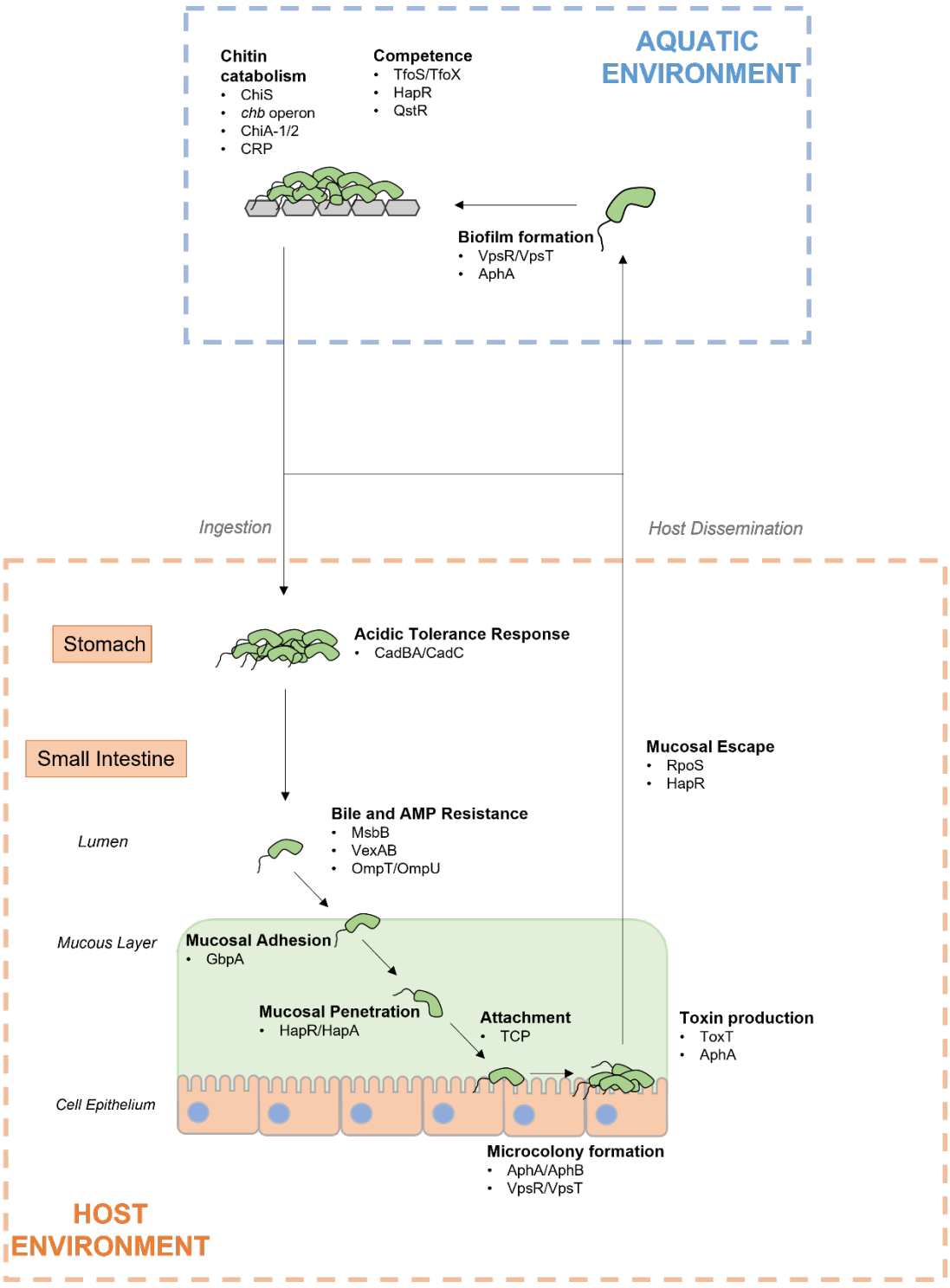

Figure 1.7 – The life cycle of pathogenic *V. cholerae*. V. cholerae, shown as individual cells or as biofilms, manages the transition between host and aquatic or host and host environments through differential regulation of genes. Stages of infection are labelled along with transcription factors important for each stage (details discussed in the text). Based on Conner et al., 2016 and Almagro-Moreno et al., 2015.

1.7.3 Evolution of *V. cholerae*

Horizontal gene transfer by bacteriophages is a driver of the evolution of *V. cholerae* (Waldor and Mekalanos, 1996; Karaolis et al., 1999). Toxigenic *V. cholerae* result from integration of transposable genetic elements (termed pathogenicity islands) into the *Vibrio* genome (Pang et al., 2007; Karaolis et al., 1998). Vibrio pathogenicity islands VPI-1 and VPI-2 are found in classical and El Tor strains (Heidelberg et al., 2000; Karaolis et al., 1998; Jermyn and Boyd, 2002). VPI-1 includes genes encoding CTX (*ctxAB*) and TCP (Karaolis et al., 1998). Acquisition of these genes was sequential, with bacteriophages CTXϕ and VPIϕ identified as the source of *ctxAB* and *tcp* respectively (Waldor and Mekalanos, 1996; Karaolis et al., 1999). 7PET strains contain two further pathogenicity islands, VSP-1 and VSP-2 (Dziejman et al., 2002). The associated genes are less well characterised but have been linked to increased survivability in host and aquatic environments. Genes on VSP-1 also modulate chemotaxis and colonisation of the host (Davies et al., 2012). The VPS-2 encoded protein, VerA, is involved in the response to zinc starvation (Murphy et al., 2021).

Horizontal gene transfer can also occur due to uptake of DNA by natural competence in *V. cholerae* (Meibom et al., 2005). This process is induced by growth on chitin and DNA uptake is driven by the Chitin regulated pilus (ChiRP) (Meibom et al., 2004). Studies have shown that natural competence allows *V. cholerae* to alter its serogroup by incorporating O-antigen genes from a donor (Blokesch and Schoolnik, 2007).

Accumulation of single-nucleotide polymorphisms in the *V. cholerae* genome also has profound effects on gene expression. The N16961 strain, for example, contains a frameshift mutation which truncates HapR (Heidelberg et al., 2000). A recent whole-genome

sequencing study analysing over 1,000 clinical 7PET isolates identified a wide array of SNPs across the genome of *V. cholerae* (Weill et al., 2017). Many SNPs were non-synonymous (i.e., alter the encoded amino acid sequence). Genes with a high ratio of non-synonymous to synonymous mutations were identified as transcription regulatory factors or cell surface proteins with functions in host colonisation and disease. Two such factors, HapR and LuxO (high ratios of non-synonymous SNPs), regulate gene expression as part of the quorum-sensing cascade (Lilley and Bassler, 2000; Jobling and Holmes, 1997; Ball et al., 2017).

1.8 Quorum-Sensing

1.8.1 Quorum-sensing in bacteria

Quorum-sensing is a mechanism by which bacteria respond to signals from neighbouring bacteria (reviewed in Miller and Bassler, 2001). Small molecules, known as auto-inducers (AIs), are continually synthesised and secreted into the environment by bacterial cells. AIs bind to receptor proteins on the bacterial cell surface or, less often, in the cytoplasm (Keller and Surette, 2006). This leads to changes in gene expression. As bacterial population density increases, AI levels in the local environment grow. Receptors that detect the AIs modulate the induction of transcription factors. Genes regulated by this process include those involved in controlling biofilm formation and pathogenesis (Keller and Surette, 2006; Miller and Bassler, 2001) .

1.8.2 The Quorum Sensing Cascade in *V. cholerae*

Quorum-sensing in *V. cholerae* (see figure 1.8) governs the expression of many genes involved in virulence, biofilm formation and dissemination from host organisms (Miller and Bassler, 2001; Margolin, 2005; Zhu et al., 2002). Key components of the quorum-sensing cascade are descrbed below.

1.8.2.1 Quorum-sensing signals and receptors

V. cholerae produces the cholera auto-inducer 1 (CAI-1) and auto-inducer 2 (AI-2). CAI-1 production is highly prevalent amongst *Vibrio* spp. and so allows regulation of genes in response to other *Vibrios* (Ng et al., 2011). By contrast, AI-2 is common to many bacteria and is a more general signal of bacterial cell density (Federle and Bassler, 2003). In *V. cholerae*, CAI-1 and AI-2 are both required for lifestyle switching, but CAI-1 is required in

lower concentrations than AI-2 (Bridges and Bassler, 2019). In a mixed-species environment, this would allow *V. cholerae* to activate genes promoting dispersal from biofilms if two criteria are met; i) the local population is at high cell density (detection of AI-2) and ii) there are enough *vibrio* spp. cells within the population (detection of CAI-1) (Bridges and Bassler, 2019). CAI-1 and AI-2 are detected by the transmembrane receptors, CqsS and LuxPQ, respectively. At low cell density, when their corresponding auto-inducers are at low concentrations, CqsS and LuxPQ phosphorylate LuxU (Bassler et al., 1994).

Phosphorylation of LuxU is also controlled by environmental signals other than those involved in quorum-sensing. For example, in *V. cholerae*, a third transmembrane receptor, CqsR, is bound by ethanolamine; a common carbon and nitrogen source for many bacteria (Watve et al., 2020). Interestingly, ethanolamine is abundant in the large intestine but is not metabolised by *V. cholerae.* Hence, CqsR can respond to a particular environment. It has been suggested that CqsR may respond to multiple ligands (Watve et al., 2020).

Nitric oxide (NO) is produced by many host organisms as an antimicrobial in response to infection (Janoff et al., 1997). While some bacteria can synthesise NO, *V. cholerae* does not encode the required synthase enzyme (Crane et al., 2010; Hossain et al., 2018).The cytosolic kinase, VpsS, phosphorylates LuxU in the absence of NO (Jung et al., 2015; Hossain et al., 2018). VpsV senses NO and inhibits the activity of VpsS. Taken together, this suggests that the VpsV/VpsS-mediated response acts as a sensor of host cell activity (Hossain et al., 2018).

Different *Vibrio* spp. have unique quorum-sensing signals and receptors. *Vibrio harveyi*, for example, uniquely encodes a regulator, LuxN, which is controlled by the ligand, HAI-1, which

is produced by LuxM (Bassler et al., 1993). Similarly, regulation of LuxU by the receptor, CqsR is found in *V. cholerae* but not in *V. harveyi.* Any of these sensors alone is sufficient to activate the LuxU-mediated pathway (Jung et al., 2015).

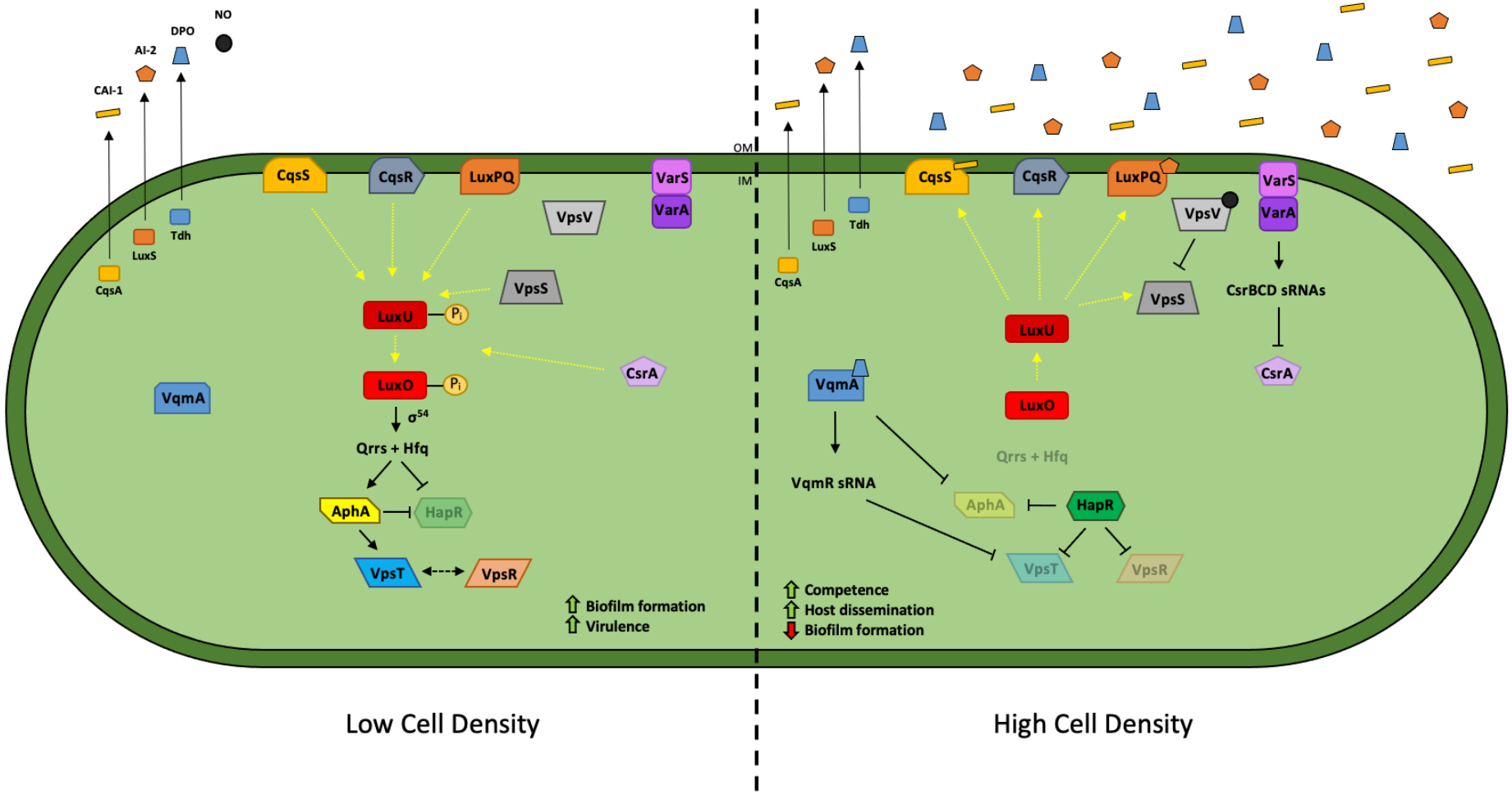

Figure 1.8 – The quorum-sensing regulatory cascade in *V. cholerae*. Yellow arrows indicate the direction of phosphorylation. Black arrows indicate activation/synthesis and blunt arrows indicate repression. As cell density increases, auto-inducer concentrations in the environment increase. Binding of these auto-inducers to their corresponding receptors results in the transition to high cell density-type behaviours, including the activation of competence and repression of biofilm formation. Nitric oxide concentrations also affect LuxU phosphorylation. *Adapted from* Eickhoff and Bassler, 2018. *CAI-1 = Cholera Auto-inducer 1, AI-1 = Auto-inducer 1, AI2 = Auto-inducer 2, DPO = 3,5-dimethylpyrazin-2-ol, NO = Nitric oxide.*

1.8.2.2 LuxU and LuxO

Once phosphorylated, LuxU phosphorylates, LuxO (Freeman and Bassler, 1999). LuxO is one of a family of proteins, known as bacterial enhancer binding proteins (bEBPs), that are activators of σ^{54}-dependent transcription (Bush and Dixon, 2012). bEBPs are AAA proteins (ATPases associated with various cellular activities), which form six-membered rings that bind activator sequences, which causes promoter DNA looping. This looping (often mediated by factors such as IHF) allows bEBPs to bind σ^{54} (see figure 1.9) (Erzberger and Berger, 2006; Joly et al., 2012; Bush and Dixon, 2012). The structure of LuxO (figure 1.10) is consistent with that of group I bEBPs, with receiver (or R) domains facing outward and catalytic ATPase (or C) domains in the centre (Boyaci et al., 2016). In an unphosphorylated state ATPase activity is inhibited by the R domain (Freeman and Bassler, 1999). Unlike other known group I bEBPs, the hexameric ring of LuxO is pre-assembled in an inactive state prior to phosphorylation which might allow more rapid activation and repression of transcription (Boyaci et al., 2016). Phosphorylation of LuxO by LuxU occurs at a conserved aspartate residue, which de-represses ATPase activity and facilitates ATP-dependent DNA unwinding (Boyaci et al., 2016). When phosphorylated, LuxO acts in conjunction with Hfq to activate the four quorum-regulatory RNAs (Qrrs) (Vincent et al., 2012).

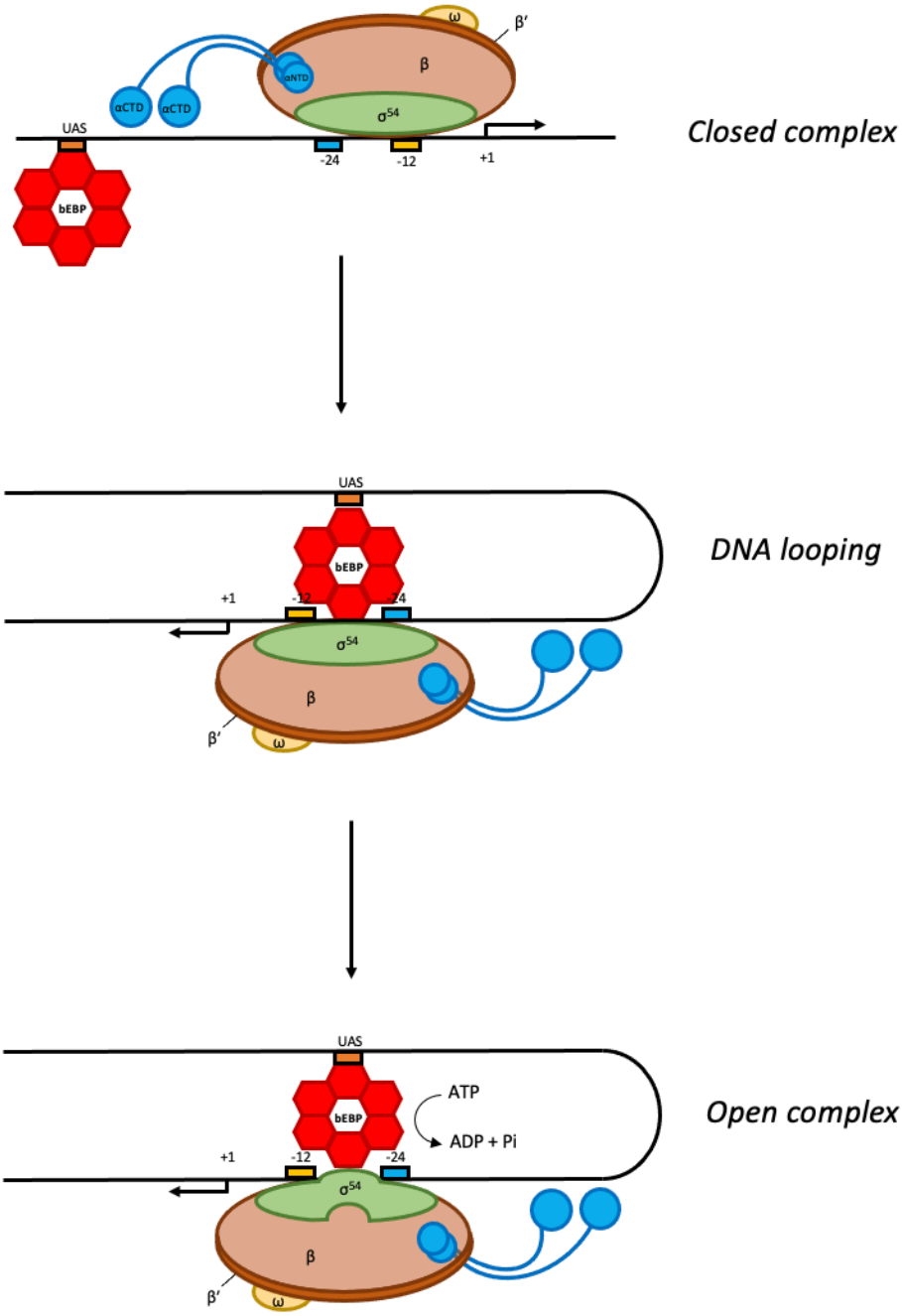

Figure 1.9 – Transcription initiation by bEBPs. RNA polymerase holoenzyme binds to σ^{54}-dependent promoters at -12 and -24 consensus sites. A bEBP binds to an upstream activator sequence (UAS) and cause DNA looping. ATP hydrolysis by bEBP results in conformational changes which unwind the DNA and form the open complex. *Based on Bush and Dixon, 2012.*

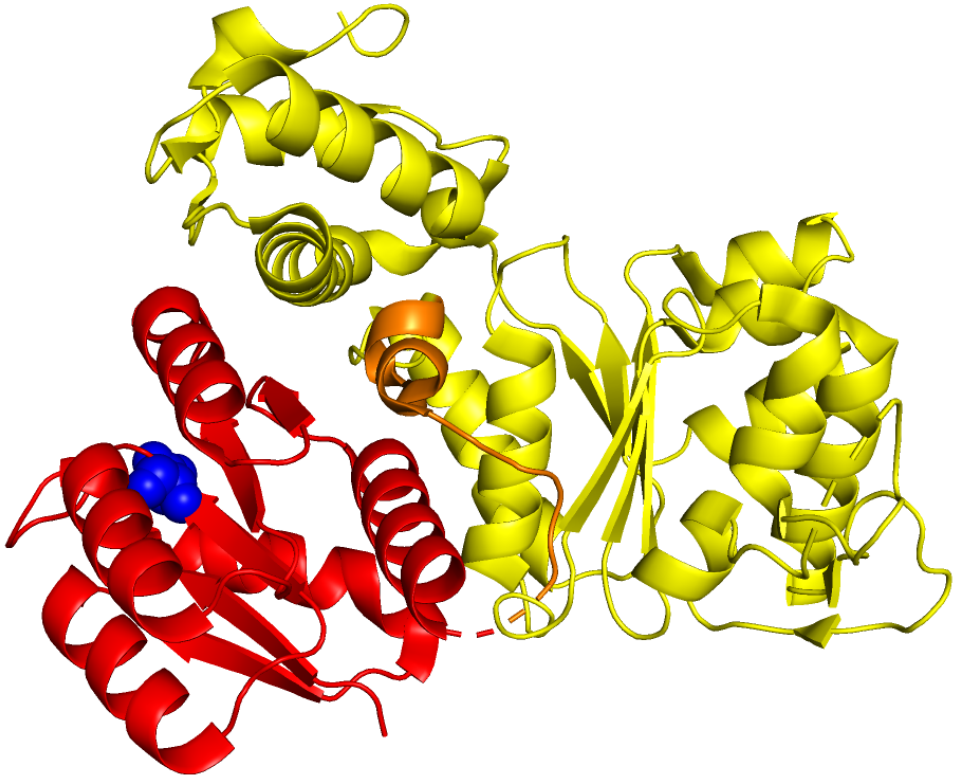

Figure 1.10 – Crystal structure of a LuxO monomer (*V. angustum*). Receiver I domain, ATPaI(C) domain and R-C linker coloured red, yellow, and orange respectively. Conserved asparate residue which is phosphorylated by LuxU is shown in blue. Monomers form a hexameric ring structure, which is inactive in the unphosphorylated state. Image produced in Pymol. Crystal structure resolved in *Vibrio angustum* by Boyaci et al. (2016).

1.8.2.3 The quorum-regulatory RNAs

The four small quorum-regulatory RNAs, Qrr1-4 (see figure 1.11), all contain a conserved sequence of 33 nucleotides for binding the *hapR* and *vca0939* mRNAs (Tu and Bassler, 2007). Qrr binding also represses transcription of the *luxO* gene and upregulates transcription of *aphA* (Tu and Bassler, 2007). Repression of *hapR* and activation of *vca0939* by Qrrs is redundant; studies have shown that, in Qrr triple deletion mutants, a 'feedback-loop' compensates for there being fewer Qrrs (Lenz et al., 2004; Svenningsen et al., 2009; Faner and Feig, 2013). Feedback is mediated by HapR, which up-regulates Qrr expression, though the mechanism is not understood (Svenningsen et al., 2009). In *Vibrio harveyi*, Qrrs are not functionally redundant as In *V. cholerae* (Tu and Bassler, 2007). Instead, *V. harveyi* is thought to have other co-factors to help finely modulate Qrr expression. Furthermore, many *Vibrio* spp., including *V. harveyi* encode a fifth Qrr, absent in *V. cholerae*, the function of which is unknown (Tu and Bassler, 2007).

1.8.2.4 AphA

AphA sits at the end of the quorum-sensing cascade and is the master transcriptional regulator of genes required at low cell density. Hence, AphA promotes so-called 'individual behaviours' in *V. cholerae* (Rutherford et al., 2011). For instance, AphA is an activator of the toxin coregulated pilus (TCP) regulators, TcpP and TcpH (Yang et al., 2010). Interaction with the promoters of *tcpP* and *tcpH* requires a co-activator, AphB. AphA also represses the high cell density regulator, HapR, and downregulates natural competence by directly repressing expression of TfoX (Papenfort et al., 2015; Haycocks et al., 2019). In *Vibrio harveyi*, AphA has been shown to modulate expression of qrrs 2, 3 and 4 (Tu and Bassler, 2007; van Kessel et al., 2013a).

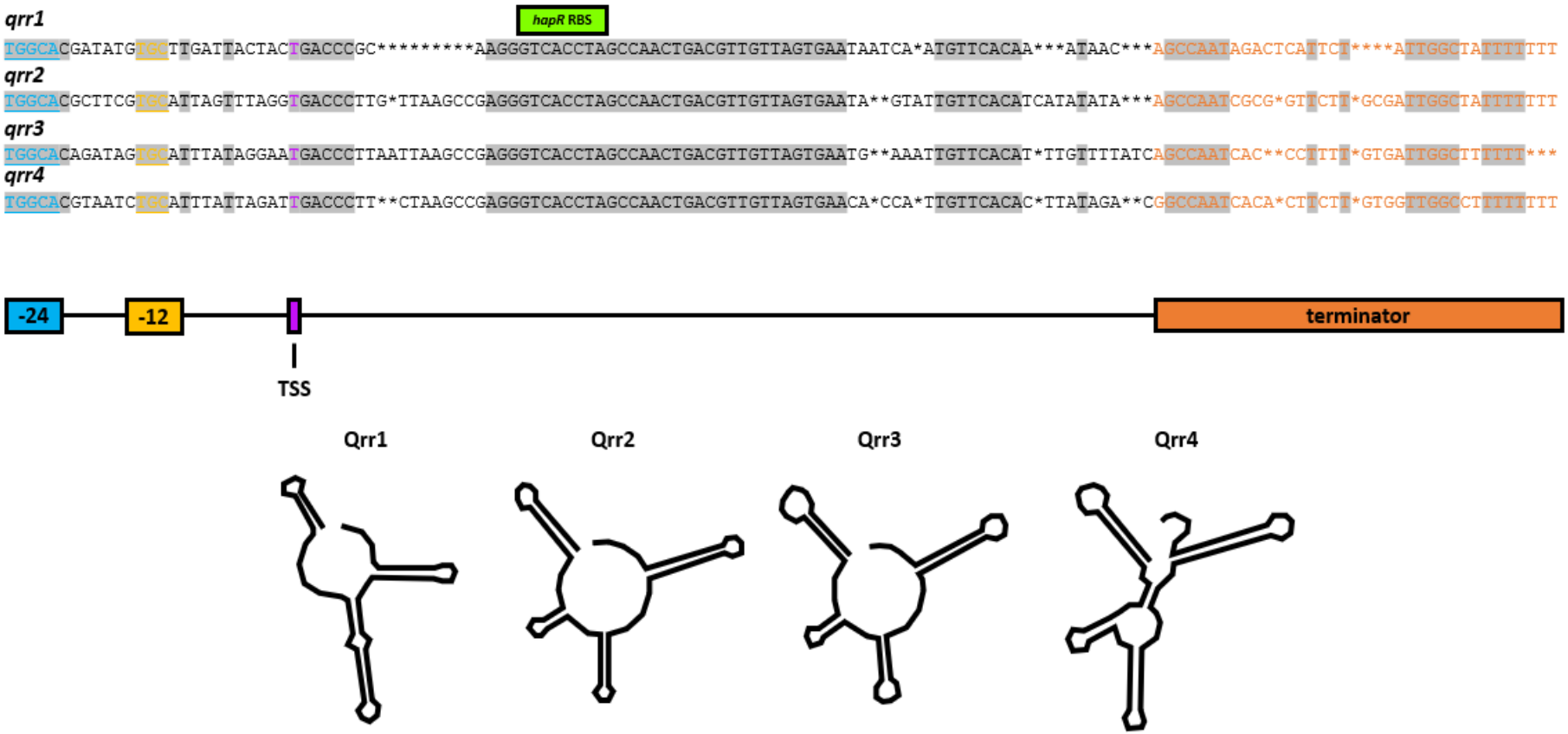

Figure 1.11 – Quorum-regulatory RNA sequences in *V. cholerae*. *-24*, *-12* and transcription start sites indicated in blue, orange and purple respectively. Sequence homologous to the ribosome binding site (RBS) of *hapR* is highlighted in green. Nucleotides conserved across all four Qrrs highlighted in grey. *Adapted from Tu and Bassler, 2007*.

1.8.3 HapR

HapR also sits at the end of the quorum-sensing cascade and is the master regulator at high population density. The factor was first identified as a regulator of haemagglutinin protease (Hap), which activates the A subunit of the cholera toxin (CTX) (Jobling and Holmes, 1997). HapR is a TetR family transcription factor homologous to LuxR in *V. harveyi*, SmcR in *V. vulnificus*, and OpaR in *V. parahaemolyticus* (de Silva et al., 2007). TetR family regulators in non-*Vibrio* species generally control the expression of one or two genes (Cuthbertson and Nodwell, 2013). HapR and homologues in other *Vibrios*, however, regulate hundreds of genes (Ball et al., 2017).

1.8.3.1 Structure and DNA binding of HapR

The structure of HapR (see figure 1.12) epharoseonsation mediated by helical motifs of the C-terminal domain (de Silva et al., 2007). It has been speculated that a small channel within this domain is bound by a ligand which subsequently alters HapR DNA-binding or transcription regulation. However, this ligand has yet to be identified. The N-terminal domain has a helix-turn-helix motif that binds DNA (de Silva et al., 2007). There is no structure of a HapR/DNA complex. However, one study has resolved the DNA-bound structure of the HapR homologue in *Staphylococcus aureus*, QacR (Schumacher et al., 2002).

The consensus DNA-binding sequence of HapR is unresolved. Studies of the HapR homologue LuxR in *V. harveyi* using chromatin immunoprecipitation and DNA sequencing (ChIP-seq) provide some insight; LuxR-bound promoters have a palindromic sequence of approximately 20 bp (van Kessel et al., 2013b; Zhang et al., 2021). Different consensus sequences are observed when comparing LuxR-activated and LuxR-repressed promoters

(van Kessel et al., 2013b; Zhang et al., 2021). Similarly, it has also been suggested that HapR may bind two distinct DNA motifs (Tsou et al., 2009). Further studies have shown that HapR and LuxR bind to DNA near the -10 and -35 elements of promoters and interact with both the N- and C-terminal domains of the RNAP α-subunits (Ball and van Kessel, 2019). The number of LuxR dimers bound at a single promoter can vary, with as many as eight identified binding sites at the *luxCDABE* promoter (Chaparian et al., 2016).

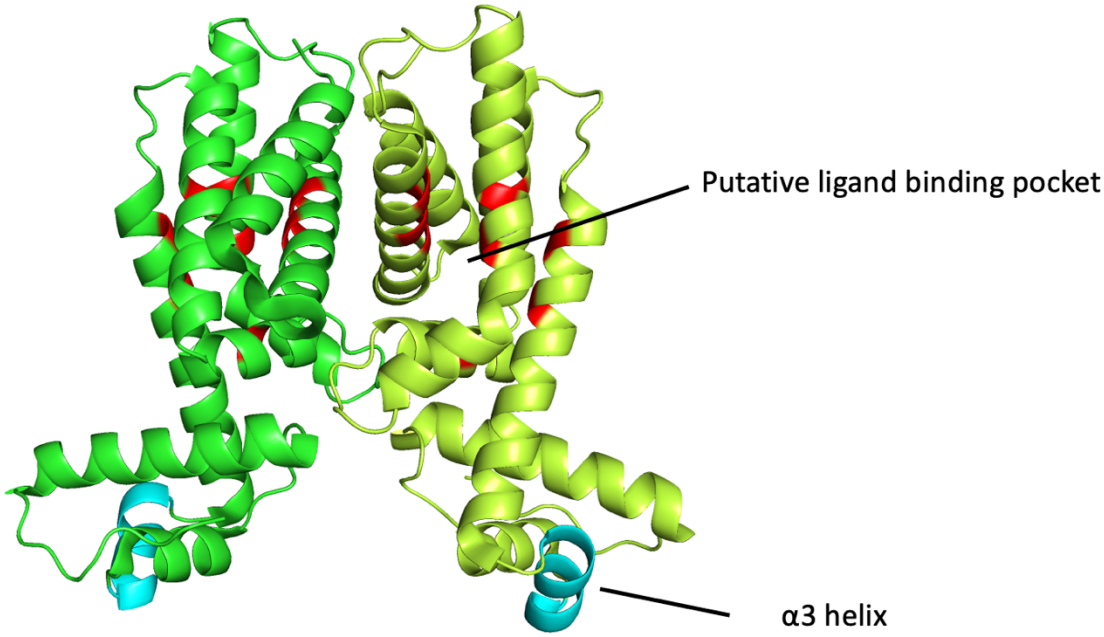

Figure 1.12 – Crystal structure of a *V. cholerae* HapR dimer. Monomers coloured separately (light and dark green). Helix associated with binding to the major groove of DNA highlighted in cyan. Residues forming a small putative ligand binding pocket highlighted in red. Crystal structure resolved by de Silva et al., 2007. Image produced in Pymol.

1.8.3.2 *Gene regulation by HapR*

HapR is thought to regulate around 100 genes in *V. cholerae*; approximately half of these genes are upregulated, and half are downregulated by HapR. (Nielsen et al., 2006). Regulation by HapR leads to *V. cholerae* exhibiting so-called 'group behaviours', such as the repression of biofilm formation and virulence gene expression (Rutherford et al., 2011). Furthermore, HapR, along with RpoS, promotes dissemination of *V. cholerae* from host organisms (mucosal escape) (Jobling and Holmes, 1997). HapR also induces the natural competence cascade by activating QstR expression (Scrudato and Blokesch, 2013; Meibom et al., 2005). In a recent ChIP and RNA-seq study, LuxR and histone-like nucleoid structuring protein (H-NS) were shown to co-regulate 124 genes in *V. harveyi* (Chaparian et al., 2020). LuxR was proposed to de-repress genes inhibited by H-NS by competitive binding at promoters. H-NS regulates a similar number of genes in *V. cholerae*, and many of these genes are related to virulence, motility and the response to stress factors (Wang et al., 2015). Therefore, it is reasonable to assume that a similar mechanism of activation by HapR occurs in *V. cholerae*. Alternatively, it has been shown that HapR and H-NS can co-operatively repress gene expression (Ayala et al., 2018).

1.8.4 The VarS/VarA two component system

A separate signalling cascade, referred to as the VarSA/CsrABCD system, influences the activity of LuxO (Lenz et al., 2005). The sensor kinase VarS responds to a currently unknown external signal by phosphorylating VarA. Phosphorylated VarA directly upregulates transcription of three sRNAs, CsrB, CsrC and CsrD. These sRNAs bind to a regulatory protein, CsrA, preventing it from binding to other mRNAs (Liu et al., 1997; Lenz et al., 2005). When uninhibited, CsrA acts to downregulate the activity of LuxO; the exact mechanism of this is

currently unknown but it is believed to involve some intermediate, as the *luxO* promoter does not contain a consensus CsrA DNA binding site (Lenz et al., 2005).

1.8.5 VqmA

A distinct quorum-sensing pathway, mediated by the cytosolic receptor, VqmA, exists in *V. cholerae* (Wang et al., 2011a). The VqmA-binding ligand, 3,5-dimethylpyrazin-2-ol (DPO), stimulates the production of the small RNA VqmR. VqmR is regulatory and represses *aphA* and *vpsT* (Herzog et al., 2019; Papenfort et al., 2015).

1.9 Overview of this study

Whole genome sequencing studies have revealed that the *hapR* and *luxO* genes are highly variable amongst clinical isolates (Weill et al., 2017). Given the critical role that HapR and LuxO have in the response of *V. cholerae* to the environment, this high degree of variability is intriguing. Furthermore, HapR is not expressed (or expressed at very low levels) in many *V. cholerae* pathogenic isolates (Joelsson et al., 2006). In some strains, such as the El Tor strain N16961, the *hapR* gene has a frameshift mutation and is non-functional (Zhu et al., 2002). Hence, the aim of this study was to characterise the role of HapR and LuxO in the quorum-sensing cascade of 7PET *Vibrio* cholerae.

First, we have determined the effect of clinically observed mutations within the promoter sequences of *hapR* and *luxO*. We show that these mutations, common in clinical isolates, can alter promoter activity substantially. Second, we have used Chromatin Immunoprecipitation and DNA sequencing (ChIP-seq) to map binding of HapR and LuxO genome wide. Though ChIP-seq studies have previously been done on HapR homologues in other *Vibrio* species (such as LuxR in *V. harveyi*), the DNA binding profile of HapR in 7PET *V. cholerae* has not been determined (Zhang et al., 2021; Ball et al., 2017).

Third, this study details the mechanism by which HapR interacts with a target promoter to regulate transcription. Using a combination of *in vitro* transcription, promoter probe assays (using β-galactosidase as a reporter), electrophoretic mobility shift assays and DNaseI footprinting, we show co-operative interactions, between HapR and CRP, important to repress transcription. Experiments in this study were done using *V. cholerae* E7946, an

Ogawa El Tor strain isolated in 1978 from a patient in Bahrain that expresses HapR (Miller et al., 1989).

Chapter 2
Materials and Methods

2.1 Cells and Culturing

2.1.1 Liquid cultures

Unless otherwise stated, all overnight cultures and subcultures of *E. coli* and *V. cholerae* were grown in Luria-Bertani (LB) broth (supplied by Sigma) with appropriate antibiotics at 37 ^{o}C. To prepare, powdered broth was dissolved in deionised water (dH_2O) at the concentration stated by the supplier, then autoclaved at 121 ^{o}C for 21 minutes. *V. cholerae* strains were grown with either 50 μg/ml (N16961) or 100 μg/ml (E7946) Streptomycin in addition to any other antibiotics required.

2.1.2 Plate cultures

Strains in this study were grown on LB agar (supplied by Sigma) with the same antibiotic concentrations as were used in liquid cultures. To prepare, powdered media was dissolved in deionised water (dH_2O) at the concentration stated by the supplier, then autoclaved at 121 ^{o}C for 21 minutes.

2.1.3 Antibiotics

Antibiotics were dissolved in dH_2O (or 100 % methanol for Tetracycline) to a stock concentration of 1000-fold the intended final concentration and filter sterilised through a 0.45 μM filter before storage at the appropriate temperature as per the supplier's instructions.

2.1.4 Bacterial Strains

See Table 2.1 for a list of bacterial strains used

2.2 Plasmids, oligonucleotides and synthesised DNA fragments

2.2.1 Plasmids

See Table 2.2 for a list of plasmids used

2.2.2 Oligonucleotides

See Table 2.3 for a list of oligonucleotides used

2.2.3 Synthesised DNA fragments

See Table 2.4 for a list of synthesised DNA fragments used

2.3 Buffers

See table 2.5 for a list of buffers used

Strain	Features	Source
***E. coli* JCB387**	*lac⁻ nir⁻*	Grainger et al., 2007
***E. coli* T7 Express**	*Detailed in product specifications*	New England Biolabs (NEB)
***E. coli* M182**	*lacIPOZY⁻*	Casadaban and Cohen, 1980
***E. coli* M182Δcrp**	*lacIPOZY⁻ crp⁻*	Casadaban and Cohen, 1980
***E. coli* S17 (λpir)**	λpir lysogen S17-1 derivative	de Lorenzo et al., 1993
***E. coli* DH5α**		Woodcock et al., 1989
***V. cholerae* N16961**	*hapR⁻*	Heidelberg et al., 2000
***V. cholerae* E7946**	*hapR⁺*	Miller et al., 1989
V. cholerae* E7946 Δ*hapR	*hapR⁻*	This study
V. cholerae* E7946 Δ*crp	*crp⁻*	This study
V. cholerae* E7946 Δ*hapR* Δ*crp	*hapR⁻ crp⁻*	This study

Table 2.1 – Strains used in this study. Key features of each strain shown.

Plasmid	Description	Selective Marker (Conc. used when culturing)	Source
pRW50-T	*E. coli*/*V. cholerae* shuttle vector with a multiple cloning site directly upstream of a LacZ gene	Tetracycline (35 µg/ml)	Lodge et al., 1992
pAMNF	pJ201-derived plasmid. Contains an N-terminal 3xFLAG tag and downstream multiple cloning site	Kanamycin (50 µg/ml)	ATUM
pAMNF HapR	pAMNF with *hapR* ORF cloned between *Hind*III and *Kpn*I restriction sites	Kanamycin (50 µg/ml)	This study
pAMCF	pJ241-derived plasmid. Contains a C-terminal 3xFLAG tag and upstream multiple cloning site	Kanamycin (50 µg/ml)	ATUM
pAMCF LuxO	pAMCF with *luxO* ORF cloned between *Hind*III and *Kpn*I restriction sites	Kanamycin (50 µg/ml)	This study
pHis-tev-HapR	Over-expression vector encoding a 6xHis tagged HapR. Tag and HapR separated by a tev protease-cleavable linker	Ampicillin (100 µg/ml)	Supplied by the Dhalia lab (Indiana University)
pHis-tev-HapR (R123A)	pHis-tev-HapR with point mutation in *hapR* ORF	Ampicillin (100 µg/ml)	This study
pHis-tev-HapR (R123E)	pHis-tev-HapR with point mutation in *hapR* ORF	Ampicillin (100 µg/ml)	This study
pSR	pBR322-derived plasmid. Cloning site upstream of a λ*oop* terminator and encodes a separate σ^{70}-dependent RNA transcript (RNA-I)	Ampicillin (100 µg/ml)	Busby and Ebright, 1999
pDCRP-*Vc*	pBR322-derived plasmid. Encodes *V. cholerae* CRP under control of its native promoter (located between *EcoRI* and *SalI* restriction sites)	Ampicillin (100 µg/ml)	Manneh-Roussel et al., 2018
pDCRP-*Vc* (E55A)	pDCRP-*Vc* with point mutation in *crp* ORF	Ampicillin (100 µg/ml)	This study
pDCRP-*Vc* (E55R)	pDCRP-*Vc* with point mutation in *crp* ORF	Ampicillin (100 µg/ml)	This study
pKAS32	*E. coli*/*V. cholerae* shuttle vector encoding a streptomycin sensitive ribosomal S12 protein, RpsL	Ampicillin (100 µg/ml)	Skorupski and Taylor, 1996
pKAS32 HapR	pKAS32 with flanking regions of *hapR* gene and promoter (as present on *V. cholerae* E7946 chromosome I) inserted	Ampicillin (100 µg/ml)	This study
pKAS32 CRP	pKAS32 with flanking regions of *crp* gene and promoter (as present on *V. cholerae* E7946 chromosome I) inserted	Ampicillin (100 µg/ml)	This study

Table 2.2 – Plasmids used in this study. Features of each plasmid and the appropriate antibiotics used to select for them in bacterial culture shown.

Oligonucleotide	Sequence (5’ -> 3’)	Features/Notes
Cloning of HapR and LuxO ORFs and promoter regions		
HapR WT Cloning fwd	GGCTGCGGTACCATGGACGCATCAATCGAAAAACGC	Amplifying HapR for cloning into pAMNF (*Kpn*I)
HapR WT Cloning rev	GCCCGAAGCTTCTAGTTCTTATAGATACACAGCATATTGAGG	Amplifying HapR for cloning into pAMNF (*Hind*III)
LuxO (KpnI removed) cloning fwd	GGCTGCGGTACCATGGTAGAAGACACGGCGTCGGTGGCGGCGCTGTATCGTTCTTACCTCACACCGCTGGATATTGATATCAATATCGTGGGTACGGGAC	Amplifying LuxO for cloning into pAMCF (*Kpn*I) (Synonymous mutation to remove *Kpn*I site)
LuxO (KpnI removed) rev	ATCGCGTCCCGTACCCACGATATTG	Amplifying LuxO for cloning into pAMCF (stop codon excluded for C-terminal tagging)
LuxO WT Cloning rev (no STOP)	GCCCGAAGCTTCCGTTCCTTCTCTTTTTCTTTCAC	*Hind*III
HapR Pro WT fwd	GGCTGCGAATTCAATCCTGTTAATCGTTTCCCTACTCATCCTCGCTTTG	*Eco*RI
HapR Pro WT rev	GCCCGAAGCTTCATAGGGGTATATCCTTGCCAATTGAGTTGTTGATTGAG	*Hind*III
HapR Pro Mut1 rev	GCCCGAAGCTTCATAGGGGTATATCCTTGCTAATTGAGTTGTTGATTGAGC	*Hind*III *C -> T mutation*
HapR Pro Mut2 rev	GCCCGAAGCTTCATAGGGGTATATCCTTGCCAATTGCGTTGTTGATTGAGCATTTTGC	*Hind*III *A -> C mutation*
HapR Pro Mut3 rev	GCCCGAAGCTTCATAGGGGTATATCCTTGCCAATTGAGTTTTTGATTGAGCATTTTGCTC	*Hind*III *G -> T mutation*
LuxO Pro WT fwd	GGCTGCGAATTCAGAGAAAAACACTGATTTCAAACACGCAG	*Eco*RI
LuxO Pro WT rev	GCCCGAAGCTTCATGAGGACATATTTTGTTTTCTGCAAAGATTGATTATG	*Hind*III
LuxO Pro Mut1 rev	GCCCGAAGCTTCATGGGGACATATTTTGTTTTCTGCAAAGATTGATTATG	*Hind*III *T -> C mutation*
LuxO Pro Mut2 rev	GCCCGAAGCTTCATGAAGACATATTTTGTTTTCTGCAAAGATTGATTATG	*Hind*III *C -> T mutation*
LuxO Pro Mut3 rev	GCCCGAAGCTTCATGAGGGCATATTTTGTTTTCTGCAAAGATTGATTATG	*Hind*III *T -> C mutation*
LuxO Pro Mut4 rev	GCCCGAAGCTTCATGAGGACATATTTTGTTTTCTGCAAAGATTAATTATGTTGCATAGCCTAGCC	*Hind*III *C -> T mutation*

Amplifying promoters for cloning into pSR and pRW50-T vectors		
HapTarget PmurQ fwd	AAAAGAATTCCACCAATCTGGCGGCCACTC	*Eco*RI
HapTarget PmurQ rev	TTTTAAGCTTCATAAGGCTTCTCGGCAAAT	*Hind*III
HapTarget PhapR fwd	AAAAGAATTCCATACCATTCTCGTTGTGTT	*Eco*RI
HapTarget PhapR rev	TTTTAAGCTTCATAGGGGTATATCCTTGCC	*Hind*III
HapTarget PVC0585 fwd	AAAAGAATTCCATAGGGGTATATCCTTGCC	*Eco*RI
HapTarget PVC0585 rev	TTTTAAGCTTCATACCATTCTCGTTGTGTT	*Hind*III
HapTarget PVC0502 fwd	AAAAGAATTCGACAAAAGTTTGTTGCCCGC	*Eco*RI
HapTarget PVC0502 rev	TTTTAAGCTTCATAGTATTGGCTTTGGCAT	*Hind*III
HapTarget PmutH fwd	AAAAGAATTCACCAGACCACATGAAGATCC	*Eco*RI
HapTarget PmutH rev	TTTTAAGCTTCATAAAGGCTTTCGGTTTGG	*Hind*III
HapTarget PleuO fwd	AAAAGAATTCTAATGAACTGACTAACTCAA	*Eco*RI
HapTarget PleuO rev	TTTTAAGCTTCATTGCGTCTTTTTTATCTA	*Hind*III
HapTarget PVC0433 fwd	AAAACAATTGTACCTGCAACTTCAAGTAGT	*Mfe*I
HapTarget PVC0433 rev	TTTTAAGCTTCATTATTTTTTAATCACCAA	*Hind*III
HapTarget PVC0241 fwd	AAAAGAATTCCTATAGATGCGAACAGTTGC	*Eco*RI
HapTarget PVC0241 rev	TTTTAAGCTTCATAGTATGCTGACTACTGC	*Hind*III
HapTarget PrfaD fwd	AAAACAATTGCATAGTATGCTGACTACTGC	*Mfe*I
HapTarget PrfaD rev	TTTTAAGCTTCATTATGAATTCCTATAGAT	*Hind*III
HapTarget PVC0620 fwd	AAAAGAATTCAAACCGTACCCGTTTTGCGAG	*Eco*RI
HapTarget PVC0620 rev	TTTTAAGCTTACTAGTAAGGAACAGCTATG	*Hind*III
HapTarget PVC0688 fwd	AAAAGAATTCCATAGCGTTTGTCCTTTTGT	*Eco*RI
HapTarget PVC0688 rev	TTTTAAGCTTCATTACTATCCATTTTTTCA	*Hind*III
HapTarget PVC1298 fwd	AAAAGAATTCCATAAACTCTTTGTATAATT	*Eco*RI
HapTarget PVC1298 rev	TTTTAAGCTTCATGATAGTTTTGTAATTAT	*Hind*III
HapTarget PVC1375 fwd	AAAACAATTGCATCCACTTCTTCCTTATTA	*Mfe*I
HapTarget PVC1375 rev	TTTTAAGCTTCATATCAAAAGTGGTTGGGA	*Hind*III
HapTarget PVC1376 fwd	AAAACAATTGCATATCAAAAGTGGTTGGGA	*Mfe*I
HapTarget PVC1376 rev	TTTTAAGCTTCATCCACTTCTTCCTTATTA	*Hind*III
HapTarget PVC1403 fwd	AAAAGAATTCCATTTTTTGGGTAATCGATA	*Eco*RI
HapTarget PVC1403 rev	TTTTGGATCCCATGGAAAACCTCGTTGTTT	*Bam*HI
HapTarget PVC1405 fwd	AAAAGAATTCCATGGAAAACCTCGTTGTTT	*Eco*RI
HapTarget PVC1405 rev	TTTTGGATCCCATTTTTTGGGTAATCGATA	*Bam*HI
HapTarget PVC1436 fwd	AAAAGAATTCCCAATTCGTAAAGAAGCTAA	*Eco*RI
HapTarget PVC1436 rev	TTTTGGATCCCATATCTGCTGAGGCTTTAG	*Bam*HI

HapTarget PVC2352 fwd	AAAAGAATTCTCAGCACAATATCTCGCGCC	*Eco*RI
HapTarget PVC2352 rev	TTTTAAGCTTCATGCCGATGAGGCTCATAA	*Hind*III
HapTarget PVCA0218 fwd	AAAAGAATTCCATATAAACCTCACTGACTC	*Eco*RI
HapTarget PVCA0218 rev	TTTTAAGCTTCATCGTTTACTTCTTATCAT	*Hind*III
HapTarget PVCA0219 fwd	AAAAGAATTCCATCGTTTACTTCTTATCAT	*Eco*RI
HapTarget PVCA0219 rev	TTTTAAGCTTCATATAAACCTCACTGACTC	*Hind*III
HapTarget PVCA0662 fwd	AAAAGAATTCTCAGTTTGTAAATTGAGGAA	*Eco*RI
HapTarget PVCA0662 rev	TTTTAAGCTTCATATCAAATATGAATCCTT	*Hind*III
HapTarget PVCA0663 fwd	AAAAGAATTCCATATCAAATATGAATCCTT	*Eco*RI
HapTarget PVCA0663 rev	TTTTAAGCTTCATGGTGTTACCTACTTGTT	*Hind*III
HapTarget PVCA0906 fwd	AAAAGAATTCATTTTTATCCTGACCCCATA	*Eco*RI
HapTarget PVCA0906 rev	TTTTGGATCCCATGCCTACGCCTATCGCCG	*Bam*HI
HapTarget PVCA0960 fwd	AAAAGAATTCCATCATGAGTTATATTTACA	*Eco*RI
HapTarget PVCA0960 rev	TTTTAAGCTTCATCCCTCAATCCTCAGTTT	*Hind*III
HapTarget PVCA0961 fwd	AAAAGAATTCCATCCCTCAATCCTCAGTTT	*Eco*RI
HapTarget PVCA0961 rev	TTTTAAGCTTCATCATGAGTTATATTTACA	*Hind*III
Oligonucleotides for sequencing cloned DNA inserts in different plasmids		
pRW50 seq fwd	GTTCTCGCAAGGACGAGAATTTC	Sequencing inserts in pRW50 constructs
pRW50 seq rev	GTCGTTGAACTGAGCCTGAAATTCAGG	Sequencing inserts in pRW50 constructs
pSR seq fwd	GTGCCACCTGACGTCTAAGAAACC	Sequencing inserts in pSR constructs
pSR seq rev	GCAACCGAGCGTTCTGAACAAATCC	Sequencing inserts in pSR constructs
pAM seq fwd	ATTTATTCCAATGTCACACACTTTTCGC	Sequencing inserts in pAMNF or pAMCF constructs
pAM seq rev	GAAACGCCGTAGCGCCGATGGTAGT	Sequencing inserts in pAMNF or pAMCF constructs
Amplifying fragments for radiolabelling		
pSR footprinting fwd (bio)	[***BIO***]-CACGAGGCCCTTTCGTCTTCTC	Amplifying promoter fragments for DNaseI footprinting, EMSA or GA ladder prepar–tion - biotinylated to prevent radiolabellin’ at 5' end
pSR footprinting rev	GGAGTTCTGAGGTCATTACTGGAG	Amplifying promoter fragments for DNaseI footprinting, EMSA or GA ladder preparation

pSR footprinting fwd	CACGAGGCCCTTTCGTCTTCTC	Amplifying promoter fragments for DNaseI footprinting, EMSA or GA ladder preparation
pSR footprinting rev (bio)	[***BIO***]-GGAGTTCTGAGGTCATTACTGGAG	Amplifying promoter fragments for DNaseI footprinting, EMSA or GA ladder prepar–tion - biotinylated to prevent radiolabellin' at 5' end
Amplifying fragments for pKAS32-mediated gene knock-outs		
pKAS32 fwd	GCAGGCACAAGCGGCCGCCTGCAGCTGGCG CCATCGATACGCGTACGTCG	Amplifying pKAS plasmid backbonephargibson assembly or restriction cloning
pKAS32 rev	CACGGTTTCATTAACAACCGGTACCTCTAGA ACTATAGCTAGCATGCGCAAATTTAAAGCGC TG	Amplifying pKAS plasmid backbonephargibson assembly or restriction cloning
CRP arm upstream fwd	CGGTTGTTAATGAAACCGTGGATATTAAATG C	Amplifying *crp* flanking regions for assembly into pKAS plasmid and subsequent *crp* gene knock-out
CRP arm upstream rev	ATCGGGGCACCTAGCCGATTTTTCCGGTTTC	Amplifying *crp* flanking regions for assembly into pKAS plasmid and subsequent *crp* gene knock-out
CRP arm downstream fwd	AATCGGCTAGGTGCCCCGATAACCCGTC	Amplifying *crp* flanking regions for assembly into pKAS plasmid and subsequent *crp* gene knock-out
CRP arm downstream rev	AGGCGGCCGCTTGTGCCTGCGCAGCCAA	Amplifying *crp* flanking regions for assembly into pKAS plasmid and subsequent *crp* gene knock-out
HapR arm1 fwd	CTAGAGGTACCGGTTGTTAATCCCAACCCCG ATTGGTAATC	Amplifying *hapR* flanking regions for assembly into pKAS plasmid and subsequent *hapR* gene knock-out

HapR arm1 rev	TGTGTTTCATTTTCTTGGGCAGCACAAAG	Amplifying *hapR* flanking regions for assembly into pKAS plasmid and subsequent *hapR* gene knock-out
HapR arm2 fwd	GCCCAAGAAAATGAAACACACAGTTGAAGTC	Amplifying *hapR* flanking regions for assembly into pKAS plasmid and subsequent *hapR* gene knock-out
HapR arm2 rev	CGCCAGCTGCAGGCGGCCGCTATGCGGTCGATGTGCTG	Amplifying *hapR* flanking regions for assembly into pKAS plasmid and subsequent *hapR* gene knock-out
Site-directed mutagenesis of hapR *and* crp *genes*		
HapR_R123E _fwd_SDM	TGCTTCAACCGAGGACGAAGTTTGGC	Introducing mutation in *hapR* ORF *GCA -> GAG mutation*
HapR_R123A _fwd_SDM	TGCTTCAACCGCTGACGAAGTTTGGCC	Introducing mutation in *hapR* ORF *GCA -> GCT mutation*
HapR_R123_rev_SDM	CTCCACTCAAACCAGACTTTG	Introducing mutation in *hapR* ORF
CRP_E55R_fwd_SDM	GATCAAAGATCGTGAAGGTAAAGAGATGATTCTC	Introducing mutation in crp ORF *GAA -> CGT mutation*
CRP_E55A_fwd_SDM	GATCAAAGATGCGGAAGGTAAAGAGATGATTC	Introducing mutation in crp ORF *GAA -> GCG mutation*
CRP_E55_rev _SDM	AGTACCGCAACTGAACCT	Introducing mutation in crp ORF

Table 2.3 – Oligonucleotides used in this study. Features within the DNA sequence such as restriction sites (e.g. *Eco*RI) highlighted. Mutations indicated in red are relative to wild-type sequence of *V. cholerae* (E7946).

Fragment	Sequence (5′ -> 3′)	Features
HapR Pro Mut4	CATAGGGGTATATCCTTGCCAATTGAGTTGTTGATTGAGCATTTTGCTCT AATGATTATTTTGTTATTTGCTACTTAAAGCCCTATGGGTGTAATGGTGC ATATATTCAAGGTCAATCTCTGTTGGGTGAAAAATGTGCAACTATGTTA ATTATTTGTCGTTTCAGCTTGTTTTATTGAGTGGGTACATAACAAAGCGA GGATGAGTAGGGAAACGATTAACAGGATT	*A -> G mutation* -10 and -35 elements
HapR Pro Mut5	CATAGGGGTATATCCTTGCCAATTGAGTTGTTGATTGAGCATTTTGCTCT AATGATTATTTTGTTATTTGCTACTTAAAGCCCTATGAGTGAAATGGTGC ATATATTCAAGGTCAATCTCTGTTGGGTGAAAAATGTGCAACTATGTTA ATTATTTGTCGTTTCAGCTTGTTTTATTGAGTGGGTACATAACAAAGCGA GGATGAGTAGGGAAACGATTAACAGGATT	*T -> A mutation* -10 and -35 elements
HapR Pro Mut6	CATAGGGGTATATCCTTGCCAATTGAGTTGTTGATTGAGCATTTTGCTCT AATGATTATTTTGTTATTTGCTACTTAAAGCCCTATGAGTGTAATGGTGC ATATATTCAAGGTTAATCTCTGTTGGGTGAAAAATGTGCAACTATGTTA ATTATTTGTCGTTTCAGCTTGTTTTATTGAGTGGGTACATAACAAAGCGA GGATGAGTAGGGAAACGATTAACAGGATT	*C -> T mutation* -10 and -35 elements
LuxO Pro Mut5	AGAGAAAAACACTGATTTCAAACACGCAGATAAAAAAATAGCCAATAG AATGAGTCTATTGGCTGTTATTTGTGAACATTGATTATTCACTAACAACG TCAGTTGGCTAGGTGACCCTTGCGGGTCAGTAGTAATCAAGCACATATC GTGCCAACTCAAATCGGTCTAGATGTGTGATGTTTAGCATCATTTATCA AGAAATTTTAATTCAAATTTGCAAAATGCAATTCCAAATGCAATTATTAC AGCAAAATGCAAAATAATATGGCTAGGCTATGCAACATAATCAATCTTT GCAGAAAACAAAATATGTCCTCATG	*G -> A mutation*

Table 2.4 – Synthesised DNA fragments used in this study. Features within the DNA sequence such as restriction sites (e.g. *Eco*RI) highlighted. Fragments synthesised by ThermoFisher. Mutations indicated in red are relative to wild-type sequence of *V. cholerae* (E7946).

Buffer	Constituents
Phenol:Choloroform:Isoamyl alcohol	Phenol 50 % (v/v) Choloroform 48 % (v/v) Isoamyl alcohol 2 % (v/v)
FA lysis buffer (150)	50 mM Hepes-KOH (pH7) 150 mM NaCl 1 mM EDTA 1 % (w/v) Triton X-100 0.1 % (w/v) Sodium deoxycholate 0.1 % (w/v) SDS
FA lysis buffer (500)	50 mM Hepes-KOH (pH7) 500 mM NaCl 1 mM EDTA 1 % (w/v) Triton X-100 0.1 % (w/v) Sodium deoxycholate 0.1 % (w/v) SDS
TE	10 mM Tris-HCl (pH 8.0) 1 mM EDTA
TBS	20 mM Tris-HCl (pH 7.4) 0.9 % (w/v) NaCl
ChIP wash buffer	10 mM Tris-HCl (pH 8.0) 250 mM LiCl 1 mM EDTA 0.5 % (w/v) Nonidet-P40 0.5 % (w/v) Sodium Deoxycholate
ChIP elution buffer	50 mM Tris-HCl (pH 7.5) 10 mM ETDA 1 % (w/v) SDS
Protein Buffer 1	25 mM Tris-HCl (pH 7.5) 1 mM EDTA 1M NaCl
Protein Buffer 2	25 mM Tris-HCl (pH 8.5) 4M urea
Protein Buffer 3	25 mM Tris-HCl (pH 8.5) 6 M guanidinium-HCl
Protein Buffer A	25mM Tris-HCl (pH 8.5) 1M NaCl
Protein Buffer B	25 mM Tris-HCl (pH 8.5) 1 M NaCl 1 M imidazole

Protein Buffer X	50 mM HEPES 1 M NaCl 1 mM DTT 5 mM EDTA 0.1 mM Triton X-100
CRP Lysis Buffer	50 mM Potassium phosphate 2 mM EDTA 0.2 M NaCl 5 % (w/v) Glycerol 2 mM DTT Protease inhibitor cocktail (–erck - added as per instructions)
CRP Dialysis Buffer	50 mM Potassium phosphate 2 mM EDTA 5 % (w/v) Glycerol 2 mM DTT
CRP Column Wash Buffer	500 mM Potassium phosphate 2 mM EDTA 5 % (w/v) Glycerol 2 mM DTT
CRP Stock Buffer	10 mM Sodium phosphate 0.1 mM EDTA 0.2 M NaCl 50 % (w/v) Glycerol
RNAP Lysis Buffer	50 mM Tris-HCl (pH 7.5) 150 mM NaCl 2 mM $MgCl_2$ 0.1 mDTT **2** 2 mMDTA **2** 1 mM β-mercaptoethanol 5 % (w/v) Glycerol 0.2 % (w/v) Triton X-100 0.25 mg/ml lysozyme Protease inhibitor cocktail (–erck - added as per instructions)
TGED Buffer	10 mM Tris-HCl (pH 7.5) 0.1 mMA **2.6** 0.1 mM DTT 5 % (w/v) Glycerol
RNAP Stock Buffer	10 mM Tris-HCl (pH 7.5) 0.2 mM EDTA 0.1 mM DTT 100 mM NaCl 50 % (w/v) Glycerol
Z-Buffer	30 mM $NaH_2PO_4 \cdot 2H_2O$ 60 mM $NaPO_4$ **2** 1 mM $MgSO_4 \cdot 7H_2O$ 10 mM KCl

5 x Protein loading buffer	10 % (w/v) SDS 10 mM DTT 20 % (w/v) Glycerol 0.2 M Tris-HCl (pH 6.8) 0.05 % Bromophenol blue
10 x TNSC buffer	400 mM Tris-acetate 100 mM $MgCl_2$ 1 M KCl
Primer extension STOP solution	97.5 % (v/v) formamide 10 mM EDTA pH 7.5 0.025 % (v/v) bromophenol blue 0.025 % (v/v) xylene cyanol FF
2 x STOP solution	660 mM Urea 100 mM EDTA 80 % (v/v) Deionised formamide 0.015 % (v/v) Bromophenol blue 0.015 % (v/v) Xylene cyanol
8 % polyacrylamide gel	27 % (v/v) Protogel (30 %) (Geneflow) 6 M Urea 1 x TBE 3.5 mM Ammonium persulphate 0.0003 % (v/v) N,N,N',N'-Tetramethyl ethylenediamine (Temed)
5 % polyacrylamide gel	16.6 % (v/v) Protogel (30 %) (Geneflow) 6 M Urea 0.5 x TBE 4.4 mM Ammonium persulphate 0.002 % (v/v) N,N,N',N'-Tetramethyl ethylenediamine (Temed)
DNaseI Blue	5 M urea 20 mM NaOH 1 mM EDTA 0.025 % (*v/v*) bromophenol blue 0.025 % (*v/v*) xylene cyanol FF
DnaseI Stop	0.3 M Sodium acetate (pH 7) 10 mM EDTA

Table 2.5 – Buffers used in this study.

2.4 PCR, restriction digests, DNA preparation and gel electrophoresis

2.4.1 Polymerase chain reactions (PCR)

PCR was done using Q5 DNA polymerase (NEB) according to the manufacturers protocol. Where required (for example, before restriction digestion or cloning) the resulting DNA was purified using a PCR purification kit (Qiagen).

2.4.2 Restriction digests

Enzymes for DNA restriction digests were supplied by NEB. Restriction digests were done using the optimal buffers and enzymes at the appropriate concentrations as stated by the supplier. Where required for restriction cloning, digested plasmid DNA was incubated at 37 ^{o}C with Calf Intestinal Phosphatase (CIP) for at least 1 hour post-digest.

2.4.3 Ligation reactions

Ligation of DNA fragments were done using Quick ligase (supplied by NEB) following the manufacturers protocol.

2.4.4 Genomic DNA extraction

Genomic DNA was extracted using a DNeasy Blood and Tissue kit (Qiagen) following the manufacturers protocol with one amendment to the first step, cells were resuspended in 180 µl ATL buffer, 20 µl of 100 mg/ml lysozyme was added and the cells were incubated at 37 ^{o}C for 30 minutes.

2.4.5 Plasmid purification

Plasmid DNA was extracted using Mini, Midi or Maxiprep kits (supplied by Qiagen) as per the supplied protocol, with the amendment of using nuclease-free dH_2O for elution instead of the supplied elution buffer.

2.4.6 Phenol-chloroform extraction/Ethanol precipitation

A phenol:choloroform:isoamyl alcohol solution (mixed at a ratio of 25:24:1) was added to an equal volume of DNA and transferred to a 5PRIME Phase Lock Gel Heavy tube (Quantabio). A vortex mixer was used to homogenise the sample and the aqueous layer were separated from the organic phase by centrifugation at 21,000 x g for 3 minutes. The aqueous upper phase was transferred to a new microfuge tube and mixed with 1/10 volume of 3 M sodium acetate (pH 5.2). When precipitating DNA fragments smaller than 100 bp in size, 1/100 volume of GlycoBlue (Thermo Fisher) was also added. DNA was then precipitated by adding cold 100 % ethanol to the mixture and storing at -80 ^oC for 30 minutes. DNA was collected by centrifugation at 4 ^oC and 21,000 x g for 45 minutes. The supernatant was removed and the DNA pellet was resuspended in cold 70 % ethanol before collecting by centrifugation at 4 ^oC and 21,000 x g for 10 minutes. The supernatant was removed and the DNA pellet was resuspended in nuclease-free dH_20.

2.4.7 Agarose gel electrophoresis

1 % (w/v) agarose gels were made by dissolving agarose powder (Bioline) in 1 x TBE. Gels were supplemented with 1/10,000 volumes ethidium bromide or Sybr Safe (Thermo Fisher) before pouring. Once set, gels were placed into electrophoresis tanks filled with 1 x TBE. DNA was mixed with 6 x gel loading dye (NEB) before loading into the wells of the gel. DNA

fragments were separated by electrophoresis at 120 V for as long as required. DNA fragments were visualised using a UV transilluminator.

2.4.8 DNA gel extraction

DNA bands were excised from agarose gels using a clean razor blade and the DNA was extracted using a Gel Extraction kit (Qiagen) following the manufacturers protocol.

2.4.9 Preparation of polyacrylamide gels

Polyacrylamide gels were made by mixing TBE, Protogel (30 % w/v acylamide/bisacryl–mide - Geneflow) and ddH_2O (see table 2.5 for final concentrations). Acrylamide was polymerised by addition of ammonium persulphate (APS) and TEMED (N,N,N',N' – Tetramethylethylenediamine) at appropriate concentrations (see table 2.5). Gels were submerged in TBE (the same concentration as the final TBE concentration within the gel) within gel tanks. 8 % polyacrylamide gels were run at 80 W for 1 hour before samples were loaded.

2.5 Bacterial transformation and chromosomal deletions

2.5.1 Preparing competent cells

To prepare competent *E. coli* cells, 1 ml of an overnight culture of JCB387 was sub-cultured into 50 ml of LB and grown at 37 ^{o}C to mid-log phase ($O.D._{650}$ – 0.3 - 0.5). Cells were incubated on ice for 10 minutes before centrifugation at 3,500 x g for 5 minutes at 4 ^{o}C. The pelleted cells were re-suspended in 25 ml pre-chilled 0.1 M $CaCl_2$ and incubated on ice for 30 minutes. Cells were centrifuged again as before and re-suspended in 3.3 ml 0.1 M $CaCl_2$. Cells were then left overnight on ice before being supplemented with 1.2 ml of 50 % glycerol (filter-sterilised and chilled). Aliquots of cells were made and stored at -80 ^{o}C.

2.5.2 Transformation by heat shock

Competent cells were thawed on ice and mixed with plasmid(s) or the final product of a ligation reaction for transformation. Mixture was chilled for at least 30 minutes before heat shock at 42 ^{o}C for 2 minutes. After recovery on ice for 3 minutes cells were supplemented with LB and incubated for 1 hour at 37 ^{o}C (with shaking) before spreading onto LB agar plates with selective antibiotics where appropriate. Colonies were selected after overnight incubation at 37 ^{o}C.

2.5.3 Transformation by electroporation

Mid-log phase *E. coli* or *V. cholerae* cells were collected by centrifugation at 3,500 x g for 10 minutes at 4 ^{o}C. The cells were then re-suspended in 15 % (v/v) glycerol. This glycerol wash was repeated three times before the cells were finally resuspended in 500 µl 15 % (v/v) glycerol and stored at -80 ^{o}C. Cells and up to 1 µg of desired plasmid DNA were mixed (50 µl total volume) and incubated for 30 minutes on ice in a 0.2 cm gap electroporation cuvette

(GeneFlow). After incubation, 2,500 V were applied to cuvettes with a capacitance of 25 µF and resistance of 200 Ω in an Eporator (Eppendorf). Immediately after electroporation, cells were supplemented with 950 µl of LB and incubated at 37 °C with shaking for 1 hour. Cells were then spread onto LB agar with appropriate antibiotics and grown overnight at 37 °C.

2.5.4 Transformation by natural competence

Mid-log phase cultures of *V. cholerae* E7946 cells were collected by centrifugation at 3,500 x g and resuspended in 1 ml 0.7 % (w/v) Instant Ocean (Aquarium Systems). 100 µl of cells were added to microfuge tubes prepared with 0.1 g sterile chitin flakes (Sigma) and 900 µl 0.7 % (w/v) Instant Ocean. The mixtures were incubated at 30 °C (non-shaking) for between 36 and 48 hours, then 1-5 µg of DNA for transformation was added. Mixtures were incubated for another 24 hours at 30 °C before addition of LB broth, vortexing and incubation at 37 °C (shaking). Cell suspensions were then spread onto LB agar plates with appropriate antibiotics and incubated overnight at 37 °C.

2.5.5 Conjugation

Conjugations were done in either a bipartite or tripartite manner. For bipartite conjugation, overnight cultures of donor *E. coli* S17 (containing a plasmid for conjugation) and recipient *V. cholerae* were collected by centrifugation at 3,500 x g. Cells were washed with 0.9 % NaCl and resuspended in LB broth. Donor and recipient cells were mixed in a 1:1 ratio.

For tripartite conjugation, overnight cultures of donor *E. coli* DH5α (containing a plasmid for conjugation), 'helper' *E. coli* DH5α (containing a plasmid, pRK2013), and recipient *V. cholerae* were collected by centrifugation at 3,500 x g. Cells were washed with 0.9 % NaCl

and resuspended in LB broth. Donor, helper, and recipient strains were mixed in a 1:2:1 ratio.

Cell mixtures were spotted onto LB agar plates and dried aseptically before incubation overnight at 30 ^{o}C. Cell clumps formed overnight were scraped and resuspended in 0.9 % NaCl before spreading onto selective LB agar plates (selecting for *V. cholerae* with the desired plasmid). Plates were incubated overnight at 37 ^{o}C and colonies were subsequently selected and re-streaked onto selective LB agar plates.

2.5.6 Chromosomal deletions in *V. cholerae*

Regions to be deleted in the *V. cholerae* genome were removed using an allelic replacement method first developed by Skorupski and Taylor. Briefly, regions of the chromosome approximately 1kb upstream and downstream of the deletion were cloned in plasmid pKAS32. This plasmid contained a faulty ribosomal subunit, *rpsL*, which sensitises *V. cholerae* to streptomycin. The pKAS32 derivatives were introduced into *E. coli* S17cells (through transformation by heat shock) and subsequently into *V. cholerae* E7946 by conjugation. pKAS32 is a suicide vector within *V. cholerae* and must be incorporated (via homologous recombination) into the genome to allow growth on LB agar supplemented with 100 µg/ml ampicillin and 6.25 µg/ml polymyxin B. Cells were then re-streaked onto LB agar supplemented with 500 µg/ml streptomycin. *V. cholerae* which do not undergo a second homologous recombination event, and remove the *rpsL* gene, are unable to grow at this stage. Cells which did grow were tested by colony PCR (using MyTaq Red Mix, Bioline) to check for the deletion of our region of interest.

2.6 Chromatin Immunoprecipitation and DNA sequencing (ChIP-seq)

2.6.1 ChIP-seq procedure

Overnight cultures of cells containing pAMNF or pAMCF (with or without *hapR* or *luxO* genes) were sub-cultured to $O.D._{650}$ 1-1.2. Cells were then fixed with formaldehyde (to a final concentration of 1 % v/v). Reactions were quenched with glycine (to a final concentration of 0.5 M). Cells were washed with TBS and resuspended in FA lysis buffer (150 nM NaCl) with 2 mg/ml lysozyme. Cells were then left at 37 ^{o}C for 30 minutes before sonication with a Bio-ruptor (Diagenode) for 3 x 10 cycles (30 second pulses each). The cell debris was removed by centrifugation at 21,000 x g for 5 minutes. The supernatant was collected.

A 50 % v/v solution of Protepharoseharose beads (GE Healthcare) in TBS was prepared and 25 µl was mixed with 800 µl of lysates along with 1 µl of anti-FLAG antibody (Sigma). After incubation and rotation at room temperature for 90 minutes, the beads were resuspended in FA lysis buffer (150 mM NaCl) and transferred to a Spin-X column (VWR). The same procedure was used to wash beads in all subsequent steps. Beads were collected and washed twice with 10mM Tris-HCl (pH 7.5). The bead-associated DNA was then blunt-ended using a Quick Blunting kit (NEB). The beads were washed twice with FA lysis buffer (150 mM NaCl) and twice with 10mM Tris-HCl (pH 8) before the DNA was poly-adenylated using Klenow Fragment (3'-->5' exo-, NEB). The beads were then washed twice with FA lysis buffer (150 mM NaCl) and twice with 10mM Tris-HCl (pH 7.5). NEXTFlex Barcodes (BioO Scientific) were ligated to the DNA with a Quick Ligase kit (NEB). The beads were then washed twice with FA lysis buffer (150 mM NaCl) and once with TE buffer (10 mM Tris-HCl, 1 mM EDTA, pH 8.0). The spin-X column was transferred to a new microfuge tube, elution buffer (50 mM

Tris-HCl, 10 mM EDTA, 1 % SDS, pH 7.5) was added and the tubes were incubated at 65 ^{o}C for 10 minutes. DNA was eluted off the beads by centrifugation at 3,500 x g for 1 minute and de-crosslinked by boiling at 100 ^{o}C for 10 minutes. To purify the DNA, Agencourt AMPure XP magnetic beads (Beckman Coulter) were added at 1.1 x volume to eluted DNA. The tubes were placed on a magnetic rack to separate the beads from the liquid phase. The liquid phase was removed and the beads were washed twice on the magnetic rack with 70 % (v/v) ethanol. The final DNA libraries were eluted by adding dH_2O to the tubes, mixing and placing the tubes on the magnetic rack to separate the beads. The liquid phase was collected in a fresh microfuge tube.

Libraries were then amplified by PCR using Q5 DNA polymerase (NEB) and NEXTflex primer mix (BioO Scientific). To determine the appropriate number of cycles used to amplify the libraries, a test amplification was done with samples taken at 18, 21, 24, 27, 30, and 33 cycles and viewed on a 1 % agarose gel post-stained with ethidium bromide diluted in 10,000 volumes of dH_2O. Once the optimal conditions for amplification had been determined, the original ChIP libraries were amplified again as before using the determined number of cycles before another AMPure bead clean-up (as described earlier, except with beads added at 0.8 x the volume of DNA library). If necessary, a further 0.8 x AMPure clean-up was done.

DNA concentrations were quantified on a Qubit 2.0 Fluorometer (ThermoFisher) and the average size of the amplified DNA was determined using an Agilent 220 TapeStation. This information was used to mix libraries at an equimolar ratio (usually 2nM of each library) before loading onto an Illumina MiSeq cartridge for sequencing.

2.6.2 ChIP-seq of HapR and LuxO

For both HapR and LuxO, two biological repeats of the ChIP-seq experiment were done. For one of the pAMNF-HapR replicates, a modified version of the previously outlined immunoprecipitation protocol was used, in which two extra wash steps preceded the TE wash; FA Lysis (500 mM NaCl) and ChIP wash buffer (10 mM Tris-HCl, 250 mM LiCl, 1 mM EDTA, 0.5 % Nonidet-P40, 0.5 % Sodium Deoxycholate, pH 8) were used in this instance.

2.6.3 Analysing ChIP-seq data

Raw .fastq files obtained after sequencing were uploaded to usegalaxy.org and sequences were trimmed with the 'FastqGroomer' programme (Carver et al., 2012). BAM files were generated with the 'Bowtie2' programme using these trimmed '.fastq' files. The BAM files were visualised on Artemis alongside the reference genome, *V. cholerae* N16961 (Chromosome 1 or 2) (Heidelberg et al., 2000). This allowed us to observe binding peaks for our protein of interest. Averages of replicate datasets were obtained using the 'multibamsummary' programme on usegalaxy.org. Averaged values were normalised (all values expressed as a fraction of the highest value), these values were then opened in DNAPlotter (Carver et al., 2009) to produce a genome-wide profile of binding peaks.

To select peaks from the data, the averaged data was loaded in Artemis and was used to create features using the 'create features from graph > peaks' function. For HapR, the window size = 100, minimum feature size = 100 and cut-off value = 10. For LuxO, the window size = 100, minimum feature size = 100 and cut-off value = 4. Where this function created multiple features for a single peak, these features were merged.

MEME analysis of ChIP-seq data was used to determine DNA binding motifs (Bailey et al., 2009). The midpoint of DNA binding features (created for each peak as described above) determined the peak centres. A 300 bp selection of the genome sequence around each peak centre was taken and processed in MEME. The parameters for this analysis included the assumption either one or zero motifs were present per sequence. For HapR, the maximum length of motif was 25 bp. For LuxO, the maximum length was 16 bp.

2.7 β-galactosidase Assays

2.7.1 Generating promoter-*lacZ* fusions

DNA regions of interest in *V. cholerae* were amplified by PCR using colonies of *V. cholerae* E7946 as the DNA template. Point mutations in promoters were introduced with modified primers or using synthesised promoter fragments (Table 2.4) as an alternative PCR template. PCR products were cloned using appropriate restriction enzymes into pRW50-T.

2.7.2 β-galactosidase assays

Overnight cultures were grown to mid-log phase (unless otherwise stated) before lysis with 3 drops each of toluene and 1 % sodium deoxycholate, mixing with a vortex mixer and aeration for 20 minutes at 37 ^{o}C. 2.5 ml of Z-buffer containing ONPG and β-mercaptoethanol was added to 100 µl of lysed cells and left at 37 ^{o}C for at least 20 minutes. Reactions were quenched with 1 ml of 1M sodium carbonate and the reaction time and the O.D.$_{420}$ of each sample was recorded. β-galactosidase activity (Miller units) (Miller, 1972) was calculated as follows:

$$Activity = \frac{1{,}000\ x\ 2.5\ x\ A\ x\ O.D.420}{4.5\ x\ T\ x\ V\ x\ O.D.650}$$

where:

A = Final volume (ml)

T = Time (minutes)

V = Volume of lysed cells (ml)

1,000/4.5 = Factor accounting for 1 mole/ml O-nitrophenol absorption - 0.0045 at O.D.$_{420}$

2.5 = Factor accounting for O.D.$_{650}$ of 1 per 0.4 mg/ml bacteria

2.8 Primer extension

Overnight cultures were grown to mid-log phase before collected by centrifugation at 3,500 x g. All subsequent centrifugation steps were done at 4 ^{o}C. Cell were resuspended in TE buffer with 40 µg/ml lysozyme and incubated at room temperature for 15 minutes. 700 µl of buffer RLT (Qiagen) with 1 % (v/v) β-mercaptoethanol was added to cells along with 500 µl 100 % ethanol and these were passed through RNeasy mini columns (Qiagen). Columns were washed once with 700 µl of buffer RW1 and twice with 500 µl of RPE (Qiagen). RNA was then eluted from the column with 30 µl RNase-free water. To remove DNA contaminants, samples were mixed with 1 µl Turbo DNase and 3.5 µl 10 x Turbo DNAse buffer (Ambion) and ioncubated for 30 minutes at 37 ^{o}C. The DNase was inactivated with 6.1 µl Dnase inactivating reagent (Ambion) at room temperature for 2 minutes. The supernatants were collected after centrifugation of samples at 21,000 x g for 90 seconds and stored at -80 ^{o}C.

0.5 µl of 100 µM primer was radiolabelled by mixing 1 µl γ^{32}-ATP, 1 µl T4 Polynucleotide Kinase (NEB), 2 µl 10 x PNK buffer and 15.5 µl DEPC-treated water. The mixture was incubated at 37 ^{o}C for 30 minutes before inactivation at 68 ^{o}C for 10 minutes. 1 µl of radiolabelled primer was mixed with 20-30 µg of extracted RNA along with 0.1 volumes of 3M sodium acetate (pH 7.0) and 2.5 volumes of cold 100 % ethanol before incubation for 30 minutes at -80 ^{o}C. RNA was then collected by centrifugation at 21,000 x g, washed with 1 ml cold 70 % ethanol and re-suspended in 30 µl hybridisation buffer (20 mM HEPES, 0.4 M NaCl, 80 % formamide). The suspension was incubated for 5 minutes at 50 ^{o}C, then 15 minutes at 75 ^{o}C and finally 3 hours at 50 ^{o}C to anneal the primer. 75 µl of 100 % cold ethanol was then added and the RNA was incubated for at least 30 minutes at -80 ^{o}C.

RNA was collected by centrifugation at 21,000 x g, washed with 1 ml cold 70 % ethanol and resuspended in 31 µl DEPC-treated water. Samples were mixed with 2.5 µl AMV reverse transcriptase (Promega), 1 µl 50 mM DTT, 5 µl 10 mM dNTPs and 0.6 µl RNasin for 1 hour at 37 ^{o}C. After inactivation at 72 ^{o}C, 1 µl of 10mg/ml RNase was added to the sample, which was incubated for 30 minutes at 37 ^{o}C. 6.7 µl of 3M sodium acetate (pH 4.8) was added along with 125 µl 100 % cold ethanol. The sample was collected by centrifugation at 21,000 x g and resuspended in 4 µl primer extension STOP solution (see table 2.5).

To prepare the A, C, G and T ladders, 10 µg of template DNA from bacteriophage M13mp18 was denatured with 8 µl of 2 M NaOH and incubated at room temperature for 10 minutes. DNA was precipitated with 7 µl of 3 M NaAc (pH 5.2), 4 µl dH_20 and 120 µl of 100 % cold ethanol for 20 minutes at -80 ^{o}C. DNA was collected by centrifugation at 21,000 x g for 15 minutes, washed with 700 µl 70 % cold ethanol, dried under a vacuum for 8 minutes and resuspended in 10 µl dH_2O. 10 pM of Universal primer (5' GTAAAACGACGGCCAGT 3') with 2 µl annealing buffer (1 M Tris-HCl pH 7.5, 100 mM $MgCl_2$, 160 mM DTT) was added to the DNA and incubated at 65 ^{o}C for 5 minutes, then at 37 ^{o}C for 10 minutes and then at room temperature for 5 minutes.

5 µl each of four termination reaction solutions (A, C, G and T) were prepared in separate tubes:

'A' mix short	840 µM dCTP, 840 µM dGTP, 840 µM dTTP, 14 µM ddATP, 93.5µM dATP, 40 mM Tris-HCl (pH 7.5), 50 mM NaCl

'C' mix short	840 µM dATP, 840 µM dGTP, 840 µM dTTP, 14 µM ddCTP, 93.5 µM dCTP, 40 mM Tris-HCl (pH 7.5), 50 mM NaCl
'G' mix short	840 µM dCTP, 840 µM dATP, 840 µM dTTP, 14 µM ddGTP, 93.5 µM dGTP, 40 mM Tris-HCl (pH 7.5), 50 mM NaCl
'T' mix short	840 µM dCTP, 840 µM dGTP, 840 µM dATP, 14 µM ddTTP, 93.5 µM dTTP, 40 mM Tris-HCl (pH 7.5), 50 mM NaCl

T7 polymerase was diluted at a 1:5 ratio of T7 dilution buffer (25 mM Tris-HCl pH 7.5, 5 mM DTT, 100 µg/ml BSA, 5 % v/v glycerol). 2 µl of diluted T7 polymerase was mixed with the M13 DNA/primer mix, 3 µl 'A' labelling mix (1.375 mM of dCTP, dGTP, and dTTP each, 333.5 mM NaCl) and 1 µl of α-P^{32} dATP (Perkin Elmer). The mixture was incubated at room temperature for 5 minutes and 4.5 µl was transferred into the four termination reaction tubes. After a further incubation for 5 minutes at 37 ^{o}C, primer extension STOP solution (see table 2.5) was added to each reaction.

Samples and the A, C, G and T ladders were run on a 6 % polyacrylamide sequence gel before drying and exposing to a phosphorscreen (BioRad). This was then imaged on a BioRad FX phosphoimager.

2.9 Protein purification

2.9.1 Purification of HapR

Protein buffers 1-3, A, B and X were prepared (see Table 2.5). *E. coli* T7 Express cells were transformed with plasmid pHis-tev-HapR (or mutant derivatives thereof), which encodes a hexa-His tag fused to HapR via a tev protease cleavage site (provided by Ankur Dalia). Cells were grown in 40 ml LB (supplemented with 100 µg/ml ampicillin) overnight. Cells were sub-cultured into 1 L of LB (supplemented with 100 µg/ml ampicillin) and grown at 37 ^{o}C to mid-log phase before being supplemented with IPTG (to a final concentration of 0.4 M). The culture was grown for a further 3 hours at 37 ^{o}C before being collected by centrifugation at 3,500 x g and stored at -80 ^{o}C.

To purify HapR, the pelleted cells (post-IPTG induction) were re-suspended in 40 ml Buffer 1 before lysis using a tip sonicator. The lysed cells were centrifuged at 75,000 x g for 30 minutes at 10 ^{o}C and the pellet was re-suspended in 40 ml Buffer 2. This was then centrifuged again at 75,000 x g for 30 minutes at 4 ^{o}C and the pellet was re-suspended in 40 ml Buffer 3. After a further 30-minute centrifugation, the supernatant was run through a nickel column using an AKTA Prime. The column was washed with Buffer A and the flow-through was collected. Thereafter the column was washed with increasing concentrations of imidazole (increasing ratio of Buffer B to Buffer A) and fractions were collected at intervals.

To identify fractions with HapR we used SDS-PAGE to analyse samples. Bands corresponding to the molecular weight of HapR+6xHis (~24.5 kDa) were found and the corresponding fractions were combined and dialysed overnight at 4 ^{o}C using SnakeSkin tubing

(ThermoFisher) in 1 L Buffer X. Dialysed protein was concentrated with a vivaspin column and concentration was determined by Bradford assay (Bradford, 1976).

2.9.2 Purification of CRP

CRP lysis, dialysis, column wash and stock buffers were prepared (see Table 2.5). *E. coli* M182Δ*crp* cells were transformed with the plasmid, pDCRP-*Vc*, which expresses *V. cholerae* CRP (or mutant derivatives thereof). Cells were grown in 300 ml LB (supplemented with 100 µg/ml ampicillin) overnight. Cells were collected by centrifugation at 3,500 x g, re-suspended in 6 ml CRP lysis buffer and lysed by sonication using a Bioruptor.

A PolyPrep chromatography column (Bio-Rad) was prepared with the addition of 60 mg adenosine 3',5'-cyclic monophosphate agarose (cAMP-agarose; Merck), rehydrated with ddH_20. Sonicated cells were centrifuged at 10,000 x g for 30 minutes at 4 ^oC and the supernatant was passed through a 0.2 µm filter and loaded onto the column. The column was washed with 5 ml CRP dialysis buffer, followed by 5 ml CRP column wash buffer supplemented with 5 mM each of 5' and 3' adenosine monophosphate (AMP). After a final wash with 5 ml CRP column wash buffer, CRP protein was eluted with 5 ml CRP column wash buffer supplemented with 5 mM adenosine 3',5'-cyclic monophosphate (cAMP). 0.5 ml fractions were taken from this wash and run on an SDS-PAGE gel to check for the presence of CRP. Fractions containing CRP were dialysed overnight at 4 ^oC using SnakeSkin tubing (ThermoFisher) in CRP stock buffer.

2.9.3 Purification of V. cholerae RNA polymerase

RNAP lysis, TGED and RNAP stock buffers were prepared (see table 2.5). To purify *V. cholerae* RNA polymerase we used a purification method as first described by Burgess and Jendrisak, 1975. An overnight culture of *V. cholerae* N16961 was sub-cultured into 8 L of LB and grown at 37^{o}C to mid-log phase. Cells were harvested by centrifugation at 3,500 x g and re-suspended in 100 ml of RNAP lysis buffer. The cells were then lysed using a tip sonicator before samples were subjected to centrifugation at 39,000 x g for 45 minutes at 4 ^{o}C. The resulting supernatant was passed through a 0.2 µm filter, then polymin P was added to a final concentration of 0.35 % (v/v). Ammonium sulphate was added gradually to a final concentration of 35 % (w/v) to precipitate RNAP. Protein precipitates were re-suspended in TGED buffer supplemented with 100 mM NaCl and loaded onto a HiTrap heparin column using a 650E advance protein purification system (Waters). The column was washed with TGED + 100 mM NaCl and then fractions were eluted using TGED with increasing concentrations of NaCl (up to 1 M). Appropriate fractions containing RNA polymerase (determined by running fractions on an SDS PAGE gel) were collected and dialysed overnight at 4 ^{o}C using SnakeSkin tubing (ThermoFisher) in RNAP stock buffer. This protocol purifies the core RNAP enzyme; the primary growth phase sigma factor, RpoD, was purified separately in a previous study (Manneh-Roussel et al., 2018).

2.10 *In vitro* transcription assays

Promoters were cloned in plasmid pSR using appropriate restriction enzymes. Resulting plasmids were purified by maxiprep and used for *in vitro* transcription reactions. Purified *Vibrio cholerae* RNAP holoenzyme (4 nM) and RpoD (100 nM) was combined with 30 ng/µl plasmid DNA in TNSC buffer supplemented with BSA (100 µg/ml), ATP (200 µM),GTP (200 µM), CTP (200 µM), UTP (10µM) and α-P^{32}-UTP (5 µCi). Where appropriate, purified CRP (with 0.2mM cAMP) and/or HapR was incubated with plasmid DNA in buffer at 37 ^{o}C for 10 minutes before the addition of polymerase and RpoD. Reactions were incubated at 37 ^{o}C for 10 minutes and stopped with the addition of 1 volume of 2 x STOP solution (see table 2.5). Reactions were run on an 8 % polyacrylamide gel at 80W for approximately 1-2 hours depending on the expected size of transcripts. Resulting gels were dried and exposed overnight to a phosphor screen.

2.11 Radiolabelling of DNA

DNA fragments were prepared prior to radiolabelling using PCR or restriction enzyme based methods. In both cases, pSR plasmid containing a cloned promoter fragment (inserted at EcoRI/HindIII sites) was used. In the enzyme-based method, this plasmid was digested by HindIII and subsequently treated with Calf Intestinal Phosphatase (CIP, supplied by NEB). This DNA was then digested with AatII, run on a 1 % agarose gel, and the desired DNA fragment purified using a gel extraction kit (Qiagen). In the PCR method, fragments were amplified using pSR footprinting fwd/rev primers (see table 2.3). One of the primers used in was tagged with biotin, which prevents radiolabelling at the 5’ end.

Prepared fragments were then radiolabelled with P^{32}-labelled γ-dATP (10 µCi/µl) and T4 polynucleotide kinase (PNK, supplied by NEB) following the manufacturers protocol. Fragments were passed sequentially through two separate columns containing 200 µl G-50 Sephadex beads in TE buffer.

2.12 Electrophoretic mobility shift assays

Protein stocks were diluted to appropriate working concentrations in 1 x TNSC buffer. Stocks of CRP (or mutant derivatives thereof) were prepared with 250 µg/ml cAMP. Herring sperm DNA (to a final concentration of 12.5 mg/ml per reaction) was mixed with radiolabelled DNA fragments as a non-specific competitive inhibitor. DNA mixtures were incubated at 37 ^{o}C for a minimum of 10 minutes with or without protein mixes (refer to figure legends of results) in 1 x TNSC buffer. After incubation, samples were separated by electrophoresis at 200 V on a 5 % (w/v) polyacrylamide gel for approximately 2-3 hours before drying and exposing overnight to a phosphor screen.

2.13 DNaseI footprinting

Radiolabelled DNA fragments (between 10 and 40 ng) and 25 µg/ml of herring sperm DNA (a non-specific competitive inhibitor) were combined in a 1 x TNSC buffer. This mixture was then incubated with HapR, and/or CRP, if required (refer to figures of results) for 15 minutes at 37 ^{o}C. Recombinant DNaseI (Thermo Fisher) was diluted in dH_2O at a ratio of 1:15 and 2 µl of this was added to the DNA mixture. The DNA was digested for 5 minutes and the reaction was then quenched with the addition of 10 volumes of DNaseI Stop solution (see table 2.5). 10 volumes of phenol:chloroform:isoamyl alcohol (25:24:1) was added, a vortex mixer was used to homogenise the sample and the aqueous layer was separated from the organic phase by centrifugation at 21,000 x g for 3 minutes. The supernatant was removed and DNA was precipitated with 450 µl 100 % (v/v) ethanol and 2 µl GlycoBlue for 1 hour at -80 ^{o}C. The DNA was centrifuged at 21,000 x g and the DNA pellet was then washed with 1 ml 70 % (v/v) ethanol. After centrifugation at 21,000 x g for 10 minutes at 4 ^{o}C, the DNA was dried under a vacuum for 8 minutes and resuspended in 8 µl of DNaseI blue (see table 2.5). Samples were heated to 80 ^{o}C before running on an 8 % (w/v) polyacrylamide gel at 80 W for approximately 2 hours. The gel was then dried and exposed overnight to a phosphor screen.

2.14 GA ladder preparation

Radiolabelled DNA fragments were treated with 50 µl formic acid and incubated at room temperature for 2.5 minutes. The reaction was stopped with 200 µl 0.3 M sodium acetate (pH 7) and 1 µl of GlycoBlue (Thermo Fisher). DNA was precipitated with 700 µl 100 % (v/v) ethanol for at least 45 minutes at -80 ^{o}C before centrifugation at 21,000 x g for 1 hour at 4 ^{o}C. The DNA pellet was washed three times with 1ml 70 % (v/v) ethanol, centrifuging at 21,000 x g for 10 minutes at 4 ^{o}C each time. The DNA was then resuspended in 100 µl 0.1 M piperidine and incubated at 90 ^{o}C for 30 minutes before precipitating with 10 µl 3 M sodium acetate (pH 7), 1 µl of GlycoBlue and 300 µl 100 % (v/v) ethanol. The DNA was incubated for 45 minutes at -80 ^{o}C before centrifugation at 21,000 x g for 1 hour at 4 ^{o}C. The pellet was washed twice with 1 ml 70 % (v/v) ethanol as before. The pellet was then dried under a vacuum for 8 minutes and resuspended in 20 µl of DNaseI blue solution (see table 2.5).

Chapter 3
Assessing **hapR** *and* **luxO** *promoter mutants*

3.1 Introduction

The promoters for expression of two quorum-sensing proteins in *Vibrio cholerae*, HapR and LuxO, were explored in this chapter. As noted earlier, these proteins are of interest because of their role in regulating the *V. cholerae* infection cycle and to their sequence variability across clinical isolates. Figure 3.1 shows the ratio of non-synonymous to synonymous mutations across *V. cholerae* chromosome I (the larger of the two chromsomes in*V. cholerae*). The plot is derived from the cumulative number of SNPs across all clinical isolates from a 2017 whole-genome sequencing study (Weill et al., 2017). Some single nucleotide polymorphisms (SNPs) at the *luxO* and *hapR* loci are found within the corresponding promoter regions. Therefore, we aimed to assess the consequences of these mutations for gene expression. To do this, we cloned wild-type and mutated versions of the *hapR* and *luxO* promoter regions in pRW50-T, upstream of a *lacZ* reporter gene. *V. cholerae* E7946 was transformed with these constructs by conjugation and β-galactosidase assays were done to determine the levels of gene expression. We detected a mixture of effects with some mutations greatly reducing promoter activity.

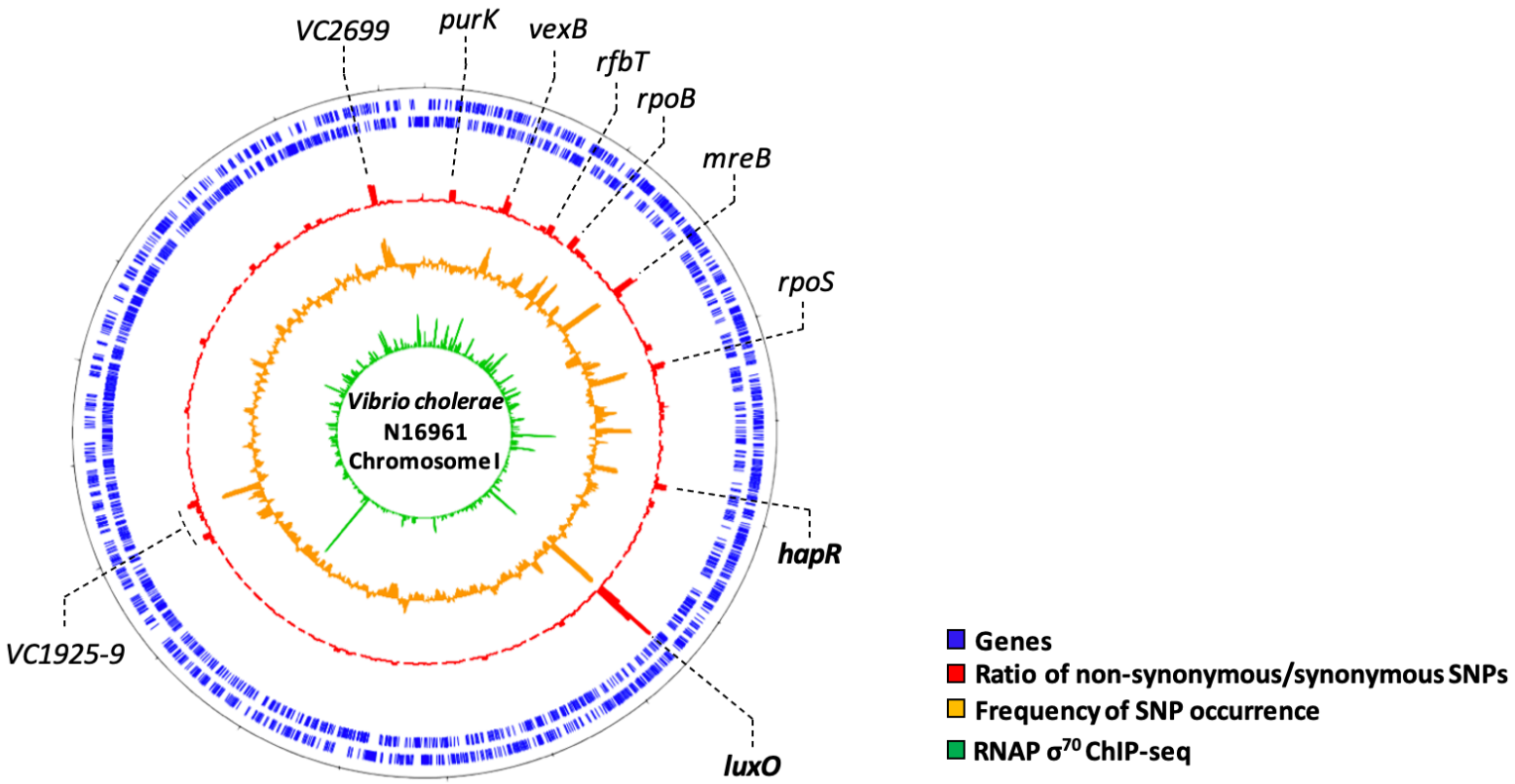

Figure 3.1 – *V. cholerae* chromosome I mutation rates within the 7PET lineage. Genes with a high ratio of non-synonymous mutations shown as peaks on the red track. The overall rate of SNP occurrence is in orange; many genes accumulate SNPs that do not cause mutations. ChIP-seq data describing the binding of the housekeeping RNA polymerase at promoters across the genome is shown in green. SNP data from Weill et al., 2017.

3.2. The effect of naturally occurring mutations within the *hapR* promoter

To replicate the occurrence of SNPs observed in clinical isolates of *V. cholerae*, we generated six mutated versions of the *hapR* promoter (referred to as P_{hapR} M1-6), each with a single nucleotide divergent from the wild-type promoter (as detailed in figure 3.2). SNPs within the promoter region of *hapR* were only observed at these six loci across clinical isolates (Weill et al. 2017). Point mutations were located downstream of the transcription start site (P_{hapR} M1-3) and within the -10 or -35 elements of the promoter (P_{hapR} M4-6). The results of β-galactosidase assays are shown in figure 3.2. pRW50-T without a promoter inserted upstream of *lacZ* was used to determine background activity. Mutant 1 showed an increase in activity compared to wild-type while Mutants 2 and 3 showed a slight decrease in activity. The P_{hapR} M4-6 derivatives showed a complete loss of activity.

3.3 The effect of naturally occurring mutations within the *luxO* promoter

Five mutant *luxO* promoters, referred to as P_{luxO} M1-5, were cloned in pRW50-T (sequences detailed in figure 3.3). Unlike the *hapR* promoter, none of the *luxO* promoters were mutated at known promoter elements. Consistent with this, P_{luxO} M1-4 showed no difference in β-galactosidase activity compared to wild-type (results presented in figure 3.3). Interestingly, P_{luxO} M5 did show a slight increase in activity.

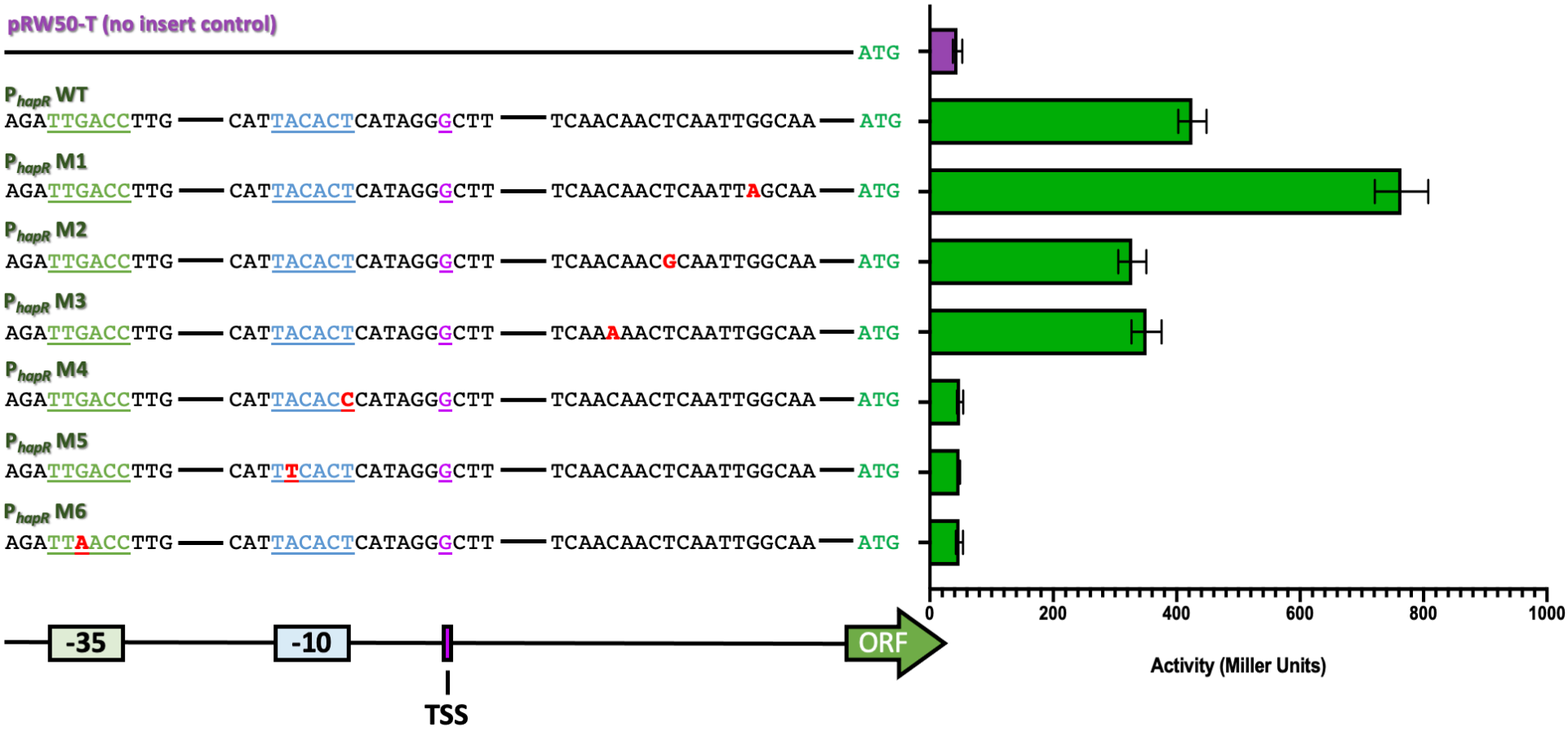

Figure 3.2 – Effect of mutations on *hapR* promoter activity. β-galactosidase assay of promoter-*lacZ* fusions in plasmid pRW50-T compared with a no-insert control (n=3). *-35*, *-10* and transcription start sites indicated in green, blue and purple respectively. Point mutations which differentiate mutant promoters from the wild-type (E7946) promoter sequence are highlighted in red. Transcription start site determined using data from Papenfort et al. (2015).

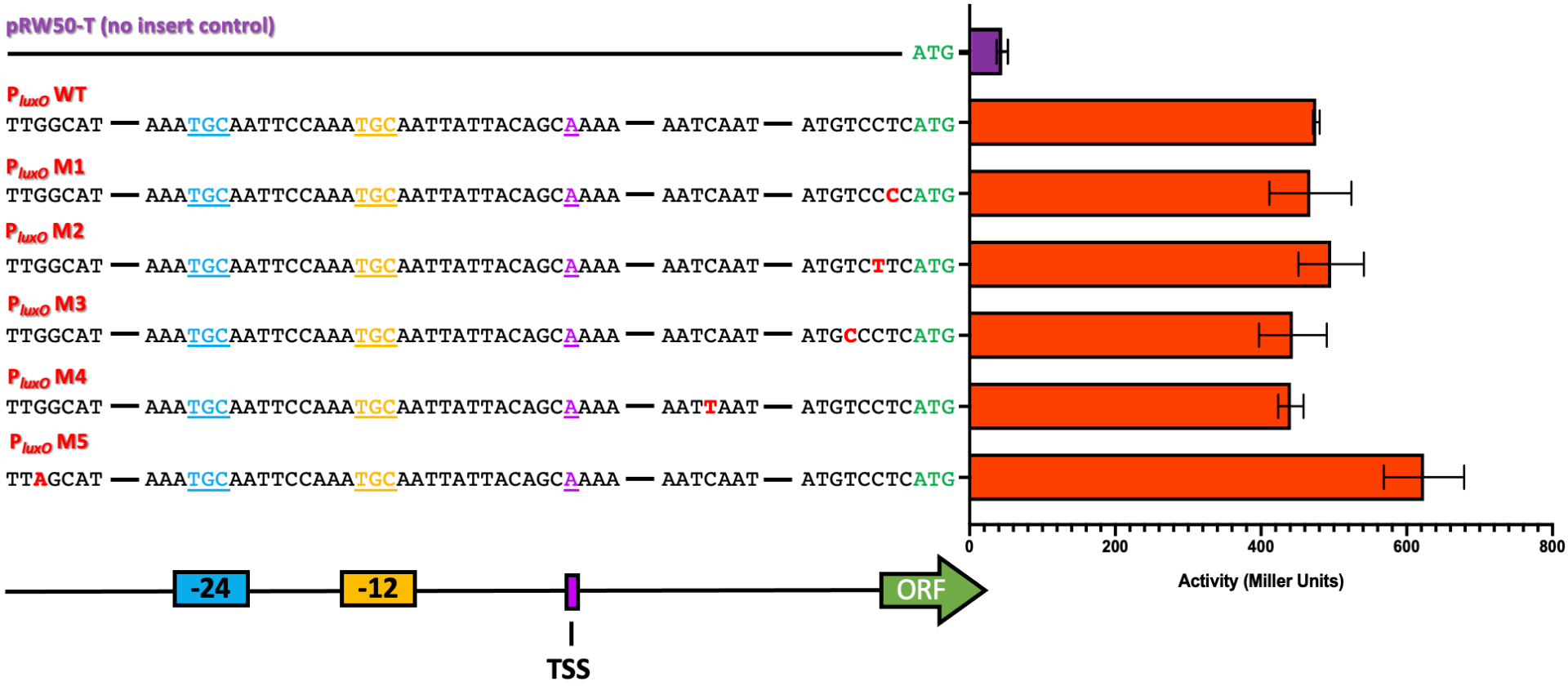

Figure 3.3 – Effect of mutations on *luxO* promoter activity. β-galactosidase assay of promoter-*lacZ* fusions in plasmid pRW50-T compared with a no-insert control (n=3). Possible *-24*, *-12* and transcription start sites indicated in blue, yellow and purple respectively. Point mutations which differentiate mutant promoters from the wild-type (E7946) promoter sequence are highlighted in red. Transcription start site determined using data from Papenfort et al. (2015).

3.4 Primer extension analysis of *hapR* and *luxO* promoter mutants

The increases in β-galactosidase activity observed for P_{hapR} M1 and P_{luxO} M5 may have been due to the introduction of additional core promoter elements. For example, the point mutation made for P_{luxO} M5 (as 'T**G**GCAT' to 'T**A**GCAT') may have resulted in the creation of a new -10 element, and transcription start site, upstream of *luxO*. Any such transcript would differ in compared to the canonical *luxO* mRNA. Hence, we used a primer extension assay, to determine the lengths of transcripts derived from the wild-type and mutant promoters. The results of the primer extension assay are shown in figure 3.4. Both P_{hapR} M1 and P_{luxO} M5 showed no difference in transcript length when compared to wild-type.

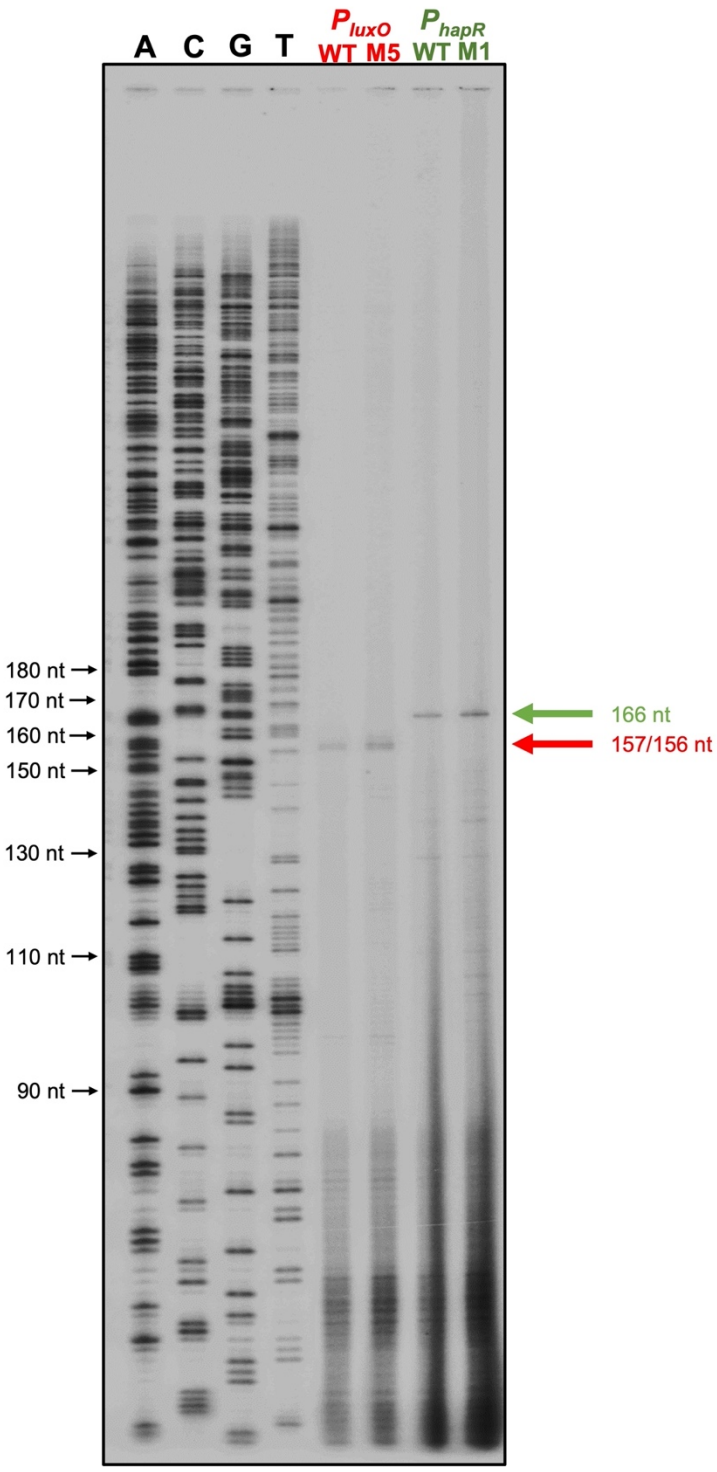

Figure 3.4 – Primer extension analysis of WT and mutant P_{luxO} and P_{hapR}. A radiolabelled (P^{32}) primer complementary to the expected mRNA, was annealed and used to prime reverse transcription. Resulting DNA products were analysed on an acrylamide gel. *luxO* promoter Mutant 5 and *hapR* promoter Mutant 1 are labelled M5 and M1 respectively. As a size standard, bacteriophage DNA (M13mp18) was used to generate dNTP sequencing ladders (labelled 'A', 'C', 'G' and 'T'). Transcription start sites for *hapR* and *luxO* are indicated by green and red arrows respectively.

3.5 Discussion

This part of the study set out to determine whether mutations in the *hapR* and *luxO* promoters, observed in clinical isolates, gave rise to changes in promoter activity. Our β-galactosidase assay results show that three of the SNPs found in the *hapR* promoter region completely ablate gene expression. We expected this because the mutations occur at highly conserved bases in the -10 or -35 elements of the promoter. Mutations in P_{hapR} M4 and M5 change the -10 element in the promoter from a consensus 'T**A**CAC**T'** to 'T**T**CACT' and 'TACAC**C**' respectively. The mutation in P_{hapR} M6 alters the -35 element from a consensus 'TT**G**ACC' to 'TT**A**ACC'. Interestingly however, we observed an almost 2-fold increase in expression from P_{hapR} M1 compared to wild-type. The M1 mutation occurs downstream of the transcription start site and does not appear to introduce a higher-consensus Shine-Dalgarno sequence, which might enhance ribosome binding. Our primer extension analysis did not shed any further light on this, as no changes to the length of the mRNA transcript were observed. It could be that this mutation results in increased mRNA stability allowing for greater gene expression.

Expression of HapR has been shown to vary across different *V. cholerae* strains, though the reason for this is unknown (Joelsson et al., 2006). It has been speculated that gene regulation by HapR may provide advantages in some environments and not others. An example of this has been observed in the fruit-fly, *Drosophila melanogaster*. During colonisation of the intestine, it was shown that uptake of host succinate by *V. cholerae* was reduced by HapR (Kamareddine et al., 2018). Succinate metabolism is important in the infectious cycles of many bacteria, including in *Salmonella* Typhimurium, where succinate is both a carbon source and an inducer of antimicrobial resistance genes (Spiga et al., 2017;

Rosenberg et al, 2021). In *V. cholerae*, reduced succinate uptake led to longer periods of infection, due to increased host survival, and would likely mean that more *V. cholerae* cells were shed from the host. It is therefore easy to see why HapR might benefit the bacterium in a host-environment. However, expressing genes which limit nutrient uptake is likely to be disadvantageous in a nutrient-limited environment. In these instances, it may be more efficient to express HapR either minimally or not at all. In contrast to *hapR*, mutations in the promoter region of *luxO* appeared to have little effect on gene expression. It is possible, however, that the mutations made affect the binding of other transcription factors expressed only under certain conditions. Most of the mutations in the *luxO* promoter were located downstream of the transcription start site, meaning they may affect the stability of the mRNA transcript and thus alter LuxO expression.

Chapter 4
ChIP-seq of HapR and LuxO

4.1 Determining DNA-binding sites of HapR and LuxO in *V. cholerae* E7946 by ChIP-seq

As shown in the previous chapter (figure 3.1), the quorum-sensing transcription factors, HapR and LuxO, are highly variable amongst clinical isolates of 7PET *V. cholerae* (Weill et al., 2017). Determining which genes are regulated by both proteins is therefore important for our understanding of this pandemic. In this chapter, we used chromatin immunoprecipitation and DNA sequencing (ChIP-seq) to map genome-wide DNA binding by HapR and LuxO in *V. cholerae* E7946. To do this, we cloned *hapR* and *luxO* in plasmids pAMNF and pAMCF respectively. pAMNF encodes a 3xFLAG tag directly upstream of a multiple cloning site and kanamycin resistance gene. pAMCF contains a 3xFLAG tag directly downstream of a multiple cloning site and kanamycin resistance gene. *V. cholerae* E7946 were transformed with these plasmids and the resulting strains were used for ChIP-seq assays. After cross-linking and sonication, immunoprecipitations were done using anti-FLAG antibody. In control experiments, we used *V. cholerae* E7946 transformed with empty pAMNF or pAMCF. DNA libraries were produced from isolated DNA and sequenced using an Illumina MiSeq. Sequencing reads were mapped to the *V. cholerae* N16961 reference genome and are presented as circular plots in figure 4.1a. Examples of identified peaks are shown in figure 4.1b and c. For HapR, the example peak centre is located directly upstream of the gene VC1280, which indicates HapR regulates this gene via interaction with its promoter. For LuxO, the example peak centre is located between genes VCA0040 and VCA0041; this coincides with the quorum-regulatory RNA 2 (*qrr2*). Overall, 32 peaks were found to meet our selection criteria for HapR, and five were observed for LuxO.

a)

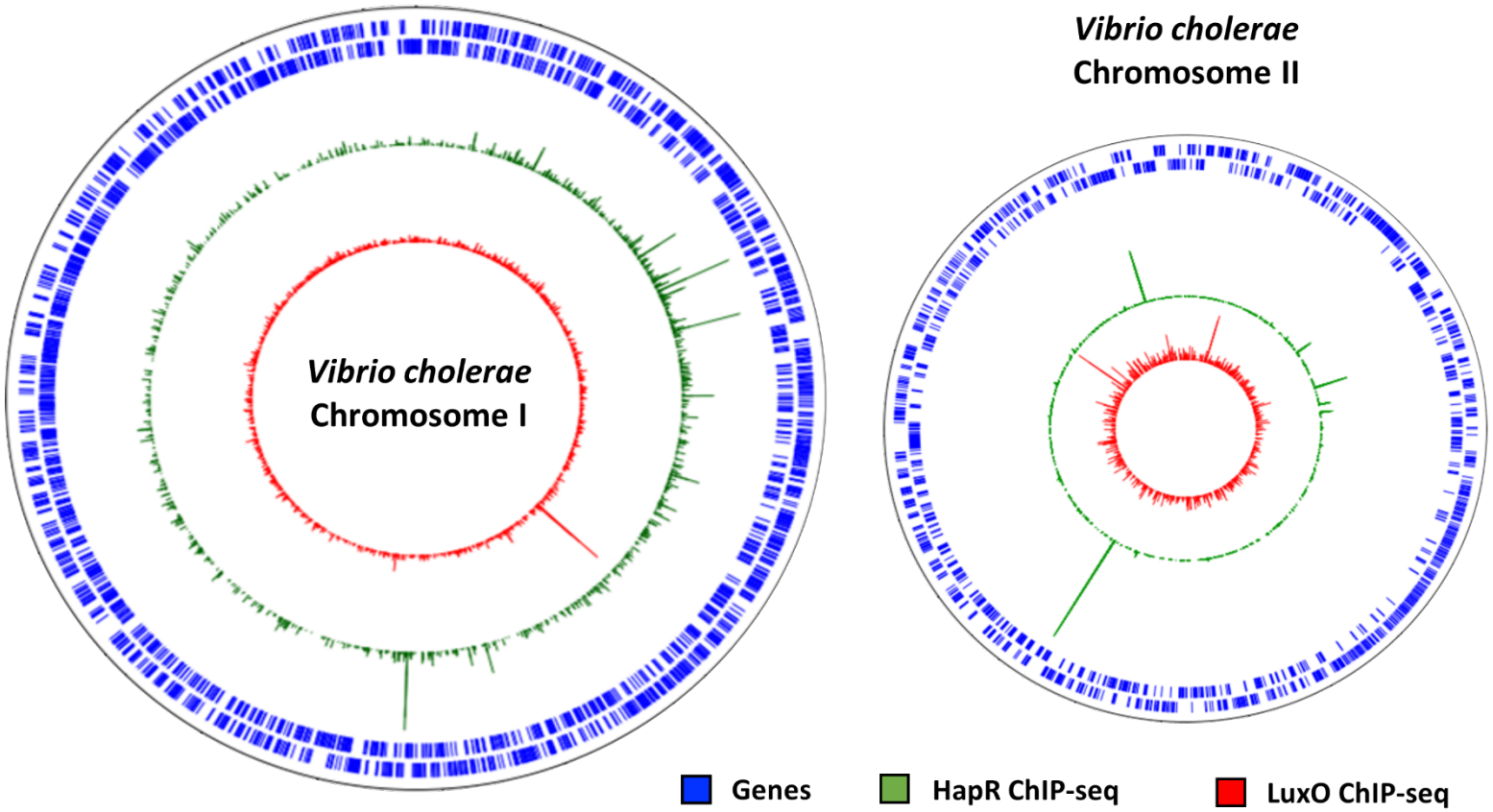
Vibrio cholerae
Chromosome I
Vibrio cholerae
Chromosome II
Genes
HapR ChIP-seq
LuxO ChIP-seq

b)

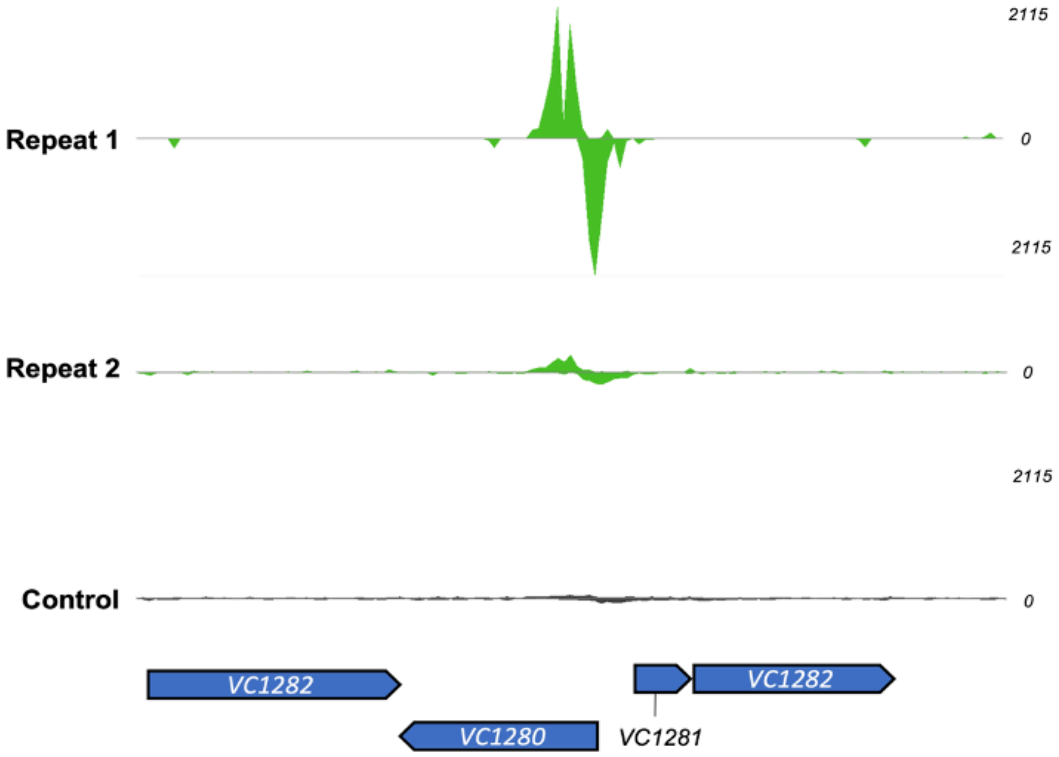
Repeat 1
2115
0
2115
Repeat 2
0
2115
Control
0
VC1282
VC1282
VC1280
VC1281

c)

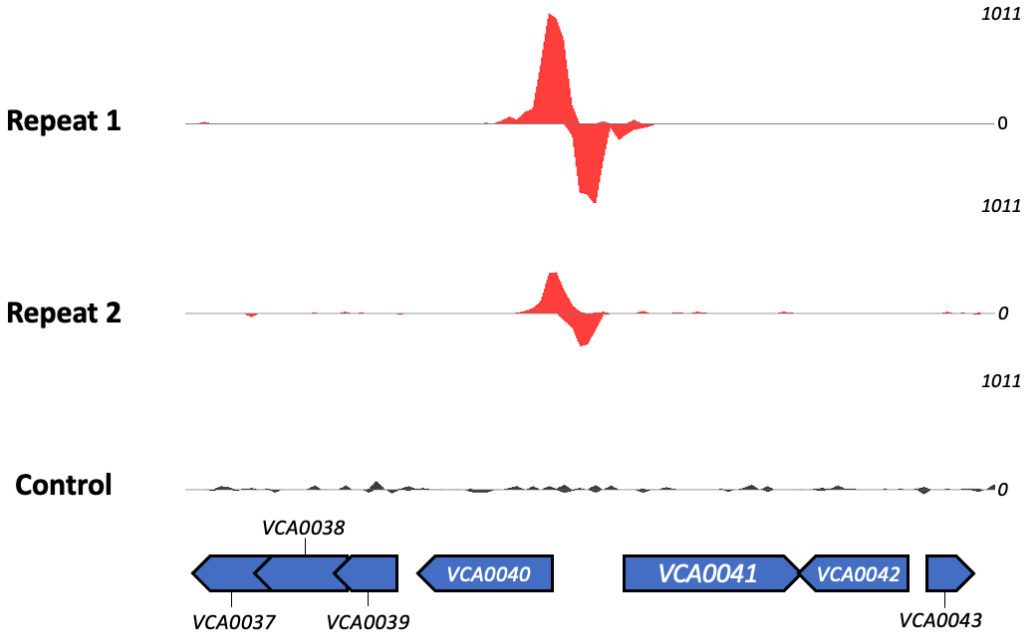
Repeat 1
1011
0
1011
Repeat 2
0
1011
Control
0
VCA0038
VCA0040
VCA0041
VCA0042
VCA0037
VCA0039
VCA0043

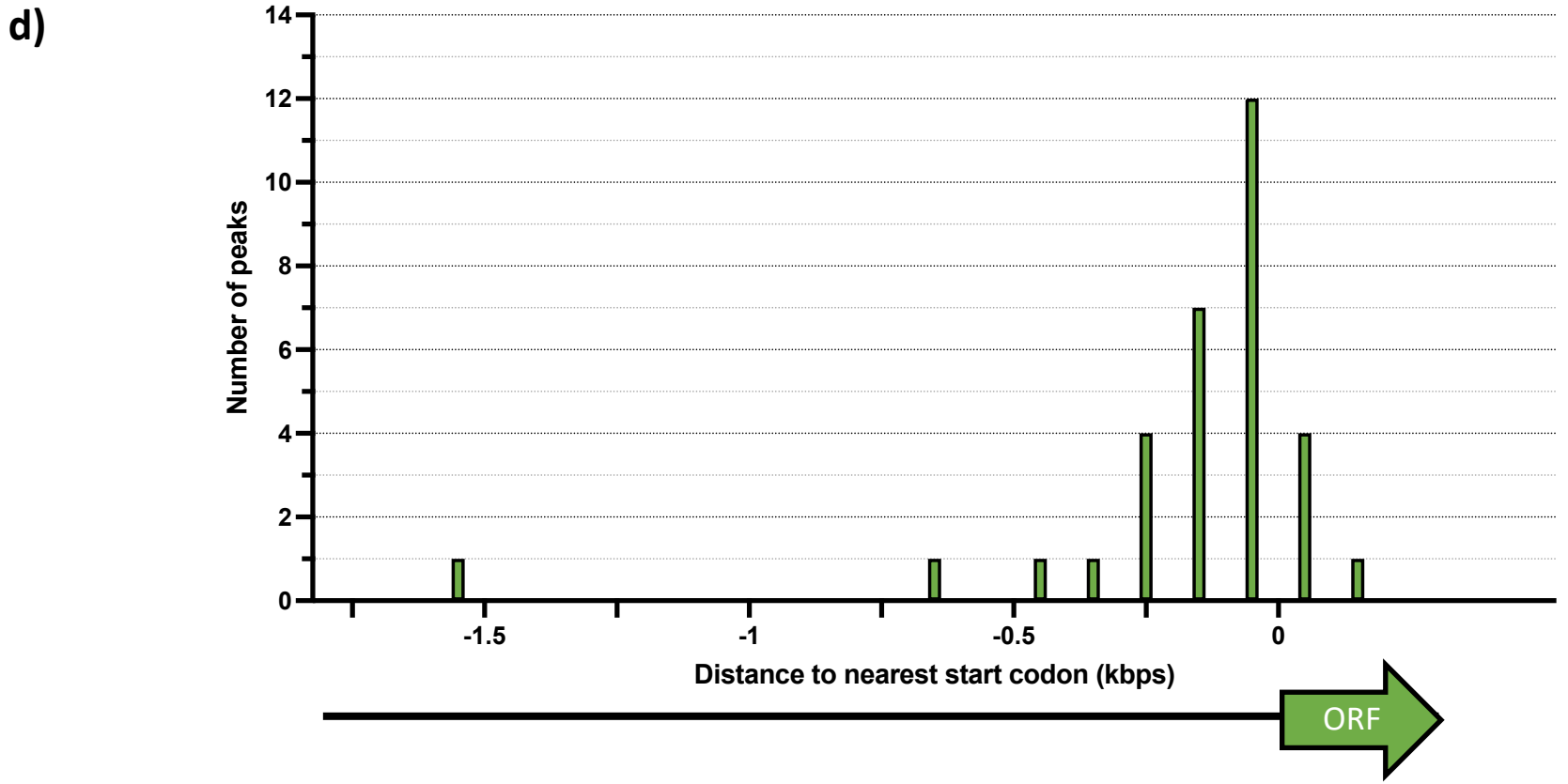

Figure 4.1 – ChIP-seq of HapR and LuxO in *V. cholerae* E7946. a) Circular plot showing the distribution of peaks displayed across both chromosomes. Examples of individual peaks (from two replicates and a negative control) and adjacent genes displayed for b) HapR and c) LuxO. Read depths for each trace are displayed on the right. d) Distance of HapR peaks from nearest start codons. *V. cholerae* N16961 was used as reference genome for ChIP-seq analysis. *Individual replicates of the ChIP-seq data across both chromosomes is displayed in a linear plot in supplementary figure 1.*

We expected most of the peaks for HapR to be in non-coding regions upstream of genes. To determine if this was the case, we mapped distances between all peak centres and their nearest gene (shown in figure 4.1c). Of the 32 peaks observed for HapR, 25 were found within 500 bp upstream of their nearest start codon. Of these, 19 were within 200 bp.

The genes adjacent to the HapR and LuxO peaks are listed in table 4.1. HapR targets are also grouped by cellular function (either known or inferred from their amino-acid sequence) and presented in figure 4.2. 27 percent of these targets are involved in metabolism, and 11.4 percent are motility and chemotaxis-related genes. Other functional categories of identified targets included gene regulation and cellular signalling. It is notable that 34 percent of gene targets were of unknown function. Unsurprisingly, four of the five peaks observed for LuxO are adjacent to the four quorum-regulatory RNAs. The fifth peak is in the intergenic region between two divergent genes encoding the cold-shock like protein, CspD and the ATP-dependent Clp protease adapter protein, ClpS (Heidelberg et al., 2000).

Gene(s)	Function(s)	Category(s)
HapR		
Chromosome I		
VC0102<(VC0103)	hypothetical protein<(hypothetical protein)	Unknown
VC0204<>VC0206	transcriptional regulator, MurR<>N-acetylmuramic acid-6-phosphate etherase, MurQ	Gene Regulation <>Metabolism
VC0240<>VC0241	ADP-L-glycero-D-mannoheptose-6-epimerase, RfaD <> mannose-1-phosphate guanylyltransferase	Metabolism<>Metabolism
VC0433	arginine/ornithine antiporter	Metabolism
VC0484	hypothetical protein	Unknown
(VC0486)	transcriptional regulator, DeoR family	Gene Regulation
(VC0502)	type IV pilin	Motility and chemotaxis
VC0515	hypothetical protein	Unknown
VC0583<>VC0585	hemagglutinin/protease regulatory protein, HapR<>Hypoxanthine phosphoribosyltransferase	Gene Regulation<>Metabolism
VC0668	DNA mismatch repair protein MutH	DNA repair
VC0687<>VC0688	carbon starvation protein A, putative <> lipoprotein, putative	Metabolism<>Structural
(VC0822)>VC0823	inner membrane protein, putative	Unknown
VC0880	conserved hypothetical protein	Unknown
VC0916	phosphotyrosine protein phosphatase	Cell Signalling
VC1280<>VC1281	hypothetical protein <> PTS system cellobiose-specific IIC, CelB	Unknown<>Metabolism
VC1298<>VC1299	methyl-accepting chemotaxis protein <> 6-pyruvoyl tetrahydrobiopterin synthase	Motility and chemotaxis<>Metabolism
VC1375<>VC1376	hypothetical protein <> GGDEF family protein	Unknown<>Cell Signalling
VC1403<>VC1405	methyl-accepting chemotaxis proteins	Motility and chemotaxis
VC1436<(VC1437)	cation transport ATPase, E1-E2 family	Cell Signalling
VC1851	phosphodiesterase	Cell Signalling
VC2211<(VC2212)	hypothetical protein	Unknown

VC2352	NupC family protein	Metabolism
VC2486	leucine transcriptional activator, LeuO	Gene Regulation
	Chromosome II	
VCA0148	TagA-related protein	Metabolism
(VCA0198)	site-specific DNA-methyltransferase, putative	Gene Regulation
VCA0218<>VCA0219	Haemolysin secretion protein HlyB <> Haemolysin, HlyA	Virulence<>Virulence
VCA0224<>VCA0225	hypothetical protein <> conserved hypothetical protein	Unknown<>Unknown
VCA0662<>VCA0663	CbbY family protein <> methyl-accepting chemotaxis protein	Metabolism<>Motility and chemotaxis
VCA0691	acetoacetyl-CoA reductase	Metabolism
VCA0906	methyl-accepting chemotaxis protein	Motility and chemotaxis
VCA0960<>VCA0961	diguanylate cyclase <> hypothetical protein	Cell signalling<>Unknown
VCA1070	sodium/proline symporter	Metabolism
	LuxO	
	Chromosome I	
***qrr*1 <> VC1021**	quorum-regulatory RNA <> transcriptional repressor, LuxO	Gene Regulation<>Gene Regulation
VC1142<>VC1143	cold shock-like protein CspD<>ATP-dependent Clp protease adapter protein, ClpS	Gene Regulation<>Metabolism
	Chromosome II	
qrr2	quorum-regulatory RNA	Gene Regulation
qrr3	quorum-regulatory RNA	Gene Regulation
qrr4	quorum-regulatory RNA	Gene Regulation

Table 4.1 – Genes adjacent to HapR and LuxO ChIP-seq peaks. Brackets indicate peak centre is within gene, arrows indicate if genes are upstream (<) or downstream (>) of peak centres. Functions of genes are given if known.

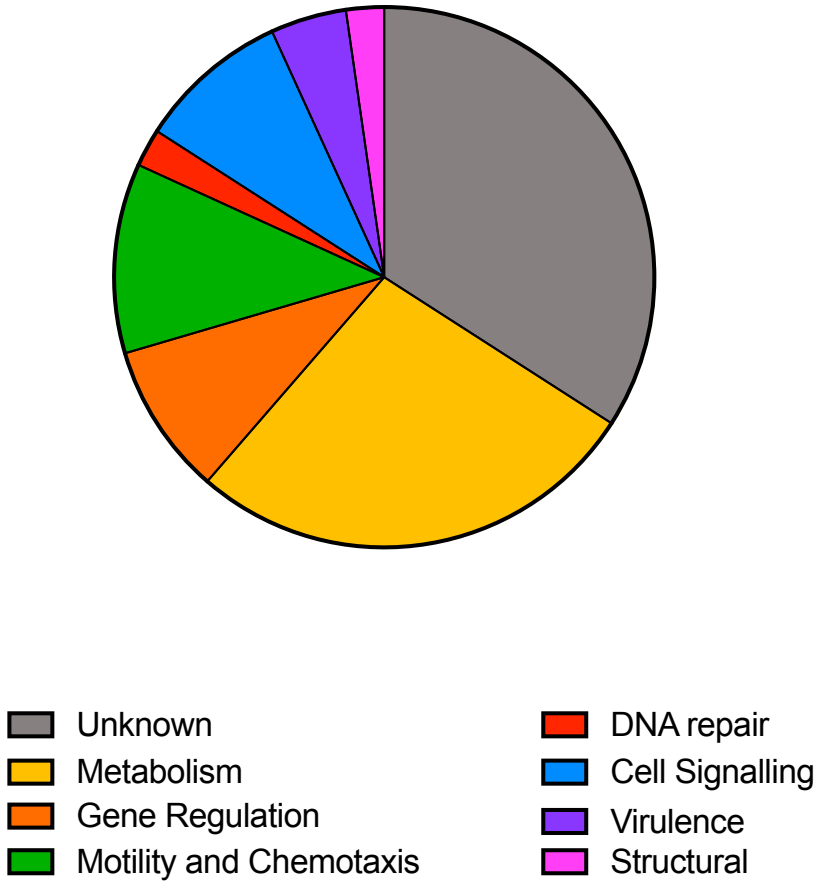

Figure 4.2 – Functional categories of genes adjacent to HapR ChIP-seq peaks. Functions categorised either by known function or assumed function based on structural homology with other proteins.

4.2 Determining DNA-binding motifs from ChIP-seq data

Next, we used MEME (Bailey et al., 2009) to identify the consensus DNA-binding motifs of HapR and LuxO. Figure 4.3 shows the results of this analysis, with the most significant motif for each protein presented. The HapR motif consists of a 22 bp, 'A/T'-rich palindromic sequence with consensus 5'-'$T_1T_2A_3N_4T_5G_6A_7T_8A_9N_{10}A_{11}T_{12}N_{13}T_{14}A_{15}T_{16}C_{17}A_{18}N_{19}T_{20}A_{21}A_{22}$-3'. The '$T_5$' and '$A_{18}$' nucleotides were completely conserved. The LuxO motif identified consists of two hexameric palindromes, 5'-'TTGCAA'-3', either side of an 'A/T' centre. We then analysed these motifs to determine their positions relative to the determined peak centres (figure 4.3c). For HapR, the determined motif trended towards the centre of the peaks, which is expected as peak centres should correspond to the precise position of HapR binding. This contrasts with the control motif (the second most significant motif identified by MEME), which shows no bias in its distribution. Analysis of the MEME-determined LuxO motif shows a similar distribution compared to the control motif, although this is harder to interpret due to the small number of peaks available.

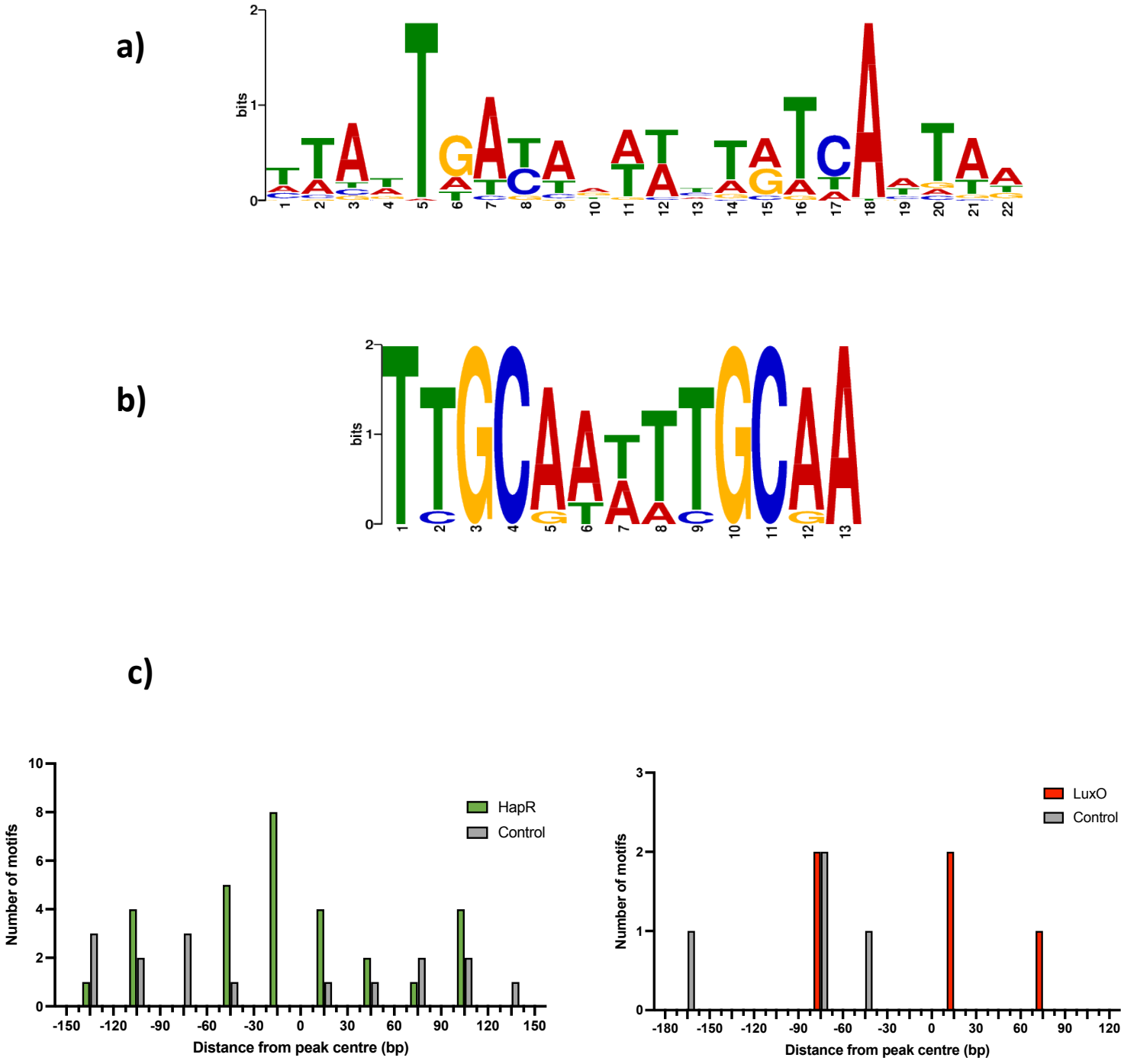

Figure 4.3 – Binding motifs of HapR and LuxO as determined by MEME. DNA-binding motif for a) HapR and b) LuxO as determined by MEME analysis. MEME output was set to determine three potential binding motifs; the most probable motif (based on e-value) is displayed. c) Distances between the DNA binding motifs and the nearest peak centre in *V. cholerae.* Top motifs for HapR and LuxO displayed against the second probable motif as control motifs.

4.3 Assessing the co-regulation of genes using ChIP-seq data

We noticed that the DNA-binding motif for HapR resembled that of the cyclic AMP-receptor protein (CRP) (see figure 4.4), which regulates genes in *V. cholerae* in response to cyclic AMP (cAMP) levels (Kolb et al., 1993; Manneh-Roussel et al., 2018). Therefore, we compared our data for HapR with CRP binding sites identified by a prior ChIP-seq analysis (Manneh-Roussel et al., 2018). In tandem, we also compared our data with binding sites for: AphA (a regulator of low cell density behaviours in *V. cholerae*) (Haycocks et al., 2019), sigma 54 (known to act in tandem with LuxO to activate the quorum-regulatory RNAs) (Dong and Mekalanos, 2012), and the 'housekeeping' sigma factor, σ^{70} (Manneh-Roussel et al., 2018). Most HapR DNA-binding motifs were within 100 bp (upstream or downstream) of the nearest ChIP-seq peak centre (figure 4.3). Therefore, we defined overlapping peaks as peaks with centres within 200 bp of one another. A control analysis, in which one of the two ChIP datasets being compared was replaced with randomised set of genomic loci, was also done. This was designed to allow for overlap between datasets that might have occurred by chance. The results are shown in figures 4.5 and 4.6. A total of 8 CRP peaks were found to coincide with HapR peaks; these loci are predominantly in intergenic regions (see table 4.2). Conversely, there was no overlap between detected HapR and AphA targets. 8 of the 32 HapR targets were bound with σ^{70}. This suggests that many HapR target promoters are inactive in our conditions. For LuxO, 4 out of 5 peaks, located upstream of the quorum-regulatory RNAs and were co-bound with σ^{54}. Three LuxO peaks were also co-bound with AphA. The fifth peak was co-bound with σ^{70}.

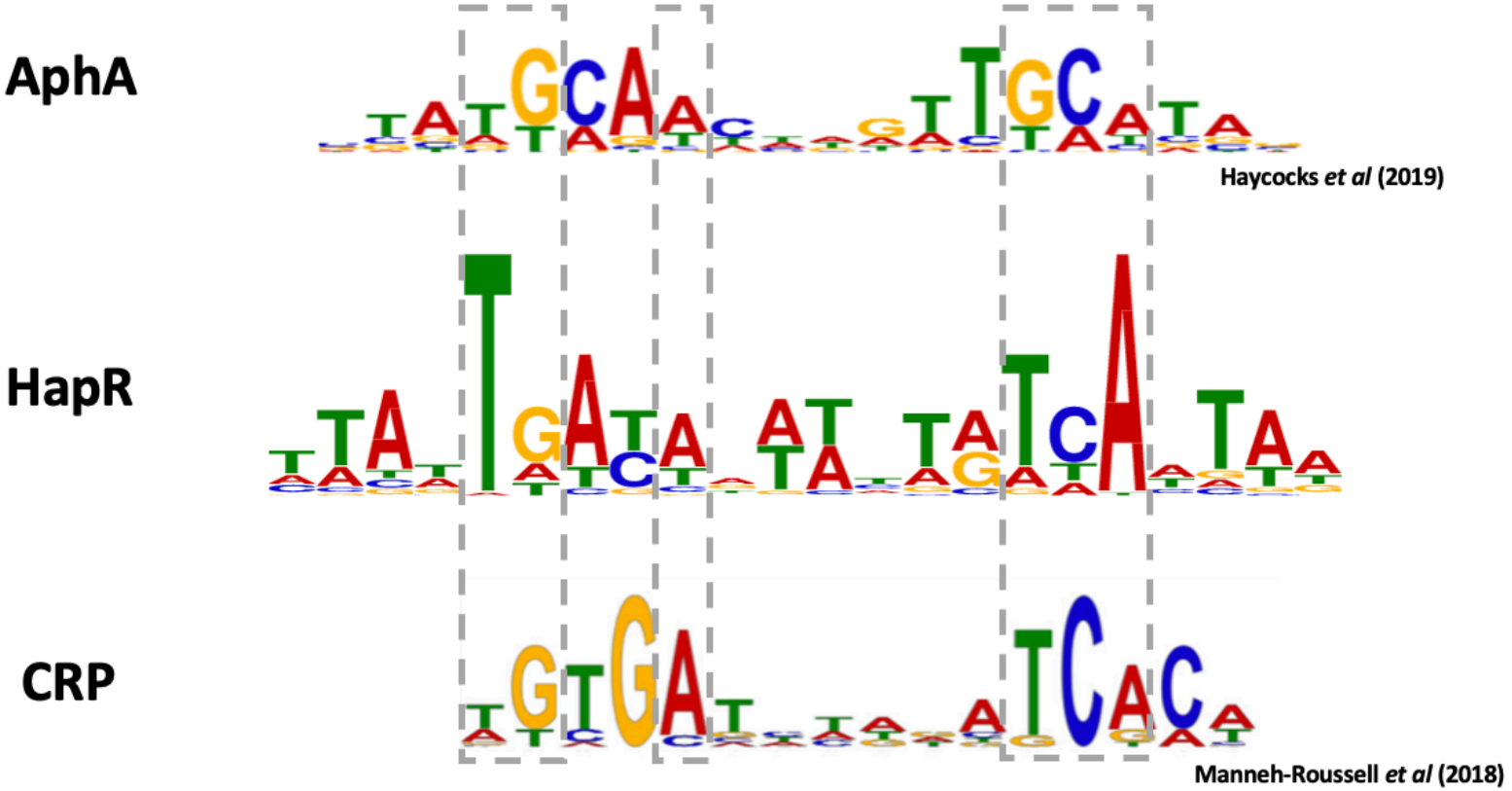

Figure 4.4 – DNA-binding motif of HapR compared to CRP and AphA motifs. Potential alignments between motifs indicated by grey boxes. HapR motif as determined in figure 4.3. CRP motif taken from Manneh-Roussell et al., 2018. AphA motif taken from Haycocks et al., 2019.

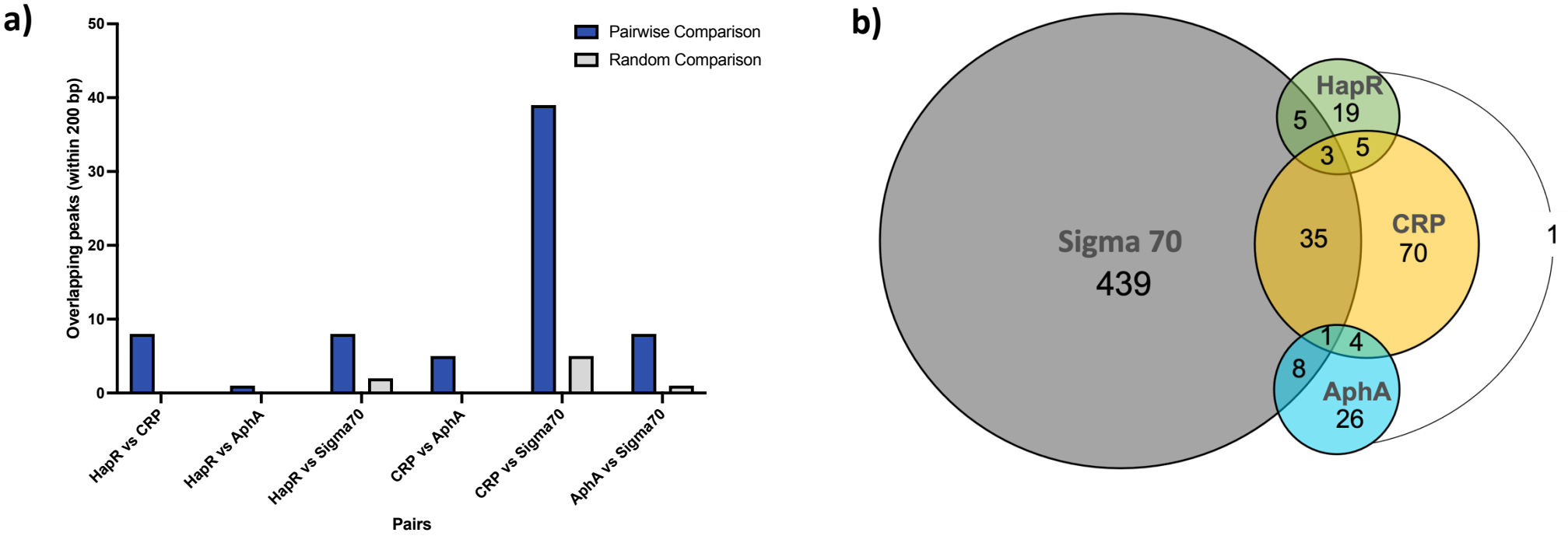

Figure 4.5 – Analysis of HapR ChIP-seq peak data. Loci of peak centres within 200 bp of one another were considered to be 'overlapping peaks'. a) Comparison of pairs of data sets are presented individually against a control analysis. Control analyses were done by generating random peak loci values across the N16961 genome (via the RAND() function in Microsoft Excel) and determining the number of overlaps occurring by chance. b) Overlapping peaks presented a Venn diagram. *ChIP data for CRP, sigma 70 and AphA obtained from other studies referenced in the text.*

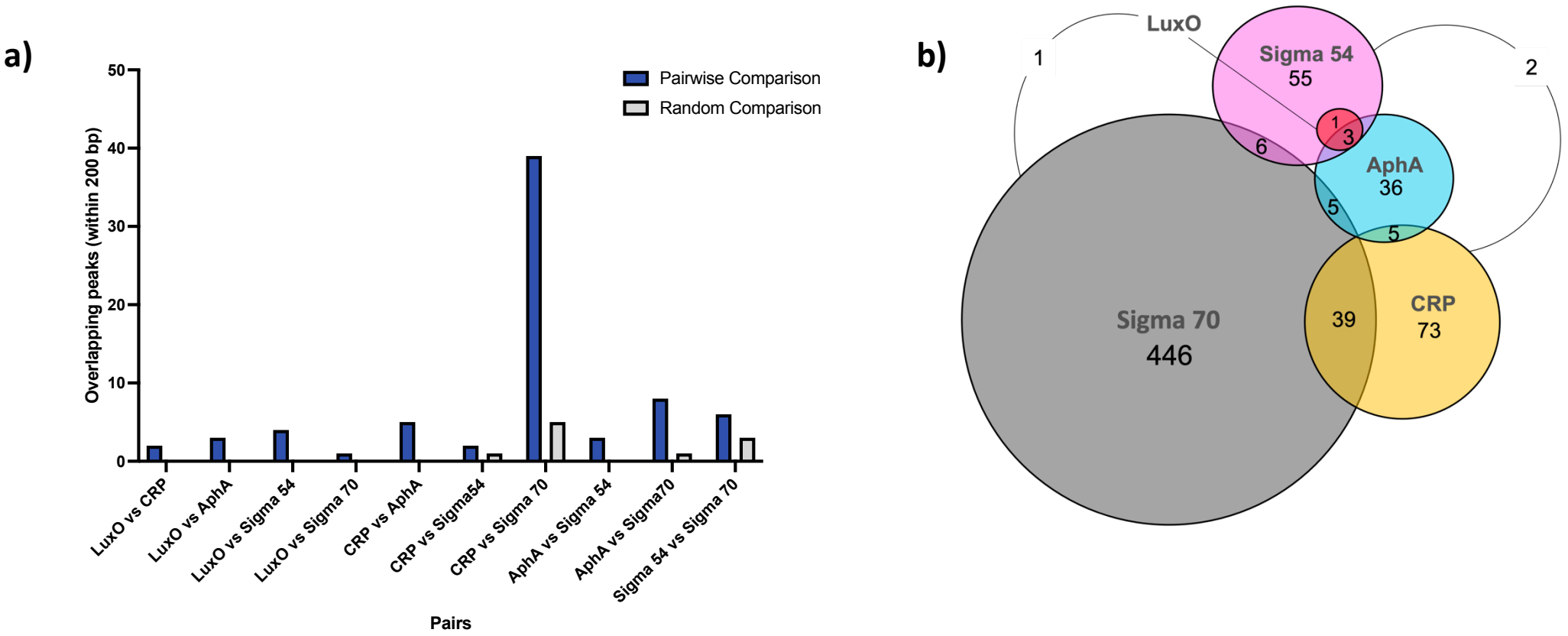

Figure 4.6 – Analysis of LuxO ChIP-seq peak data. Loci of peak centres within 200 bp of one another were considered to be 'overlapping peaks'. a) Comparison of pairs of data sets are presented individually against a control analysis. Control analyses were done by generating random peak loci values across the N16961 genome (via the RAND() function in Microsoft Excel) and determining the number of overlaps occurring by chance. b) Overlapping peaks presented a Venn diagram. *ChIP data for CRP, sigma 70, sigma 54 and AphA obtained from other studies referenced in the text.*

	Chromosome I	Chromosome II
Adjacent Genes	*VC0102<(VC0103)*	*VCA0218<>VCA0219*
	VC0485<>VC0486	*VCA0224<>VCA0225*
	VC1851	*VCA0662<>VCA0663*
	leuO	*VCA0691*

Table 4.2 – Chromosomal loci potentially co-bound by CRP and HapR. ChIP-seq peak centres for HapR (this study) and CRP (Manneh-Rousell et al., 2018)92 were determined and their relative positions on the V. cholerae N16961 reference genome were compared. Overlaps between CRP and HapR binding loci were defined as peak centres within 200 bp of one another. Results in the table show the nearest genes adjacent to these loci. '<>' indicates loci positioned between two divergent genes. Peaks positioned within the ORF of a gene are indicated by brackets.

4.4 Discussion

In this chapter, we aimed to identify novel DNA-binding targets of HapR and LuxO in *V. cholerae*. In the case of HapR, our ChIP-seq data identified 32 peaks, 25 of which were within promoter regions. This expands our list of potential targets to more than 45 transcription units. In these instances, further studies are required to determine if HapR regulates the transcription of one or both genes. In transcriptome analysis, HapR was found to influence the expression of 100 transcription units (Nielsen et al., 2006). Only 21 of the genes identified by this analysis are also identified by our ChIP-seq data, 9 of which are part of a single operon, VC1394-VC1403. It is likely that many of these genes are indirectly regulated by HapR and so not observed by ChIP-seq. Some, targets previously shown to be directly regulated by HapR (i.e., at the level of transcription) such as qstR (Scrudato and Blokesch, 2013), *vpsR* (Lin et al., 2007)*, dns* (Scrudato and Blokesch, 2013), *tcpA* and *tcpP* (Gao et al., 2020) were not identified by our ChIP-seq. This may be due to low levels of HapR binding in our conditions. For example, the well-known HapR target, *hapA* (Jobling and Holmes, 1997), was not recovered, but we did observe a peak in the promoter in one ChIP-seq replicate only. We also identified peaks in the promoters of known HapR targets. For instance, HapR regulates transcription for the *hapR* promoter and a peak was identified at this locus (Lin et al., 2005). Other targets of interest include the genes encoding the haemolysin, *hlyA* and haemolysin secretion protein, *hlyB*, as well as six genes involved in motility and chemotaxis (Yamamoto et al., 1990). A previous study reported 16 chemotaxis-related genes that appeared to be regulated (either directly or indirectly) by HapR (Nielsen et al., 2006).

Targets found closer to the chromosomal origin of replication are more enriched in the data, this can be observed in figure 4.1a. At the point of formaldehyde crosslinking, the cells in our experiment would have been at different stages of genome replication, resulting in a higher copy number of sequences closer to the origin of replication. This may have raised the cut-off threshold for peaks that we have used and peaks closer to the *ter* region of the chromosome may be missed in our analysis as a result. It is also possible that HapR does not bind certain sites under the conditions used in our ChIP-seq experiment and therefore were not found in this study.

In the case of LuxO five peaks were identified in our study. Four of these are at the quorum-regulatory RNA (qrr) 1-4 loci, known to interact with LuxO. The fifth peak is between two divergent genes encoding the cold-shock like protein, CspD and the ATP-dependent Clp protease adapter protein, ClpS. The functions of these proteins have been characterised in *E. coli*. CspD is a protein induced by stationary phase growth as part of the SOS response to carbon starvation (Yamanaka and Inouye, 1997). ClpS is part of the N-end rule pathway in bacteria, which governs the degradation of proteins (Erbse et al., 2006).Given that LuxO phosphorylation is controlled by environmental signals other than cell density, *cspD* is the more likely target of regulation by LuxO. This may indicate a previously undescribed mechanism by which the SOS response and quorum-sensing are linked. It is noteworthy that four out of the five LuxO peaks overlapped with sigma 54 (RpoN) ChIP-seq targets (Dong and Mekalanos, 2012). Unsurprisingly, these peaks all corresponded to the qrrs. Three of these four LuxO peaks also overlapped with AphA targets. This is unsurprising as AphA is known to directly control expression of qrrs 2, 3 and 4 in *Vibrio harveyi* (which were identified by their homology with qrrs 2-4 in *V. cholerae*) (Tu and Bassler, 2007; van Kessel et al., 2013a). The

fifth LuxO peak, located between the two divergent genes mentioned earlier, did not overlap with either σ^{54} or AphA but did overlap with a peak from a σ^{70} ChIP-seq (Manneh-Roussel et al., 2018). It is possible that LuxO may have an extra regulatory role than has hitherto been described in the literature, involving some interaction with σ^{70}.

Previous ChIP-seq studies on the HapR homolog in *V. harveyi*, LuxR, identified a similar DNA target motif to that identified for HapR in our analysis (van Kessel et al., 2013b). Both motifs are a 22 bp palindrome containing the sequences 'TGA' and 'TCA' separated by 8 bp (see figure 4.7). As noted earlier, the motif for HapR resembles the consensus CRP binding site that is also palindromic and contains the sequences 'TGTGA' and 'TCACA' separated by 6 bp (Manneh-Roussel et al., 2018). Hence, it is possible to align the consensus binding motifs for HapR and CRP so that many of the preferred bases match (figure 4.4). This is particularly striking given the significant coincidence of CRP and HapR binding peaks derived from ChIP-seq experiments. We hypothesise that CRP and HapR might co-regulate genes, in either a cooperative or competitive manner, and that this may sometimes involve co-recognition of the same binding sequence. It should be noted however, that the experimental conditions under which ChIP-seq data was obtained may have varied between different studies.

The DNA binding consensus for the low cell density master regulator, AphA, resembles that of both CRP and HapR. This is significant because a previous study has shown that AphA and CRP co-regulate genes and this is sometimes via recognition of the same sequence (Haycocks et al., 2019). Gene regulation by AphA at low cell density leads to the downregulation of natural competence, increase in biofilm formation and the upregulation of virulence factors (Rutherford et al., 2011). This is antithetical to the role played by HapR,

which is a direct repressor of AphA (Kovacikova and Skorupski, 2002). Given the opposing functions of these two genes, we hypothesised that some genes would be competitively co-regulated by HapR and AphA. We therefore compared our ChIP-seq data for HapR to that of AphA as determined by a previous study (Haycocks et al., 2019). Interestingly, only one instance of overlapping peaks was observed. The peaks were located upstream of the gene *VC0102*, which encodes a hypothetical protein of 46 amino acids and unknown function. Because the ChIP-seq of AphA did not identify HapR in its list of targets, it is possible that other HapR/AphA co-regulated genes are missed by one or both datasets. Further investigation into the role of AphA at HapR-regulated promoters is beyond the scope of this project, however, the relationship between HapR and CRP is explored in later chapters.

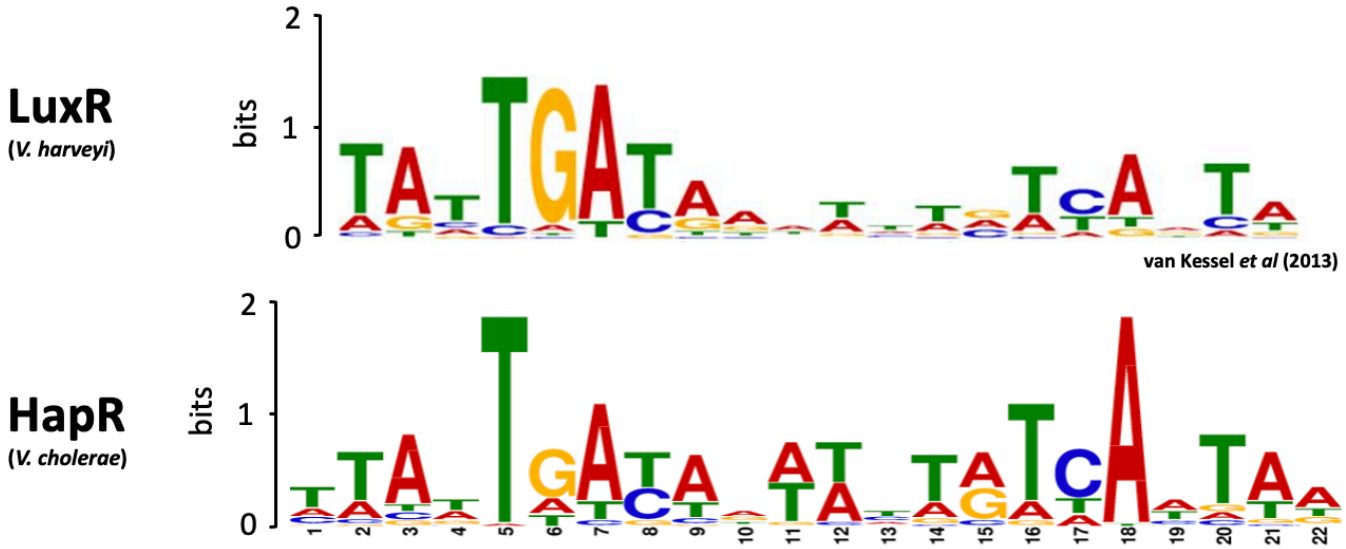

Figure 4.7 – DNA-binding motif of HapR compared to LuxR. HapR motif as determined in figure 4.3. LuxR motif taken from van Kessel et al., 2013b.

Chapter 5

Measuring the impact of HapR at target promoters

5.1 Introduction

Analysis of our ChIP-seq data identified 32 loci of the *V. cholerae* genome to which HapR binds. Binding by HapR at these loci may regulate the transcription of over 40 genes. A selection of HapR targets with functions of interest such as chemotaxis, cell wall metabolism and virulence were the subject of further analysis as described below. Targets of unknown function were excluded. We also analysed the promoter region of the *chb* operon (P_{VC0620}), which regulates chiotbiose utilisation (Meibom et al., 2004). While a peak was not observed at this locus in our ChIP-seq data, *chb* was identified in another study as being directly repressed by HapR (Klancher et al., 2020a).

To analyse promoters of interest, we used *in vitro* transcription and β-galactosidase assays. *In vitro* transcription allows us to identify if HapR acts directly upon promoters to regulate transcription. β-galactosidase assays indicate if HapR controls transcription at promoters, *in vivo,* potentially indirectly or in combination with other factors.

5.2 β-galactosidase assays

To determine the effect of HapR binding on transcription *in vivo*, we cloned 25 of the HapR-targeted promoter regions upstream of a *lacZ* reporter in the plasmid pRW50-T. *V. cholerae* E7946 cells containing the resulting plasmids were transformed with pAMNF (with or without HapR) as in our ChIP-seq assays (Chapter 4). The pAMNF has been used in previous studies for the ectopic expression of *V. cholerae* transcription factors in β-galactosidase assays (Haycocks et al., 2019). Promoter activity, in the presence and absence of plasmid encoded HapR, was the determined by β-galactosidase assay. Cells were grown to mid-log phase ($O.D._{650}$ of approximately between 0.8 and 1.1) before lysis. The results of β-

galactosidase activity of lysates are shown in figure 5.1. All promoters tested were either inactive or not affected by ectopic HapR. We reasoned that this may be due to HapR expression from the E7946 chromosome masking the impact of ectopic HapR. Hence, to minimise chromosomal HapR expression, we repeated the experiment after growing the cells to a lower density before lysis ($O.D._{650}$ of approximately between 0.2 and 0.4). The results (Figure 5.2) show only two promoters, P_{VC1403} and $P_{VCA0219}$, are activated in the presence of HapR.

To ensure no native expression of HapR, we deleted the *hapR* gene of *V. cholerae* E7946. Our pRW50-T promoter fusions were transfered to this strain, and the wild type parent, by conjugation. Because HapR is expressed at high cell density, cells were lysed after growth overnight, rather than being sub-cultured to a specific $O.D._{650}$. The results of this comparison, presented in figure 5.3, show that transcription often differed between the wild-type and *ΔhapR* strains. Five promoters showed an increase in activity upon deletion of *hapR*. Activity from two promoters, P_{V1375} and P_{VC1403}, decreased in the absence of *hapR*.

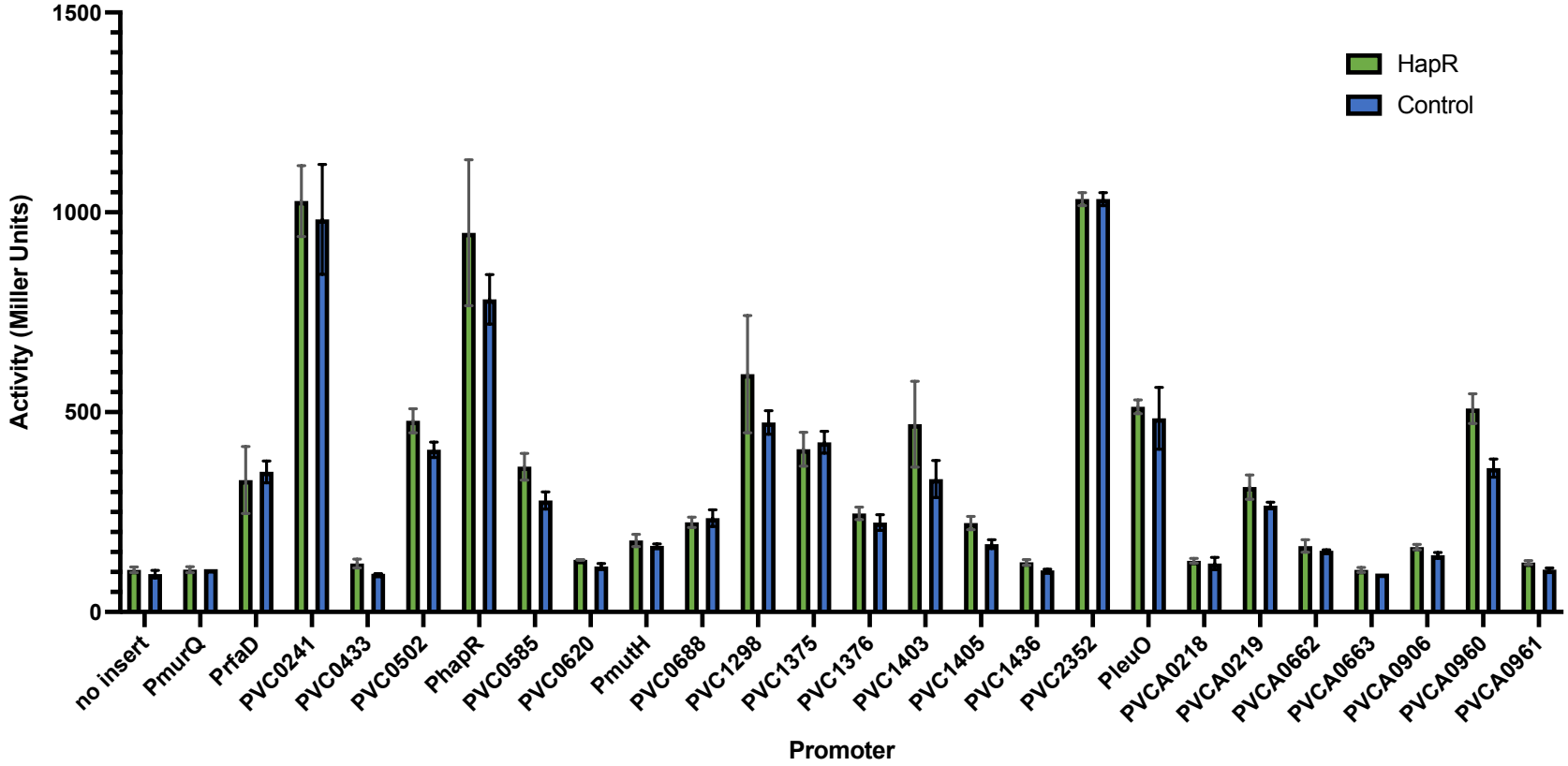

Figure 5.1 – Transcription from HapR-target promoters with and without ectopically expressed HapR in *V. cholerae* E7946. β-galactosidase assay of promoter-*lacZ* fusions in plasmid pRW50-T compared with a no-insert control (n=3). Strains were transformed with a plasmid ectopically expressing HapR (pAMNF-HapR, shown in green) or with a control plasmid (pAMNF, shown in blue).

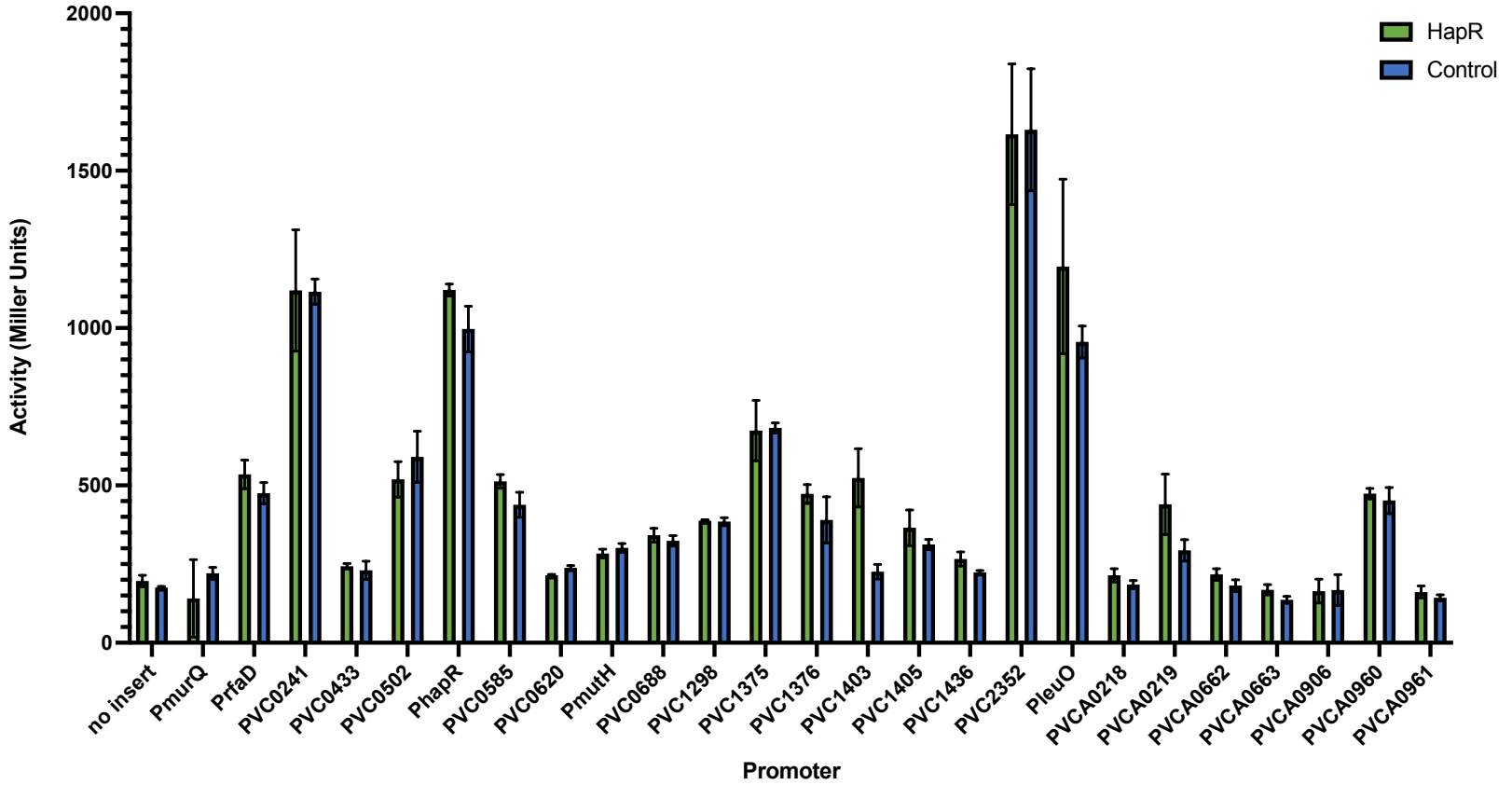

Figure 5.2– Transcription from HapR-target promoters with and without ectopically expressed HapR in *V. cholerae* E7946 (grown to low cell density). β-galactosidase assay of promoter-*lacZ* fusions in plasmid pRW50-T compared with a no-insert control (n=3). Strains were transformed with a plasmid ectopically expressing HapR (pAMNF-HapR, shown in green) or with a control plasmid (pAMNF, shown in blue)

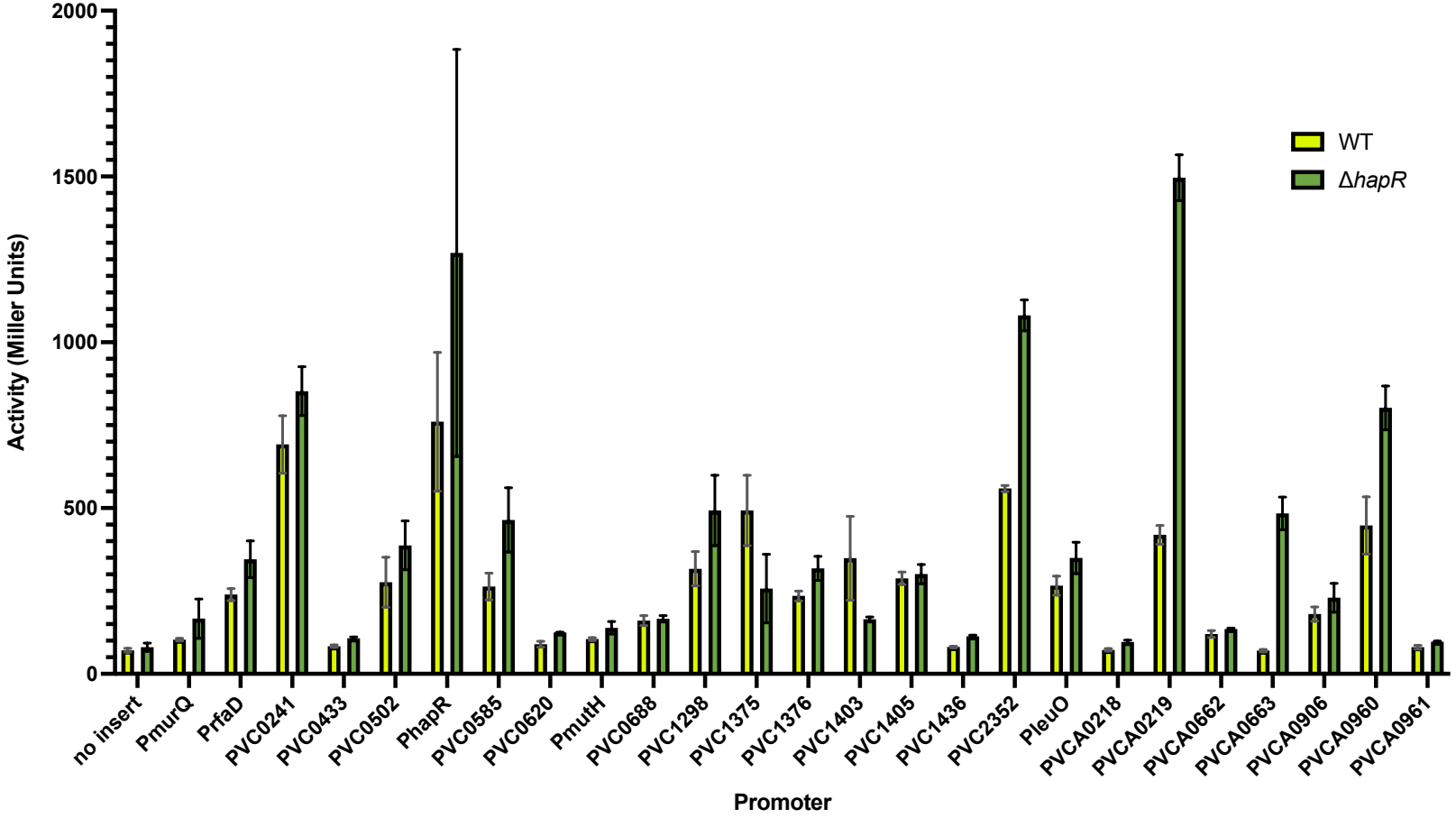

Figure 5.3 – Transcription from HapR-target promoters in WT and Δ*hapR V. cholerae* E7946. β-galactosidase assay of promoter-*lacZ* fusions in plasmid pRW50-T compared with a no-insert control (n=3).

5.3 *In vitro* transcription

Our *in vivo* experiments, while informative, do not confirm direct regulation by HapR at promoters. For example, HapR may act indirectly via the regulation of other genes. Other repressors or activators factors may also confound results *in vivo*.

To determine if effects of HapR on transcription *in vivo* could be explained by direct interaction between HapR and RNAP, we used an *in vitro* transcription assay. Promoters of interest were cloned in a plasmid, pSR, that contains a λ*oop* transcription terminator downstream of the cloned promoter. Transcripts terminating at λ*oop* can be compared to those from a separate σ^{70}-dependent promoter, at the plasmid replication origin, that drives production of the RNA-I transcript. Experiments were done without HapR or with HapR at concentrations ranging from 0.25 μM to 5 μM. For seven target promoters, no transcripts were observed (figure 5.4). Presumably, an undefined activator is needed at these promoters. For six promoters, transcripts observed were unaffected by HapR (figure 5.5). We detected 12 HapR repressed promoters (figure 5.6). For each gel, the red arrow shows the predicted transcript size. The RNA-I band serves as an internal control and is also indicated. The results are summarised alongside our results *in vivo* in table 5.1. In one case (PVC_{1375}) repression of one transcript coincided with increased production of an alternative transcript.

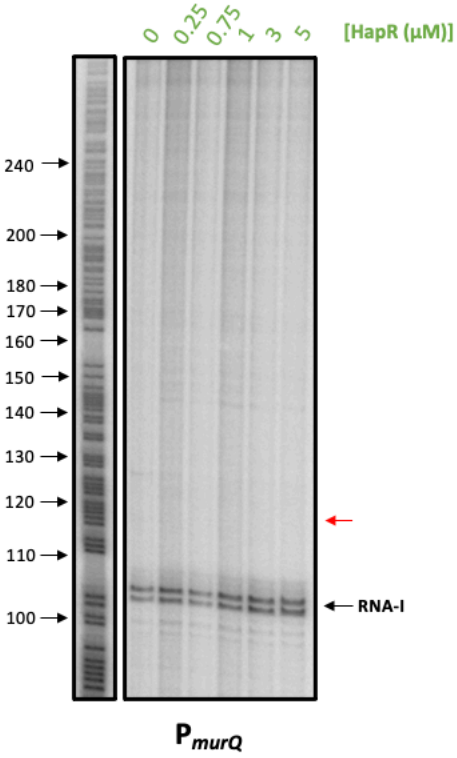

P_{murQ}

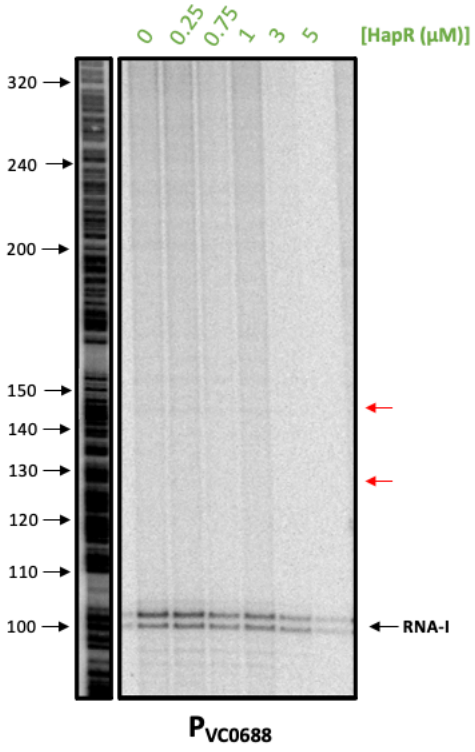

P_{VC0688}

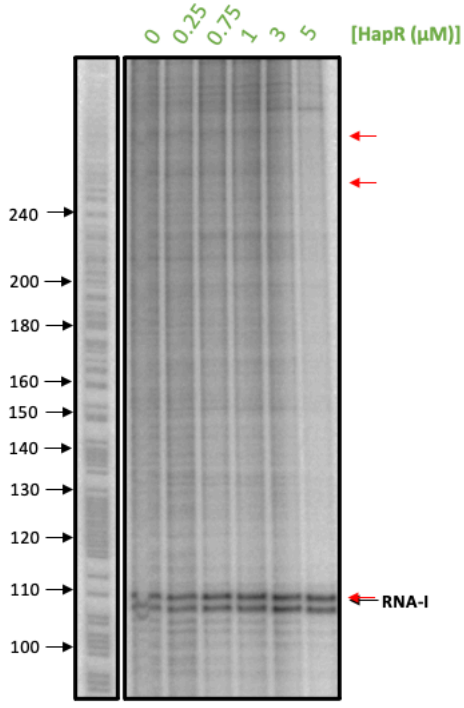

P_{VC1405}

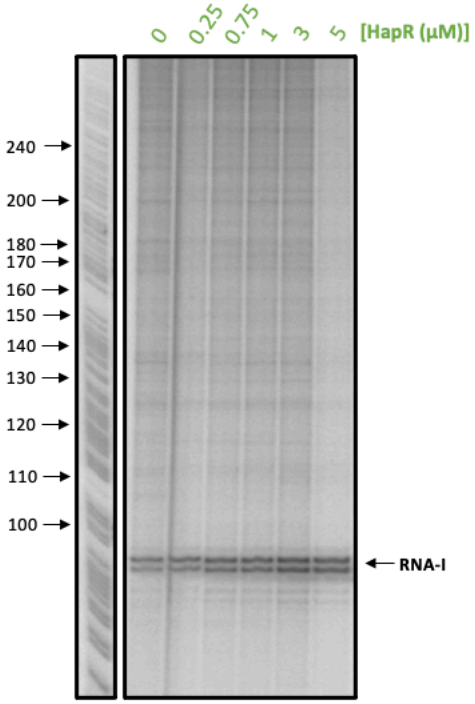

$P_{VCA0218}$

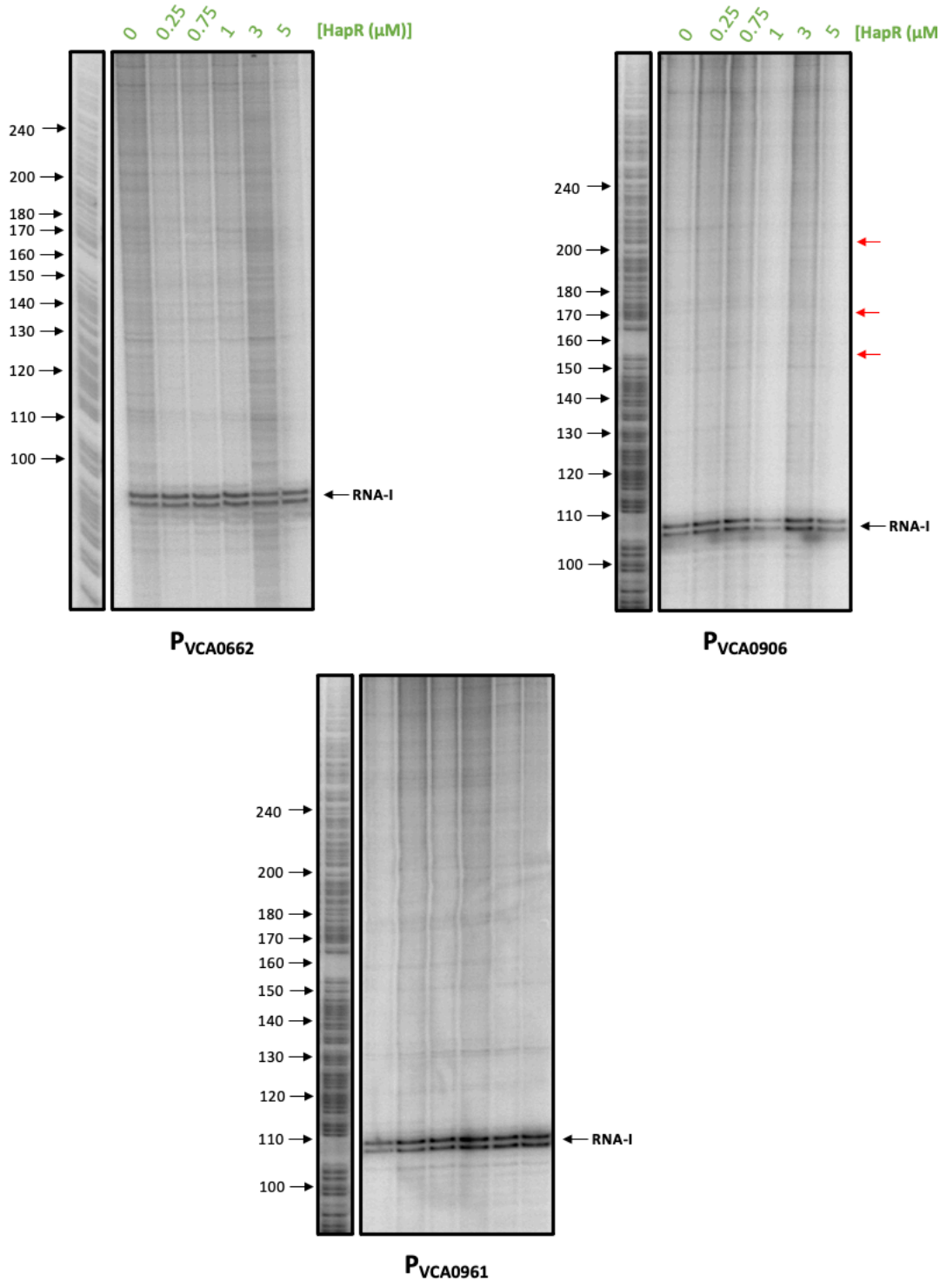

Figure 5.4 – HapR-target promoters with no observed transcription *in vitro*. Promoters of interest cloned upstream of a *λoop* transcription terminator and a separate σ^{70}-dependent transcript (RNA-I). Plasmid DNA was mixed with RNA polymerase, α-UTPs, σ^{70} and purified HapR-6xHis of varying concentration. Reactions were run alongside GA ladders (left) for size reference. Red arrows indicate the expected size of transcripts (based on RNA-seq data from Papenfort et al. (2015)). *N.B. Some GA ladders appear mutltiple times where samples were run on same gel.*

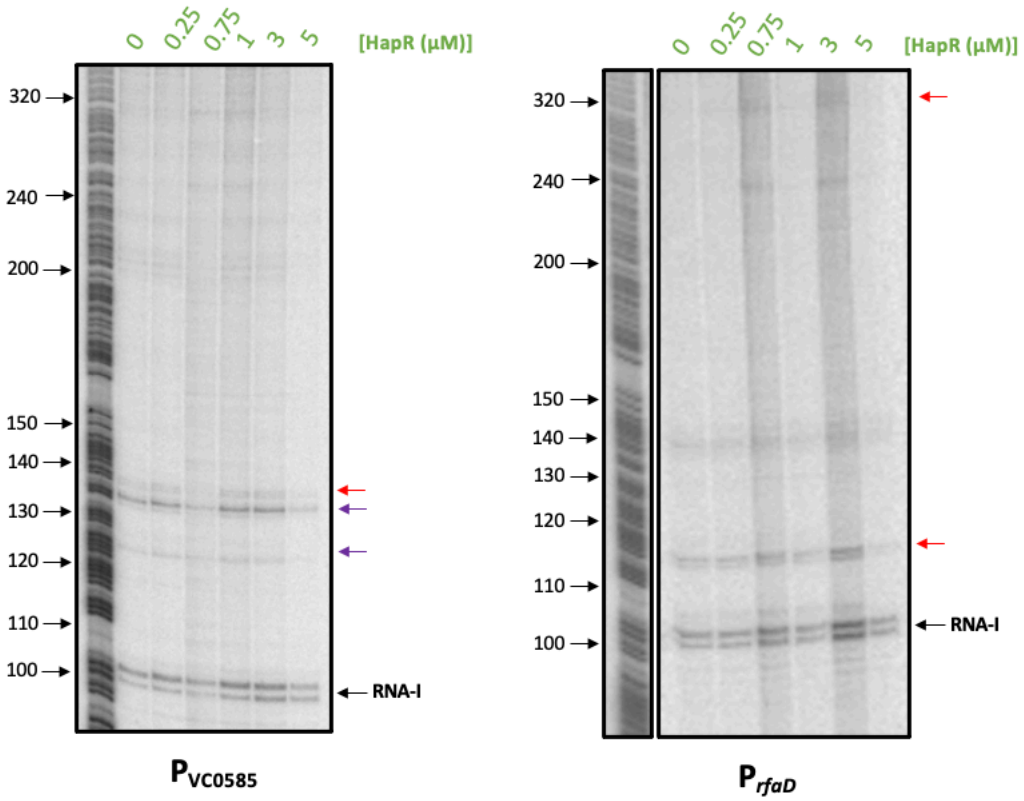
0 0.25 0.75 1 3 5 [HapR (μM)]
320
240
200
150
140
130
120
110
100
RNA-I
P_{VC0585}
0 0.25 0.75 1 3 5 [HapR (μM)]
320
240
200
150
140
130
120
110
100
RNA-I
P_{rfaD}

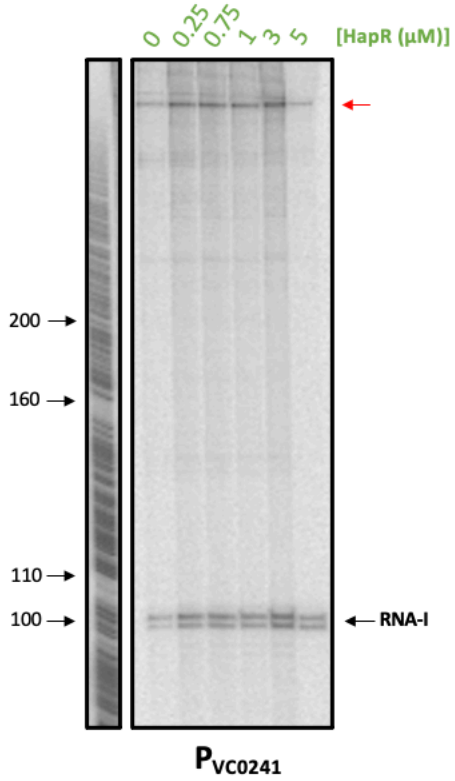
0 0.25 0.75 1 3 5 [HapR (μM)]
200
160
110
100
RNA-I
P_{VC0241}

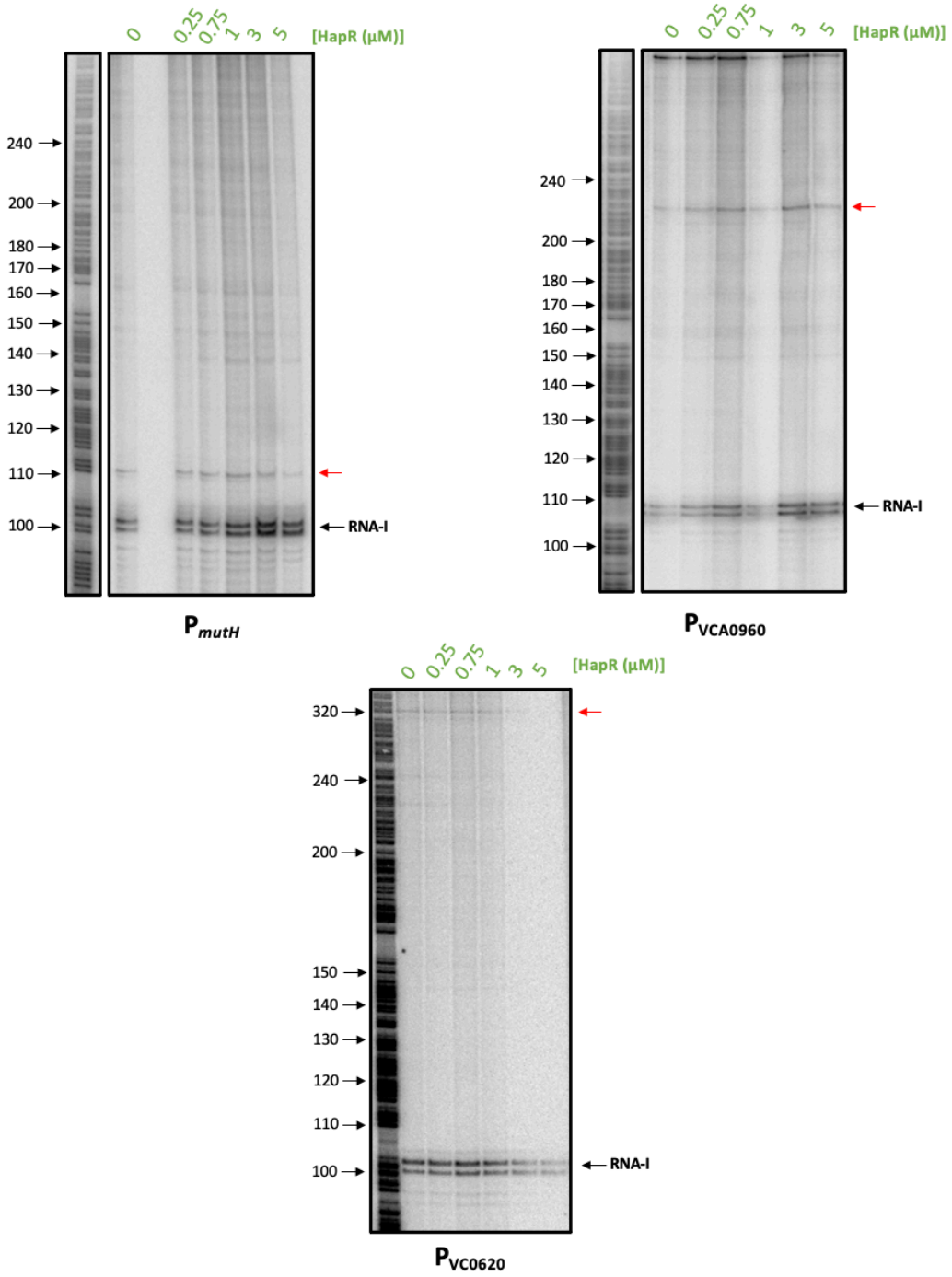

Figure 5.5 – HapR-target promoters with transcripts unaffected by HapR *in vitro*. Promoters of interest cloned upstream of a *λoop* transcription terminator and a separate σ^{70}-dependent transcript (RNA-I). Plasmid DNA was mixed with RNA polymerase, α-UTPs, σ^{70} and purified HapR-6xHis of varying concentration. Reactions were run alongside GA ladders (left) for size reference. Red arrows indicate the expected size of transcripts (based on RNA-seq data from Papenfort et al. (2015)). Purple arrows indicate other transcripts observed. *N.B. Some GA ladders appear multiple times where samples were run on same gel.*

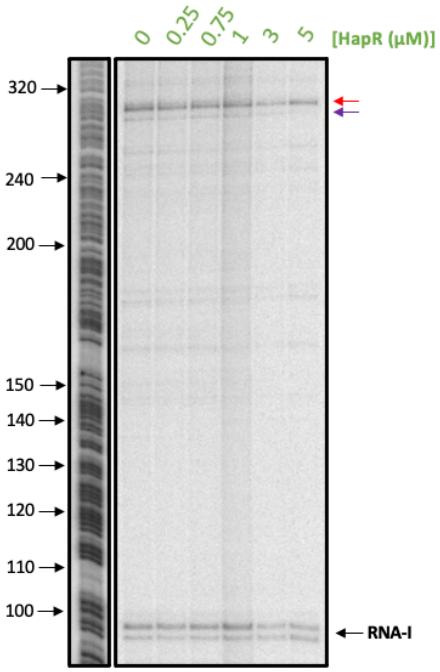

P_{VC0502}

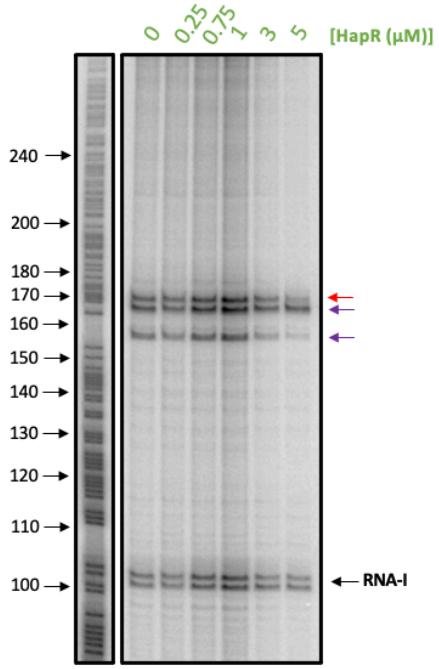

P_{hapR}

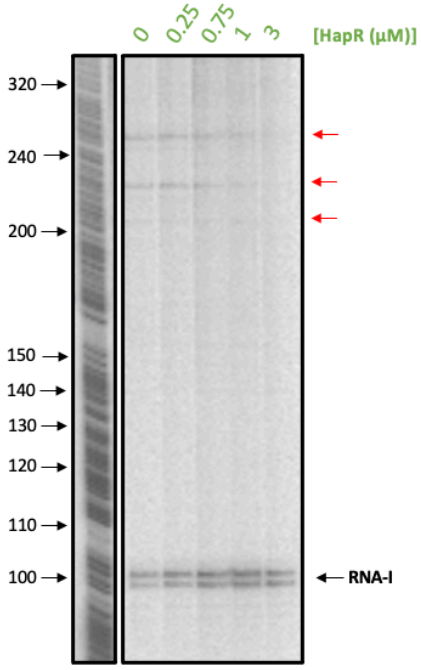

P_{VC0433}

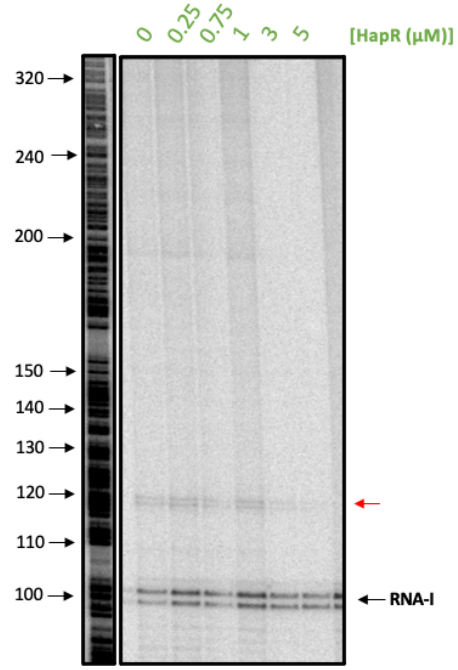

P_{VC1298}

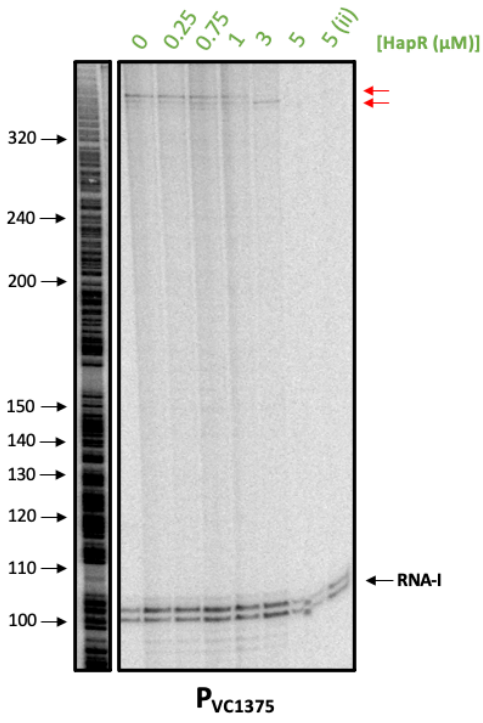

P_{VC1375}

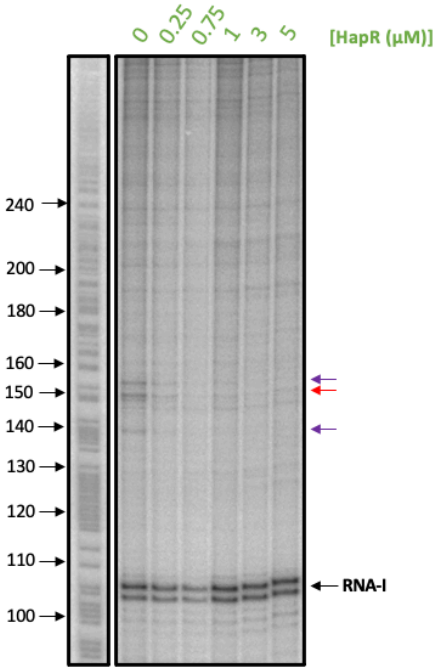

P_{VC1376}

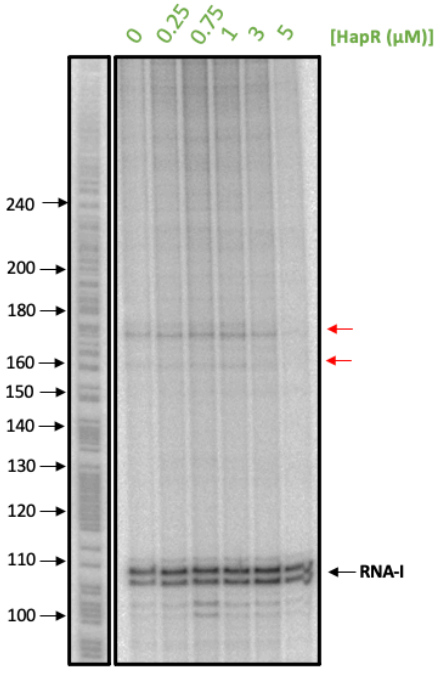

P_{VC1436}

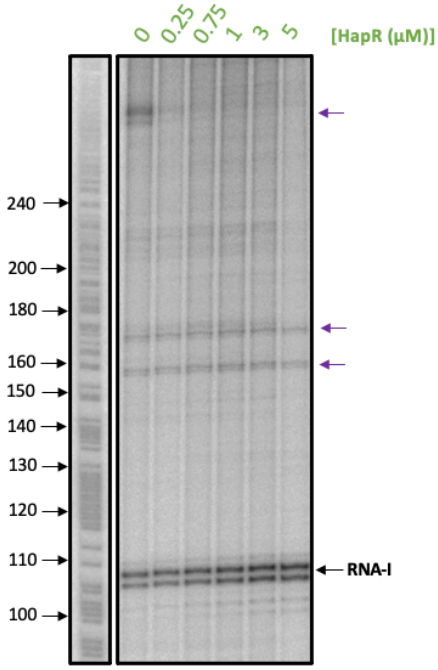

P_{VC1403}

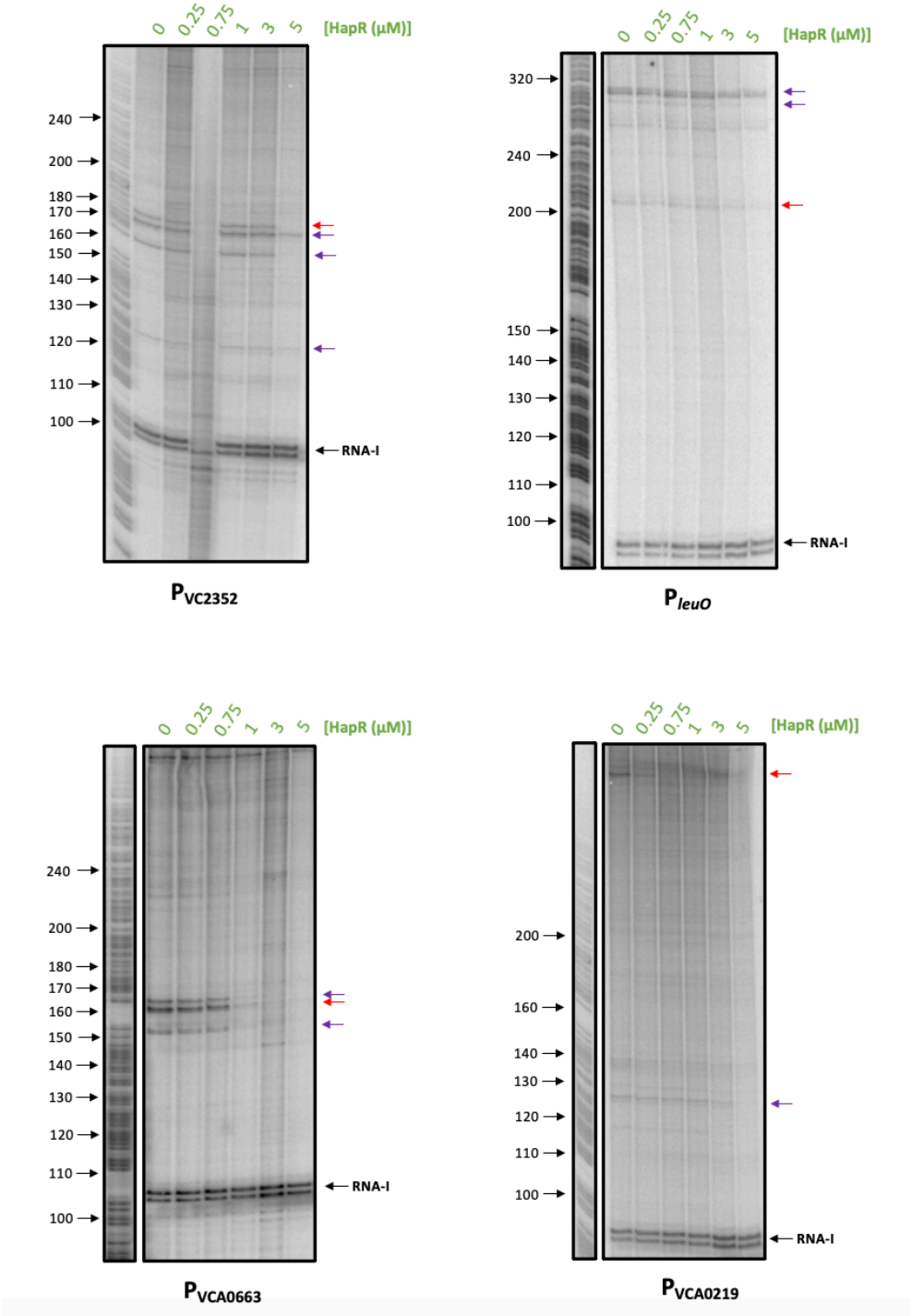

Figure 5.6 – HapR-target promoters repressed by HapR *in vitro*. Promoters of interest cloned upstream of a *λoop* transcription terminator and a separate σ^{70}-dependent transcript (RNA-I). Plasmid DNA was mixed with RNA polymerase, α-UTPs, σ^{70} and purified HapR-6xHis of varying concentration. Reactions were run alongside GA ladders (left) for size reference. Red arrows indicate the expected size of transcripts (based on RNA-seq data from Papenfort et al. (2015)). Purple arrows indicate other transcripts observed. *N.B. Some GA ladders appear multiple times where samples were run on same gel.*

Promoter	Predicted transcript size(s) (nt)	Observed transcript size(s) (nt)	Effect of HapR *in vitro*	Effect of HapR *in vivo*
P*murQ*	116	None	I	R
P*rfaD*	119	119*	N	N
PVC0241	516	300+**	N	N
PVC0433	211/232/269	211/232/269	R	I
PVC0502	297	290/297	R (transcript at 290 nt only)	N
P*hapR*	169	156/165/169	R (transcript at 156 nt only)	N
PVC0585	137	125/137/140	N	R
PVC0620	311	311	N	I
P*mutH*	117	117*	N	I
PVC0688	128/146	None	I	N
PVC1298	123	123*	R	N
PVC1375	362/401	300+**	R/A	A
PVC1376	150	140/150/154	R	N
PVC1403	Undetermined	160/175/300+**	R (transcript at 300+ nt only)	A
PVC1405	108/263/299	None**	I	N
PVC1436	165	165*	R	I
PVC2352	177	128/164/173/177	R	R
P*leuO*	215	215/300-320*	R	N
PVCA0218	514	None**	I	I
PVCA0219	524	139*/524**	R	R
PVCA0662	372/450	None	I	I
PVCA0663	161	152/161/164	R	R
PVCA0906	154/172/205	None	I	N
PVCA0960	211/367	211*	N	N
PVCA0961	Undetermined	None	I	I

Table 5.1 – Summary of *in vitro* and *in vivo* transcription from HapR target promoters. Predicted transcript sizes are based on data from Papenfort et al. (2015). ***In vitro***, promoters were characterised as inactive (I), repressed by HapR (R), activated by HapR (A) or not affected by HapR (N). Inactive promoters showed no transcript both in the presence and absence of HapR. Promoters at which a reduction or increase in at least one transcript was observed were classified as repressed or activated respectively. Promoters at which no change in transcription was observed in the presence of HapR were classified as not affected. ***In vivo***, promoters were characterised as inactive (I), repressed by HapR (R), activated by HapR (A) or not affected by HapR (N) in the conditions of our experiment. Inactive promoters gave less than twice the no insert control activity both in the presence and absence of HapR. Promoters activated or repressed by HapR showed at least a 2-fold decrease or increase in activity respectively, following HapR deletion, after no insert activity values had been subtracted from the overall activity. All other promoters were classified as not affected.
** Refer to original image, **Out of visible GA ladder range.*

5.4 Discussion

Frequently, ectopic expression of HapR *in vivo* did not alter transcription from promoters of interest. Most likely, this is because native HapR expression confounds our results. Consistent with this, deletion of chromosomal *hapR* did impact transcription from many HapR target promoters. Specifically, transcription was increased from five promoters and decreased from two promoters when *hapR* was deleted. In conjunction with these experiments, we also assessed transcription from these promoters *in vitro*. The genes for which we observed HapR-mediated regulation and the possible reasons for such regulation are discussed in the sections below. ChIP-seq data at some of these gene loci is presented in figure 5.7.

5.4.1 HapR auto-regulation

Given that HapR a known auto-repressor, we expected to observe an increase in gene expression from P_{hapR} in our Δ*hapR* strain (Lin et al., 2005). *In vivo*, deletion of *hapR* resulted in no change in activity. While this is not what was expected, we note that there was a high degree of error in our data for this promoter in the Δ*hapR* strain, which may be the result of an outlier. *In vitro*, we observe three transcripts one of which is repressed by HapR (figure 5.6). It is possible that assessing transcription *in vitro* using RpoS (a known activator of HapR) instead of RpoD would yield a different result (Nielsen et al., 2006). Additionally, we note that the divergent promoter, P_{VC0585}, shows repression by HapR both *in vitro* and *in vivo*. VC0585 encodes a hypoxanthine phosphoribosyl transferase, important in the GMP synthesis pathway (Heidelberg et al., 2000).

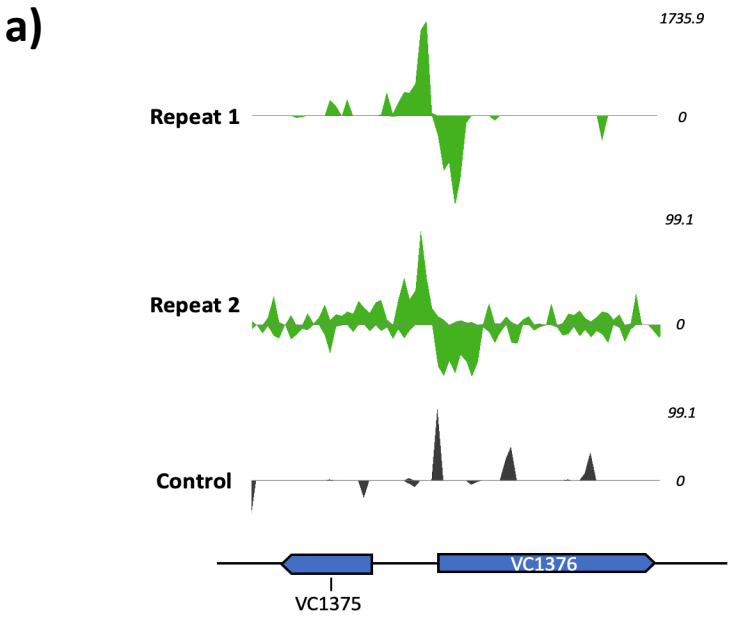
a)
1735.9
Repeat 1
0
99.1
Repeat 2
0
99.1
Control
0
VC1376
VC1375

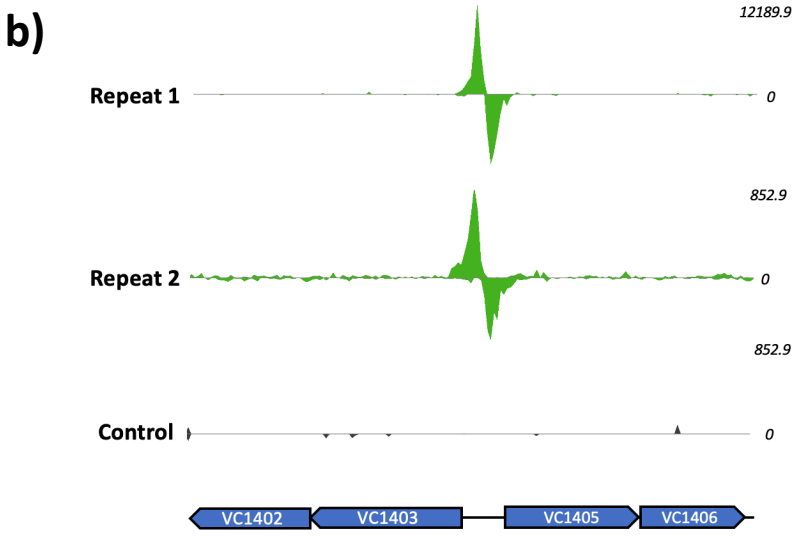
b)
12189.9
Repeat 1
0
852.9
Repeat 2
0
852.9
Control
0
VC1402
VC1403
VC1405
VC1406

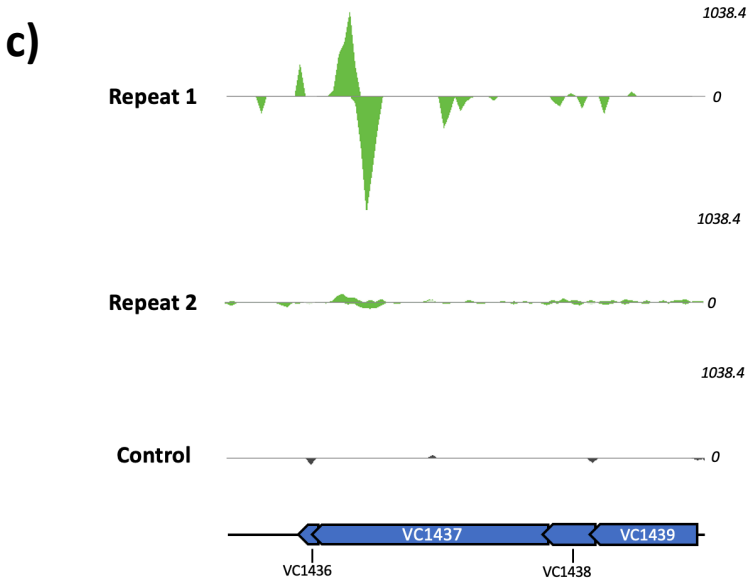
c)
1038.4
Repeat 1
0
1038.4
Repeat 2
0
1038.4
Control
0
VC1437
VC1439
VC1436
VC1438

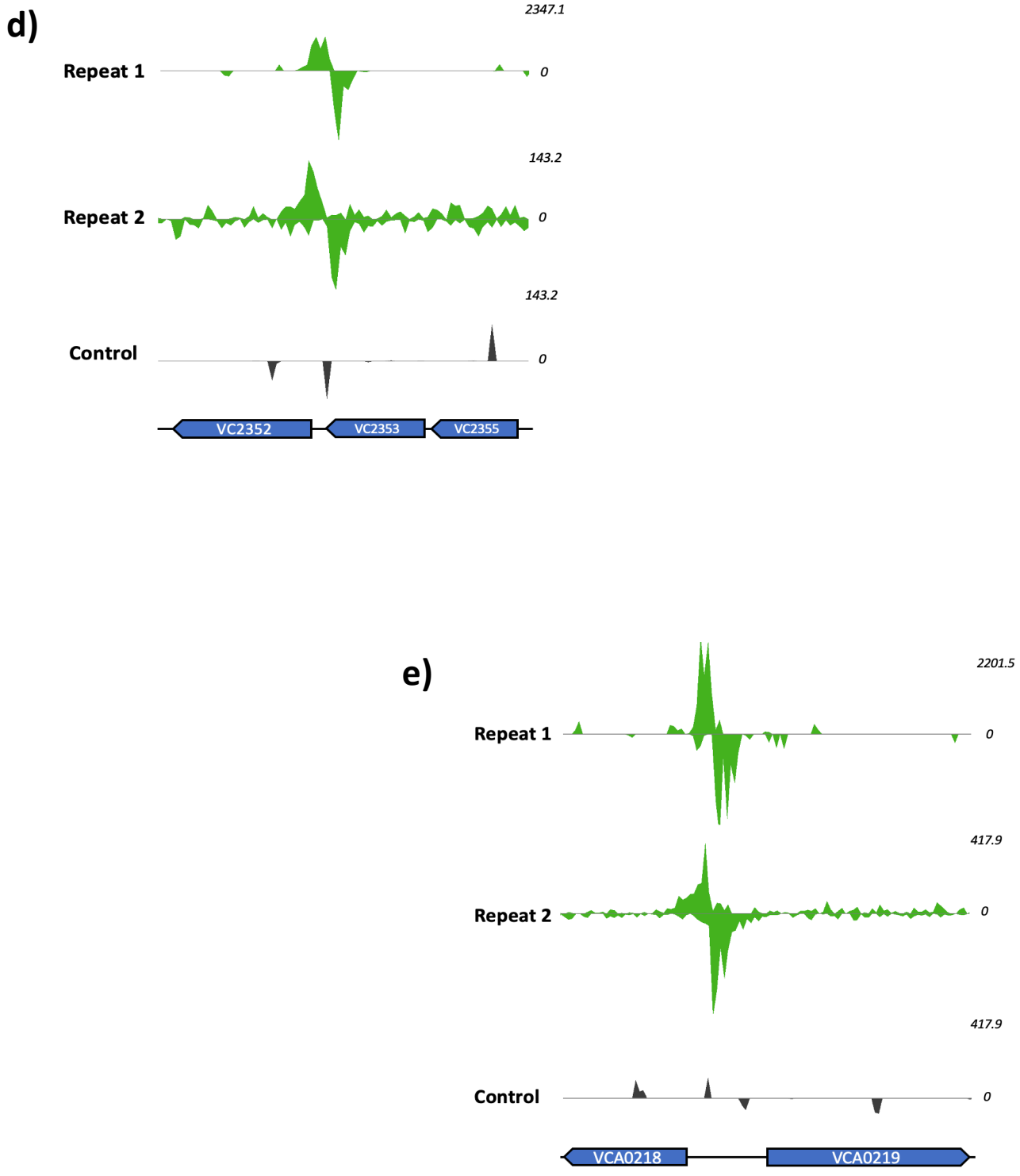

Figure 5.7 – ChIP-seq peaks at HapR target loci in *V. cholerae* E7946. Peaks adjacent to genes a) VC1375/VC1376, b) VC1403/VC1405, c) VC1436, d) VC2352 and e) VCA0218/VCA0219 (from two replicates and a negative control). Genes represented by blue bars. Read depths for each trace are displayed on the right. *V. cholerae* N16961 was used as reference genome for ChIP-seq analysis.

5.4.2 Haemolysin

VCA0219 (*hlyA*), encodes a haemolysin which lyses mammalian red blood cells and is involved in the pathogenicity of 7PET *V. cholerae* (Ichinose et al., 1987). Divergent VCA0218 (*hlyB*) encodes HlyB, which governs the secretion of HlyA indirectly through the sensing of external factors such as nutrients (Jeffery and Koshland, 1993). Previous studies have shown that expression of HlyA and its activator, HlyU, are repressed by HapR (Gao et al., 2018). Our *in vitro* and *in vivo* data show that HapR represses transcription from the VCA0219 promoter. We conclude, therefore, that HapR represses transcription of *hlyA*. We observe no effect of HapR on transcription from the VCA0218 promoter, however, no transcript was observed *in vitro* either with or without HapR. Activation by another transcription factor may be required. We note that no peaks were observed in our ChIP-seq data near the gene encoding *hlyU* (VC0678).

5.4.3 Methyl-accepting chemotaxis proteins

Three of the HapR target promoters assessed in this chapter control the expression of methyl-accepting chemotaxis proteins (MCPs). These MCPs are encoded by the genes VC1298, VC1403 and VCA0663. Our *in vitro* data shows HapR represses transcription from the VC1298 promoter but no HapR-mediated effect was observed *in vivo*. Interestingly, in the case of the VC1403 promoter, our *in vitro* data contradicts our findings *in vivo*. *In vivo*, deletion of *hapR* decreases promoter activity. By contrast, our *in vitro* data suggests there are three promoters in the P_{VC1403} fragment, one of which is repressed by HapR. It is possible that the 'HapR-sensitive' transcript is in some way detrimental to gene expression, perhaps at the level of translation; as the most strongly expressed transcript, it may be that the translational machinery is diverted from the other two transcripts. VCA0663 encodes

another MCP, although not one hitherto identified as part of the HapR regulon. Our *in vitro* and *in vivo* data show transcription from the VCA0663 promoter is repressed by HapR.

5.4.4 Diguanylate cyclase

Transcription from the intergenic region of divergent genes VC1375 and VC1376 was also assessed. We observed repression of transcription from P_{VC1376} by HapR *in vitro* but not *in vivo*. VC1376 (*cdgM*) encodes a diguanylate cyclase, which regulates c-di-GMP levels in *V. cholerae* in response to temperature (Townsley and Yildiz, 2015; Conner et al., 2017). It is also thought that CdgM increases c-di-GMP levels to promote biofilm formation in response to host bile (Koestler and Waters, 2014; Conner et al., 2017). HapR-mediated repression of biofilm formation via the downregulation of the *vps* genes, is well-characterised in *V. cholerae* (Hammer and Bassler, 2003; Yildiz et al., 2004). Previous studies have shown HapR also directly regulates expression of the diguanylate cyclase encoding gene, *cdgA* (VCA0074) to control biofilm formation (Waters et al., 2008). Our results indicate that HapR also controls *cdgM*.

We observed an unusual result in our *in vitro* transcription assay of the VC1375 promoter; HapR represses one transcript and promotes another. The role of the protein encoded by VC1375 in *V. cholerae* is also not currently known, nor has it been categorised into a subfamily of proteins based on its predicted structure.

5.4.5 Cytochrome c oxidase

One of our candidate promoters in this study, P_{VC1436}, is not intergenic. Instead, the promoter is located within the open reading frame of VC1437 (*ccoI*), and is directly

upstream of VC1436 (*ccoS*), both of which are part of the *ccoGHIS* gene cluster (Koch et al., 2000; Heidelberg et al., 2000). This cluster is found downstream of the co-regulated cluster *ccoNOQP*, which forms a cbb_3-type cytochrome c oxidase (Thöny-Meyer et al., 1994). Genes in the *ccoGHIS* cluster are expressed independently and not as a single operon (Koch et al., 2000). Our *in vitro* data shows that HapR represses transcription of *ccoS*. Cytochrome c oxidase is critical for aerobic respiration and without CcoS the enzyme is inactive (Thöny-Meyer et al., 1994; Koch et al., 2000). Our study finds no evidence that HapR regulates other genes in the *ccoGHIS* or *ccoNOQP* clusters. Regulation of CcoS expression by HapR may therefore provide a rapid off-switch which downregulates aerobic respiration in anaerobic conditions.

5.4.6 Metabolism

VC2352 encodes a nucleoside transporter, which is part of the NupC-family of proteins which take up extracellular DNA (Heidelberg et al., 2000). VC2352 expression induced by CRP is vital in the aquatic environment, where extracellular DNA is a major carbon source (Gumpenberger et al., 2016). We note that HapR and CRP have adjacent ChIP-seq peaks at the VC2352 promoter region (Manneh-Roussel et al., 2018). Our *in vitro* and *in vivo* data shows that HapR represses transcription from the VC2352 promoter. Exogenous DNA is degraded by the nuclease, Dns, and imported by nucleoside uptake proteins such as VC2352. It has been proposed that HapR downregulates this in favour of the uptake of larger fragments of DNA as part of natural competence (Gumpenberger et al., 2016; Blokesch and Schoolnik, 2008). Here we provide evidence which supports this hypothesis. We also note that transcription from this promoter is not dependent on CRP. Further investigation into the activity of CRP, HapR and another known inhibitor of the VC2352

promoter, CytR, would shed light on when and how *V. cholerae* controls the uptake of DNA in different environments (Tozzi et al., 2006; Gumpenberger et al., 2016).

VC0433 is believed to encode an ornithine/arginine antiporter, which exports ornithine in exchange for arginine, producing ATP (Heidelberg et al., 2000; Verhoogt et al., 1992; R et al., 1986). While VC0433 is not well characterised, it is known that deletion of the VC0433 gene in *V. cholerae* results in increased biofilm formation (Seper et al., 2014). Given that HapR is a repressor of biofilm formation, it is not clear why HapR represses transcription of VC0433 as our *in vitro* data suggests. It is possible that HapR activity is part of a negative feedback loop which helps to fine-tune biofilm production.

5.4.7 HapR as a repressor of transcription

In this chapter we have examined the role of HapR at several chromosomal loci. We note that we observed only one instance of HapR-mediated activation of transcription *in vitro* (from the promoter P_{VC1375}), which was coupled with repression of another transcript. Homologues of HapR have been shown to directly activate genes. For example, LuxR activates transcription at the *luxCDABE* operon in *Vibrio harveyi* (Chaparian et al., 2016). A recent study showed that the HapR homologue, SmcR (in *Vibrio vulnificus*), can exist in a 'wide-dimer' or 'narrow-dimer' conformation due to flexibility in its DNA-binding domain (Newman et al., 2021). Mutants stuck in the 'wide-dimer' conformation are only able to bind SmcR-repressed promoters. HapR lacks this flexibility and is only observed in the 'wide-dimer' conformation (Newman et al., 2021). This may explain why HapR has a smaller regulon than its homologues in other *Vibrio* spp.; LuxR is thought to regulate over 600 genes in *V. harveyi*, whereas the HapR regulon is believed to consist of only 100 genes (van Kessel

et al., 2013a; Ball et al., 2017; Nielsen et al., 2006). This might also explain why we only observe transcription repression by HapR *in vitro*.

Chapter 6
Co-regulation of the murQ *promoter by HapR and CRP*

6.1 Introduction

Bacterial cell walls are chains of alternating MurNAc and GlcNAc, with peptide crosslinks between them (Vollmer et al., 2008). Figure 6.1 outlines how cell wall components can be recycled by MurP and MurQ. MurQ catalyses the conversion of MurNAc 6P to GlcNAc 6P (Jaeger et al., 2005). MurP transports MurNAc into the cytoplasm. Transport into the cytoplasm is coupled with phosphorylation of MurNAc to MurNAc 6P (Dahl et al., 2004). GlcNAc 6P can be further converted to fructose 6 phosphate, which is used in glycolysis, or recycled into new cell wall constituents (Uehara et al., 2006).

Crucially, MurP activity is regulated by binding of glucose-specific enzyme IIA ($EIIA^{Glc}$). $EIIA^{Glc}$ is a critical component of the phosphotransferase system (PTS), the core sugar transport system in bacteria. Phosphorylated $EIIA^{Glc}$ stimulates adenylate cyclase to produce cAMP, resulting in the regulation of CRP-dependent genes (Deutscher et al., 2006). The transport of sugars (by MurP, for example) dephosphorylates $EIIA^{Glc}$ and therefore reduces cAMP production (Deutscher et al., 2006). In *V. cholerae*, unphosphorylated $EIIA^{Glc}$ downregulates chitin utilisation via repression of ChiS (Yamamoto and Ohnishi, 2017). This highlights the likely importance of HapR regulation at the *murQ* promoter; repression of MurQP expression by HapR downregulates dephosphorylation of $EIIA^{Glc}$ and thereby upregulates ChiS, which is important for chitin utilisation at high cell density.

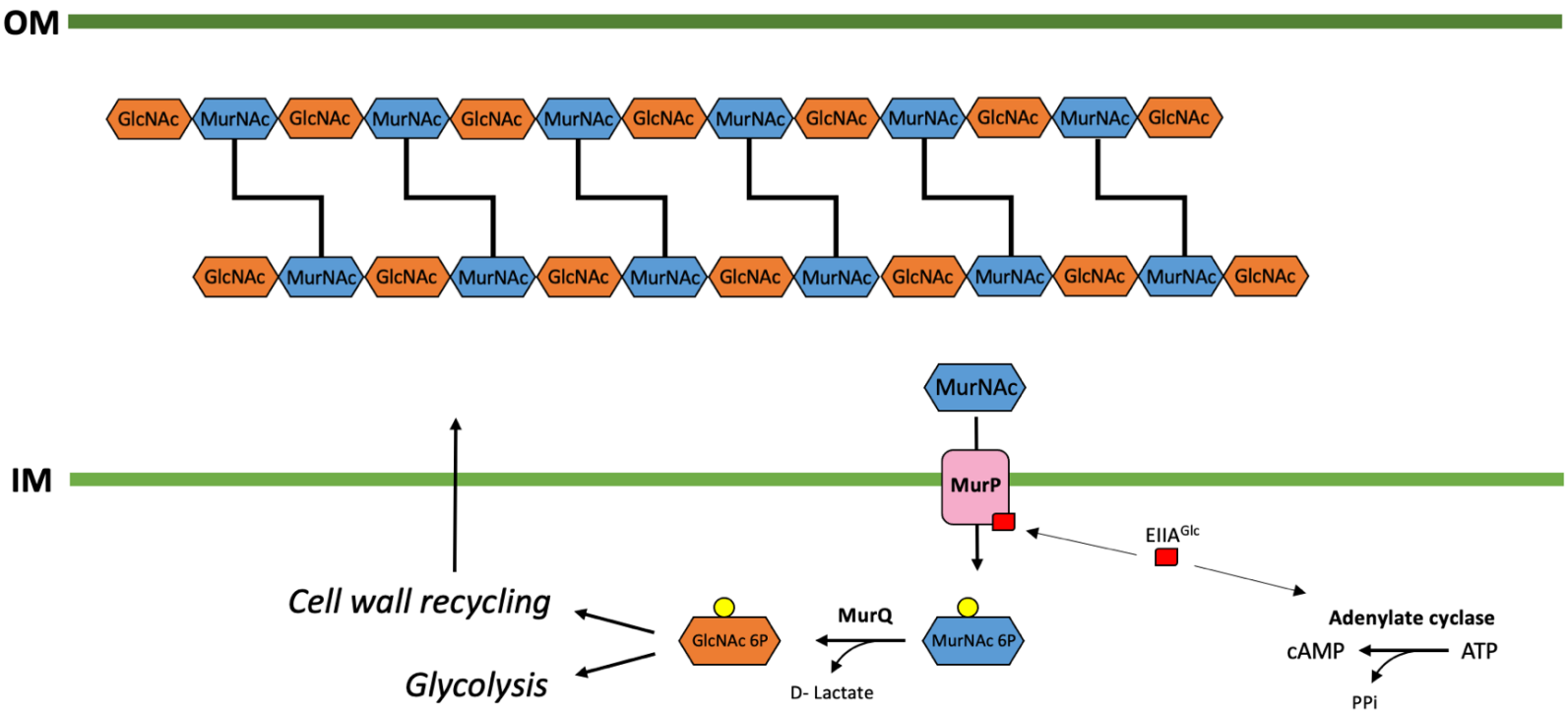

Figure 6.1 – Cell wall turnover and utilisation by MurQ and MurP. Bacterial peptidoglycan chains formed of alternate GlcNAc and MurNAc. Peptide crosslinks formed between MurNAc amino sugars of different chains. MurNAc is transported across the inner membrane by MurP, which requires $EIIA^{Glc}$. MurNAc is phosphorylated upon translocation into the cell. MurQ converts MurNAc 6P into GlcNAc 6P and D-lactate. GlcNAc 6P can be used in glycolysis or for reconstitution into new cell wall components. $EIIA^{Glc}$ also promotes cAMP production by adenylate cyclase. Adapted from Jaeger et al. (2008). *OM = Outer membrane, IM = Inner membrane, ATP = Adenosine triphosphate, PPi = pyrophosphate.*

In the previous chapter, we reported that many HapR target promoters were either inactive, or did not respond to HapR, in the conditions of our experiments. Both HapR ChIP-seq replicates showed binding at the *murQ* promoter (shown in figure 6.2), and we observe a decrease in activity between the wild-type and Δ*hapR* strains of *V. cholerae* E7946 containing a P_{murQ}-*lacZ* fusion. However, the *murQ* promoter was inactive in the absence of HapR *in vitro* and we observed no effect of HapR on transcription in this experiment (figure 5.4). Presumably, other transcription factors may be required to observe a HapR-dependent phenotype *in vitro*. In this chapter, we sought to determine how HapR regulates transcription from the *murQ* promoter.

6.1.1 The *murQ* regulatory region

Figure 6.2b shows the sequence of P_{murQ}, which we define as a section of the *V. cholerae* genome 300 bp upstream of the *murQ* open reading frame. The centre of the ChIP-seq peak is labelled, along with the predicted site of HapR binding, based on the results of our MEME analysis in chapter 4 (figure 4.4). We noticed, in chapter 4, that HapR and CRP ChIP-seq peaks often co-locate. No CRP ChIP-seq peak was observed at the *murQ* locus (Manneh-Roussel et al., 2018). However, we did note a 9/10 match to a consensus sequence for CRP binding located within the predicted HapR binding site. This CRP site is located 41.5 bp upstream of the *murQ* TSS; a position consistent with P_{murQ} being a class II CRP activated promoter. We predicted that CRP activates and HapR represses transcription from the *murQ* promoter.

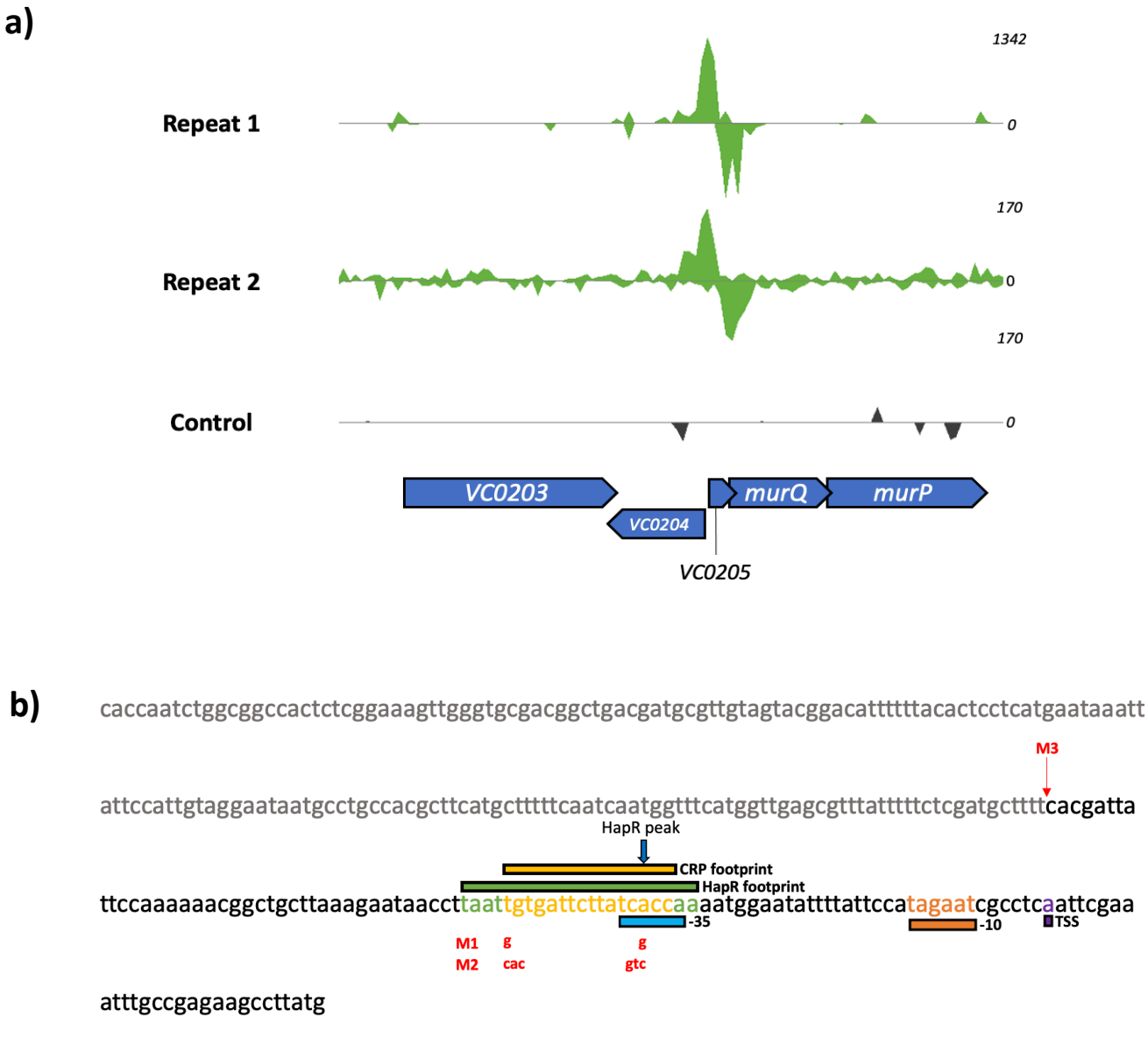

Figure 6.2 – The *murQ* promoter. a) ChIP-seq data at the *murQ* locus. Peaks from two replicates and a negative control and adjacent genes displayed. Read depths for each trace are displayed on the right. *V. cholerae* N16961 was used as reference genome. b) Sequence of P_{murQ}. Includes start codon of the *murQ* ORF and upstream intergenic region. Transcription start site (TSS), -10 and -35 promoter elements shown in purple, orange and blue respectively. Predicted HapR and CRP binding motifs are shown in green and yellow respectively. Binding site of HapR and CRP as determined by DNaseI footprinting shown by green and yellow lines respectively. Base located at the centre of HapR ChIP-seq peak indicated by the blue arrow. Point mutations and truncations made in this study indicated by red text and red arrow.

6.2 CRP binds to the *murQ* promoter *in vitro*

To determine if CRP bound the *murQ* promoter we used an electrophoretic mobility shift assay (EMSA). Briefly, the *murQ* promoter sequence, shown in figure 6.2, was end-labelled with ^{32}P and incubated with different concentrations of purified *V. cholerae* CRP protein. The resulting complexes were then separated by electrophoresis using a non-denaturing acrylamide gel. The results are shown in figure 6.3. In the absence of CRP we observed a single band, corresponding to the unbound promoter DNA. The electrophoretic mobility of the band changed upon addition of 0.5 µm CRP. When the concentration of CRP was increased to 1 µm, free promoter DNA was no longer observed. From this, we conclude that CRP binds to the *murQ* promoter.

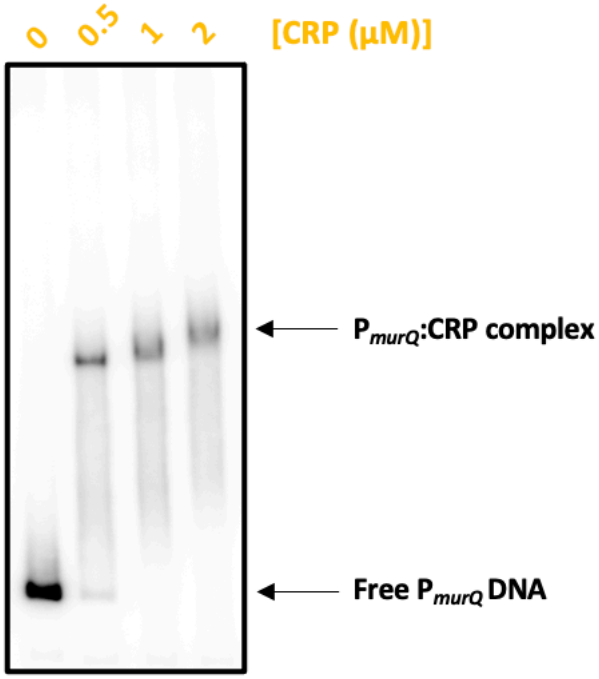

Figure 6.3 – EMSA of CRP and P_{murQ}. P^{32}-labelled promoter DNA fragments were mixed with CRP as required and herring sperm DNA as a non-specific inhibitor. Mixtures were run on a 5 % (w/v) polyacrylamide gel.

6.3 HapR and CRP co-regulate expression of *murQ*

Recall that the putative CRP binding site identified, centred at -41.5, is consistent with Class II CRP-dependent activation (Busby and Ebright, 1997). To determine if CRP activated the *murQ* promoter we used an *in vitro* transcription assay. The results are presented in figure 6.4. The DNA template used was the purified P_{murQ}-pSR plasmid construct described in the previous chapter. As expected, addition of CRP resulted in the production of a transcript approximately 120 nucleotides in length. The addition of HapR, in tandem with CRP, resulted in the loss of this transcript.

Next, we sought to determine if transcription regulation by HapR and CRP could be observed *in vivo*. We tested the P_{murQ}-*lacZ* fusion described in the previous chapter in both wild-type and Δ*hapR V. cholerae* by β-galactosidase assay. To gain further insight, we also made Δ*crp* and Δ*crp*Δ*hapR* derivations of *V. cholerae* E7946 by allelic exchange. The results are shown in figure 6.5. Deletion of *crp* resulted in a decrease of LacZ activity, whereas deletion of *hapR* resulted in an increase in activity. The Δ*crp*Δ*hapR* strain showed no difference in activity when compared to the Δ*crp* strain. Taken together with our *in vitro* transcription data, we conclude that HapR represses CRP-activated transcription from the *murQ* promoter.

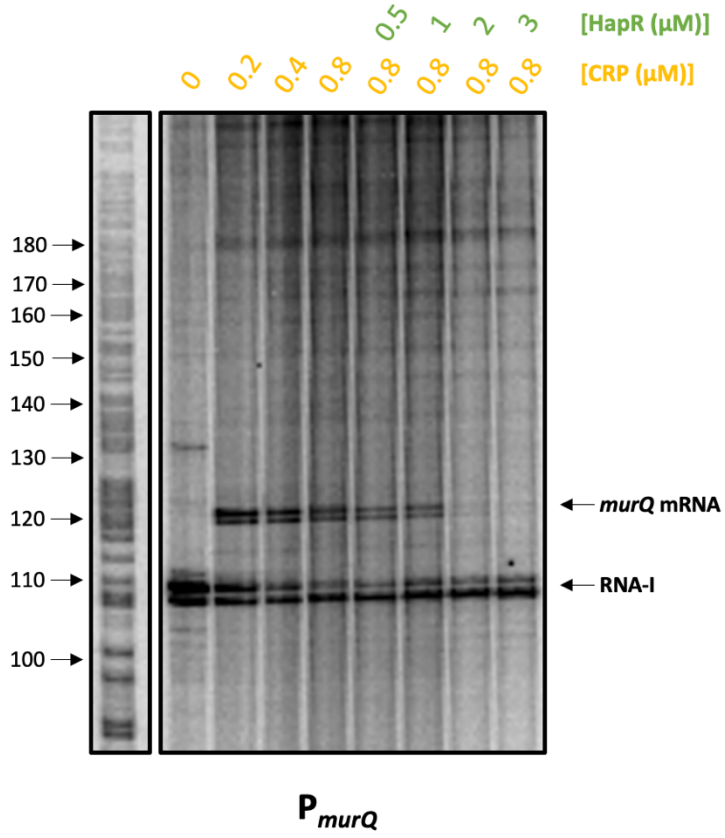

Figure 6.4 – The effect of CRP and HapR on transcription from P_{murQ} *in vitro*. P_{murQ} was cloned upstream of a λ*oop* transcription terminator and a separate σ^{70}-dependent transcript (RNA-I). Plasmid DNA was mixed with RNA polymerase, α-UTPs, σ^{70} and purified CRP/HapR of varying concentrations. Reactions run alongside GA ladders (left) for size reference.

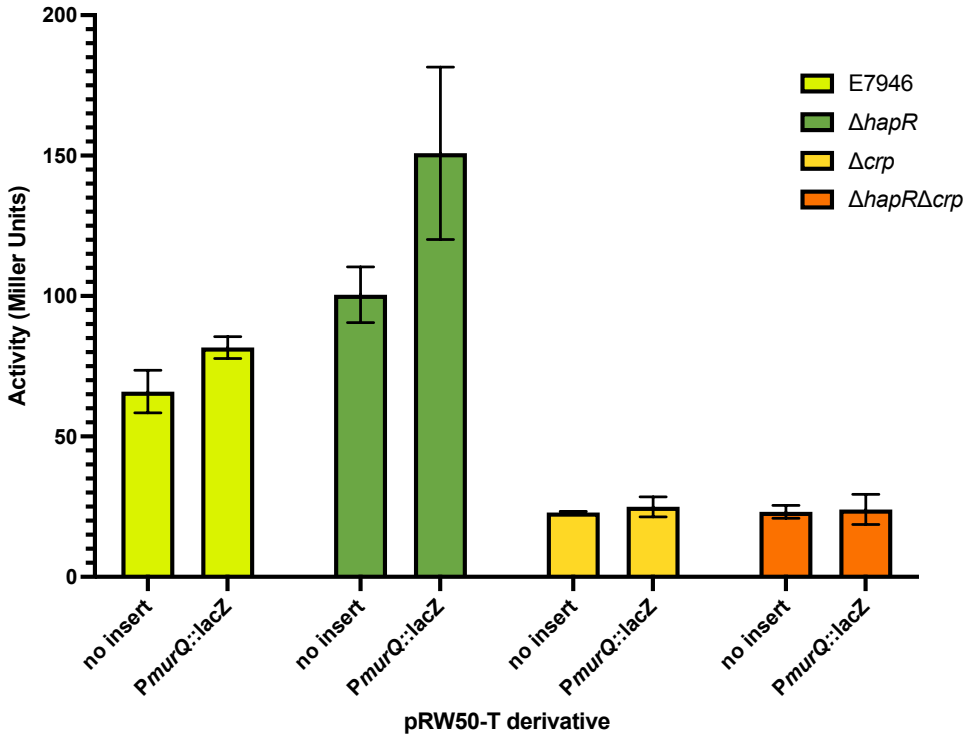

Figure 6.5 – The effect of CRP and HapR on transcription from P_{murQ} in *V. cholerae* E7946. β-galactosidase assay of WT, *Δcrp, ΔhapR* and *ΔcrpΔhapR* strains transformed with promoter-*lacZ* fusions in plasmid pRW50-T and no insert controls (n=3).

6.4 HapR and CRP bind co-operatively at the *murQ* promoter

We next sought to determine the mechanism by which HapR repressed CRP-mediated transcription at the *murQ* promoter. Assuming correct prediction of binding sites for both transcription factors, we hypothesised that HapR would compete with CRP for promoter binding. To test this, we used DNaseI footprinting. ^{32}P-labelled *murQ* promoter DNA was incubated with varying concentrations of HapR and/or CRP prior to DNaseI digestion. Digested DNA fragments were separated by electrophoresis on an 8 % polyacrylamide gel and the results are presented in figure 6.6. The pattern of DNaseI digestion in the absence of other factors is shown in lane 1. The addition of CRP (lanes 2-4) resulted in a region of protection that contained three hypersensitive bands, labelled by yellow arrows in the figure. These hypersensitive bands are likely caused by CRP bending the DNA, increasing accessibility of the double helix to DNAseI. Addition of HapR (lanes 5-8) resulted in a region of DNaseI protection approximately 28 nucleotides in length (outlined in green), but none of the hypersensitive bands observed in the presence of CRP were detected. Instead, we observed a change in the pattern of DNaseI hypersensitivity just upstream of the HapR protected DNA (outlined in purple). Our results indicate that HapR and CRP bind to the *murQ* promoter at regions centred at position -43 and -41.5 respectively. This is precisely consistent with our ChIP-seq analysis. The pattern of DNaseI digestion detected in the presence of both CRP and HapR is shown in lanes 9-12. The banding pattern resembled a mix of the individual HapR and CRP reactions. For instance, DNaseI addition resulted in HapR-mediated protection but also the emergence of CRP-dependent hypersensitive bands 1 and 2. Hence, HapR does not prevent CRP binding at the *murQ* promoter.

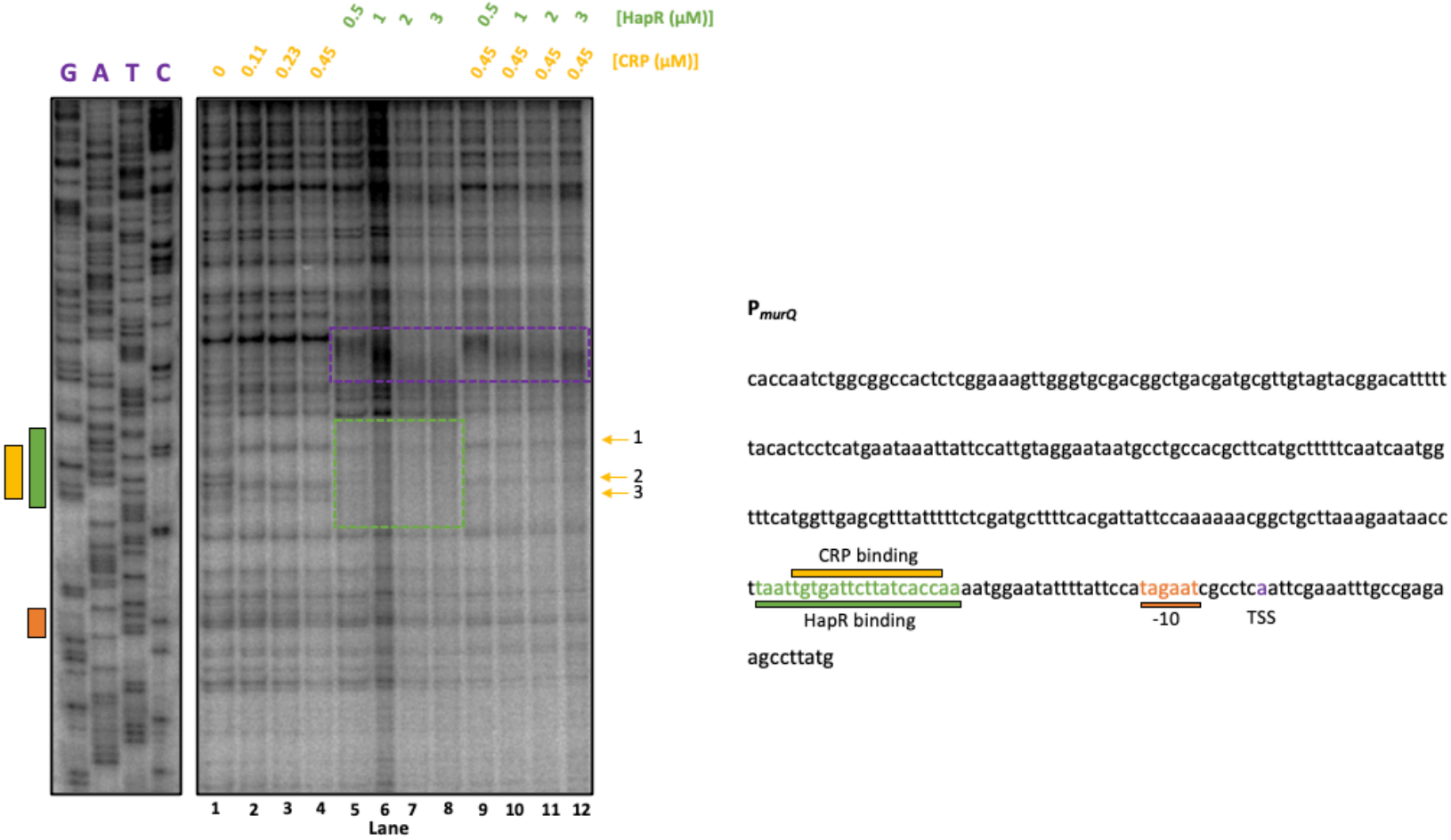

Figure 6.6 – DNaseI footprinting of P_{murQ}. ^{32}P-labelled promoter DNA fragments were incubated with or without HapR/CRP proteins before digesting with DNaseI. Samples were phenol/chloroform extracted and ethanol precipitated before running on 8 % (w/v) polyacrylamide gel alongside G/A/T/C sequencing ladders. Lane numbers 1-12 indicated. Footprinting gel image shown alongside promoter sequence. Transcription start site (based on Papenfort et al. 2015) indicated. -10 promoter element, CRP binding site and HapR binding site (based on known consensus sequences) are highlighted in orange, yellow and green respectively. Yellow arrows indicate hyper-sensitive bands observed upon addition of CRP. Section of DNA protected from DNaseI activity by HapR outlined by green box on gel image. Region of an unknown HapR-mediated effect outlined by a purple box.

Our DNaseI footprints cannot differentitate between a mixed population of P_{murQ} fragments bound to either HapR or CRP and P_{murQ} fragments bound to both factors simultaneously. Both scenarios could generate a similar overall pattern of DNaseI digestion. Hence, we used EMSAs to further assess HapR and CRP interaction at the *murQ* promoter. We incubated *murQ* promoter DNA with HapR and CRP either separately or in tandem before running complexes on a non-denaturing gel. Our results, presented in figure 6.7, show that CRP binds to the *murQ* promoter at concentrations of 0.025 µM or higher. However, incubation of HapR up to 0.75 µM with the *murQ* promoter fragment resulted in smearing, rather than a clear shift as expected. Interestingly, when we tested the same concentrations of HapR in tandem with 0.2 µM CRP, both proteins bound to the DNA. These results suggest that CRP and HapR bind co-operatively at the *murQ* promoter. By contrast, when we tested a DNA fragment containing the *hapR* promoter, HapR alone bound to the DNA at concentrations of 0.25 µM or higher and this binding was not altered by CRP.

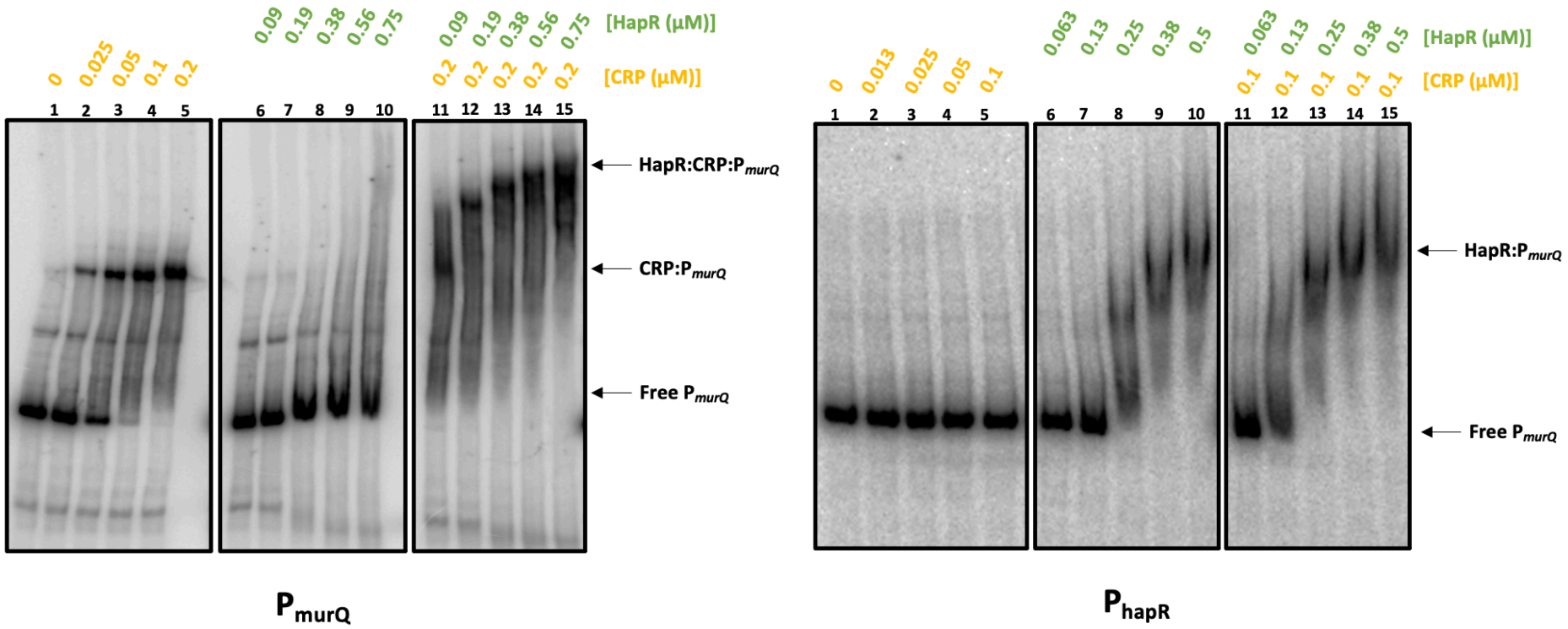

Figure 6.7 – EMSAs of promoters bound by HapR and CRP. P^{32}-labelled promoter DNA fragments were mixed with proteins and herring sperm DNA as a non-specific inhibitor. Mixtures were run on a 5 % (w/v) polyacrylamide gel.

6.5 Mutation of the *murQ* promoter alters binding of HapR and CRP

To further characterise the HapR and CRP binding sites at the *murQ* promoter we made mutations within the DNA sequence of P_{murQ}. The precise sequence changes are shown in figure 6.2, and a schematic is shown in figure 6.8. Mutant 1 was made by changing the T and A bases, within the conserved TGA and TCA motifs, shared by the HapR and CRP DNA binding consensus sequence. We predicted that this would inhibit binding by both HapR and CRP. We also mutated all six bases of the conserved TGA and TCA motifs (mutant 2) to ensure abolition of HapR and CRP binding. For mutant 3, the sequence of P_{murQ} was truncated. We reasoned that truncating the promoter in this way would ensure HapR and CRP binding was entirely dependent on the single locus we had identified. We also predicted this would minimise the effects of any other transcription factors which might confound our results *in vivo*. ^{32}P-labelled promoter fragments were incubated with HapR and CRP, both separately and in tandem, before running on a non-denaturing gel. Figure 6.9 shows a comparison of the WT and mutant 3 promoters. We observe co-operative binding of HapR and CRP in both cases. Figure 6.10 shows wild-type P_{murQ}, mutant 1 and mutant 2. Neither mutant 1 and mutant 2 were bound by HapR or CRP.

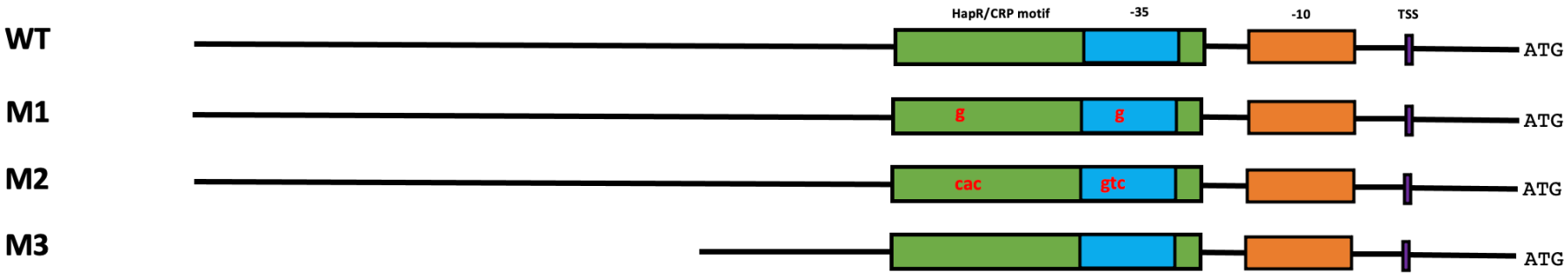

Figure 6.8 – Schematic diagrams wild-type and mutant P_{murQ} used in this study. Mutations are displayed in red. Transcription start site (TSS), -10 and -35 promoter elements and HapR/CRP binding motif highlighted in purple, orange, blue and green respectively.

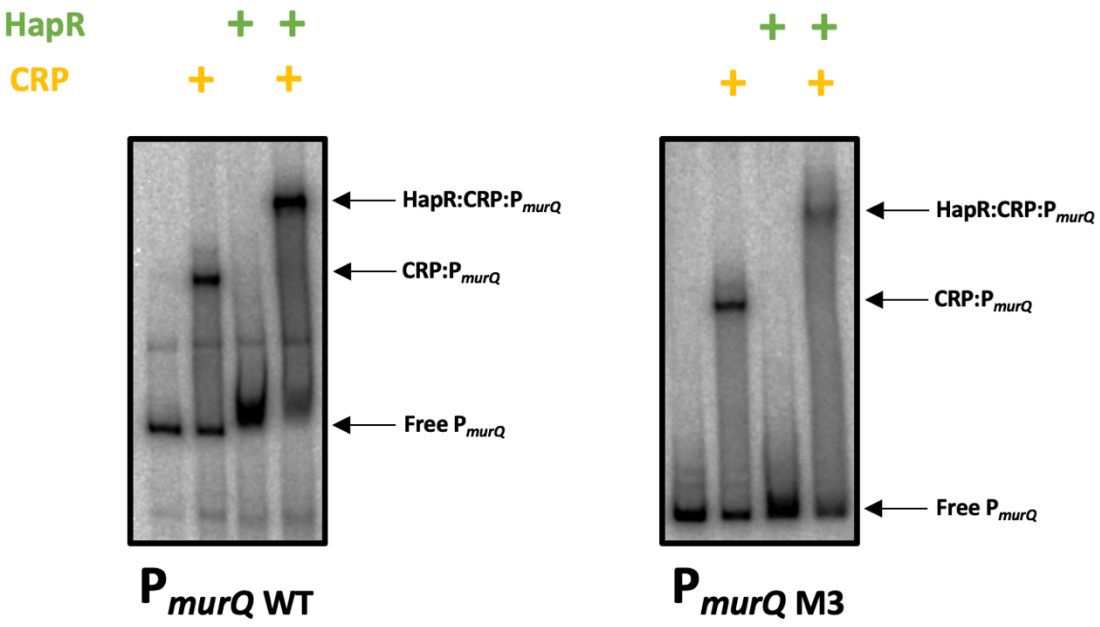

Figure 6.9 – Effect of truncating P_{murQ} on binding by HapR and CRP. P^{32}-labelled promoter DNA fragments were mixed with proteins and herring sperm DNA as a non-specific inhibitor. Mixtures were run on a 5 % (w/v) polyacrylamide gel. CRP and HapR final concentrations were 0.1 µM and 1 µM respectively.

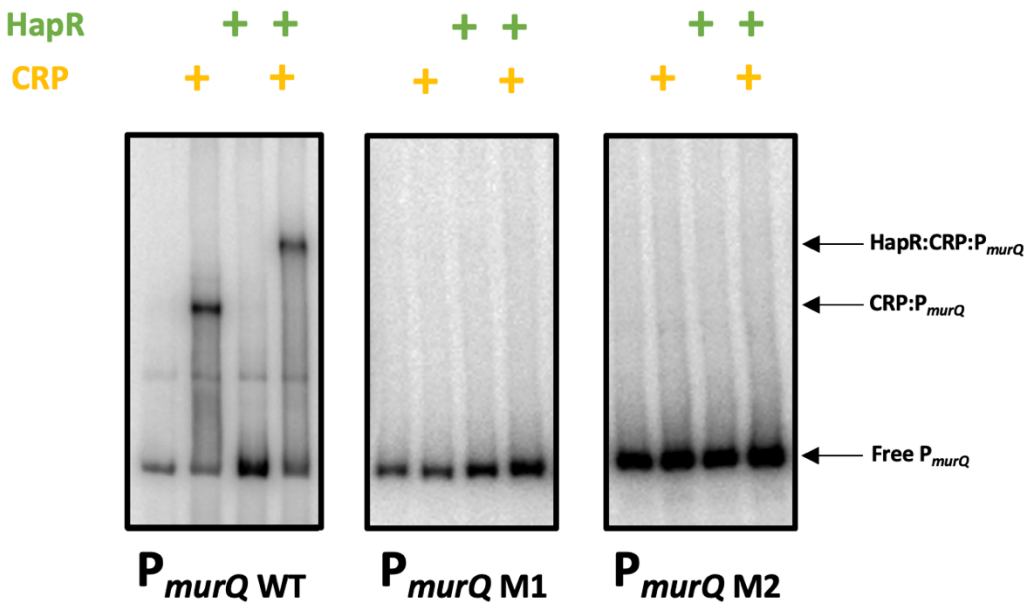

Figure 6.10 – Effect of mutating identified CRP/HapR binding site of P_{murQ}. P^{32}-labelled promoter DNA fragments were mixed with proteins and herring sperm DNA as a non-specific inhibitor. Mixtures were run on a 5 % (w/v) polyacrylamide gel. CRP and HapR final concentrations were 0.1 µM and 0.5 µM respectively.

6.6 Mutation of the *murQ* promoter alters HapR and CRP-mediated expression

To compare the effects of CRP and HapR on transcription from our wild-type and mutant promoters *in vivo*, we used β-galactosidase assays. Briefly, P_{murQ} (either wild-type, mutant 1, mutant 2 or mutant 3) was cloned upstream of *lacZ* in pRW50-T. The resulting plasmids are used to transform *V. cholerae* E7946 wild-type, *Δcrp, ΔhapR* and *ΔcrpΔhapR* strains. The strains were also transformed with empty pRW50-T as a no-insert control. The results of the β-galactosidase assays are shown in figure 6.11. Activity from both the wild-type and mutant 3 *murQ* promoter increased in *ΔhapR* strains compared to wild-type E7946. The cause of the increase in transcription from mutant 3 is speculated upon in the discussion of this chapter. However, *murQ* mutants 1 and 2 show no difference between the wild-type and *ΔhapR* strains. No change in activity was observed between different promoter constructs in *Δcrp* and *ΔcrpΔhapR* strains. Hence, mutation of conserved bases for HapR and CRP binding abolishes transcription activation by CRP and repression by HapR. In addition, truncation of the *murQ* promoter did not alter transcription regulation by CRP and HapR. Overall, we conclude that HapR and CRP bind to a shared binding locus at the *murQ* promoter and that co-binding prevents activation by CRP.

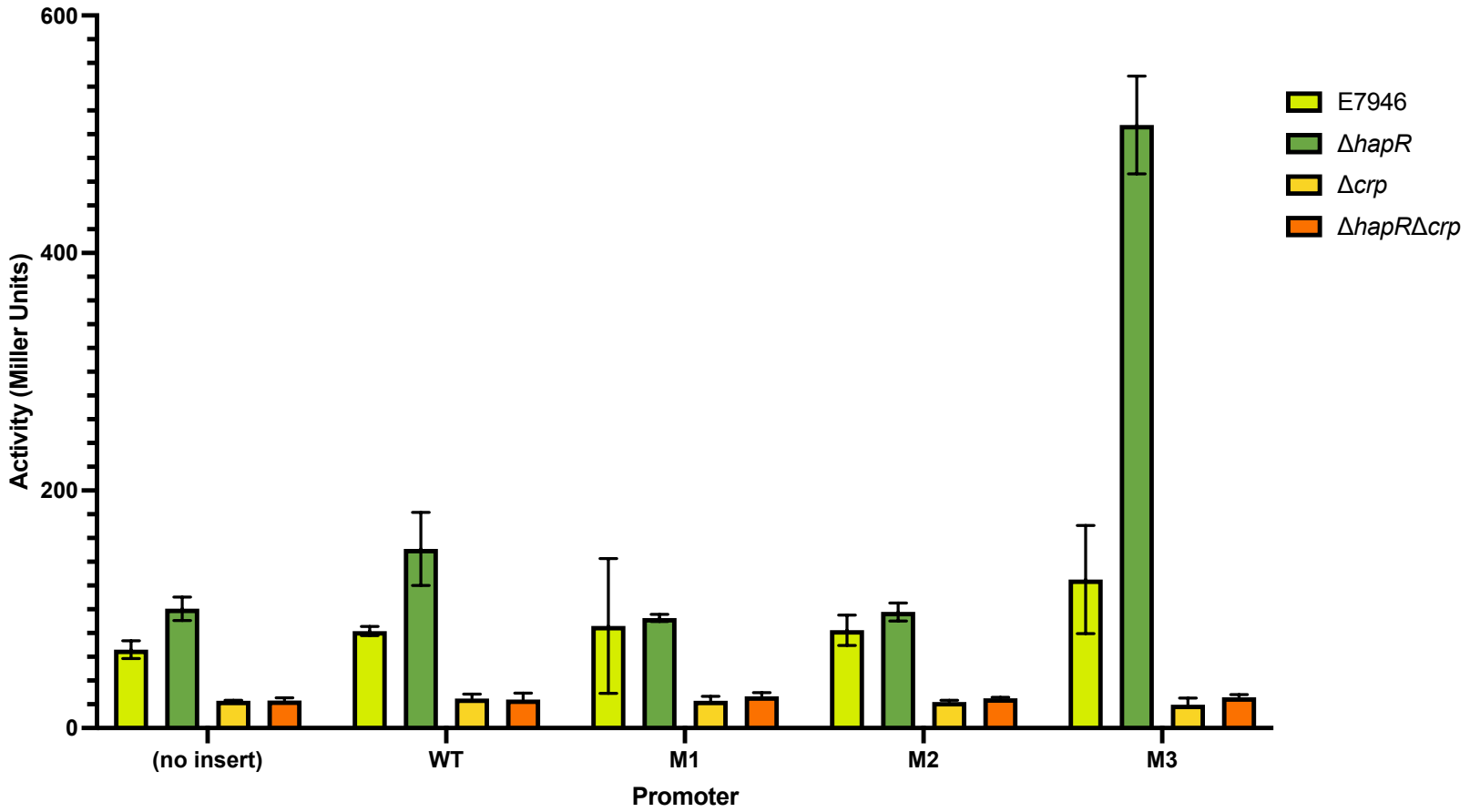

Figure 6.11 – The effect of mutants of P_{murQ} on transcription regulation by HapR and CRP in *V. cholerae* E7946. β-galactosidase assay of WT, *Δcrp, ΔhapR* and *ΔcrpΔhapR* strains transformed with promoter-*lacZ* fusions in plasmid pRW50-T or no insert controls (n=3). *N.B. 'no insert' and 'WT' data also used in figure 6.5.*

6.7 Mutations in HapR and CRP affect binding to the *murQ* promoter

We aimed to determine the mechanism of co-operative binding by HapR and CRP at the *murQ* promoter. We reasoned that HapR and CRP must bind different faces of the P_{murQ} DNA to avoid competing with each other. A DNA-bound structure of a HapR homologue in *Staphylococcus aureus,* QacR, has been resolved (Schumacher et al., 2002). We aligned this with an equivalent CRP-DNA structure (Parkinson et al., 1996). We used this to build a hypothetical model of a QacR-CRP-DNA complex, which is presented in figure 6.12. In our model, each monomer of QacR and CRP has a loop that protrudes towards the DNA (highlighted in figure 6.12) (Parkinson et al., 1996; Schumacher et al., 2002). In CRP, the loop is comprised of $D_{54}E_{55}E_{56}G_{57}$ residues that form AR3. In QacR, the loop comprises residues $K_{108}T_{109}N_{110}S_{111}$. In HapR, the analogous loop is comprises the sequence $R_{123}D_{124}E_{125}V_{126}$ (de Silva et al., 2007). We predicted that the arginine in the 'HapR loop' (R123) might interact with the negatively charged loop in CRP. Such an interaction might be critical for DNA binding co-operativity between CRP and HapR. To test this, we used site-directed mutagenesis to introduce non-synonymous mutations in the *hapR* and *crp* genes. In HapR, we replaced R123 with either an alanine (R123A, no charge) or a glutamic acid (R123E, negatively charged). In CRP, we replaced E55 with either an alanine (E55A, no charge) or arginine (E55R, positively charged). All mutant proteins were purified as described in materials and methods.

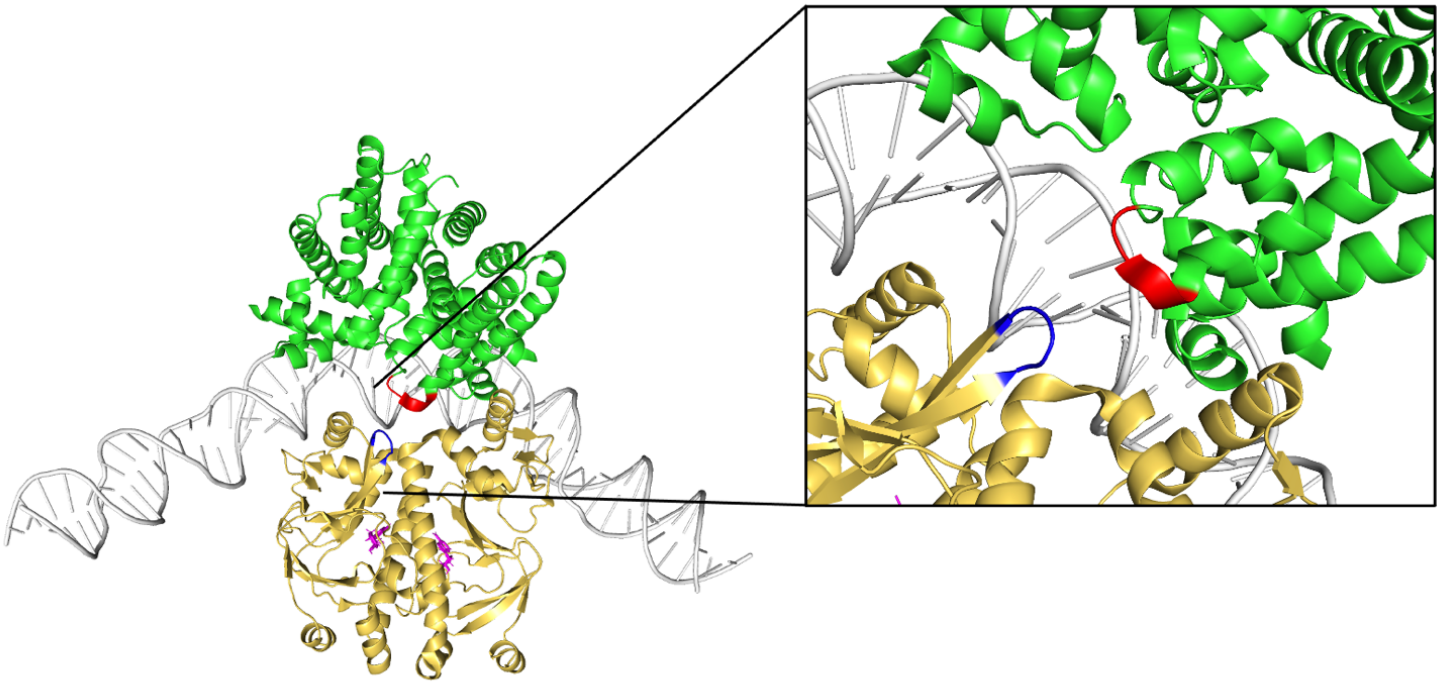

Figure 6.12 – Putative binding model of QacR/HapR and CRP at the *murQ* promoter. Crystal structure of HapR structural homologue, QacR (green) bound to DNA, resolved in *S. aureus* by Schumacher et al. (2002). Crystal structure of CRP dimer (yellow) bound to DNA (grey) resolved in *E. coli* by Parkinson et al. (1996). Motifs predicted to mediate interaction between proteins are highlighted in red and blue on HapR and CRP respectively. QacR-associated DNA aligned with DNA bound by CRP and hidden for the purposes of this model. Image generated in Pymol.

In an initial experiment, we checked binding of the individual CRP and HapR derivatives to P_{murQ}. Whilst HapR binds to P_{murQ} at sufficient concentrations, both HapR mutants are unable to bind. By contrast, mutations in CRP do not prevent binding to P_{murQ} (figure 6.13). Hence, we did not use the HapR derivatives in further experiments. Figure 6.14 shows EMSAs assessing the effect of CRP mutations on DNA binding co-operativity with HapR at P_{murQ}. Wild-type CRP binds co-operatively with HapR (lanes 5-8). However, we noticed that co-operative binding is altered for both CRP mutants; binding affinity at 2 µM CRP and 0.19 µM HapR resulted in a smear instead of a distinct band (compare lanes 6, 14 and 22). Furthermore, when the concentration of HapR was increased further, we observed an increase in unbound P_{murQ} DNA for both CRP mutants. This was most pronounced in the E55R mutant (compare lanes 7-8, 15-16, and 23-24).

To further assess how mutations in CRP affect its activity, and interactions with HapR, we used *in vitro* transcription. The results are shown in figure 6.15. As previously observed, wild-type CRP activates transcription from P_{murQ} and this transcript is repressed upon addition of HapR. Interestingly, both mutant derivatives of CRP activated transcription and this could not be repressed by HapR. Taken together, our results suggest that the CRP mutants are not deficient in transcription activation but are deficient in binding co-operativity with HapR at the *murQ* promoter.

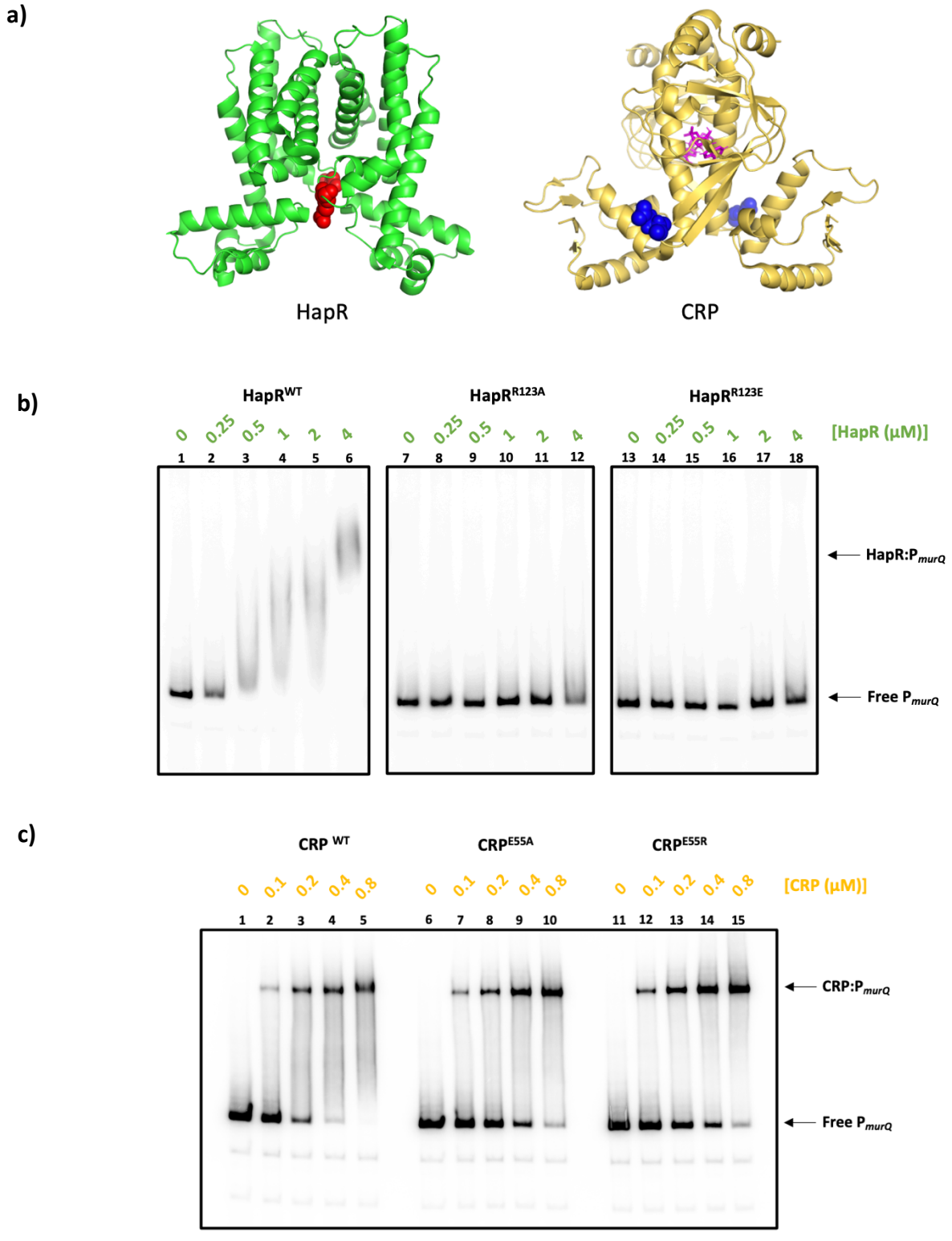

Figure 6.13 – The effect mutations in HapR and CRP on DNA binding P_{murQ}. a) Crystal structures of showing the loci of R123 (red) and E55 (blue) amino acid residues in HapR and CRP respectively. **b+c)** P^{32}-labelled promoter DNA fragments were mixed with proteins and herring sperm DNA as a non-specific inhibitor. Mixtures were run on a 5 % (w/v) polyacrylamide gel. Comparisons between wild-type and mutant derivatives of **b)** HapR and **c)** CRP on binding to P_{murQ}.

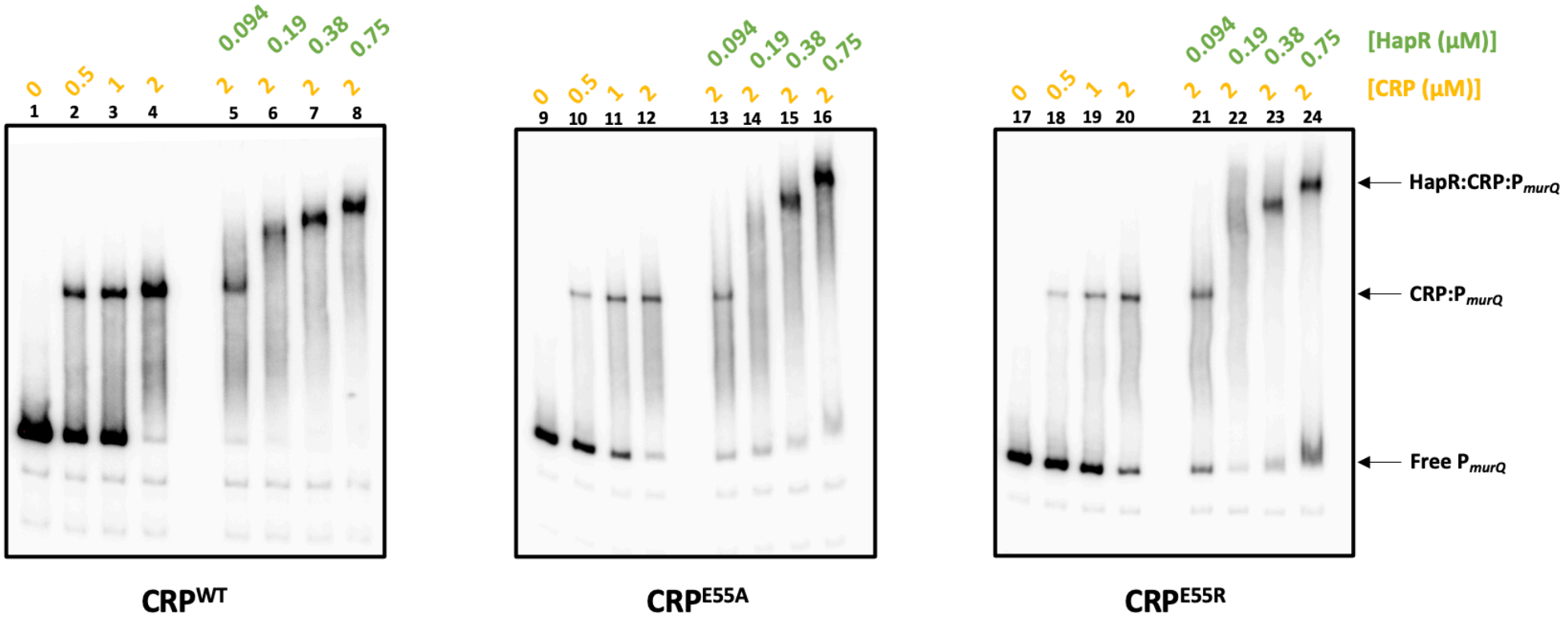

Figure 6.14 – The effect mutations in HapR and CRP on DNA binding co-operativity at P_{murQ}. P^{32}-labelled promoter DNA fragments were mixed with proteins and herring sperm DNA as a non-specific inhibitor. Mixtures were run on a 5 % (w/v) polyacrylamide gel.

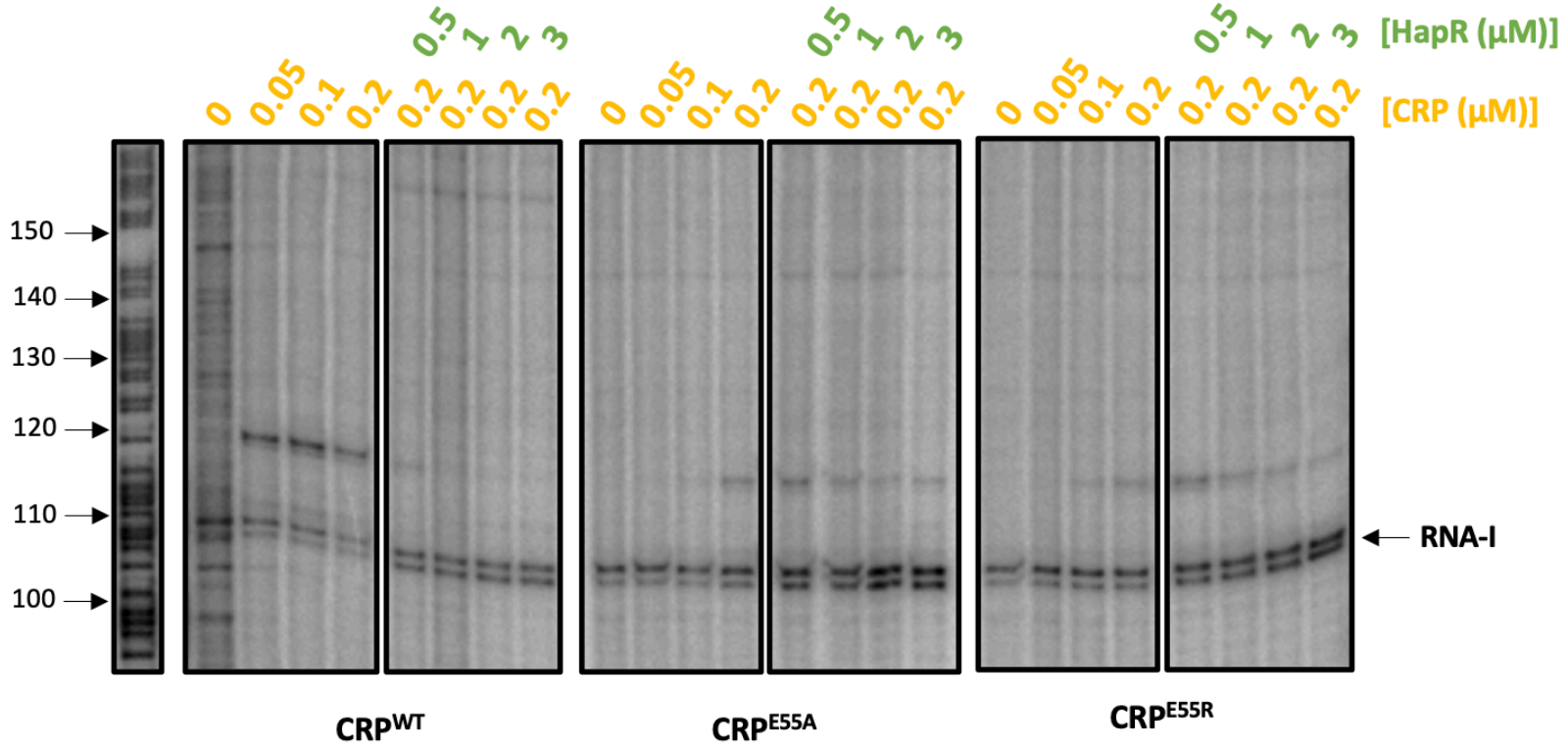

Figure 6.15 – The effect of CRP mutants on transcription and inhibition by HapR at P_{murQ}. P_{murQ} was cloned upstream of a λ*oop* transcription terminator and a separate σ^{70}-dependent transcript (RNA-I). Plasmid DNA was mixed with RNA polymerase, α-UTPs, σ^{70} and purified CRP/HapR of varying concentrations. Reactions run alongside GA ladders (left) for size reference.

6.8 Discussion

6.8.1 HapR and CRP co-regulation of the *murQ* promoter

In this chapter, we have assessed how HapR and CRP regulate transcription at the *murQ* promoter. CRP is essential for transcription activation, as indicated by both our *in vitro* transcription (figure 6.4) and our β-galactosidase assays (figure 6.5). Interestingly, β-galactosidase activity from truncated P_{murQ} (mutant 3) was over 3.5-fold higher in the *ΔhapR* strain compared to wild-type E7946. This difference may be due to other transcription factors, that bind the full-length promoter and repress transcription. We could not identify any other regions of CRP binding in our DNase I footprinting experiments (figure 6.6), consistent with CRP binding a single site. We conclude that activation of transcription at the *murQ* promoter requires binding of a single CRP dimer.

Regulation of MurQ expression by CRP has previously been reported in *E. coli* (Jaeger and Mayer, 2008). The *murQ* promoter in *E. coli* is a class I CRP activated promoter, with a CRP binding site -71.5 upstream of the transcription start site. This an interesting contrast to the *murQ* promoter in *V. cholerae*, which we have shown is a class II CRP-dependent promoter. Differences in the mechanisms of activation between *V. cholerae* and *E. coli* might reflect the distinct environments and nutrient sources utilised by both species.

We have shown that HapR and CRP bind to overlapping regions of the *murQ* promoter, which reflects similarities in their consensus DNA binding motifs. Our results show that HapR represses transcription from P_{murQ}. Surprisingly, we demonstrate that the affinity of HapR for the *murQ* promoter increases when CRP is bound. We conclude, therefore, that CRP and HapR bind co-operatively at this promoter.

In *E. coli*, transcription from the *murQ* promoter is regulated by another repressor, MurR, which binds to inverted repeats centred around -11 and -42 (Jaeger and Mayer, 2008). *V. cholerae* expresses MurR (VC0204), however MurR binding sites at the *murQ* promoter have not been determined (Heidelberg et al., 2000). Given that we have shown HapR binds at the -43 position, the co-regulation of *murQ* by MurR and HapR requires further investigation. Indeed, it is possible that transcription repression by MurR may have influenced results for the non-truncated *murQ* promoters *in vivo* (figure 6.11).

HapR and CRP co-regulation of the *murQ* promoter in *V. cholerae* is likely important to prevent ChiS repression by CRP at high-cell density. Chitin is a polymer of GlcNAc which *V. cholerae* can utilise as a source of carbon (Meibom et al., 2004). Like MurNAc, GlcNAc is also imported into the cytoplasm for recycling (John Rogers et al., 1988). GlcNAc import is controlled by NagE, which, like MurP is upregulated by CRP in *E.coli* (Plumbridge and Kolb, 1991). Our ChIP-seq data has not identified *nagE* in *V. cholerae* (VC0995) as a HapR target, however. We might conclude that CRP upregulates MurNAc and GlcNAc metabolism indiscriminately, but HapR (which is upregulated when *V. cholerae* is on chitin), might promote a preference for GlcNAc metabolism by downregulating MurQ and MurP. Alternatively, inhibition by HapR may prevent excessive removal of MurNAc from the cell wall which may be detrimental to bacterial morphology.

6.8.2 The mechanism of CRP and HapR binding co-operativity

We have identified the E55 residue in CRP as important for co-operative binding by HapR and CRP at the *murQ* promoter. The R123 residue in HapR is the most likely point of contact for CRP E55. However, mutation of R123 caused a loss of DNA binding by HapR. It is likely

that this is because R123 in one HapR monomer forms a salt bridge with E117 in the other (de Silva et al., 2007). Mutations in R123 are therefore potentially disruptive to the formation of the HapR dimer. To study the role of R123 in binding co-operativity with CRP further, a mutation which compensates for the loss of dimerization might be considered. For example, an E117R mutation might be used in tandem with R123E to restore the salt bridge that is disrupted in an R123E mutant. The loop region of CRP, which we predicted would mediate binding co-operativity with HapR at the *murQ* promoter, contains three negatively charged residues. Although this study has focused on mutating only one of these residues (E55), we acknowledge that D54 and E56 may also be critical for co-operativity.

Chapter 7
Final Conclusions and Future Directions

7.1 Conclusions

This study sought to determine the role of HapR and LuxO in the regulation of genes in *V. cholerae*. The high prevalence of non-synonymous mutations in *hapR* and *luxO* amongst clinical isolates of *V. cholerae* suggests that changes in expression or activity of these factors are important in the emergence of pathogenic strains (Weill et al., 2017). Three of the six mutations in the promoters of *hapR*, observed in clinical isolates and reproduced in this study, abolished transcription. It is likely, therefore, that the clinical isolates in which the mutations were found did not express *hapR*. Furthermore, one of the *luxO* promoter mutants tested resulted in increased expression and would likely result in repression of HapR *in vivo*. Taken together, our studies suggest that HapR-deficient strains are more likely to be pathogenic. Indeed, 50% of naturally-derived *V. cholerae* analysed in another study were found to be quorum-sensing deficient (Wang et al., 2011b). It has been suggested that strains of *V. cholerae* with this phenotype have a selective advantage over other bacteria within certain environments such as in biofilms (Katzianer et al., 2015). Quorum-sensing deficiency might not always be advantageous to the bacterium, however. For example, expression of HapR was shown to increase the survival of *V. cholerae* within the intestines of fruit flies (Kamareddine et al., 2018).

The fact that clinical isolates of 7PET *V. cholerae* are often HapR-deficient may explain why these strains do not persist in the environment (Mutreja et al., 2011). HapR controls the utilisation of chitin and induces natural competence, which are both key survival mechanisms within the aquatic environment (Meibom et al., 2005; Scrudato and Blokesch, 2013). Hence, HapR-deficient strains are likely to have reduced survivability outside of the

host. We note that the gene encoding the sigma factor, RpoS, a positive regulator of HapR, is also highly variable amongst clinical isolates (Weill et al., 2017).

Our ChIP-seq data has identified 32 DNA binding targets of HapR and 5 targets of LuxO. LuxO has previously only been described as a regulator of Qrr expression, however, we have identified another DNA-binding target between two divergent genes. These genes, ClpS and CspD are involved in protein degradation and carbon starvation respectively. Our data suggests that LuxO co-binds with σ^{70} at this locus, whereas σ^{54} co-binds with LuxO upstream of the four Qrrs (Dong and Mekalanos, 2012; Manneh-Roussel et al., 2018). Transcription co-regulation by bEBPs such as LuxO and σ^{54} is well-established (figure 1.9), further work is required to determine if LuxO also regulates the expression of σ^{70}-dependent genes.

We have identified 13 promoters which are directly repressed by HapR. The genes controlled by these promoters have roles in motility, respiration, chemotaxis and virulence. In addition, we have identified another promoter, *murQ*, which controls the expression of MurQ and MurP and is co-regulated by HapR and CRP. Transcription from the *murQ* promoter is activated by CRP in a class II-dependent manner and is repressed by HapR. We propose that HapR and CRP bind co-operatively at a single *murQ* promoter locus and that AR3 of CRP is important for this interaction. MurQ controls the metabolism of MurNAc, a key component of the cell wall. MurP imports MurNAc into the cytoplasm and dephosphorylates $EIIA^{Glc}$. This likely explains the importance of repression by HapR at this locus. CRP promotes the metabolism of alternative carbon sources but indirectly represses chitin catabolism. To counter this, HapR represses MurQ and MurP expression, thereby increasing the pool of phosphorylated $EIIA^{Glc}$ and subsequently upregulating ChiS.

7.2 Future Directions

We have established a model of co-operative binding by HapR and CRP at the *murQ* promoter, however, we have yet to fully characterise this interaction. Specifically, we have not yet confirmed if the negatively charged AR3 of CRP interacts with a positively charged amino acid residue in HapR. Mutation of R123 in HapR caused loss of DNA binding, which we speculated was due to the disruption of a salt bride crucial for HapR dimerisation (de Silva et al., 2007). A HapR E117R/R123E double mutant might preserve this salt bridge, whilst allowing us to investigate the interaction between R123 and residues within AR3. Other regulatory factors may control *murQ* expression besides HapR and CRP.

In our *in vivo* transcription assays we observed that truncation of the *murQ* intergenic region resulted in an increase in transcription, which was not observed *in vitro*. It may be that another repressor regulates this promoter by binding upstream of the HapR/CRP site we have identified. In *E. coli*, the *murR* gene is divergent from *murQ* and expresses a repressor of MurQP expression (Jaeger and Mayer, 2008). *murR* is also present in *V. cholerae*, and the interaction between HapR, CRP and MurR at the *murQ* promoter should therefore be characterised (Heidelberg et al., 2000).

In addition to the *murQP*, we have identified up to 13 other genes that may be co-regulated by HapR and CRP (summarised in table 4.2). Some of these genes may be regulated by HapR and CRP in a similar manner to *murQ* and future experiments should aim to determine this. Potentially co-regulated targets include the haemolysin and haemolysin export proteins, HlyA and HlyB. HapR has previously been shown to repress haemolysin expression (Gao et

al., 2018). Future experiments should compare the haemolytic activity of wild-type *V. cholerae* with that of Δ*hapR*, Δ*crp* and Δ*hapR*Δ*crp* strains.

We have not investigated the role of HapR at all the loci identified by our ChIP-seq analysis, many of which are upstream of genes of unknown function. Of the HapR-targeted genes for which a function is either known or inferred from their homology with genes in other bacteria, several have roles in motility and chemotaxis (Heidelberg et al., 2000). Further studies should therefore include deleting the genes regulated by HapR and assessing the motility of the resulting strains.

As previously discussed, HapR and LuxO displayed a high incidence of SNPs across clinical isolates of 7PET *V. cholerae*, the phenotypic effects of which are currently unknown. Further experiments should introduce the observed point mutations within the *hapR* and *luxO* genes and assess what effect, if any, this has on the growth, competence, motility, and pathogenesis of *V. cholerae*. Considering the observations made on *hapR* promoter mutants in chapter 3, we expect that some of the clinically observed SNPs render HapR inactive.

Appendices

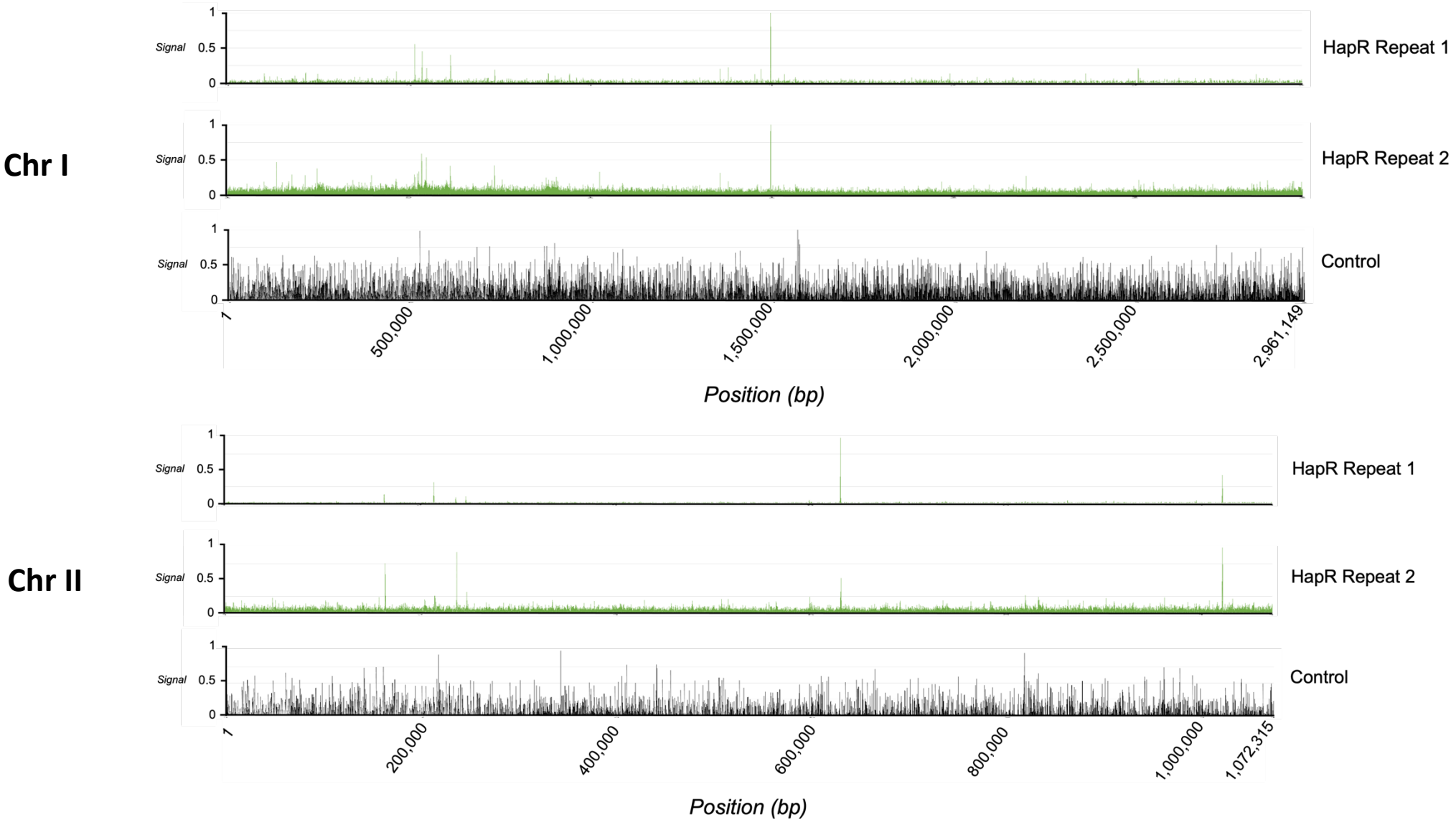
Chr I
Signal
1
0.5
0
HapR Repeat 1
HapR Repeat 2
Control
1
500,000
1,000,000
1,500,000
2,000,000
2,500,000
2,961,149
Position (bp)
Chr II
HapR Repeat 1
HapR Repeat 2
Control
1
200,000
400,000
600,000
800,000
1,000,000
1,072,315
Position (bp)

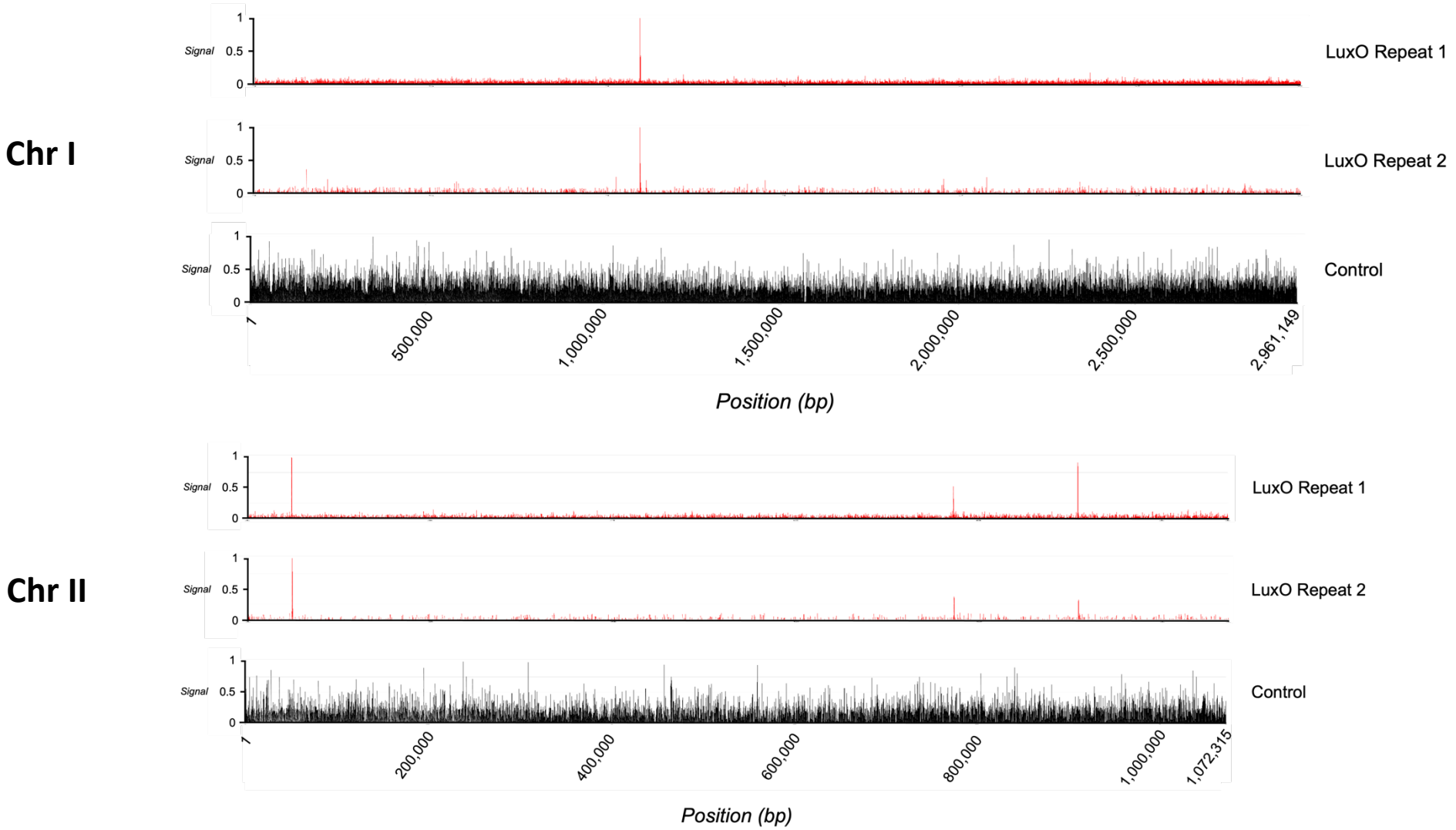

Supplementary figure 1 – Linear tracks of HapR and LuxO ChIP-seq data presented in figure 4.1. Reads across both chromosomes of *V. cholerae* N16961 were sorted into 10 bp bins using the 'multibamsummary' tool on usegalaxy.org. For each dataset, the read depths were normalised so that the highest signal was equal to 1.

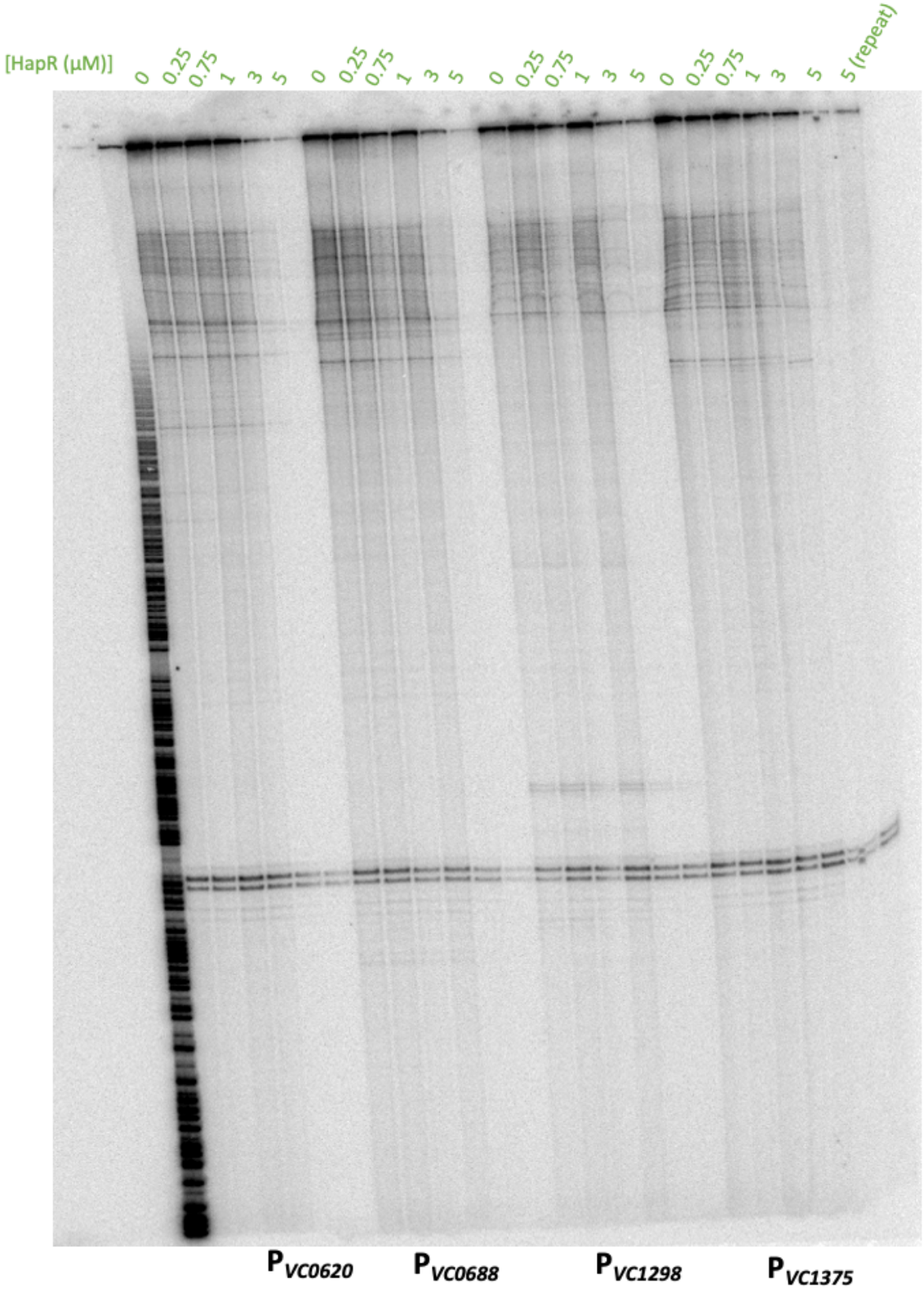
[HapR (μM)]
0 0.25 0.75 1 3 5 0 0.25 0.75 1 3 5 0 0.25 0.75 1 3 5 0 0.25 0.75 1 3 5 5 (repeat)
P VC0620
P VC0688
P VC1298
P VC1375

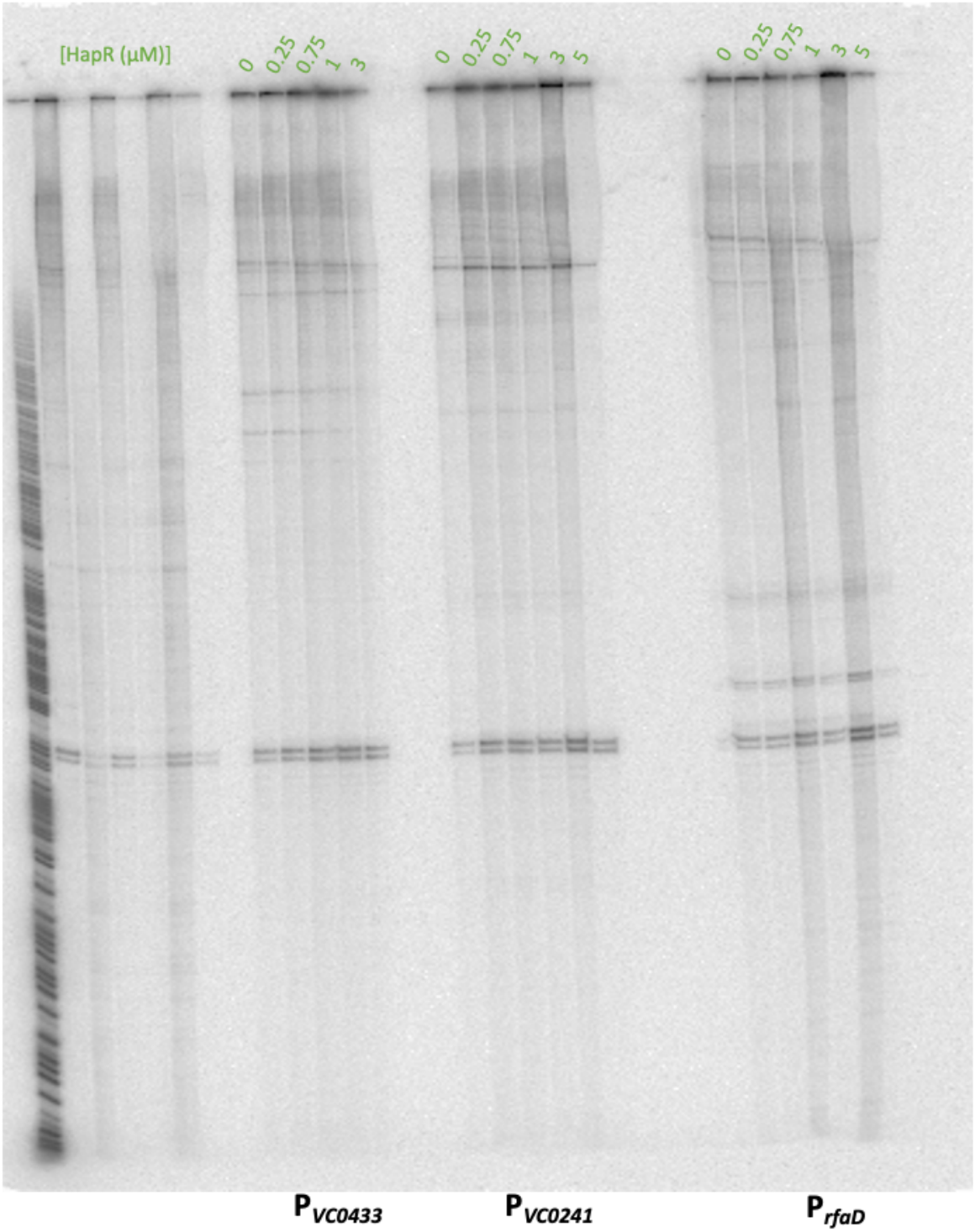
[HapR (μM)]
0 0.25 0.75 1 3
0 0.25 0.75 1 3 5
0 0.25 0.75 1 3 5
P_{VC0433}
P_{VC0241}
P_{rfaD}

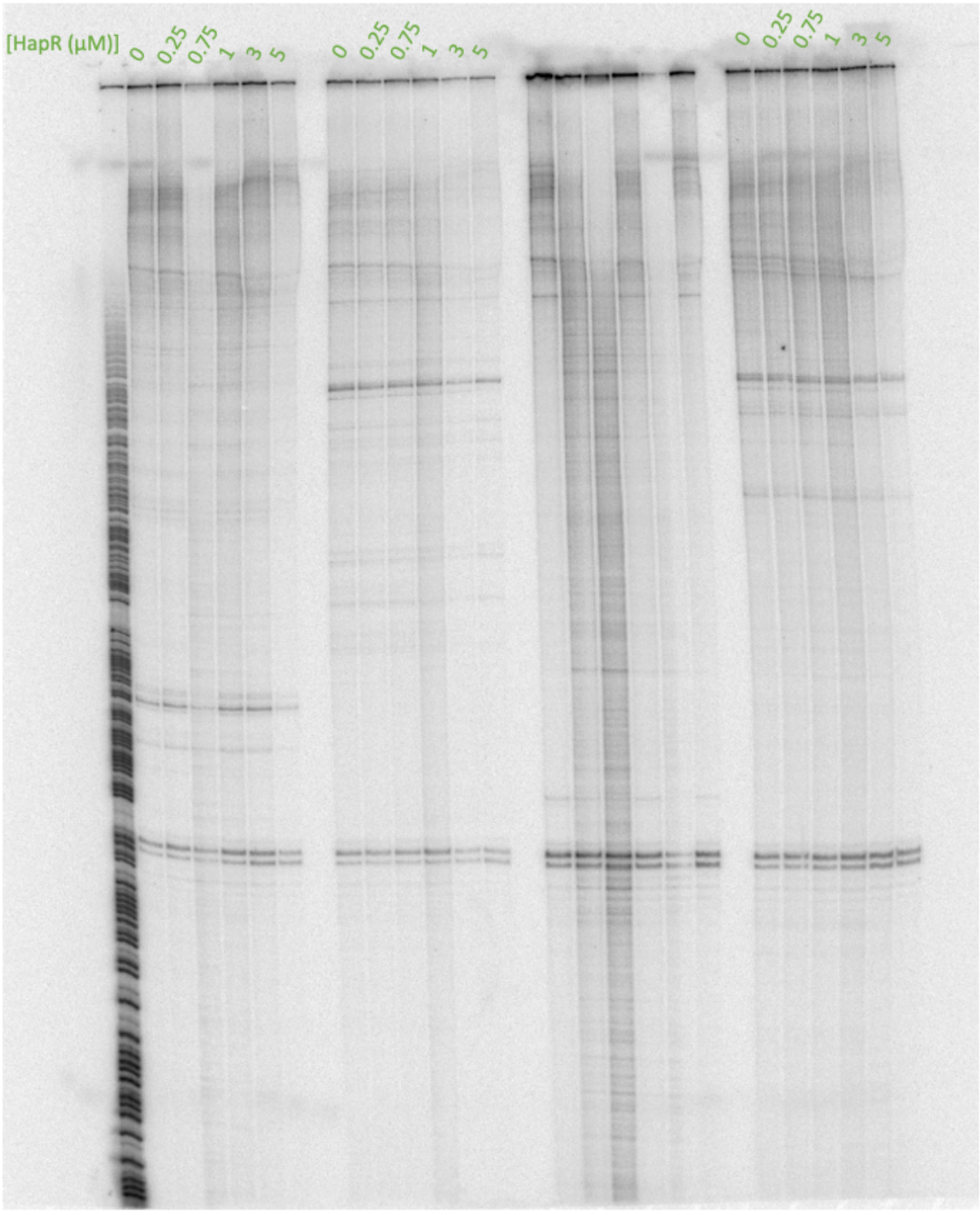
[HapR (μM)]
0
0.25
0.75
1
3
5
0
0.25
0.75
1
3
5
0
0.25
0.75
1
3
5
P VC0585
P VC0502
P leuO

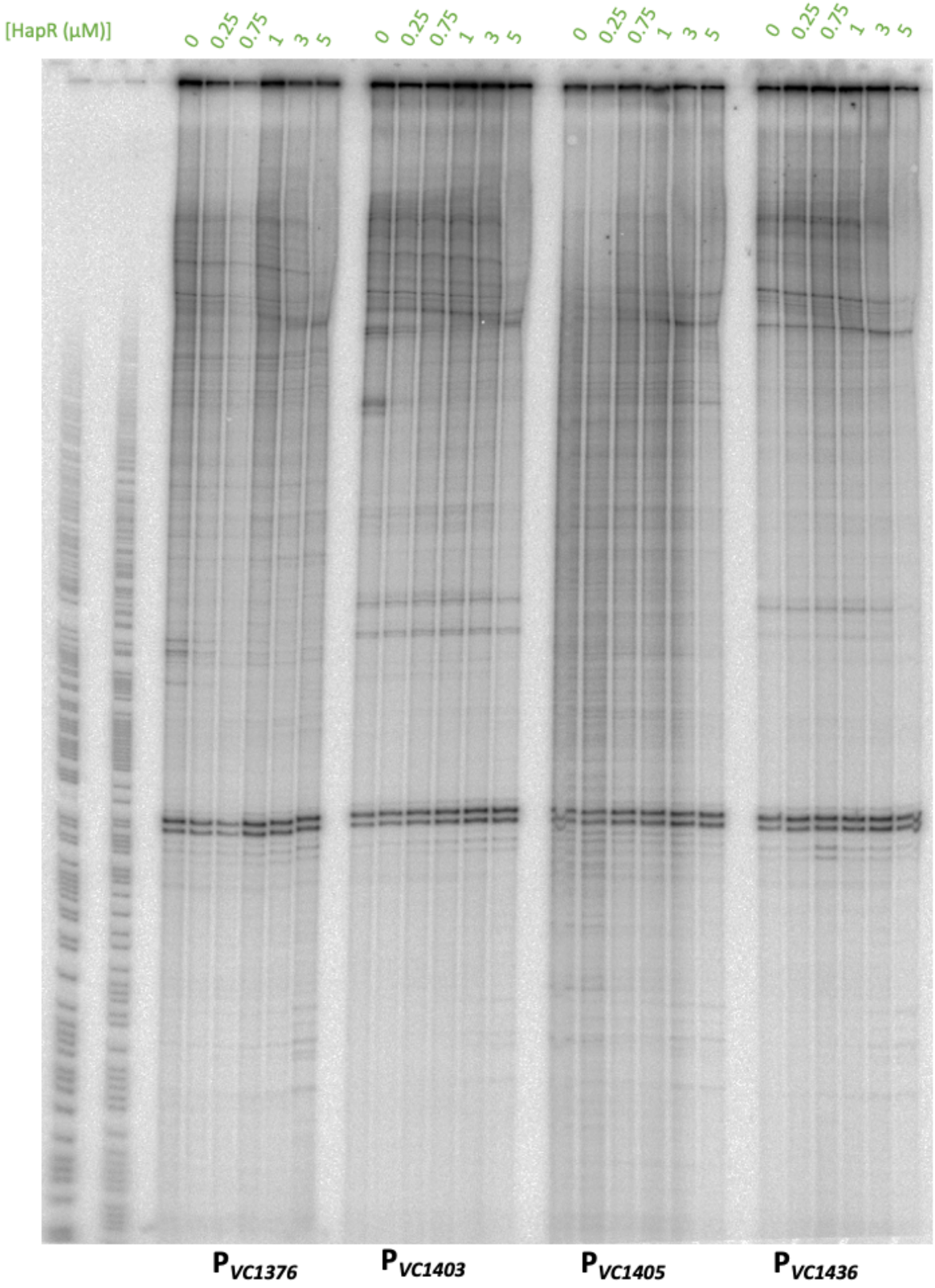
[HapR (μM)]
0 0.25 0.75 1 3 5
0 0.25 0.75 1 3 5
0 0.25 0.75 1 3 5
0 0.25 0.75 1 3 5
P VC1376
P VC1403
P VC1405
P VC1436


[HapR (μM)]
0 0.25 0.75 1 3 5
0 0.25 0.75 1 3 5
0 0.25 0.75 1 3 5
0 0.25 0.75 1 3 5 (5) (5)
P VC2352
P VCA0218
P VCA0219
P VCA0662

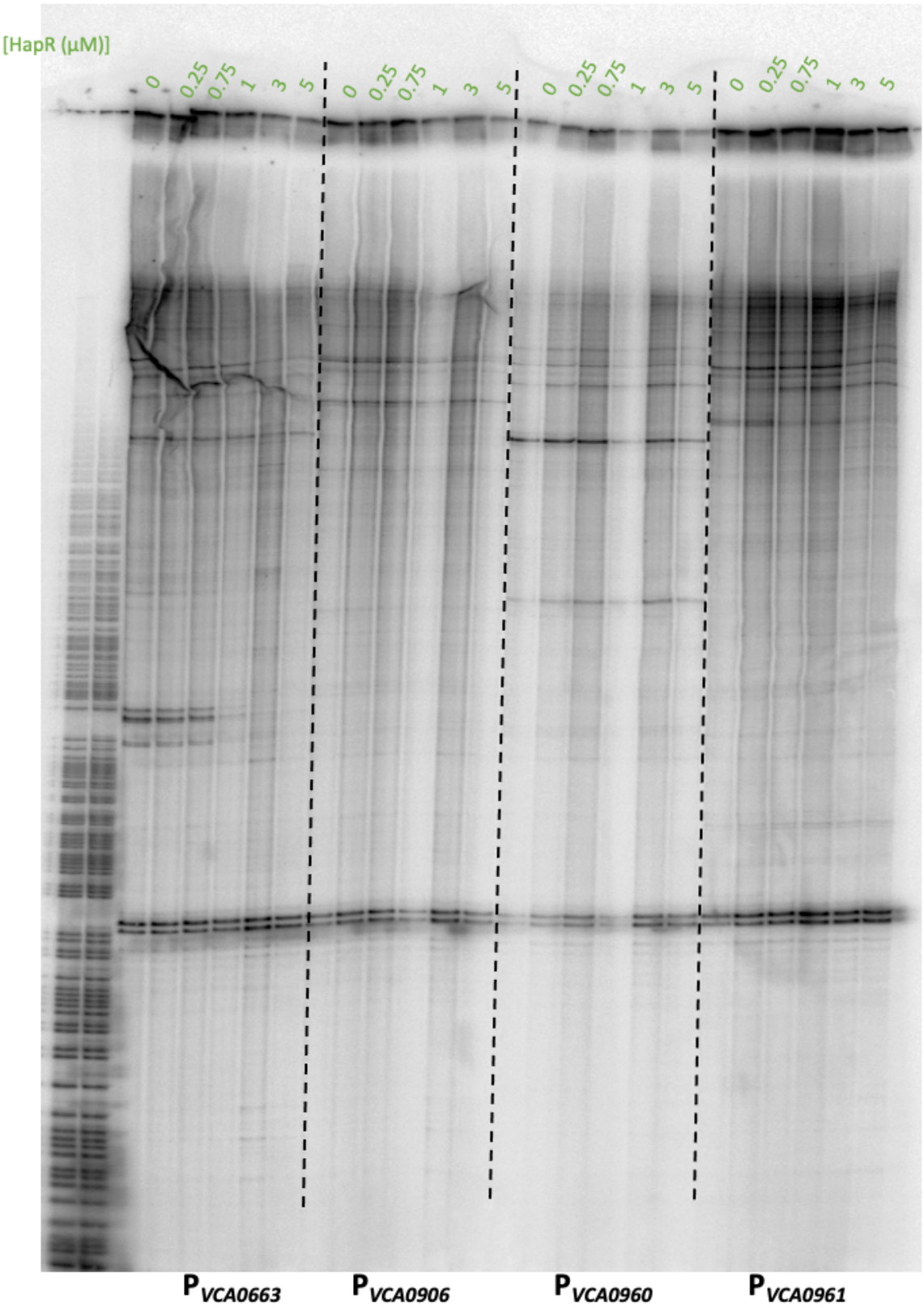
[HapR (μM)]
0
0.25
0.75
1
3
5
0
0.25
0.75
1
3
5
0
0.25
0.75
1
3
5
0
0.25
0.75
1
3
5
P VCA0663
P VCA0906
P VCA0960
P VCA0961

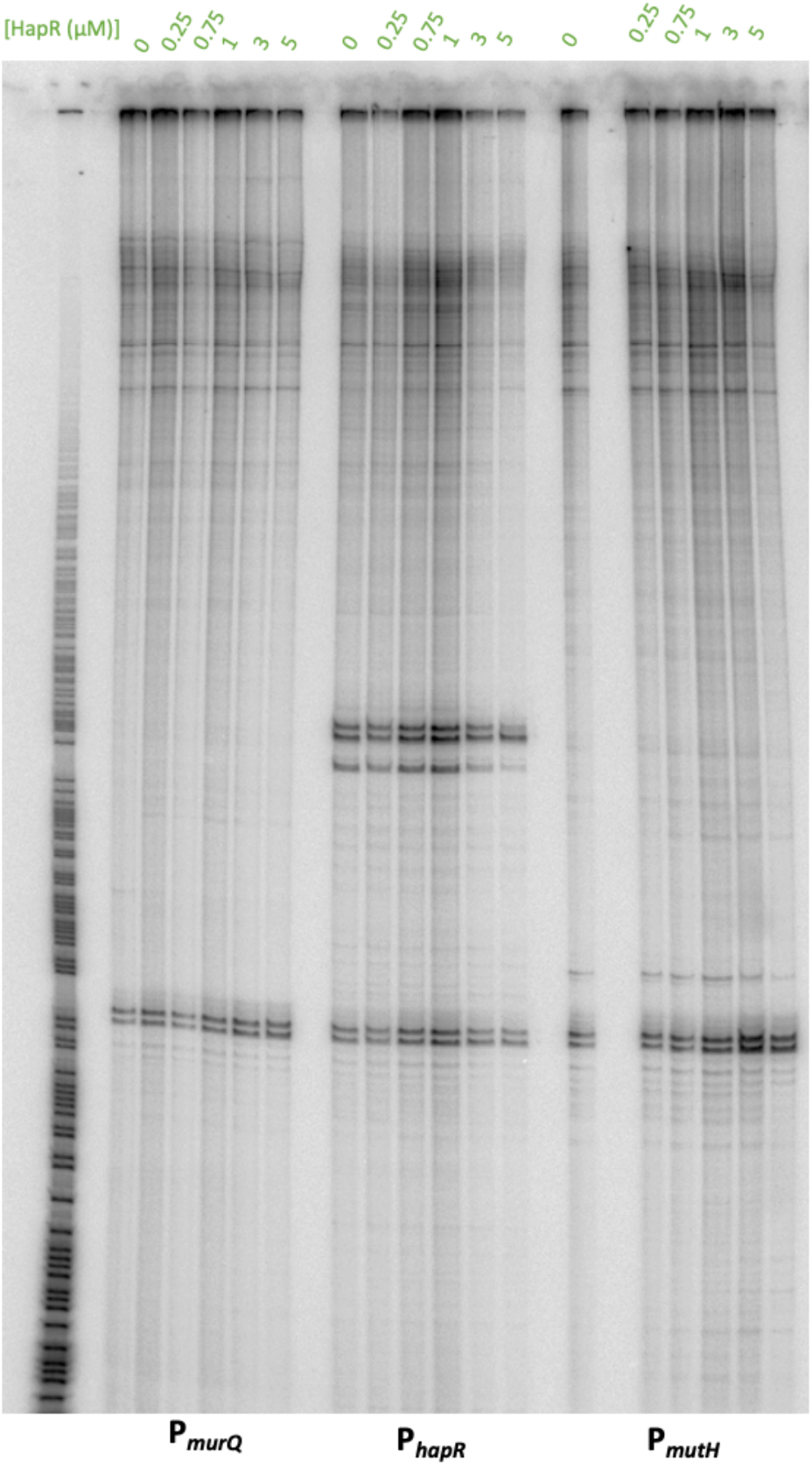
[HapR (μM)]
0
0.25
0.75
1
3
5
0
0.25
0.75
1
3
5
0
0.25
0.75
1
3
5
P murQ
P hapR
P mutH

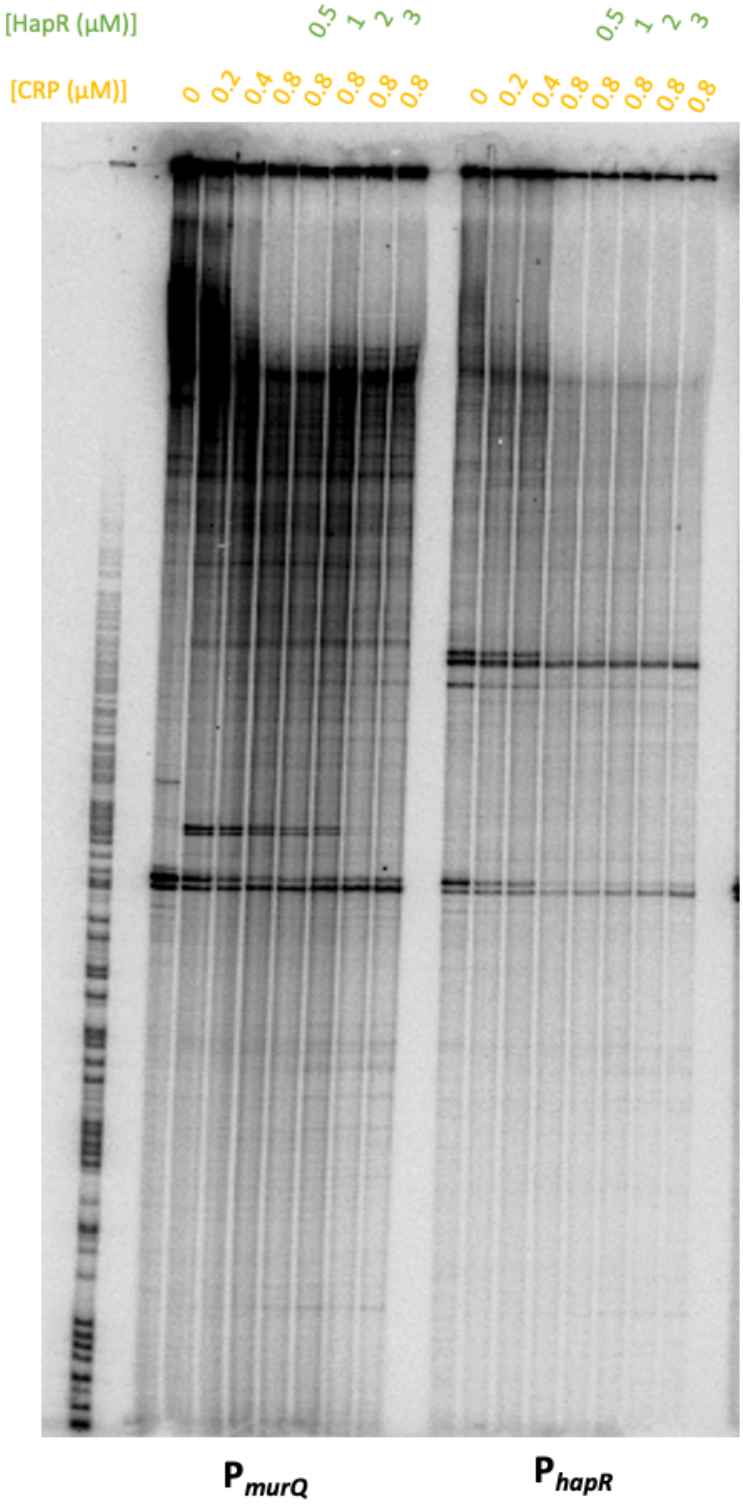

Supplementary figure 2 – Original *in vitro* transcription gel images used in this study.

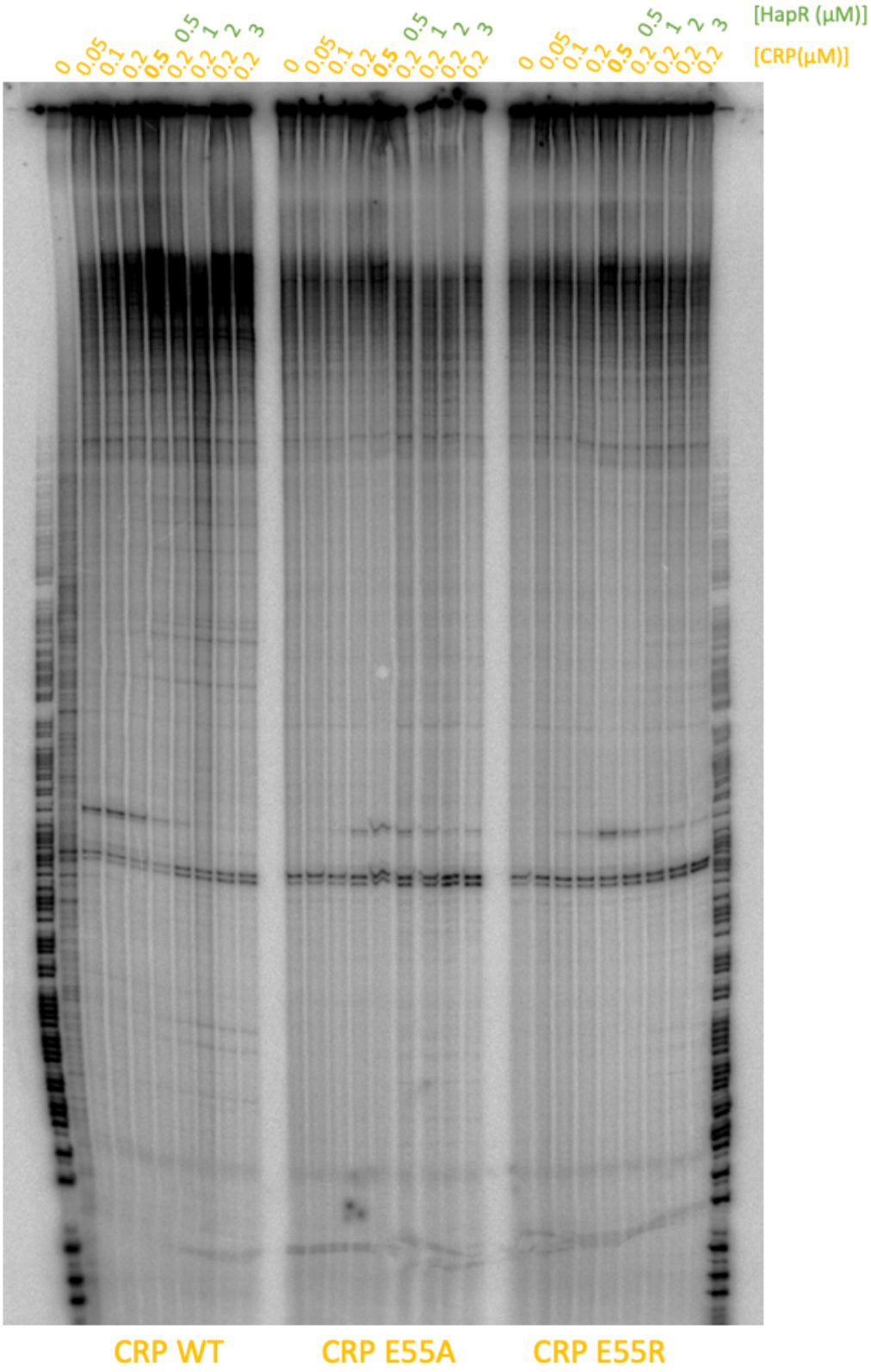
[HapR (μM)]
[CRP(μM)]
0 0.05 0.1 0.2 0.5 0.2 0.2 0.2 0.2
0.5 1 2 3
0 0.05 0.1 0.2 0.5 0.2 0.2 0.2 0.2
0.5 1 2 3
0 0.05 0.1 0.2 0.5 0.2 0.2 0.2 0.2
0.5 1 2 3
CRP WT
CRP E55A
CRP E55R

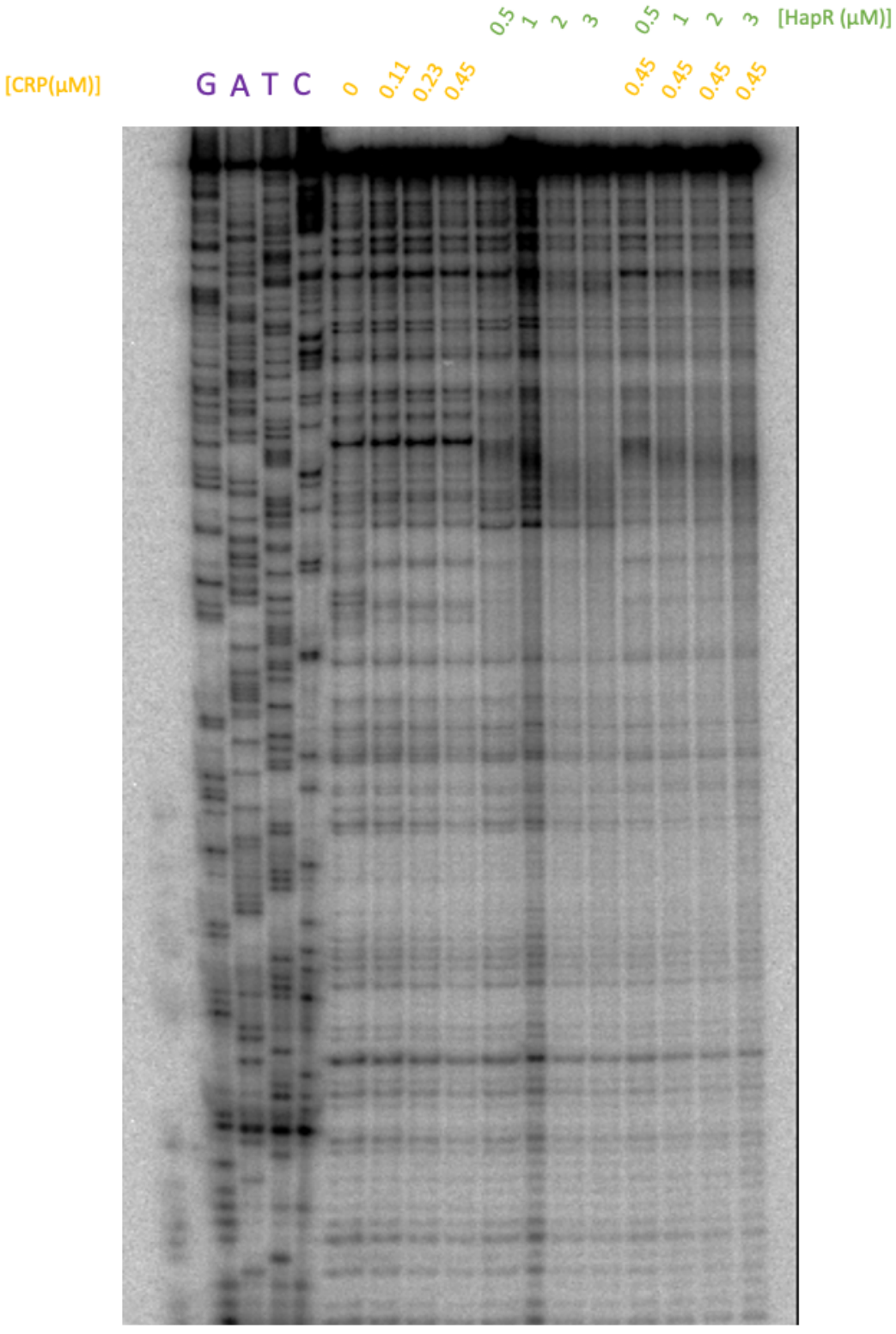

P_{murQ}

Supplementary figure 3 – Original images of DNAseI footprinting gel used in this study. *See relevant chapter for further details.*

References

Absalon, C., van Dellen, K. and Watnick, P.I. (2011) A communal bacterial adhesin anchors biofilm and bystander cells to surfaces. *PLoS pathogens*, 7 (8).

Abuaita, B.H. and Withey, J.H. (2009) Bicarbonate Induces *Vibrio cholerae* virulence gene expression by enhancing ToxT activity. *Infection and immunity*, 77 (9): 4111–4120.

Alam, M., Sultana, M., Nair, G.B., Sack, R.B., Sack, D., Siddique, A.A., Huq, A., Colwell, R. (2006) Toxigenic *Vibrio cholerae* in the aquatic environment of Mathbaria, Bangladesh. *Applied and environmental microbiology*, 72 (4): 2849–2855.

Alam, M., Sultana, M., Nair, G.B., Siddique, A., Hasan, N., Sack, R.B., Sack, DA., Ahmed, K., Sadique, A., Watanbe, W., Grim, C., Huq, A., Colwell, R. (2007) Viable but nonculturable *Vibrio cholerae* O1 in biofilms in the aquatic environment and their role in cholera transmission. *Proceedings of the National Academy of Sciences of the United States of America*, 104 (45): 17801–6.

Ali, M., Lopez, A.L., Ae You, Y., Eun Kim, Y., Sah, B., Maskery, B., Clemens, J. (2012) The global burden of cholera. *Bulletin of the World Health Organization*, 90 (3): 209–218.

Almagro-Moreno, S., Pruss, K. and Taylor, R.K. (2015) Intestinal Colonization Dynamics of *Vibrio cholerae*. *PLoS Pathogens*, 11 (5).

Angerer, A., Enz, S., Ochs, M., Braun., V. (1995) Transcriptional regulation of ferric citrate transport in *Escherichia coli* K-12. FecI belongs to a new subfamily of sigma 70-type factors that respond to extracytoplasmic stimuli. *Molecular microbiology*, 18 (1): 163–174.

Ayala, J.C., Wang, H., Benitez, J.A., Silva, A. (2018) Molecular basis for the differential expression of the global regulator VieA in *Vibrio cholerae* biotypes directed by H-NS, LeuO and quorum sensing. *Molecular Microbiology*, 107 (3): 330–343.

Bailey, T.L., Boden, M., Buske, F.A., Frith, M., Grant, C., Clementi, L., Ren, J., Li, W., Noble, W. et al. (2009) MEME SUITE: tools for motif discovery and searching. *Nucleic Acids Research*, 37

Ball, A.S., Chaparian, R.R. and van Kessel, J.C. (2017) Quorum Sensing Gene Regulation by LuxR/HapR Master Regulators in *Vibrios*. *Journal of Bacteriology*, 199 (19).

Ball, A.S. and van Kessel, J.C. (2019) The master quorum-sensing regulators LuxR/HapR directly interact with the alpha subunit of RNA polymerase to drive transcription activation in *Vibrio harveyi* and *Vibrio cholerae*. *Molecular microbiology*, 111 (5): 1317–1334.

Bassler, B.L., Wright, M., Showalter, R.E., Silverman, M. (1993) Intercellular signalling in *Vibrio harveyi*: sequence and function of genes regulating expression of luminescence. *Molecular Microbiology*, 9 (4): 773–786.

Bassler, B.L., Wright, M. and Silverman, M.R. (1994) Multiple signalling systems controlling expression of luminescence in *Vibrio harveyi* : sequence and function of genes encoding a second sensory pathway. *Molecular Microbiology*, 13 (2): 273–286.

Bina, J.E., Provenzano, D., Wang, C., Bina, R., Mekalanos, J. (2006) Characterization of the *Vibrio cholerae vexAB* and *vexCD* efflux systems. *Archives of Microbiology*, 186 (3): 171–181.

Blokesch, M. (2012) Chitin colonization, chitin degradation and chitin-induced natural competence of *Vibrio cholerae* are subject to catabolite repression. *Environmental Microbiology*, 14 (8): 1898–1912.

Blokesch, M. and Schoolnik, G.K. (2007) Serogroup conversion of *Vibrio cholerae* in aquatic reservoirs. *PLoS Pathogens*, 3 (6): 0733–0742.

Blokesch, M. and Schoolnik, G.K. (2008) The Extracellular Nuclease Dns and Its Role in Natural Transformation of *Vibrio cholerae*. *Journal of Bacteriology*, 190 (21): 7232.

Booth, B.A., Boesman-Finkelstein, M. and Finkelstein, R.A. (1984) *Vibrio cholerae* hemagglutinin/protease nicks cholera enterotoxin. *Infection and immunity*, 45 (3): 558–560.

Borukhov, S. and Nudler, E. (2008) RNA polymerase: the vehicle of transcription. *Trends in Microbiology*, 16 (3): 126–134.

Borukhov, S. and Severinov, K. (2002) Role of the RNA polymerase sigma subunit in transcription initiation. *Research in Microbiology*, 153 (9): 557–562.

Boyaci, H., Shah, T., Hurley, A., Kokona, B., Li, Z., Ventocilla, C., Jeffrey, P., Semmelhack, M., Fairman, R., Bassler, B., Hughson, F. (2016) Structure, Regulation, and Inhibition of the Quorum-Sensing Signal Integrator LuxO Stock, A.M. (ed.). *PLoS Biology*, 14 (5): e1002464.

Bradford, M.M. (1976) A rapid and sensitive method for the quantitation of microgram quantities of protein utilizing the principle of protein-dye binding. *Analytical Biochemistry*, 72 (1–2): 248–254.

Bridges, A.A. and Bassler, B.L. (2019) The intragenus and interspecies quorum-sensing autoinducers exert distinct control over *Vibrio cholerae* biofilm formation and dispersal Sourjik, V. (ed.). *PLoS Biology*, 17 (11): e3000429.

Browning, D.F. and Busby, S.J.W. (2004) The regulation of bacterial transcription initiation. Nature Reviews Microbiology, 2 (1): 57–65.

Browning, D.F. and Busby, S.J.W. (2016) Local and global regulation of transcription initiation in bacteria. *Nature Reviews Microbiology*, 14 (10): 638–650.

Burgess, R. and Jendrisak, J. (1975) A procedure for the rapid, large-scale purification of *Escherichia coli* DNA-dependent RNA polymerase involving Polymin P precipitation and DNA-cellulose chromatography. *Biochemistry*, 14 (21): 4634–4638.

Burgess, R.R. and Anthony, L. (2001) How sigma docks to RNA polymerase and what sigma does. *Current opinion in microbiology*, 4 (2): 126–31.

Busby, S. and Ebright, R.H. (1997) Transcription activation at Class II CAP-dependent promoters. *Molecular Microbiology*, 23 (5): 853–859.

Busby, S. and Ebright, R.H. (1999) Transcription activation by catabolite activator protein (CAP). *Journal of Molecular Biology*. 293 (2) pp. 199–213.

Bush, M. and Dixon, R. (2012) The role of bacterial enhancer binding proteins as specialized activators of σ54-dependent transcription. *Microbiology and Molecular Biology Reviews*, 76 (3): 497–529.

Campbell, E.A., Muzzin, O., Chlenov, M., Sun, J., Olson, a., Weinman, O., Trester-Zedlitz, M., Darst (2002) Structure of the bacterial RNA polymerase promoter specificity sigma subunit. *Molecular Cell*, 9 (3): 527–39.

Carver, T., Harris, S.R., Berriman, M., Parkhill, J., McQuillan J. (2012) Artemis: an integrated platform for visualization and analysis of high-throughput sequence-based experimental data. *Bioinformatics*, 28 (4): 464–469.

Carver, T., Thomson, N., Bleasby, A., Berriman, M., Parkhill, J. (2009) DNAPlotter: circular and linear interactive genome visualization. *Bioinformatics*, 25 (1): 119–120.

Casadaban, M.J. and Cohen, S.N. (1980) Analysis of gene control signals by DNA fusion and cloning in *Escherichia coli*. *Journal of Molecular Biology*, 138 (2): 179–207.

Chaparian, R.R., Olney, S.G., Hustmyer, C.M., et al. (2016) Integration host factor and LuxR synergistically bind DNA to coactivate quorum-sensing genes in *Vibrio harveyi*. *Molecular Microbiology*, 101 (5): 823–840.

Chaparian, R.R., Tran, M.L.N., Miller Conrad, L.C., et al. (2020) Global H-NS counter-silencing by LuxR activates quorum sensing gene expression. *Nucleic Acids Research*, 48 (1): 171–183.

Chatterjee, S.N. and Chaudhuri, K. (2003) Lipopolysaccharides of *Vibrio cholerae*: I. Physical and chemical characterization. *Biochimica et Biophysica Acta (BBA) - Molecular Basis of Disease*, 1639 (2): 65–79.

Chaudhuri, K. and Chatterjee, S.N. (2009) Cholera toxins. pp. 1–321.

Cheetham, G.M. and Steitz, T.A. (1999) Structure of a transcribing T7 RNA polymerase initiation complex. *Science*, 286 (5448): 2305–9.

Chin, C.-S., Sorenson, J., Harris, J.B., et al. (2011) The Origin of the Haitian Cholera Outbreak Strain. *New England Journal of Medicine*, 364 (1): 33–42.

Cho, B.K., Kim, D., Knight, E.M., Zengler, K., Palsson, B. (2014) Genome-scale reconstruction of the sigma factor network in *Escherichia coli*: Topology and functional states. *BMC Biology*, 12 (1): 1–11.

Colwell, R.R. (1996) Global Climate and Infectious Disease: The Cholera Paradigm. *Science*, 274 (5295): 2025–2031.

Conner, J.G., Teschler, J.K., Jones, C.J., Yildiz, F. (2016) Staying alive: *Vibrio cholerae*'s cycle of environmental survival, transmission, and dissemination. *Microbiology Spectrum*, 4 (2).

Conner, J.G., Zamorano-Sánchez, D., Park, J.H., Sondermann, H., Yildiz, F. (2017) The ins and outs of cyclic di-GMP signaling in *Vibrio cholerae*. *Current opinion in microbiology*, 36: 20.

Cramer, P., Bushnell, D.A. and Kornberg, R.D. (2001) Structural basis of transcription: RNA polymerase II at 2.8 angstrom resolution. *Science*, 292 (5523): 1863–76.

Crane, B.R., Sudhamsu, J. and Patel, B.A. (2010) Bacterial nitric oxide synthases. *Annual review of biochemistry*, 79: 445–470.

de Crombrugghe, B., Busby, S. and Buc, H. (1984) Cyclic AMP receptor protein: role in transcription activation. *Science*, 224 (4651): 831–838.

Cuthbertson, L. and Nodwell, J.R. (2013) The TetR Family of Regulators. *Microbiology and Molecular Biology Reviews*, 77 (3): 440.

Dahl, U., Jaeger, T., Nguyen, B.T., Sattler, J., Mayer, C. (2004) Identification of a phosphotransferase system of *Escherichia coli* required for growth on N-acetylmuramic acid. *Journal of Bacteriology*, 186 (8): 2385–2392.

Dalia, A.B., Lazinski, D.W. and Camilli, A. (2014) Identification of a membrane-bound transcriptional regulator that links chitin and natural competence in *Vibrio cholerae*. *mBio*, 5 (1).

Dallas, W.S. and Falkow, S. (1980) Amino acid sequence homology between cholera toxin and *Escherichia coli* heat-labile toxin. *Nature*, 288 (5790): 499–501.

Davies, B.W., Bogard, R.W., Young, T.S., Mekalanos, J. (2012) Coordinated regulation of accessory genetic elements produces cyclic di-nucleotides for *V. cholerae* virulence. *Cell*, 149 (2): 358–370.

deHaseth, P.L. and Helmann, J.D. (1995) Open complex formation by *Escherichia coli* RNA polymerase: the mechanism of polymerase-induced strand separation of double helical DNA. *Molecular Microbiology*, 16 (5): 817–824.

Dell, C.L., Neely, M.N. and Olson, E.R. (1994) Altered pH lysine signalling mutants of *cadC*, a gene encoding a membrane-bound transcriptional activator of the *Escherichia coli cadBA* operon. *Molecular Microbiology*, 14 (1): 7–16.

Deutscher, J., Francke, C. and Postma, P.W. (2006) How phosphotransferase system-related protein phosphorylation regulates carbohydrate metabolism in bacteria. *Microbiology and molecular biology reviews*, 70 (4): 939–1031.

Dong, T.G. and Mekalanos, J.J. (2012) Characterization of the RpoN regulon reveals differential regulation of T6SS and new flagellar operons in *Vibrio cholerae* O37 strain V52. *Nucleic Acids Research*, 40 (16): 7766–75.

Dubnau, D. and Losick, R. (2006) Bistability in Bacteria. *Molecular Microbiology,* 61 (3): 564-572.

Dutta, T. and Srivastava, S. (2018) Small RNA-mediated regulation in bacteria: A growing palette of diverse mechanisms. *Gene*, 656: 60–72.

Dziejman, M., Balon, E., Boyd, D., Fraser, C., Heidelberg, J., Mekalanos, J. (2002) Comparative genomic analysis of *Vibrio cholerae*: genes that correlate with cholera endemic and pandemic disease. *Proceedings of the National Academy of Sciences of the United States of America*, 99 (3): 1556–1561.

Ebright, R.H. (1993) Transcription activation at Class I CAP-dependent promoters. *Molecular Microbiology*, 8 (5): 797–802.

Eickhoff, M.J. and Bassler, B.L. (2018) SnapShot: Bacterial Quorum Sensing. *Cell*, 174 (5): 1328-1328.e1.

Erbse, A., Schmidt, R., Bornemann, T., Schneider-Mergener, J., Mogk, A., Zahn, R., Dougan, D., Bukau, B. (2006) ClpS is an essential component of the N-end rule pathway in *Escherichia coli*. *Nature*, 439 (7077): 753–756.

Erzberger, J.P. and Berger, J.M. (2006) Evolutionary relationships and structural mechanisms of AAA+ proteins. *Annual review of biophysics and biomolecular structure*, 35: 93–114.

Faner, M.A. and Feig, A.L. (2013) Identifying and characterizing Hfq-RNA interactions. *Methods*, 63 (2): 144–59.

Faruque, S.M., Biswas, K., Nashir Udden, S.M., Ahmad, Q. S., Sack, D., Nair, G.B., Mekalanos, J. (2006) Transmissibility of cholera: *in vivo*-formed biofilms and their relationship to infectivity and persistence in the environment. *Proceedings of the National Academy of Sciences of the United States of America*, 103 (16): 6350–6355.

Federle, M.J. and Bassler, B.L. (2003) Interspecies communication in bacteria. *The Journal of Clinical Investigation*, 112 (9): 1291–9.

Ferrell, J. E. (2002) Self-perpetuating states in signal transduction: positive feedback, double-negative feedback and bistability. *Current opinion in cell biology*, 14 (2): 140-148.

Flemming, H.C. and Wingender, J. (2010) The biofilm matrix. *Nature Reviews Microbiology*, 8 (9): 623–633.

Fong, J.C.N., Karplus, K., Schoolnik, G.K., Yildiz, F. (2006) Identification and characterization of RbmA, a novel protein required for the development of rugose colony morphology and biofilm structure in *Vibrio cholerae*. *Journal of Bacteriology*, 188 (3): 1049–1059.

Fong, J.C.N. and Yildiz, F.H. (2007) The *rbmBCDEF* gene cluster modulates development of rugose colony morphology and biofilm formation in *Vibrio cholerae*. *Journal of Bacteriology*, 189 (6): 2319–2330.

Fong, J.C.N. and Yildiz, F.H. (2008) Interplay between cyclic AMP-cyclic AMP receptor protein and cyclic di-GMP signaling in *Vibrio cholerae* biofilm formation. *Journal of Bacteriology*, 190 (20): 6646–6659.

Freeman, J.A. and Bassler, B.L. (1999) A genetic analysis of the function of LuxO, a two-component response regulator involved in quorum sensing in *Vibrio harveyi*. *Molecular microbiology*, 31 (2): 665–677.

Gao, H., Xu, J., Lu, X., Li, J., Lou, J., Zhao, H., Diao, B., Shi, Q., Zhang, Y., Kan, B. (2018) Expression of hemolysin is regulated under the collective actions of HapR, Fur, and HlyU in *Vibrio cholerae* El Tor serogroup O1. *Frontiers in Microbiology*, 9: 1310.

Gao, H., Zhang, J., Lou, J., Li, J., Qin, Q., Shi, Q., Zhang, Y., Kan, B. (2020) Direct Binding and Regulation by Fur and HapR of the Intermediate Regulator and Virulence Factor Genes Within the ToxR Virulence Regulon in *Vibrio cholerae*. *Frontiers in Microbiology*, 11.

Grainger, D.C., Aiba, H., Hurd, D., Browning, D., Busby, S. (2007) Transcription factor distribution in *Escherichia coli* : studies with FNR protein. *Nucleic Acids Research*, 35 (1): 269–278.

Gumpenberger, T., Vorkapic, D., Zingl, F.G., Pressler, K., Lackner, S., Seper, A., Reidl, J., Schild, S. (2016) Nucleoside uptake in *Vibrio cholerae* and its role in the transition fitness from host to environment. *Molecular Microbiology*, 99 (3): 470–483.

Halpern, M. and Izhaki, I. (2017) Fish as Hosts of *Vibrio cholerae*. *Frontiers in Microbiology*, 8: 282.

Hammer, B.K. and Bassler, B.L. (2003) Quorum sensing controls biofilm formation in *Vibrio cholerae*. *Molecular Microbiology*, 50 (1): 101–104.

Häse, C.C. and Mekalanos, J.J. (1998) TcpP protein is a positive regulator of virulence gene expression in *Vibrio cholerae*. *Proceedings of the National Academy of Sciences*, 95 (2): 730–734.

Haycocks, J.R.J., Warren, G.Z.L., Walker, L.M., Chlebek, J., Dalia, T., Dalia, A., Grainger, D.C. (2019) The quorum sensing transcription factor AphA directly regulates natural competence in *Vibrio cholerae. PLoS Genetics*, 15 (10): e1008362.

Hayden, J.D. and Ades, S.E. (2008) The Extracytoplasmic Stress Factor, σE, Is Required to Maintain Cell Envelope Integrity in *Escherichia coli*. *PLoS ONE*, 3 (2): e1573.

Heidelberg, J.F., Eisen, J.A., Nelson, W.C., Clayton, R., Gwinn, M., Dodson, D., Hickey, E., Peterson, J., Umayam, L., Gill, S., Nelson, K., Read, T., Tettelin, H., Richardson, D., Ermolaeva, M., Vamathevan, J., Bass, S., Qin, H., Dragoi, I., Sellers, P., McDonald, l., Utterback, T., Fleishmann, R., Nierman, W., White, O., Salzberg, S., Smith, H., Colwell, R., Mekalanos, J., Venter, J., Fraser, C. (2000) DNA sequence of both chromosomes of the cholera pathogen *Vibrio cholerae*. *Nature*, 406 (6795): 477–483.

Helene Thelin, K. and Taylor, R.K. (1996) Toxin-coregulated pilus, but not mannose-sensitive hemagglutinin, is required for colonization by *Vibrio cholerae* O1 El Tor biotype and O139 strains. *Infection and Immunity*, 64 (7): 2853–2856.

Hengge-Aronis, R. (1993) Survival of hunger and stress: The role of *rpoS* in early stationary phase gene regulation in *E. coli*. *Cell*, 72 (2): 165–168.

Herrington, D.A., Hall, R.H., Losonsky, G., Mekalanos, J., Taylor, R., Levine, M. (1988) Toxin, toxin-coregulated pili, and the toxR regulon are essential for *Vibrio cholerae* pathogenesis in humans. *The Journal of experimental medicine*, 168 (4): 1487–1492.

Herzog, R., Peschek, N., Fröhlich, K.S., Schumacher, K., Papenfort, K. (2019) Three autoinducer molecules act in concert to control virulence gene expression in *Vibrio cholerae*. *Nucleic Acids Research*, 47 (6): 3171–3183.

Hossain, S., Heckler, I. and Boon, E.M. (2018) Discovery of a Nitric Oxide Responsive Quorum Sensing Circuit in *Vibrio cholerae*. *ACS chemical biology*, 13 (8): 1964–1969.

Hulbert, R.R. and Taylor, R.K. (2002) Mechanism of ToxT-Dependent Transcriptional Activation at the *Vibrio cholerae tcpA* Promoter. *Journal of Bacteriology*, 184 (20): 5533.

Ichinose, Y., Yamamoto, K., Nakasone, N., Tanabe, M., Takeda, T., Miwatani, T., Iwanaga, M. (1987) Enterotoxicity of El Tor-like hemolysin of non-O1 *Vibrio cholerae*. *Infection and Immunity*, 55 (5): 1090–1093.

Jaeger, T., Arsic, M. and Mayer, C. (2005) Scission of the lactyl ether bond of N-acetylmuramic acid by *Escherichia coli* "etherase." *The Journal of Biological Chemistry*, 280 (34): 30100–30106.

Jaeger, T. and Mayer, C. (2008) The transcriptional factors MurR and catabolite activator protein regulate N-acetylmuramic acid catabolism in *Escherichia coli*. *Journal of Bacteriology*, 190 (20): 6598–6608.

Janoff, E.N., Hayakawa, H., Taylor, D.N., Fasching, C., Kenner, J., Jaimes, E., Raij, L. (1997) Nitric oxide production during *Vibrio cholerae* infection. *The American Journal of Physiology*, 273 (5).

Jeffery, C.J. and Koshland, D.E. (1993) *Vibrio cholerae hlyB* is a member of the chemotaxis receptor gene family. *Protein Science : A Publication of the Protein Society*, 2 (9): 1532.

Jermyn, W.S. and Boyd, E.F. (2002) Characterization of a novel *Vibrio* pathogenicity island (VPI-2) encoding neuraminidase (*nanH*) among toxigenic *Vibrio cholerae* isolates. *Microbiology*, 148 (Pt 11): 3681–3693.

Jobling, M.G. and Holmes, R.K. (1997) Characterization of *hapR*, a positive regulator of the *Vibrio cholerae* HA/protease gene *hap*, and its identification as a functional homologue of the *Vibrio harveyi luxR* gene. *Molecular Microbiology*, 26 (5): 1023–1034.

Joelsson, A., Liu, Z. and Zhu, J. (2006) Genetic and Phenotypic Diversity of Quorum-Sensing Systems in Clinical and Environmental Isolates of *Vibrio cholerae*. *Infection and Immunity*, 74 (2): 1141.

John Rogers, M., Ohgi, T., Plumbridge, J., Söll, D. (1988) Nucleotide sequences of the *Escherichia coli nagE* and *nagB* genes: the structural genes for the N-acetylglucosamine transport protein of the bacterial phosphoenolpyruvate: sugar phosphotransferase system and for glucosamine-6-phosphate deaminase. *Gene*, 62 (2): 197–207.

Joly, N., Zhang, N., Buck, M., Zhang, X. (2012) Coupling AAA protein function to regulated gene expression. *Biochimica et Biophysica Acta (BBA) - Molecular Cell Research*, 1823 (1): 108–116.

Jung, S.A., Chapman, C.A. and Ng, W.-L. (2015) Quadruple Quorum-Sensing Inputs Control *Vibrio cholerae* Virulence and Maintain System Robustness Weiss, D. (ed.). *PLoS Pathogens*, 11 (4): e1004837.

Kamareddine, L., Wong, A.C.N., Vanhove, A.S., Hang, S., Purdy, A., Kierek-Pearson, K., Asara, J., Ali, A., Glenn Morris Jr, J., Watnick, P. (2018) Activation of *Vibrio cholerae* quorum sensing promotes survival of an arthropod host. *Nature Microbiology*, 3 (2): 243–252.

Kaper, J.B., Morris, J.G. and Levine, M.M. (1995) Cholera. *Clinical Microbiology Reviews*, 8 (1): 48–86.

Karaolis, D.K.R., Johnson, J.A., Bailey, C.C., Boedeker, E., Kaper, J., Reeves, P. (1998) A *Vibrio cholerae* pathogenicity island associated with epidemic and pandemic strains. *Proceedings of the National Academy of Sciences*, 95 (6): 3134–3139.

Karaolis, D.K.R., Somara, S., Maneval, D.R., Johnson, J., Kaper, J. (1999) A bacteriophage encoding a pathogenicity island, a type-IV pilus and a phage receptor in cholera bacteria. *Nature*, 399 (6734): 375–379.

Katzianer, D.S., Wang, H., Carey, R.M., Zhu, J. (2015) “Quorum Non-Sensing”: Social Cheating and Deception in *Vibrio cholerae*. *Applied and Environmental Microbiology*, 81 (11): 3856.

Keller, L. and Surette, M.G. (2006) Communication in bacteria: an ecological and evolutionary perspective. *Nature Reviews Microbiology*, 4 (4): 249–258.

van Kessel, J.C., Rutherford, S.T., Shao, Y., Utria, A., Bassler, B. (2013a) Individual and combined roles of the master regulators AphA and LuxR in control of the *Vibrio harveyi* quorum-sensing regulon. *Journal of Bacteriology*, 195 (3): 436–443.

van Kessel, J.C., Ulrich, L.E., Zhulin, I.B., Bassler, B. (2013b) Analysis of activator and repressor functions reveals the requirements for transcriptional control by LuxR, the master regulator of quorum sensing in *Vibrio harveyi*. *mBio*, 4 (4).

Klancher, C.A., Hayes, C.A. and Dalia, A.B. (2017) The nucleoid occlusion protein SlmA is a direct transcriptional activator of chitobiose utilization in *Vibrio cholerae*. *PLoS Genetics*, 13 (7): e1006877.

Klancher, C.A., Newman, J.D., Ball, A.S., van Kessel, J., Dalia, A. (2020a) Species-specific quorum sensing represses the chitobiose utilization locus in *Vibrio cholerae*. *Applied and Environmental Microbiology*, 86 (18).

Klancher, C.A., Yamamoto, S., Dalia, T.N., Dalia, A. (2020b) ChiS is a noncanonical DNA-binding hybrid sensor kinase that directly regulates the chitin utilization program in *Vibrio cholerae*. *Proceedings of the National Academy of Sciences of the United States of America*, 117 (33): 20180–20189.

Koch, H.G., Winterstein, C., Saribas, A.S., Alben, J., Daldal, F. (2000) Roles of the *ccoGHIS* gene products in the biogenesis of the cbb3-type cytochrome c oxidase. *Journal of Molecular Biology*, 297 (1): 49–65.

Koestler, B.J. and Waters, C.M. (2014) Bile acids and bicarbonate inversely regulate intracellular cyclic di-GMP in *Vibrio cholerae*. *Infection and Immunity*, 82 (7): 3002–3014.

Kolb, A., Busby, S., Buc, H., Garges, S., Adhya, S. (1993) Transcriptional Regulation by cAMP and Its Receptor Protein. *Annual Review of Biochemistry*, 62 (1): 749–797.

Kovacikova, G. and Skorupski, K. (2002) Regulation of virulence gene expression in *Vibrio cholerae* by quorum sensing: HapR functions at the *aphA* promoter. *Molecular Microbiology*, 46 (4): 1135–1147.

Kumar, A., Malloch, R.A., Fujita, N., Smillie, D., Ishihama, A., Hayward, R. (1993) The Minus 35-Recognition Region of *Escherichia coli* Sigma 70 is Inessential for Initiation of Transcription at an “Extended Minus 10” Promoter. *Journal of Molecular Biology*, 232 (2): 406–418.

Lee, D.J., Minchin, S.D. and Busby, S.J.W. (2012) Activating Transcription in Bacteria. *Annual Review of Microbiology*, 66 (1): 125–152.

Lencer, W.I., Constable, C., Moe, S., Rufo, P., Wolf, A., Jobling, M., Ruston, S., Madara, J., Holmes, R., Hirst, T. (1997) Proteolytic activation of cholera toxin and *Escherichia coli* labile toxin by entry into host epithelial cells. Signal transduction by a protease-resistant toxin variant. *The Journal of Biological Chemistry*, 272 (24): 15562–15568.

Lenz, D.H., Miller, M.B., Zhu, J., Kulkarni, R., Bassler, B. (2005) CsrA and three redundant small RNAs regulate quorum sensing in *Vibrio cholerae*. *Molecular Microbiology*, 58 (4): 1186–1202.

Lenz, D.H., Mok, K.C., Lilley, B.N., Kulkarni, R., Wingreen, N., Bassler, B. (2004) The small RNA chaperone Hfq and multiple small RNAs control quorum sensing in *Vibrio harveyi* and *Vibrio cholerae*. *Cell*, 118 (1): 69–82.

Li, X. and Roseman, S. (2004) The chitinolytic cascade in *Vibrios* is regulated by chitin oligosaccharides and a two-component chitin catabolic sensor/kinase. *Proceedings of the National Academy of Sciences of the United States of America*, 101 (2): 627–631.

Li, X.-Y. and McClure, W.R. (1998) Characterization of the Closed Complex Intermediate Formed during Transcription Initiation by *Escherichia coli* RNA Polymerase. *Journal of Biological Chemistry*, 273 (36): 23549–23557.

Lilley, B.N. and Bassler, B.L. (2000) Regulation of quorum sensing in *Vibrio harveyi* by LuxO and Sigma-54. *Molecular Microbiology*, 36 (4): 940–954.

Lin, W., Kovacikova, G. and Skorupski, K. (2005) Requirements for *Vibrio cholerae* HapR binding and transcriptional repression at the *hapR* promoter are distinct from those at the *aphA* promoter. *Journal of Bacteriology*, 187 (9): 3013–9.

Lin, W., Kovacikova, G. and Skorupski, K. (2007) The quorum sensing regulator HapR downregulates the expression of the virulence gene transcription factor AphA in *Vibrio cholerae* by antagonizing Lrp- and VpsR-mediated activation. *Molecular Microbiology*, 64 (4): 953–967.

Liu, M.Y., Gui, G., Wei, B., Preston, J., Oakford, L., Yüksel, Ü., Giedroc, D., Romeo, T. (1997) The RNA molecule CsrB binds to the global regulatory protein CsrA and antagonizes its activity in *Escherichia coli*. *The Journal of Biological Chemistry*, 272 (28): 17502–17510.

Lodge, J., Fear, J., Busby, S., Gunasekeran, P., Kamini, N. (1992) Broad host range plasmids carrying the *Escherichia coli* lactose and galactose operons. FEMS microbiology letters, 74 (2–3): 271–276.

de Lorenzo, V., Cases, I., Herrero, M., Timmis, K. (1993) Early and late responses of TOL promoters to pathway inducers: identification of postexponential promoters in

Pseudomonas putida with *lacZ-tet* bicistronic reporters. *Journal of Bacteriology*, 175 (21): 6902–6907.

Lowden, M.J., Skorupski, K., Pellegrini, M., Chiorazzo, M., Taylor, R. (2010) Structure of *Vibrio cholerae* ToxT reveals a mechanism for fatty acid regulation of virulence genes. *Proceedings of the National Academy of Sciences of the United States of America*, 107 (7): 2860–2865.

Manneh-Roussel, J., Haycocks, J.R.J., Magán, A., Perez-Soto, N., Voelz, K., Camili, A., Karchler, A., Grainger, D.C. (2018) cAMP Receptor Protein Controls *Vibrio cholerae* Gene Expression in Response to Host Colonization. *mBio*, 9 (4).

Margolin, W. (2005) FtsZ and the division of prokaryotic cells and organelles. Nature reviews. *Molecular Cell Biology*, 6 (11): 862–71.

Matson, J.S., Yoo, H.J., Hakansson, K., DiRita, V. (2010) Polymyxin B resistance in El Tor *Vibrio cholerae* requires lipid acylation catalyzed by MsbB. *Journal of Bacteriology*, 192 (8): 2044–2052.

Meibom, K.L., Blokesch, M., Dolganov, N.A., Wu, C., Schoolnik, G. (2005) Chitin Induces Natural Competence in *Vibrio cholerae*. *Science*, 310 (5755): 1824–1827.

Meibom, K.L., Li, X.B., Nielsen, A.T., Wu, C., Roseman, S., Schoolnick, G. (2004) The *Vibrio cholerae* chitin utilization program. *Proceedings of the National Academy of Sciences of the United States of America*, 101 (8): 2524.

Merrell, D.S. and Camilli, A. (1999) The *cadA* gene of *Vibrio cholerae* is induced during infection and plays a role in acid tolerance. *Molecular Microbiology*, 34 (4): 836–849.

Merrick, M.J. (1993) In a class of its own? the RNA polymerase sigma factor (σN). *Molecular Microbiology*, 10 (5): 903–909.

Miller, J.H. (1972) Experiments in molecular genetics. *Cold Spring Harbor Laboratory*.

Miller, M.B. and Bassler, B.L. (2001) Quorum Sensing in Bacteria. *Annual Review of Microbiology*, 55 (1): 165–199.

Miller, V.L., DiRita, V.J. and Mekalanos, J.J. (1989) Identification of *toxS*, a regulatory gene whose product enhances *toxR*-mediated activation of the cholera toxin promoter. *Journal of Bacteriology*, 171 (3): 1288–1293.

Minakhin, L., Bhagat, S., Brunning, A., Campbell, E., Darst, S. (2001) Bacterial RNA polymerase subunit ω and eukaryotic RNA polymerase subunit RPB6 are sequence, structural, and functional homologs and promote RNA polymerase assembly. *Proceedings of the National Academy of Sciences*, 98 (3): 892–897.

Murakami, K.S., Masuda, S., Campbell, E.A., Muzzin, O., Darst, S. (2002) Structural Basis of Transcription Initiation: An RNA Polymerase Holoenzyme-DNA Complex. *Science*, 296 (5571): 1285–1290.

Murphy, S.G., Johnson, B.A., Ledoux, C.M., Dörr, T. (2021) *Vibrio cholerae*'s mysterious Seventh Pandemic island (VSP-II) encodes novel Zur-regulated zinc starvation genes involved in chemotaxis and cell congregation. *PLoS Genetics*, 17 (6): e1009624.

Mutreja, A., Kim, D.W., Thomson, N.R., Connor, T., Lee, J., Karikuri, S., Croucher, N., Choi, S., Harris, S., Lebens, M., Niyogi, S., Kim, E., Ramamurthy, T., Chun, J., Wood, J., Clemens, J., Czerkinsky, C., Nair, G.B. Holmgren, J., Parkhill, J. Dougan, G. (2011) Evidence for several waves of global transmission in the seventh cholera pandemic. *Nature*, 477 (7365): 462–465.

Newman, J.D., Russell, M.M., Fan, L., Wang, Y., Gonzalezz-Gutierrez, G., van Kessel, J. (2021) The DNA binding domain of the *Vibrio vulnificus* SmcR transcription factor is flexible and binds diverse DNA sequences. *Nucleic Acids Research*, 49 (10): 5967–5984.

Ng, W.-L., Perez, L.J., Wei, Y., Kraml, C., Semmelhack, M., Bassler, B. (2011) Signal production and detection specificity in *Vibrio* CqsA/CqsS quorum-sensing systems. *Molecular Microbiology*, 79 (6): 1407–1417.

Nielsen, A.T., Dolganov, N.A., Otto, G., Miller, M., Wu, C., Schoolnick, G. (2006) RpoS Controls the *Vibrio cholerae* Mucosal Escape Response. *PLoS Pathogens*, 2 (10): e109.

Nielsen, A.T., Dolganov, N.A., Rasmussen, T., Otto, G., Miller, M., Felt, A., Torreilles, S., Schoolnik, G. (2010) A bistable switch and anatomical site control *Vibrio cholerae* virulence gene expression in the intestine. *PLoS pathogens*, 6 (9).

Niu, W., Kim, Y., Tau, G., Heyduk, T., Ebright, R. (1996) Transcription activation at class II CAP-dependent promoters: two interactions between CAP and RNA polymerase. *Cell*, 87 (6): 1123–34.

Niu, W., Zhou, Y., Dong, Q., Ebright, Y., Ebright, R. (1994) Characterization of the activating region of *Escherichia coli* catabolite gene activator protein (CAP) I. Saturation and alanine-scanning mutagenesis. *Journal of Molecular Biology*, 243 (4): 595–602.

Nudler, E., Gusarov, I., Avetissova, E., Kozlov, M., Goldfarb, A. (1998) Spatial Organization of Transcription Elongation Complex in *Escherichia coli*. *Science*, 281 (5375): 424–428.

Pang, B., Yan, M., Cui, Z., Ye, X., Diao, B., Ren, Y., Gao, S., Zhang, L., Kan, B. (2007) Genetic diversity of toxigenic and nontoxigenic *Vibrio cholerae* serogroups O1 and O139 revealed by array-based comparative genomic hybridization. *Journal of Bacteriology*, 189 (13): 4837–4849.

Papenfort, K., Förstner, K.U., Cong, J.-P., Sharma, C., Bassler, B. (2015) Differential RNA-seq of *Vibrio cholerae* identifies the VqmR small RNA as a regulator of biofilm formation.

Proceedings of the National Academy of Sciences of the United States of America, 112 (7): E766-75.

Parkinson, G., Wilson, C., Gunasekera, A., Ebright, Y., Ebright, R., Berman, H. (1996) Structure of the CAP-DNA complex at 2.5 angstroms resolution: a complete picture of the protein-DNA interface. *Journal of Molecular Biology*, 260 (3): 395–408.

Plumbridge, J. and Kolb, A. (1991) CAP and Nag repressor binding to the regulatory regions of the *nagE-B* and *manX* genes of *Escherichia coli*. *Journal of Molecular Biology*, 217 (4): 661–679.

Cunin, R., Glansdorff, N., Piérard, A., Stalon, V. (1986) Biosynthesis and metabolism of arginine in bacteria. *Microbiological Reviews*, 50 (3): 314–352.

Revyakin, A., Liu, C., Ebright, R.H., Strick, T. (2006) Abortive initiation and productive initiation by RNA polymerase involve DNA scrunching. *Science* (New York, N.Y.), 314 (5802): 1139–43.

Rhodius, V.A. and Busby, S.J.W. (2000) Interactions between activating region 3 of the *Escherichia coli* cyclic AMP receptor protein and region 4 of the RNA polymerase σ70 subunit: application of suppression genetics. *Journal of Molecular Biology*, 299 (2): 311–324.

Rojo, F. (1999) Repression of transcription initiation in bacteria. *Journal of Bacteriology*, 181 (10): 2987–91.

Rombel, I., North, A., Hwang, I., Wyman, C., Kustu, S. (1998) The bacterial enhancer-binding protein NtrC as a molecular machine. *Cold Spring Harbor symposia on quantitative biology*, 63: 157–66.

Rosenberg, G., Yehezkel, D., Hoffman, D., Mattioli, C.C., Fremder, M., Ben-Arosh, H., Vainman, L., Nissani, N., Hen-Avivi, S., Brenner, S., Itkin, M., Malitsky, S., Ohana, E., Ben-Moshe, N.B., Avraham, R. (2021) Host succinate is an activation signal for Salmonella virulence during intracellular infection. Science 371 (6527): 400-405

Ross, W., Ernst, A. and Gourse, R.L. (2001) Fine structure of *E. coli* RNA polymerase-promoter interactions: alpha subunit binding to the UP element minor groove. *Genes & Development,* 15 (5): 491–506.

Rutherford, S.T., van Kessel, J.C., Shao, Y., Bassler, B. (2011) AphA and LuxR/HapR reciprocally control quorum sensing in *Vibrios*. *Genes & Development*, 25 (4): 397–408.

Sabo, D.L., Boeker, E.A., Byers, B., Waron, H., Fischer, E. (1974) Purification and physical properties of inducible *Escherichia coli* lysine decarboxylase. *Biochemistry*, 13 (4): 662–670.

Sanderson, A., Mitchell, J.E., Minchin, S.D., Busby, S. (2003) Substitutions in the *Escherichia coli* RNA polymerase σ70 factor that affect recognition of extended −10 elements at promoters. *FEBS Letters*, 544 (1–3): 199–205.

Savery, N.J., Lloyd, G.S., Kainz, M., Gaal, T., Ross, W., Ebright, R., Gourse, R., Busby, S. (1998) Transcription activation at Class II CRP-dependent promoters: identification of determinants in the C-terminal domain of the RNA polymerase alpha subunit. *The EMBO Journal*, 17 (12): 3439.

Schumacher, M.A., Miller, M.C., Grkovic, S., Brown, M., Skurray, R., Brennan, R. (2002) Structural basis for cooperative DNA binding by two dimers of the multidrug-binding protein QacR. *The EMBO Journal*, 21 (5): 1210.

Scott, S., Busby, S. and Beacham, I. (1995) Transcriptional co-activation at the *ansB* promoters: involvement of the activating regions of CRP and FNR when bound in tandem. *Molecular Microbiology*, 18 (3): 521–531.

Scrudato, M. lo and Blokesch, M. (2013) A transcriptional regulator linking quorum sensing and chitin induction to render *Vibrio cholerae* naturally transformable. *Nucleic Acids Research*, 41 (6): 3644.

Sengupta, C., Mukherjee, O. and Chowdhury, R. (2016) Adherence to Intestinal Cells Promotes Biofilm Formation in *Vibrio cholerae*. *The Journal of Infectious Diseases*, 214 (10): 1571–1578.

Seper, A., Pressler, K., Kariisa, A., Haid, A., Roier, S., Leitner, D., Reidl, J., Tamayo, R., Schild, S. (2014) Identification of genes induced in *Vibrio cholerae* in a dynamic biofilm system. *International Journal of Medical Microbiology*, 304 (5–6): 749.

Seshasayee, A.S.N., Sivaraman, K. and Luscombe, N.M. (2011) An Overview of Prokaryotic Transcription Factors. *Sub-Cellular Biochemistry*. (52) pp. 7–23.

Shimada, T., Fujita, N., Yamamoto, K., Ishihama, A. (2011) Novel Roles of cAMP Receptor Protein (CRP) in Regulation of Transport and Metabolism of Carbon Sources. *PLoS ONE*, 6 (6): 20081.

Silva, A.J. and Benitez, J.A. (2016) *Vibrio cholerae* Biofilms and Cholera Pathogenesis. *PLoS neglected tropical diseases*, 10 (2): e0004330.

Silva, A.J., Pham, K. and Benitez, J.A. (2003) Haemagglutinin/protease expression and mucin gel penetration in El Tor biotype *Vibrio cholerae*. *Microbiology*, 149 (Pt 7): 1883–1891.

de Silva, R.S., Kovacikova, G., Lin, W., Taylor, R., Skorupski, K., Kull, F. (2007) Crystal structure of the *Vibrio cholerae* quorum-sensing regulatory protein HapR. *Journal of Bacteriology*, 189 (15): 5683–91.

Skorupski, K. and Taylor, R.K. (1996) Positive selection vectors for allelic exchange. *Gene*, 169 (1): 47–52.

Skorupski, K. and Taylor, R.K. (1997a) Cyclic AMP and its receptor protein negatively regulate the coordinate expression of cholera toxin and toxin-coregulated pilus in *Vibrio cholerae*. *Proceedings of the National Academy of Sciences*, 94 (1): 265–270.

Skorupski, K. and Taylor, R.K. (1997b) Sequence and functional analysis of the gene encoding *Vibrio cholerae* cAMP receptor protein. *Gene*, 198 (1–2): 297–303.

Slamti, L., Livny, J. and Waldor, M.K. (2007) Global Gene Expression and Phenotypic Analysis of a *Vibrio cholerae rpoH* Deletion Mutant. *Journal of Bacteriology*, 189 (2): 351.

Spangler, B.D. (1992) Structure and function of cholera toxin and the related *Escherichia coli* heat-labile enterotoxin. *Microbiological Reviews*, 56 (4): 622–647.

Spiga, L., Winter, M.G., Furtado de Carvalho, T., Zhu, W., Hughes, E.R, Gillis, C.C., Behrendt, C.L., Kim, J., Chessa, D., Andrews-Polymenis, H.L., Beiting, D.P., Santos, R.L., Hooper, L.V. Winter, S.E. (2017) An Oxidative Central Metabolism Enables Salmonella to Utilize Microbiota-Derived Succinate. Cell Host & Microbe, 22 (3): 291-301

Starnbach, M.N. and Lory, S. (1992) The fliA (rpoF) gene of *Pseudomonas aeruginosa* encodes an alternative sigma factor required for flagellin synthesis. *Molecular Microbiology*, 6 (4): 459–469.

Stroeher, U.H., Karageorgos, L.E., Morona, R., Manning, P. (1992) Serotype conversion in *Vibrio cholerae* O1. *Proceedings of the National Academy of Sciences*, 89 (7): 2566–2570.

Svenningsen, S.L., Tu, K.C. and Bassler, B.L. (2009) Gene dosage compensation calibrates four regulatory RNAs to control *Vibrio cholerae* quorum sensing. *The EMBO journal*, 28 (4): 429–39.

Thöny-Meyer, L., Beck, C., Preisig, O., Hennecke, H. (1994) The *ccoNOQP* gene cluster codes for a cb-type cytochrome oxidase that functions in aerobic respiration of *Rhodobacter capsulatus*. *Molecular Microbiology*, 14 (4): 705–716.

Tintut, Y., Wang, J.T. and Gralla, J.D. (1995) Abortive cycling and the release of polymerase for elongation at the sigma 54-dependent *glnAp2* promoter. *The Journal of Biological Chemistry*, 270 (41): 24392–24398.

Townsley, L. and Yildiz, F.H. (2015) Temperature affects c-di-GMP signaling and biofilm formation in *Vibrio cholerae*. *Environmental Microbiology*, 17 (11): 4290–4305.

Tozzi, M.G., Camici, M., Mascia, L., Sgarella, F., Ipata, P. (2006) Pentose phosphates in nucleoside interconversion and catabolism. *The FEBS Journal*, 273 (6): 1089–1101.

Tsang, J. and Hoover, T.R. (2014) Themes and Variations: Regulation of RpoN-Dependent Flagellar Genes across Diverse Bacterial Species. *Scientifica*, 2014: 1–14.

Tsou, A.M., Cai, T., Liu, Z., Zhu, J., Kulkarni, R. (2009) Regulatory targets of quorum sensing in *Vibrio cholerae*: evidence for two distinct HapR-binding motifs. *Nucleic Acids Research*, 37 (8): 2747–56.

Tu, K.C. and Bassler, B.L. (2007) Multiple small RNAs act additively to integrate sensory information and control quorum sensing in *Vibrio harveyi*. *Genes & Development*, 21 (2): 221–33.

Uehara, T., Suefuji, K., Jaeger, T., Mayer, C., Park, J. (2006) MurQ Etherase is required by *Escherichia coli* in order to metabolize anhydro-N-acetylmuramic acid obtained either from the environment or from its own cell wall. *Journal of Bacteriology*, 188 (4): 1660–1662.

Valentin-Hansen, P., Søgaard-Andersen, L. and Pedersen, H. (1996) A flexible partnership: the CytR anti-activator and the cAMP-CRP activator protein, comrades in transcription control. *Molecular Microbiology*, 20 (3): 461–466.

Vassylyev, D.G., Vassylyeva, M.N., Zhang, J., Palangat, M., Artsimovitch, I., Landick, R. (2007) Structural basis for substrate loading in bacterial RNA polymerase. *Nature*, 448 (7150): 163–168.

Verhoogt, H.J.C., Smit, H., Abee, T., Gamper, M., Driessen, A., Haas, D., Konings, W. (1992) *arcD*, the first gene of the *arc* operon for anaerobic arginine catabolism in *Pseudomonas aeruginosa*, encodes an arginine-ornithine exchanger. *Journal of Bacteriology*, 174 (5): 1568–1573.

Vincent, H.A., Henderson, C.A., Ragan, T.J., Garza-Garcia, A., Cary, P., Gowers, D., Malfois, M., Driscoll, P., Sobott, F., Callaghan, A. (2012) Characterization of *Vibrio cholerae* Hfq provides novel insights into the role of the Hfq C-terminal region. *Journal of Molecular Biology*, 420 (1–2): 56–69.

Vollmer, W., Blanot, D. and de Pedro, M.A. (2008) Peptidoglycan structure and architecture. *FEMS Microbiology Reviews*, 32 (2): 149–167.

Waldor, M.K. and Mekalanos, J.J. (1996) Lysogenic conversion by a filamentous phage encoding cholera toxin. *Science* (New York, N.Y.), 272 (5270): 1910–1913.

Wang, H., Ayala, J.C., Benitez, J.A., Silva, A. (2015) RNA-seq analysis identifies new genes regulated by the histone-like nucleoid structuring protein (H-NS) affecting *Vibrio cholerae* virulence, stress response and chemotaxis. *PloS ONE*, 10 (2).

Wang, H., Wu, J.-H., Ayala, J.C., Benitez, J., Silva, A. (2011a) Interplay among cyclic diguanylate, HapR, and the general stress response regulator (RpoS) in the regulation of *Vibrio cholerae* hemagglutinin/protease. *Journal of Bacteriology*, 193 (23): 6529–38.

Wang, L. and Gralla, J.D. (1998) Multiple *in vivo* roles for the -12-region elements of sigma 54 promoters. Journal of bacteriology, 180 (21): 5626–31.

Wang, Y., Wang, H., Cui, Z., Chen, H., Zhong, Z., Kan, B., Zhu, J. (2011b) The Prevalence of Functional Quorum-Sensing Systems in Recently Emerged *Vibrio cholerae* Toxigenic Strains. *Environmental Microbiology Reports*, 3 (2): 218.

Waters, C.M., Lu, W., Rabinowitz, J.D., Bassler, B. (2008) Quorum Sensing Controls Biofilm Formation in *Vibrio cholerae* through Modulation of Cyclic Di-GMP Levels and Repression of *vpsT*. *Journal of Bacteriology*, 190 (7): 2527–2536.

Watve, S., Barrasso, K., Jung, S.A., Davis, K., Hawver, L., Khataokar, A., Palaganas, R., Neiditch, M., Perez, L., Ng, W.L. (2020) Parallel quorum-sensing system in *Vibrio cholerae* prevents signal interference inside the host. *PLoS Pathogens*, 16 (2).

Weill, F. X., Domman, D., Njamkepo, E., Tarr, C., Rauzier, J., Fawal, N., Keddy, K. H., Salje, H., Moore, S., Mukhopadhyay, A. K., Bercion, R., Luquero, F. J., Ngandjio, A., Dosso, M., Monakhova, E., Garin, B., Bouchier, C., Pazzani, C., Mutreja, A., Grunow, R., Sidikou, F., Bonte, L., Breurec, S., Damian, M., Njanpop-Lafourcade, B.M., Sapriel, G., Page, A.L., Hamze, M., Henkens, M., Chowdhury, G., Mengel, M., Koeck, J.L., Fournier, J.M., Dougan, G., Grimont, P.A.D., Parkhill, J., Holt, K.E., Piarroux, R., Ramamurthy, T., Quilici, M.L., Thomson, N.R., Thomson, N. R. (2017) Genomic history of the seventh pandemic of cholera in Africa. *Science*, 358 (6364): 785 LP – 789.

WHO EMRO (n.d.) Outbreak update – Cholera in Yemen, 12 January 2020 | Cholera | *Epidemic and pandemic diseases*.

Wibbenmeyer, J.A., Provenzano, D., Landry, C.F., Klose, K., Delcour, A. (2002) *Vibrio cholerae* OmpU and OmpT porins are differentially affected by bile. *Infection and Immunity*, 70 (1): 121–126.

Woodcock, D.M., Crowther, P.J., Doherty, J., Jefferson, S., DeCruz, E., Noyer-Weidner, M., Smith, S.S., Michael, M. Z., Graham, M. W. (1989) Quantitative evaluation of *Escherichia coli* host strains for tolerance to cytosine methylation in plasmid and phage recombinants. *Nucleic Acids Research*, 17 (9): 3469.

Yamamoto, K., Ichinose, Y., Shinagawa, H., Makino, K., Nkata, A., Iwanaga, M., Hona, T., Miwatani, T. (1990) Two-step processing for activation of the cytolysin/hemolysin of *Vibrio cholerae* O1 biotype El Tor: nucleotide sequence of the structural gene (*hlyA*) and characterization of the processed products. *Infection and Immunity*, 58 (12): 4106–16.

Yamamoto, S., Mitobe, J., Ishikawa, T., Wai, S. N., Ohnishi, M., Watanbe, H., Izumiya, H. (2014) Regulation of natural competence by the orphan two-component system sensor kinase ChiS involves a non-canonical transmembrane regulator in *Vibrio cholerae*. *Molecular Microbiology*, 91 (2): 326–347.

Yamamoto, S. and Ohnishi, M. (2017) Glucose-Specific Enzyme IIA of the Phosphoenolpyruvate:Carbohydrate Phosphotransferase System Modulates Chitin Signaling Pathways in *Vibrio cholerae*. *Journal of Bacteriology*, 199 (18).

Yamanaka, K. and Inouye, M. (1997) Growth-phase-dependent expression of *cspD*, encoding a member of the CspA family in *Escherichia coli*. *Journal of Bacteriology*, 179 (16): 5126.

Yang, M., Frey, E.M., Liu, Z., Bishar, R., Zhu, J., (2010) The virulence transcriptional activator *aphA* enhances biofilm formation by *Vibrio cholerae* by activating expression of the biofilm regulator VpsT. *Infection and Immunity*, 78 (2): 697–703

Yang, Y., Darbari, V.C., Zhang, N., Lu, D., Glyde, R., Wang, Y., Winkelman, J., Gourse, R., Murakami, K., Buck, M., Zhang, X. (2015) Structures of the RNA polymerase-σ54 reveal new and conserved regulatory strategies. *Science* (New York, N.Y.), 349 (6250): 882–5.

Yildiz, F.H. and Schoolnik, G.K. (1998) Role of *rpoS* in stress survival and virulence of *Vibrio cholerae*. *Journal of Bacteriology*, 180 (4): 773–784.

Yildiz, H., Liu, X.S., Heydorn, A., Schoolnik, G. (2004) Molecular analysis of rugosity in a *Vibrio cholerae* O1 El Tor phase variant. *Molecular Microbiology*, 53 (2): 497–515.

Yura, T., Nagai, H. and Mori, H. (1993) Regulation of the heat-shock response in bacteria. *Annual Review of Microbiology*, 47: 321–350.

Zamorano-Sánchez, D., Fong, J.C.N., Kilic, S., Erill, I., Yildiz, F. (2015) Identification and characterization of VpsR and VpsT binding sites in *Vibrio cholerae*. *Journal of Bacteriology*, 197 (7): 1221–1235.

Zampini, M., Pruzzo, C., Bondre, V.P., Tarsi, R., Cosmo, M., Bacciaglia, A., Chhabra, A., Srivastava, R., Srivasata, B. (2005) *Vibrio cholerae* persistence in aquatic environments and colonization of intestinal cells: involvement of a common adhesion mechanism. *FEMS microbiology letters*, 244 (2): 267–273.

Zhang, G., Campbell, E.A., Minakhin, L., Severinov, K., Darst, S. (1999) Crystal structure of *Thermus aquaticus* core RNA polymerase at 3.3 A resolution. *Cell*, 98 (6): 811–24.

Zhang, J., Liu, B., Gu, D., Hao, Y., Chen, M., Ma, Y., ZZhou, X., Reverter, D., Zhang, Y., Wang, Q. (2021) Binding site profiles and N-terminal minor groove interactions of the master quorum-sensing regulator LuxR enable flexible control of gene activation and repression. *Nucleic Acids Research*, 49 (6): 3274–3293.

Zheng, D., Constantinidou, C., Hobman, J.L., Minchin, S. (2004) Identification of the CRP regulon using *in vitro* and *in vivo* transcriptional profiling. *Nucleic Acids Research*, 32 (19): 5874–5893.

Zhou, Y., Kolb, A., Busby, S.J.W., Wang, Y. (2014) Spacing requirements for Class I transcription activation in bacteria are set by promoter elements. *Nucleic Acids Research*, 42 (14): 9209–16.

Zhou, Y., Zhang, X. and Ebright, R.H. (1993) Identification of the activating region of catabolite gene activator protein (CAP): isolation and characterization of mutants of CAP

specifically defective in transcription activation. *Proceedings of the National Academy of Sciences of the United States of America*, 90 (13): 6081–6085.

Zhu, J., Miller, M.B., Vance, R.E., Dziejman, M., Bassler, B. (2002) Quorum-sensing regulators control virulence gene expression in *Vibrio cholerae*. *Proceedings of the National Academy of Sciences*, 99 (5): 3129–3134.